Acoustics Provide Insight in the Neonatal Brain and Cerebral Perfusion

Marlou Raets

Acoustics Provide Insight in the Neonatal Brain and Cerebral Perfusion

Marlou Raets

ISBN: 978-94-6169-495-9

Layout and printing: Optima Grafische Communicatie, Rotterdam, The Netherlands

Acoustics Provide Insight in the Neonatal Brain and Cerebral Perfusion

Echografie geeft inzicht in de neonatale hersenen en hersendoorbloeding

Proefschrift

ter verkrijging van de graad van doctor aan de
Erasmus Universiteit Rotterdam
op gezag van de
rector magnificus

prof.dr. H.A.P. Pols

en volgens besluit van het College voor Promoties.
De openbare verdediging zal plaatsvinden op

Woensdag 26 maart 2014 om 13.30 uur

Maria Margaritha Albertina Raets
geboren te Heerlen

Promotiecommissie

Promotor:	Prof.Dr. I.K.M. Reiss
Overige leden:	Prof.Dr. D. Tibboel
	Prof.Dr. G.P. Krestin
	Prof.Dr. B. Urlesberger
Co-promotoren:	Dr. P. Govaert
	Dr. J. Dudink

Table of contents

PART I

CHAPTER 1

GENERAL INTRODUCTION

Preterm birth and neurodevelopmental outcome

The incidence of preterm birth is increasing. Preterm infants are all infants born before 37 weeks of gestation. The incidence of preterm birth in the Netherlands is 7.8% of all deliveries, with 1.4% very preterm infants (below 32 weeks of gestation) [1]. Advances in prenatal and neonatal care have led to increased survival of infants born preterm, however neonatal morbidity is still of concern [2-6].

Preterm brain injury leads to problems of cognition, attention and behavior in 25-50% and to major motor problems (e.g. cerebral palsy) in 5-10% [7]. Various lesions are the neuropathological substrate of this encephalopathy, including periventricular leucomalacia (PVL), germinal matrix hemorrhage/intraventricular hemorrhage and neuronal/axonal deficits of cerebral white matter, cerebellum and basal ganglia. The prevalence in the literature of PVL or neuronal/axonal deficits in preterm infants is 50% [7].

During our study period 336 preterm infants below 29 weeks of gestation were admitted to Sophia's Children's hospital neonatal intensive care unit. Of these infants, 61 preterm infants died during the neonatal period and 157 infants developed apparent brain injury (documented with cranial ultrasound (CUS) or conventional Magnetic Resonance Imaging (MRI)). Data on long term neurodevelopmental outcome will follow in subsequent years.

Normal brain development

Knowledge of normal development is important in the understanding of different lesions or malformations. Normal brain development has a few major events at known time periods (table 1). At 3 to 4 weeks the neural tube is formed and closed, the *primary neurulation* [8]. Disturbances in this stage can lead to anencephaly, encephalocele and myelomeningocele (Chiari type II malformation). *Prosencephalic development* follows primary neurulation at 2 to 3 months of gestation [8]. At the end of the first month prosencephalic formation begins at the rostral end of the neural tube. After this formation prosencephalic cleavage occurs horizontally to form optic vesicles, olfactory bulbs and tracts; transversely to separate telencephalon from diencephalon and sagitally to form cerebral hemispheres, lateral ventricles and basal ganglia. The third event in this stage is midline prosencephalic development where the commissural, chiasmatic and hypothalamic plates become apparent. These structures are important for the development of corpus callosum, septum pellucidum, optic nerve-chiasm and hypothalamic structures. Disorders of prosencephalic development include aprosencephaly, holoprosencephaly, agenesis of corpus callosum or septum pellucidum and septo-optic dysplasia. *Neuronal proliferation* occurs at 3 to 4 months of gestation [8]. The germinal matrix or subventricular zone is a transient layer at the surface of the lateral ventricles and is considered the 'factory' for production of most brain cells [8, 9]. Disturbances in this phase lead to primary microcephaly. A remarkable series of

Table 1 Normal brain development

Major Development Event	Time period	Disorders/disturbances
Primary Neurulation	3-4 Weeks of gestation	Anencephaly Encephalocele Myelomeningocele (Chiari type II)
Prosencephalic Development	2-3 Months of gestation	Aprosencephaly Holoprosencephaly Agenesis of corpus callosum or septum pellucidum Septo-optic Dysplasia
Neuronal Proliferation	3-4 Months of gestation	Microcephaly
Neuronal Migration	3-5 Months of gestation	Schizencephaly Lissencephaly Polymicrogyria Heterotopia
Organization	5 Months of gestation to years postnatally	Mental retardation Fragile X syndrome Down syndrome Angelmann syndrome After prematurity Other perinatal/postnatal insults
Myelination	Birth to years postnatally	Cerebral white matter hypoplasia Prematurity Hypothyroidism Postnatal undernutrition Iron deficiency

events whereby millions of nerve cells move from their origin to different loci within the central nervous system is called *neuronal migration* [8]. Radial (projection neurons) and tangential (interneurons) migration can be distinguished [8, 9]. Disorders in this stage include schizencephaly, lissencephaly, polymicrogyria and heterotopia. After migration, *organization* takes place. For the cerebral cortex the major features of organization include the following: 1. establishment of the subplate neurons; 2. attainment of proper alignment, orientation and layering of cortical neurons; 3. elaboration of dendritic and axonal ramifications; 4. establishment of synaptic contacts; 5. cell death and selective elimination of neuronal processes and synapses and 6. proliferation and differentiation of glia [8]. Disturbances in this stage can be primary (mental retardation, fragile X syndrome, Down syndrome, Angelmann syndrome) or can be a result of perinatal/postnatal insults (prematurity, malnutrition and other insults). *Myelination* occurs from the second trimester of pregnancy and continues into adult life. It is characterized by acquisition of myelin membrane around axons. Disorders of myelination occur as a result of prematurity, hypothyroidism, postnatal malnutrition, cerebral white matter injury and iron deficiency [8].

The following stages of normal brain development: neuronal proliferation and migration, organization and myelination take place during the NICU admission of preterm infants (24 to 32 weeks of gestation). Different stress factors, like inflammation, hypoxia, hyperoxia,

hemodynamic instability and mechanical ventilation can interfere with these different stages and can lead to disorders mentioned above and in table 1. Therefore monitoring of brain development and early, objective definition of brain injury is important for treatment, parental counseling and further research to reduce neurological morbidity.

Besides neuronal development, the maturation of cerebral vascular system plays an important role in different types of brain lesions. The development of the cerebral arterial system starts with the formation of six pairs of primitive branchial arch arteries (figure 1). These arteries either regress completely or are modified during development [10]. The cranial part of the internal carotid artery terminates in the olfactory area, forming the anterior cerebral artery. At 12-14 mm CRL a midline plexus connects the distal parts of the ACA's forming the anterior communicating artery and completing the circle of Willis (in the 52-day-embryo) [10, 11]. At 16-18 mm CRL both middle cerebral arteries and the posterior cerebral arteries are developed [10]. At 24

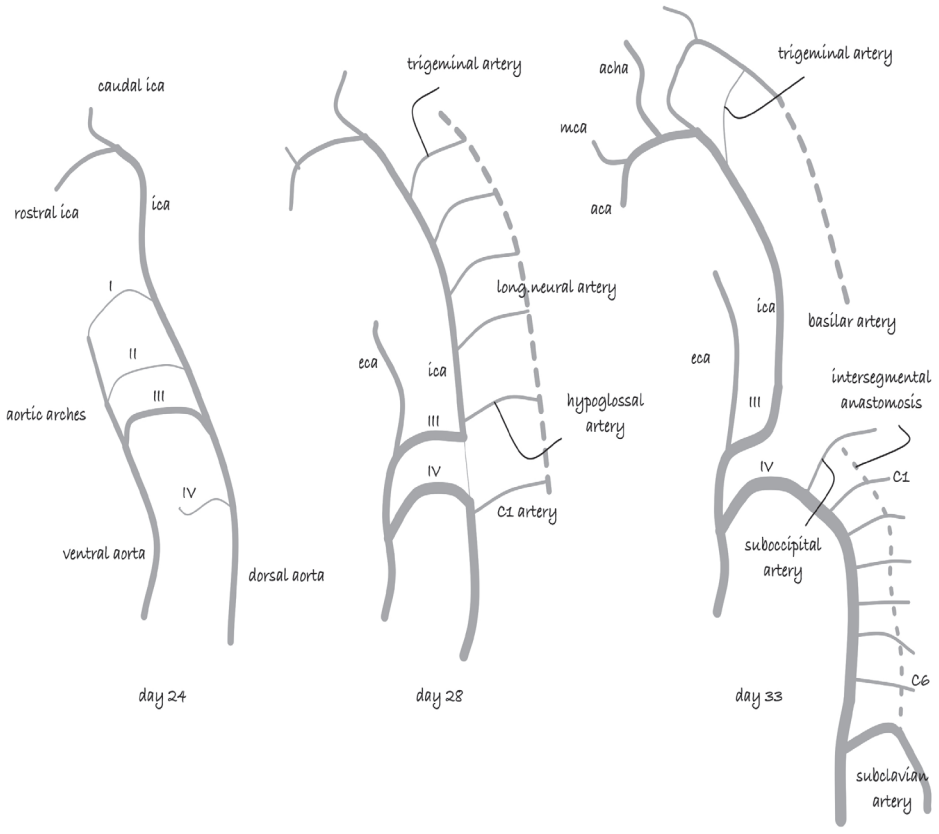

Gillilan 1958-1969

Figure 1 Development of arterial vasculature in early fetal period

mm crown-rump length (CRL) the period of actual remodeling of the primitive branchial arch arteries is generally over, the postbranchial phase continues into adulthood [10]. At an early fetal stage arterial vasculature has its adult form. Variations of the circle of Willis are described and may result from different mechanisms [11, 12]. The circle can be incomplete because of a lack of polygonal components or can have more than nine vessels forming the polygon [13]; vessels may also be present but exhibit asymmetrical caliber and flow [14].

In the early fetal period (CRL 80 mm) some definitive adult veins are formed, but many embryonic veins are still present. After the third fetal month superior striate and medullary veins draining into anterior and posterior terminal veins, form around the ICV (figure 2 and 3). In contrary to the arterial system, the transverse sinus develops asymmetrical. All studies confirmed drainage mainly to the right side in 41 %, equal drainage in 38 %, drainage mainly to the left in 19 % [15-17]. Variations of venous anatomy may play an important role in different types of brain injury (for example sinovenous thrombosis).

In viable preterm infants and around term, brain veins are therefore still in a phase of remodeling. Brain imaging techniques permit to study these veins during this remodeling phase.

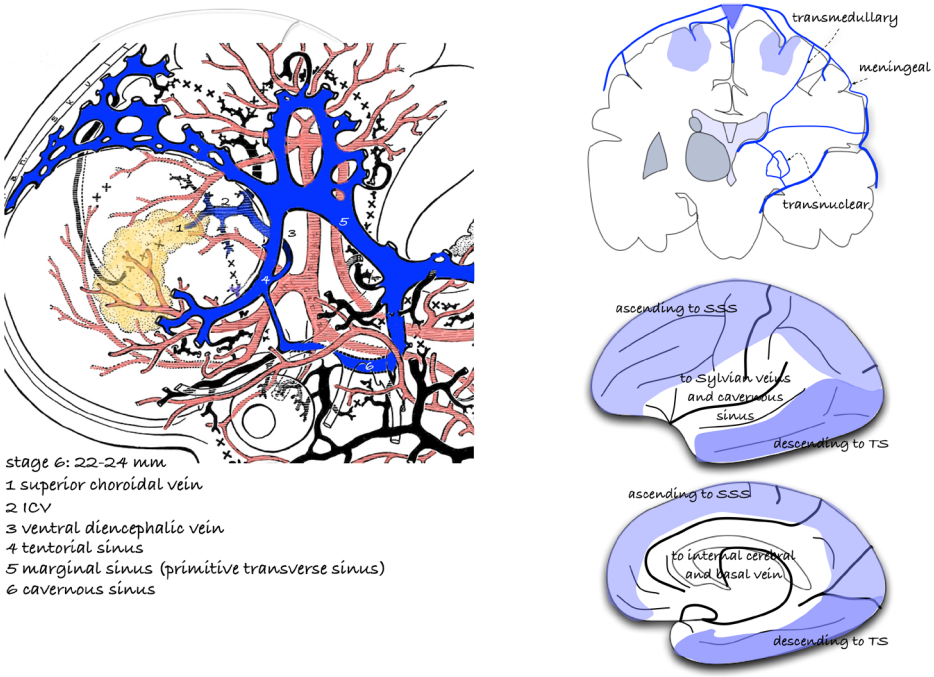

Figure 2 By courtesy of Paul Govaert. Left image: venous development in early fetal period, Right image: top and bottom: schematic images showing venous drainage patterns to sinuses

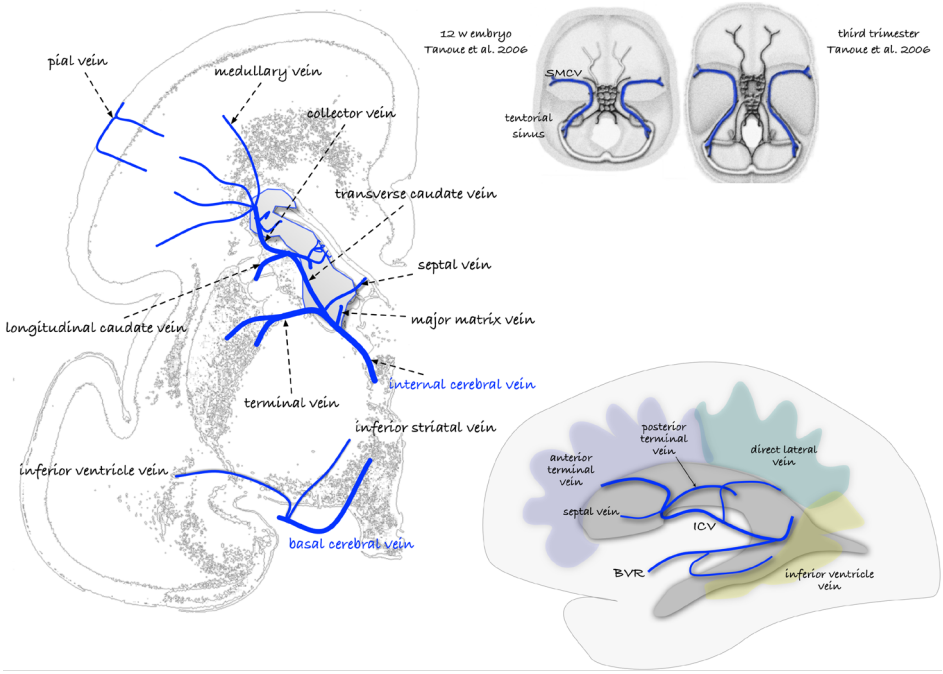

Figure 3 By courtesy of Paul Govaert
Left: schematic coronal view of right hemisphere indicating location of different veins with respect to the lateral ventricle; Right top image axial view of sinus development at 12 weeks and in third trimester. Right bottom: Sagittal schematic view of location of different veins with respect to the lateral ventricle and their different draining area's

Neuroimaging

Neonatal neuroimaging has advanced over the past decades. Starting in the early 1970's computed topography (CT) allowed detailed visualization of brain lesions in (pre)term infants, providing better understanding of the correlation between these lesions and outcome [18-20]. Major hemorrhagic lesions in preterm infants were well recognized by CT [21]. Recently CT imaging is hardly used due to the ionizing radiation. Other imaging modalities, such as cranial ultrasound (CUS) and Magnetic resonance imaging (MRI), are nowadays the most favorably used imaging techniques in neonatology.

Cranial ultrasound

CUS is used for three decades [22, 23]. Transfontanellar CUS transmits sound waves with a high frequency; the echoes are detected and processed, leading to an image of the neonatal brain. Anatomical structures and abnormalities can be distinguished by differences in echogenicity.

The technique is still improving with the use of higher frequencies (7.5-13 MHz), 3D possibilities and advances in Doppler technique and image processing techniques.

CUS is a non-invasive and safe method [24], which can be performed bedside [25]. Also CUS is relatively cheap and available in nearly all centers.

Traditionally CUS is used tot detect major cerebral abnormalities, such as intraventricular hemorrhage (IVH), periventricular hemorrhagic infarction (PVHI), post-hemorrhagic ventricular dilatation (PHVD) and (cystic) periventricular leukomalacia (cPVL). With the use of different acoustic windows, such as the mastoid (posterolateral) and posterior fontanel, and ongoing technical developments, other lesion patterns are recognized (e.g. cerebellar hemorrhage, perforator stroke)[26-30].

CUS including color Doppler allows visualization of intracranial vessels and measurement of velocities. Nowadays, ultrasound techniques permit visualization of micro vessels with flow velocities of 1-2 cm/s. With this technique, we are able to follow medial and lateral subependymal veins along their path of drainage into the terminal and internal cerebral veins (figure 3).

MR imaging

In the past two decades MRI, beside CUS, is increasingly used in neonatal intensive care. MRI is a non-ionizing imaging technique, using the properties of protons and their behavior in an external magnetic field to provide images. MRI provides unique anatomical detail of neonatal brain tissue. It offers good spatial resolution and excellent soft-tissue contrast and moreover, MRI allows quantitative measurement of brain injury [31-33]. Unfortunately, availability of MRI is limited in the majority of hospitals; it requires transport, sometimes sedation, and critically ill neonates may not be stable enough to be scanned. Therefore, serial imaging is difficult. However, MRI in preterm infants is safe, provided that guidelines are followed [34]. Research and improvement of the technique has led to advanced MR techniques like diffusion weighted imaging (DWI), diffusion tensor imaging (DTI), susceptibility weighted imaging (SWI), MR spectroscopy, functional MRI, MR angiography and arterial spin labeling. These techniques provide (patho-) physiological insights in the developing brain and cerebral blood flow [35-39].

CUS versus MRI

Several studies evaluated the detection of preterm brain injury with CUS compared with MRI [40-43]. Meta-analysis is difficult to perform given the heterogeneity of the studies and prognostic values of CUS and MRI are based on small cohort studies [44]. Horsch et al. described that CUS was able to detect all severe white matter (WM) injury [40]. Normal CUS at term equivalent age corresponded with a normal MRI or only mild WM abnormalities [40]. Another study illustrated that CUS detected most abnormalities associated with abnormal neurodevelopmental outcome [42]. Term equivalent MRI is more sensitive in predicting cerebral palsy in very low birth weight infants compared to CUS, however both imaging techniques have a high specificity [41].

Aims and outline of this thesis

The general aim of this thesis was to provide more insight in cerebral blood flow and brain maturation of preterm infants, both related to lesions.

In the first part of this thesis we focus on venous origin of many neonatal brain lesions. In **chapter 2** we start with an extensive review of disorders of newborns cerebral veins. Veins play an important part in several types of perinatal brain injury. Improving imaging techniques allow to study cerebral veins and their diseases. In **chapter 3** we study the incidence of cerebral sinovenous thrombosis in asymptomatic preterm infants.

The topic of the second part of this thesis is arterial blood flow in preterm and term neonates. In **chapter 4** we describe six neonates with carotid occlusion diagnosed with CUS. In **chapter 5** we analyze perforator stroke in the neonatal period. In **chapter 6** we evaluate the incidence of brain injury during neonatal ECMO. In **chapter 7** we analyze whether CUS including color Doppler is able to study preterm cerebral microcirculation.

In the final part of this thesis we study echogenicity in basal ganglia of preterm infants with serial imaging (**chapter 8)**, we describe the rivalry or synergy between CUS and MRI in detecting preterm brain injury (**chapter 9)** and review neonatal disorders of germinal matrix (**chapter 10)**. In **chapter 11** our findings reported in this thesis will be discussed, including future perspectives.

References

1. Stichting Perinatale Registratie Nederland.
2. Doyle LW, Roberts G, Anderson PJ. Outcomes at age 2 years of infants < 28 weeks' gestational age born in Victoria in 2005. J Pediatr. 2010; **156**(1): 49-53 e1.
3. Draper ES, Zeitlin J, Fenton AC, Weber T, Gerrits J, Martens G, et al. Investigating the variations in survival rates for very preterm infants in 10 European regions: the MOSAIC birth cohort. Arch Dis Child Fetal Neonatal Ed. 2009; **94**(3): F158-63.
4. Schlapbach LJ, Adams M, Proietti E, Aebischer M, Grunt S, Borradori-Tolsa C, et al. Outcome at two years of age in a Swiss national cohort of extremely preterm infants born between 2000 and 2008. BMC Pediatr. 2012; **12**: 198.
5. Stoll BJ, Hansen NI, Bell EF, Shankaran S, Laptook AR, Walsh MC, et al. Neonatal outcomes of extremely preterm infants from the NICHD Neonatal Research Network. Pediatrics. 2010; **126**(3): 443-56.
6. Moore T, Hennessy EM, Myles J, Johnson SJ, Draper ES, Costeloe KL, et al. Neurological and developmental outcome in extremely preterm children born in England in 1995 and 2006: the EPICure studies. BMJ. 2012; **345**: e7961.
7. Volpe JJ. Brain injury in premature infants: a complex amalgam of destructive and developmental disturbances. Lancet Neurol. 2009; **8**(1): 110-24.
8. Volpe. Neurology of the newborn. In: Saunders E, editor.; 2008. p. 3-118.
9. Raets MM, Dudink J, Govaert P. Neonatal disorders of germinal matrix. J Matern Fetal Neonatal Med. 2013.
10. Kathuria S, Gregg L, Chen J, Gandhi D. Normal cerebral arterial development and variations. Semin Ultrasound CT MR. 2011; **32**(3): 242-51.
11. Arey B. Developmental Anatomy. 6th Edn Saunders, Philadelphia. 1954: 364-73.
12. Vasovic L, Milenkovic Z, Pavlovic S. Comparative morphological variations and abnormalities of circles of Willis: a minireview including two personal cases. Neurosurg Rev. 2002; **25**(4): 247-51.
13. Vasovic LP. The tenth vascular component in a rare form of the cerebral arterial circle of fetuses. Cells Tissues Organs. 2004; **178**(4): 231-8.
14. Raets MM, Lequin MH, Plaisier A, Dudink J, Govaert P. Incidental sonographic diagnosis of neonatal carotid occlusion. Acta Paediatr. 2013; **102**(4): e187-90.
15. Ayanzen RH, Bird CR, Keller PJ, McCully FJ, Theobald MR, Heiserman JE. Cerebral MR venography: normal anatomy and potential diagnostic pitfalls. AJNR Am J Neuroradiol. 2000; **21**(1): 74-8.
16. Fukusumi A, Okudera T, Takahashi S, Taoka T, Sakamoto M, Nakagawa H, et al. Anatomical evaluation of the dural sinuses in the region of the torcular herophili using three dimensional CT venography. Acad Radiol. 2010; **17**(9): 1103-11.
17. Raets MM, Sol JJ, Govaert P, Lequin MH, Reiss IK, Kroon AA, et al. Serial Cranial US for Detection of Cerebral Sinovenous Thrombosis in Preterm Infants. Radiology. 2013.
18. El-Tatawy S, Shukry AS, Badrawi N, Hamed Z. CT of the normal brain in preterm infants. AJNR Am J Neuroradiol. 1983; **4**(3): 685-8.
19. Lazzara A, Ahmann P, Dykes F, Brann AW, Jr., Schwartz J. Clinical predictability of intraventricular hemorrhage in preterm infants. Pediatrics. 1980; **65**(1): 30-4.
20. Papile LA, Burstein J, Burstein R, Koffler H. Incidence and evolution of subependymal and intraventricular hemorrhage: a study of infants with birth weights less than 1,500 gm. J Pediatr. 1978; **92**(4): 529-34.
21. Pape KE, Bennett-Britton S, Szymonowicz W, Martin DJ, Fitz CR, Becker L. Diagnostic accuracy of neonatal brain imaging: a postmortem correlation of computed tomography and ultrasound scans. J Pediatr. 1983; **102**(2): 275-80.
22. Pape KE, Blackwell RJ, Cusick G, Sherwood A, Houang MT, Thorburn RJ, et al. Ultrasound detection of brain damage in preterm infants. Lancet. 1979; **1**(8129): 1261-4.

23. Levene MI. Measurement of the growth of the lateral ventricles in preterm infants with real-time ultrasound. Arch Dis Child. 1981; **56**(12): 900-4.
24. Torloni MR, Vedmedovska N, Merialdi M, Betran AP, Allen T, Gonzalez R, et al. Safety of ultrasonography in pregnancy: WHO systematic review of the literature and meta-analysis. Ultrasound Obstet Gynecol. 2009; **33**(5): 599-608.
25. van Wezel-Meijler G, Steggerda SJ, Leijser LM. Cranial ultrasonography in neonates: role and limitations. Semin Perinatol. 2010; **34**(1): 28-38.
26. Ecury-Goossen GM, Raets MM, Lequin M, Feijen-Roon M, Govaert P, Dudink J. Risk factors, clinical presentation, and neuroimaging findings of neonatal perforator stroke. Stroke. 2013; **44**(8): 2115-20.
27. McCarthy LK, Donoghue V, Murphy JF. Ultrasonically detectable cerebellar haemorrhage in preterm infants. Arch Dis Child Fetal Neonatal Ed. 2011; **96**(4): F281-5.
28. Soudack M, Jacobson J, Raviv-Zilka L, Ben-Shlush A, Kuint J. Cerebellar hemorrhage in very low birth weight premature infants: The advantage of the posterolateral fontanelle view. J Clin Ultrasound. 2013; **41**(7): 395-401.
29. Steggerda SJ, de Bruine FT, Smits-Wintjens VE, Walther FJ, van Wezel-Meijler G. Ultrasound detection of posterior fossa abnormalities in full-term neonates. Early Hum Dev. 2012; **88**(4): 233-9.
30. Steggerda SJ, Leijser LM, Wiggers-de Bruine FT, van der Grond J, Walther FJ, van Wezel-Meijler G. Cerebellar injury in preterm infants: incidence and findings on US and MR images. Radiology. 2009; **252**(1): 190-9.
31. Huppi PS, Dubois J. Diffusion tensor imaging of brain development. Semin Fetal Neonatal Med. 2006; **11**(6): 489-97.
32. Rutherford MA. What's new in neuroimaging? Magnetic resonance imaging of the immature brain. Eur J Paediatr Neurol. 2002; **6**(1): 5-13.
33. Counsell SJ, Rutherford MA, Cowan FM, Edwards AD. Magnetic resonance imaging of preterm brain injury. Arch Dis Child Fetal Neonatal Ed. 2003; **88**(4): F269-74.
34. Plaisier A, Raets MM, van der Starre C, Feijen-Roon M, Govaert P, Lequin MH, et al. Safety of routine early MRI in preterm infants. Pediatr Radiol. 2012; **42**(10): 1205-11.
35. Counsell SJ, Allsop JM, Harrison MC, Larkman DJ, Kennea NL, Kapellou O, et al. Diffusion-weighted imaging of the brain in preterm infants with focal and diffuse white matter abnormality. Pediatrics. 2003; **112**(1 Pt 1): 1-7.
36. De Vis JB, Petersen ET, de Vries LS, Groenendaal F, Kersbergen KJ, Alderliesten T, et al. Regional changes in brain perfusion during brain maturation measured non-invasively with Arterial Spin Labeling MRI in neonates. Eur J Radiol. 2013; **82**(3): 538-43.
37. Dubois J, Benders M, Borradori-Tolsa C, Cachia A, Lazeyras F, Ha-Vinh Leuchter R, et al. Primary cortical folding in the human newborn: an early marker of later functional development. Brain. 2008; **131**(Pt 8): 2028-41.
38. Dudink J, Counsell SJ, Lequin MH, Govaert PP. DTI reveals network injury in perinatal stroke. Arch Dis Child Fetal Neonatal Ed. 2012; **97**(5): F362-4.
39. Dudink J, Kerr JL, Paterson K, Counsell SJ. Connecting the developing preterm brain. Early Hum Dev. 2008; **84**(12): 777-82.
40. Horsch S, Skiold B, Hallberg B, Nordell B, Nordell A, Mosskin M, et al. Cranial ultrasound and MRI at term age in extremely preterm infants. Arch Dis Child Fetal Neonatal Ed. 2010; **95**(5): F310-4.
41. Mirmiran M, Barnes PD, Keller K, Constantinou JC, Fleisher BE, Hintz SR, et al. Neonatal brain magnetic resonance imaging before discharge is better than serial cranial ultrasound in predicting cerebral palsy in very low birth weight preterm infants. Pediatrics. 2004; **114**(4): 992-8.
42. Leijser LM, de Bruine FT, Steggerda SJ, van der Grond J, Walther FJ, van Wezel-Meijler G. Brain imaging findings in very preterm infants throughout the neonatal period: part I. Incidences and evolution of lesions, comparison between ultrasound and MRI. Early Hum Dev. 2009; **85**(2): 101-9.

43. Rademaker KJ, Uiterwaal CS, Beek FJ, van Haastert IC, Lieftink AF, Groenendaal F, et al. Neonatal cranial ultrasound versus MRI and neurodevelopmental outcome at school age in children born preterm. Arch Dis Child Fetal Neonatal Ed. 2005; **90**(6): F489-93.
44. Nongena P, Ederies A, Azzopardi DV, Edwards AD. Confidence in the prediction of neurodevelopmental outcome by cranial ultrasound and MRI in preterm infants. Arch Dis Child Fetal Neonatal Ed. 2010; **95**(6): F388-90.

CHAPTER 2

DISORDERS OF NEWBORN BRAIN VEINS

M.M.A. Raets, J. Dudink, C. Raybaud, L.A. Ramenghi,
M.H. Lequin, P. Govaert

Submitted

Abstract

In the early fetal period most of definitive adult veins have been formed but many embryonic veins are still present. Perinatal brain veins are thus in a phase of remodelling, which brain imaging techniques permit to study. Insight in venous developmental anatomy and disease is imperative to understand several types of injury. This review aims to provide a comprehensive background to encourage further research into prevention or mitigation of parenchymal injury related to perinatal diseases of veins.

Introduction

Veins are involved in several types of perinatal brain injury. Magnetic resonance venography and susceptibility weighted imaging, together with increasingly resolved sonographic Doppler facilities have provided the neonatal brain specialist tools to study venous developmental anatomy and disease. This review aims to provide interested parties a comprehensive background for that purpose, foremost to encourage research into prevention or mitigation of parenchymal injury related to perinatal diseases of veins (Table 1).

Table 1 Veins and neonatal brain injury

Preterm brain lesions	Medullary haemorrhagic venous infarction	Associated with GMH/IVH
		Primary (prothrombotic conditions, collagen A4 mutation)
	Punctate lesions of the white matter	
	Cerebellar haematoma	
Term brain lesions	Thrombosis	Sinovenous; general
		Internal cerebral vein
		Basal vein
		Transverse sinus
	Lobar haematoma	Major lobar haematoma
		ECMO-related haematoma
		Contusion
	Open vessel ischaemia	Polycythaemia, dehydration, severe congestion
Other	Vascular anomaly	AVM, Vein of Galen malformation
		DVA
		Sinus pericranii
		Cerebral angiodysplasia
		Cerebellar vascular dysplasia
		Sturge-Weber syndrome
		Hereditary haemorrhagic telangiectasia
	Infantile subdural haematoma	
	Infectious thrombophlebitis	
	Plexusbleeding with IVH	
	Emissary vein leakage due to jugular vein thrombosis	

Vein development

In the early fetal period [vascular stage 7a (80 mm CRL)[1], Figure 1, Table 2] some definitive adult veins are formed, but many embryonic veins are still present. The primitive transverse sinus (TS) receives an elongated tentorial sinus, itself continuous with the superficial middle cerebral

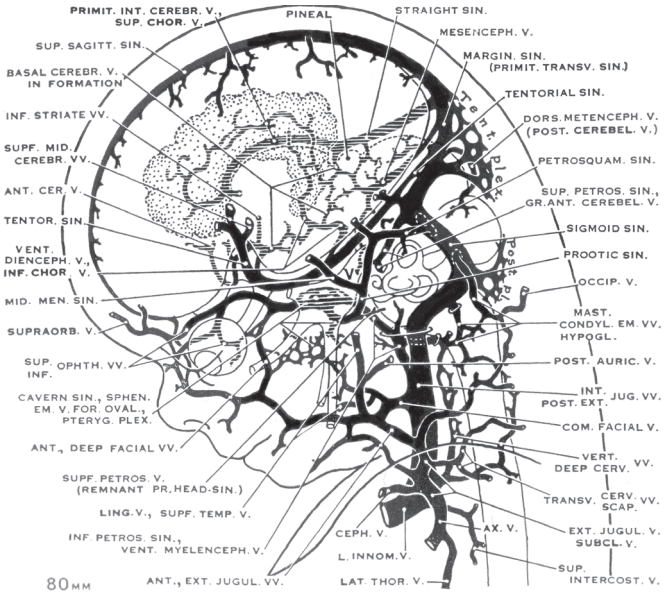

Figure 1 Vascular stage 7a (80 mm CRL, week 12), adapted from Padget 1956.

veins (SMCVs). The primitive internal cerebral vein (ICV) drains the large superior choroidal vein into the straight sinus (StS) and has only one feeder, a thalamic tributary. The basal vein of Rosenthal (BVR) is formed by coalescence of the deep middle cerebral, inferior striate and diencephalic veins, a mesencephalic vein and a tributary of the StS. The lateral mesencephalic vein, connected to the primitive metencephalic or great anterior cerebellar vein, may drain the BVR or just merely become a collateral when the BVR drains into the great cerebral vein (GCV). The stem of the great anterior cerebellar vein will become the superior petrosal sinus, outlet of the cavernous into the sigmoid sinus (SiS). The dwindling pro-otic sinus is continuous with the petrosquamosal sinus. Both become diploic in adult life. After the third fetal month superior striate and medullary veins draining into anterior and posterior terminal veins, form around the ICV. Anastomosing veins of Trolard and Labbé on the cerebral convexity - connecting SMCVs, superior sagittal and transverse sinuses - are in fact only shaped in the fetal period. In viable preterm infants and around term, brain veins are therefore still in a phase of remodelling, which can be studied both ex and in utero by visualisation of the vessels, and by measurements of flow indices and velocities[2].

During the second half of gestation, the brain presents a multilayered pattern that reflects the histological development at that stage. This includes, from the depth to the surface: the highly cellular *germinal matrices* (ventricular/subventricular zone); the *intermediate zone (IZ)*, which contains the main bundles of axons; the *subplate (SP)*, a transient neuronal structure which serves as a wait zone for the outgoing and incoming axons, and as an intermediate relay until the cortex itself becomes connected between week 22 and week 47; and the *cortical plate*

Table 2 Development of brain veins

Stage	Venous changes
28d, CRL 4 mm	Primary head plexus drain into anterior cardinal veins (later internal jugular veins)
32d, CRL 5-6 mm	Superficial anastomosing loops from head plexus (anterior: forebrain and midbrain; middle: cerebellum) from paired paramedian sinus
37d, CRL 7-12 mm	Paramedian sinus forms marginal sinus (anterior plexus); marginal sinus will become SSS and TS Emergence of paired primitive telencephalic (later superficial middle cerebral vein) and diencephalic veins
41d, CRL 12-14 mm	Meninges separate into dura and pia/arachnoid; pial veins traverse arachnoid space to dural sinus and run perpendicular to overlying pial arteries; parallel course predisposes to AVM Diencephalic veins form dorsal and ventral branches Mesencephalic veins emerge from anterior dural plexus
44-48d, CRL 16-18 mm	Middle and posterior dural plexus form sigmoid sinus; residual stem is pro-otic sinus
51d, CRL 20-24 mm	Anterior and middle plexus become tentorial plexus
56d, CRL 40 mm	Medial marginal sinus fuse to one SSS Pro-otic sinus forms cavernous sinus Inferior petrosal sinus forms caverno-jugular connection Choroid plexus drains into single median prosencephalic vein
10-12w, CRL 60-80 mm	Transverse sinus lateralizes Superior petrosal sinus forms Paired internal cerebral veins replace median prosencephalic vein and drain growing basal ganglia Basal vein of Rosenthal forms by anastomosis of telencephalic, diencephalic and mesencephalic veins

itself [3]. Before midgestation, the majority of telencephalic cortical pyramidal neurons have formed and migrated into the cortical plate (last wave about the 16th gestational week), but the germinal matrices are still active, until week 27 for the cortical mantle, and until week 34 for the ganglionic eminence. They still produce interneurons for the cortical plate and SP, and for the thalamus, respectively. They also produce oligodendrocytic precursors, microglia and possibly astroglia [4]. In this cluster of (sub)ventricular neuroepithelial cells, and reflecting the proliferative activity, a rich network of micro size vessels persists [5]. Beyond it, capillaries have progressively extended to the deep layers of the cortex (before week 15) to accompany the cellular development in the IZ and the SP [4]. These capillary networks initially are supplied by, and drained toward, the pial vascular network by transcerebral "arteries" and "veins", all very simple, embryonic vessels. Very early however (9th gestational week) anastomotic venous channels develop along the ependymal surface and connect with the vessels of the tela choroidea to form the subependymal venous system [6, 7], while the transcerebral "veins" progressively regress. As a consequence the deep medullary veins become mostly disconnected from the surface network. It is not before the thalamo-cortical connections develop from week 22 to week 47 that capillaries develop in the cortex as well, with their own drainage toward the

pial veins, separately from the subependymal system. Microangiographic studies of the fetal venous system have shown that in the second half of gestation until well into the 7th month, the deep medullary and the cortical venous systems are clearly separated and leave a gap between them [8-10].

The cerebral veins in fetuses (and premature infants) are fragile. They are primitive endothelial (sinusoid) channels, and remain so until late. The subependymal veins do not develop a mature appearance until week 27 [11], and the veins of the germinal matrix never mature. Another developmental risk factor is the fact that while the brain perfusion in fetuses is very low, it increases steeply within three days after birth, *whatever the gestational age*, probably because of the birth-related re-organization of the cardio-pulmonary circulation [4, 12, 13]; these immature veins may not be able to sustain such a sudden perinatal perfusion overload. Particularities of sinus development relative to thrombosis are described below.

Preterm venous lesions: mainly haemodynamic disruption.

Periventricular venous haemorrhagic infarction (PVHI)

Vascular rupture inherent to GMH (germinal matrix haemorrhage) occurs at the level of the fragile capillaro-venous transition. Subsequently some infants develop a haemorrhagic infarct in adjacent white (medullary) or grey matter. This occurs from a few hours up to a few days after the initial GMH. Quite often in the course of the second week the infarct shrinks by better delineation. 7.5 to 10 MHz ultrasound scanning is reliable for investigating parenchymal involvement [14-17]. Post mortem studies [18-22] strongly suggest that this parenchymal lesion equals venous infarction: venules and veins around a secluded, large GMH become occluded, probably due to compression. The venous confluences at the outer angle of the lateral ventricle and near the caudothalamic groove are especially prone to this type of injury, but veins in the roof of the temporal horn or along the atrium of the lateral ventricle can also be involved [23]. Although it is not exceptional to find thrombosis in the smaller veins around and inside a GMH, this does not appear to be the dominating event, but thrombosis may still be relevant in progression to infarction. Because of a time window, progression from GMH to venous infarction might in the future be amenable to drug manipulation. Increasing size of the GMH and increased velocity in the transverse caudate vein due to compression, may help to predict venous infarction [24, 25]. It has recently grown customary to search for prothrombotic conditions in atypical presentations of medullary infarction [26, 27]. Such an abnormal coagulation status could explain why PVHI are commonly associated with superficial cerebellar hemorrhages even though the factors related to the venous anatomy are different in the two locations [4].

Location and extent of medullary venous infarction both depend on venous anatomy (Figure 2). The territories of the different subependymal collectors may be more or less extensive. Although individual variations occur, the most extensive usually is the territory of the terminal

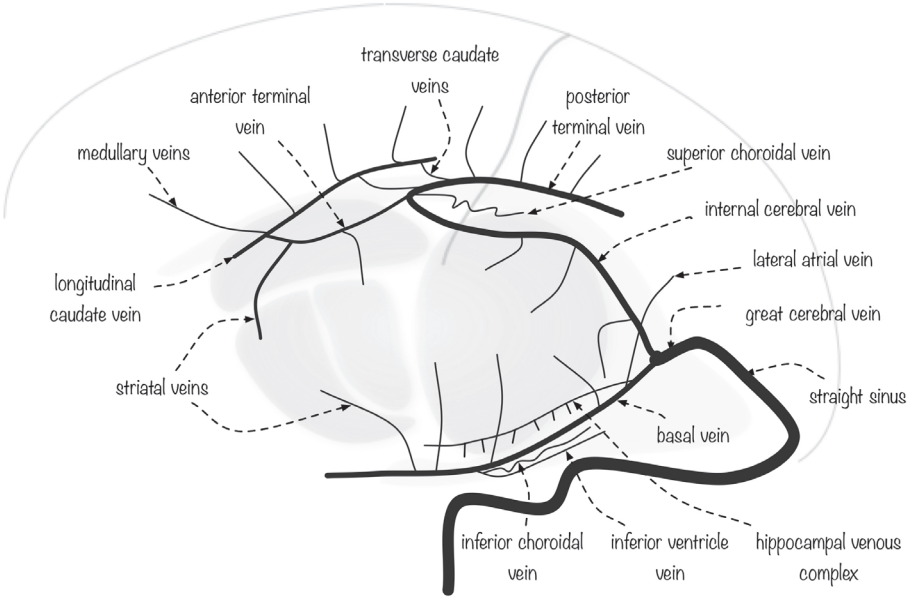

Figure 2 Venous infarction in deep medullary/subependymal veins: medullary veins affected may cover the entire frontal white matter up to the atrium, a limited area along the caudate head (anterior terminal vein), an area drained by the thalamostriate vein (posterior terminal vein), the white matter above and aside the temporal horn (inferior ventricle vein), an area of white matter above the insula (direct lateral vein) or along the atrium (lateral atrial vein), structures around the midline (medial subependymal veins), superior striatum (thalamostriate vein) or inferior striatum and amygdaloid area (basal vein).

(thalamostriate) veins which collect the deep medullary veins of the posterior frontal, central and parietal regions. Radially, as mentioned above, the territory of the deep medullary veins is restricted to the deep white matter (IZ): in PVHI, the subcortical SP and the cortex remain essentially unaffected [4]. Importantly, this preserves the possibility of some degree of "collateral plasticity" for sensory thalamo-cortical afferents, via the subplate connections, while the motor efferents are destroyed in their paraventricular course [28]. Assumedly because of the alterations of the late migration and connectivity, venous infarction associated with GMH/IVH may induce cortical dysplasia [29], as well as polymicrogyria below 25 weeks of gestation [30].

There are not enough human neonatal data on the relevance of variation in the disposition of either superficial venous trunks (intracortical, subcortical or superficial medullary), deep medullary veins (at four confluence zones: outer, candelabra, palmate and subependymal) and intermixed anastomosing or transmedullary veins that span the entire mantle [10]. It is going to be of interest, facing unilateral medullary venous infarction, to study developmental variation in relation to the lesions (Figures 3 and 4).

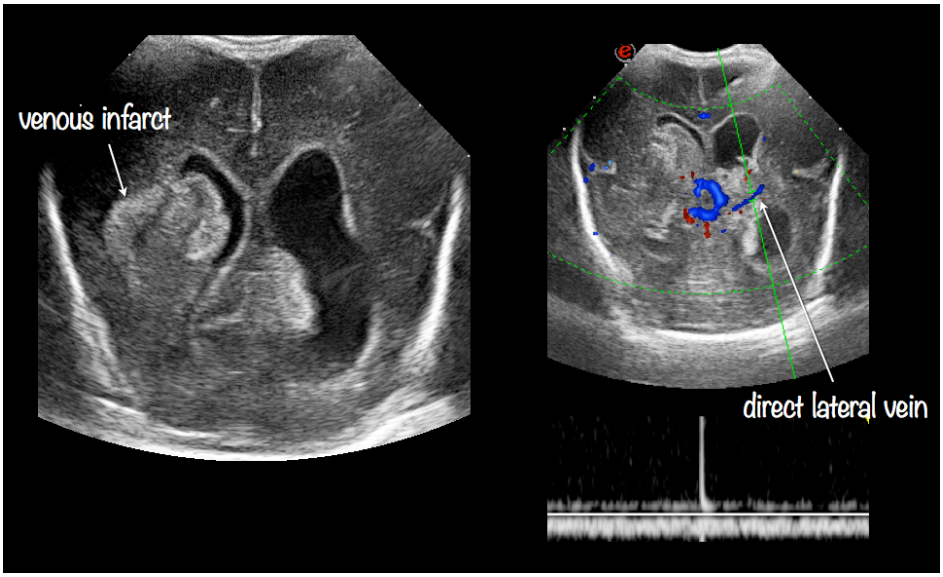

Figure 3 Right direct lateral vein infarction: observe the unaffected left vein in Doppler imaging (arrow).

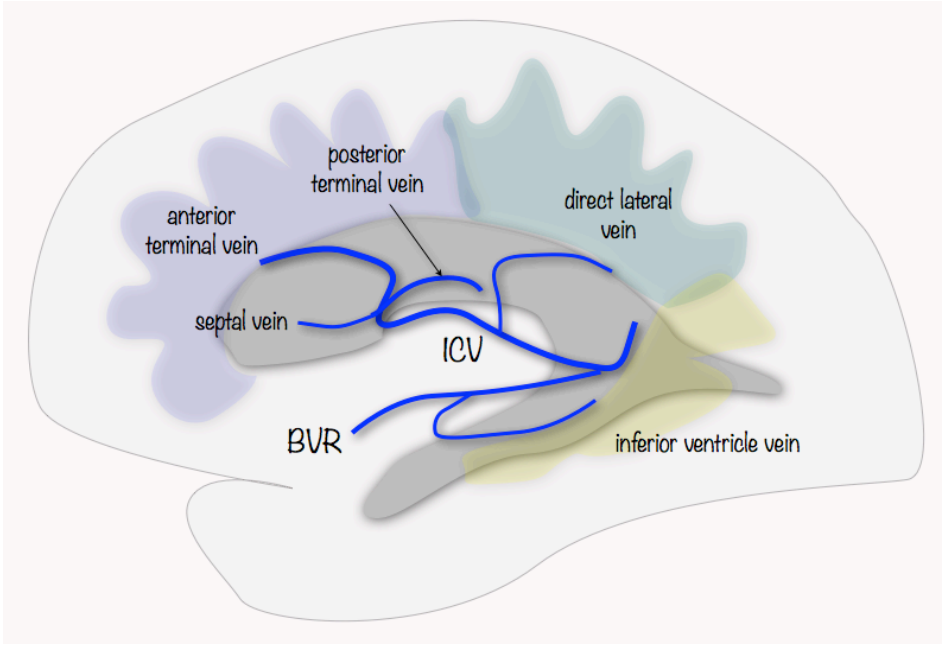

Figure 4 Medullary drainage according to lateral subependymal vein territories. In the majority, drainage of white matter towards the ventricle margins is divided into three areas: the thalamostriate vein (draining anterior and posterior terminal veins), the direct lateral vein and the inferior ventricle vein.

A component of linear venous ischaemia may also play a role in primary white matter injury of the preterm infant, suggesting a common pathway with medullary infarction following GMH [31, 32]. Conversely, venous obstruction probably leads to proximal arteriolar and capillary vasoconstriction. Other entities besides GMH, that affect veins around the ventricle margins, may lead to periventricular venous infarction: primary thrombosis, ventriculitis and tumor. The primary mechanism in which collagen A4 mutations lead to fetal IVH and parenchymal haemorrhage is not known, but a venous contribution is also possible [33, 34]. Tight junction molecule mutations have been recently added to the list of causes of neonatal brain haemorrhage [35].

Punctate lesions of the white matter

The punctate lesions of the white matter have been recognized only relatively recently as a specific manifestation in the premature infant. Their distribution matches the anatomy of the deep medullary veins, but a venous or perivenous origin, although suspected, is not proven. Their MR presentation is specific: restricted diffusion/low ADC; bright T1and low T2 (usually faint), not consistent with ischaemia; and no blooming artefact to suggest haemorrhage. They can be seen early after birth in infants of any gestational age [4], and may persist for weeks, up to term-equivalent age. As the restriction cannot be explained by an ischaemic cyto-toxic edema because of the T1/T2 signals, it has to reflect a focus of hypercellularity, and indeed, in one post-mortem study, a focus of activated microglia with vascular congestion was demonstrated [36]. Their occurrence in the premature brain can be correlated with the fact that the density of microglia is very high in fetal white matter from 19 to 30 weeks, and decreases abruptly afterward [37].

Punctate lesions may be isolated or multiple, forming alignments along the IZ-SP junction: this is where the density of microglia is highest [38]. Their distribution is usually symmetrical, even if individual dots are not [4]. They may be extensive, forming finger-like patches that extend medially across the IZ, sometimes confluent to the point of mimicking PVL on DWI/ADC: however the subventricular zone and ependyma are spared, and PVL characteristically presents, like ischemia, with low T1, high T2 signals [39]. In good agreement with the deep medullary venous anatomy, they are usually more prominent in the territory of the terminal (thalamocaudate) veins, and do not extend peripherally into the SP [4]. Depending on their size and extent, they may leave no apparent abnormality on late follow-up imaging (after 2 years), or leave patches of hypomyelination, or result if extensive, in a significant loss of white matter/corpus callosum somewhat similar to chronic PVL but again, without a destruction of the ventricular wall [4]. Their impact on neurodevelopmental outcome is still unclear [36, 40], probably related to both location and extent.

Cerebellar haematoma

Preterm primary cerebellar haemorrhage develops in germinative cortical areas under the same clinical circumstances as GMH [41-45]. Progressive apnoea is associated with a falling haematocrit, in some with motor hyperactivity (possibly due to cerebellar disinhibition) [46]. Few symptomatic cerebellar haematomas present with a tense fontanelle, because they are often

unilateral and not big enough. The extensive lobar nature of some haematomas argues against a primary pial arterial occlusion, although extensive subarachnoid haemorrhage might occlude adjacent pial arteries due to spasm and lead to secondary cerebellar infarction. A strong case was made for venous injury leading to cerebellar bleeding associated with face-mask ventilation of preterm infants [47], and a similar mechanism may well be operative in many preterms. Alternatively, secondary subarachnoid bleeding may be scattered across foliae in case of lateral ventricle IVH, following passage of clot fragments through the outlet foramina of the fourth ventricle: this mimicks cerebellar parenchymal haemorrhage. To think of preventive strategies, we need to study veins of the cerebellum in infants with neonatal cerebellar haematoma and consequences of such events, both before and after birth [48]. In adults, cerebellar haematoma due to transverse sinus thrombosis is rare [49], because it is considered that there is much more collateral circulation in the infratentorial than in the supratentorial region; this does not exclude a role for venous thrombosis in the perinatal variant of this disease entity. We are merely beginning to understand the pathogenesis of cerebellar bleeding in the preterm [50].

Term venous lesions; diverse mechanisms

Sinovenous thrombosis

Sinovenous thrombosis is less common than arterial ischaemic stroke, but likely underreported [51]. Seizures are the presenting sign in around two thirds. Other clinical signs may be jitteriness, lowered consciousness or low platelet count. TS thrombosis in small preterm infants may be entirely asymptomatic [52]. A list of risk factors and causes is gathered in Table 3. Embolism is not a cause of sinus thrombosis, but the reverse might exist: fragmentation of clot in a thrombosed sinus, next migration of a fragment along the jugular vein into the heart and finally, paradoxically into an (brain) artery. Hyperviscosity has been mentioned as a risk factor, e.g. in infants of a diabetic mother (see below). Dehydration as a cause was decades ago referred to as marantic thrombosis. Neonatal brain haemorrhage together with sinus thrombosis has been recently linked to von Willebrand type 3 disease.

Almost all infarctions due to venous thrombosis are haemorrhagic. Typical SSS thrombosis can lead to parasagittal infarction particularly in the arm area of the motor homunculus, explaining hemimotor sequelae in some children. Thrombosis within the SSS usually starts in the vicinity of the parietal lobe, probably due to the peculiar forward course - against sinus flow direction - course of the posterior frontal, parietal and occipital bridging veins as they drain the convexity. Underneath the anterior fontanelle and further distally under the tip of the occipital squame the sinus is exposed to mechanical forces during (difficult) delivery. It is long known that about half of SSS thromboses are associated with TS thrombosis and that about a third of sinus thromboses are associated with deep involvement [53-56] Sinus thrombosis can propagate into the deep venous system, and probably the reverse exists as well. There have

Table 3 Mechanisms of sinovenous thrombosis (references in Govaert et al. 2009)

Infection		- scalp infection, with phlebitis into intracranial sinus via emissary veins, e.g. with aplasia cutis - as a complication of meningitis/septicaemia - cavernous thrombosis from orbital cellulitis
Trauma		- infected cephalhaematoma, osteitis, transverse sinus thrombosis - superior sagittal sinus thrombosis, impressed occcipital squame - propagated thrombosis from superior sagittal sinus into deep veins - transverse sinus thrombosis - contusion with direct vein laceration - penetrating scalp electrode
Obstructed venous outflow		- misplaced, upstream central venous catheter - tight nuchal ventilator collar - triple nuchal cord coil - superior vena cava obstruction with anomalous pulmonary venous connection or jugular vein hypoplasia - ECMO
Prothrombotic condition	polycythemia	cyanotic congenital heart disease, in infants of a diabetic mother
	dehydration	marantic thrombosis, often insufficient breast feeding with hypernatraemia
	dysfunctional haemostasis	- antithrombin III - homozygous protein C (or S) - fV Leiden mutation - antiphospholipid antibodies - f II mutation - tPAI1 polymorphism - high lipoprotein A - factor VII replacement - congenital nephrotic syndrome - (post hepatitis B vaccination) antinuclear antibodies
	asphyxia	congestion, endothelial injury and intravascular coagulation
Other		endovascular treatment of vein of Galen malformation; other vascular anomalies
Unknown		multiple intermixed causes

been anecdotal reports of neonatal cavernous sinus thrombosis with eyelid chemosis, facial swelling and external ophtalmoplegia [50].

Exceptionally an infarct is purely ischaemic but clearly related to sinus thrombosis, which is possibly due to reactive arterial or arteriolar spasm. For unknown reasons haemorrhagic infarction associated with SSS thrombosis is within the parasagittal cerebral (sub)cortex and not within parenchyma bordering the interhemispheric fissure or deeper down along the convexity (Figure 5). The existence of transmedullary, transnuclear (through basal ganglia) and meningeal collaterals is of importance in avoiding infarction, depending on many factors such as the speed of vessel occlusion, the rheology of blood and the presence of prothrombotic risk factors. A typical red infarct leaves haemosiderin and gliosis in the residual scar, sometimes with figured calcification along the vein. Over a period of weeks to months a sinus usually gradually recanalizes [57, 58].

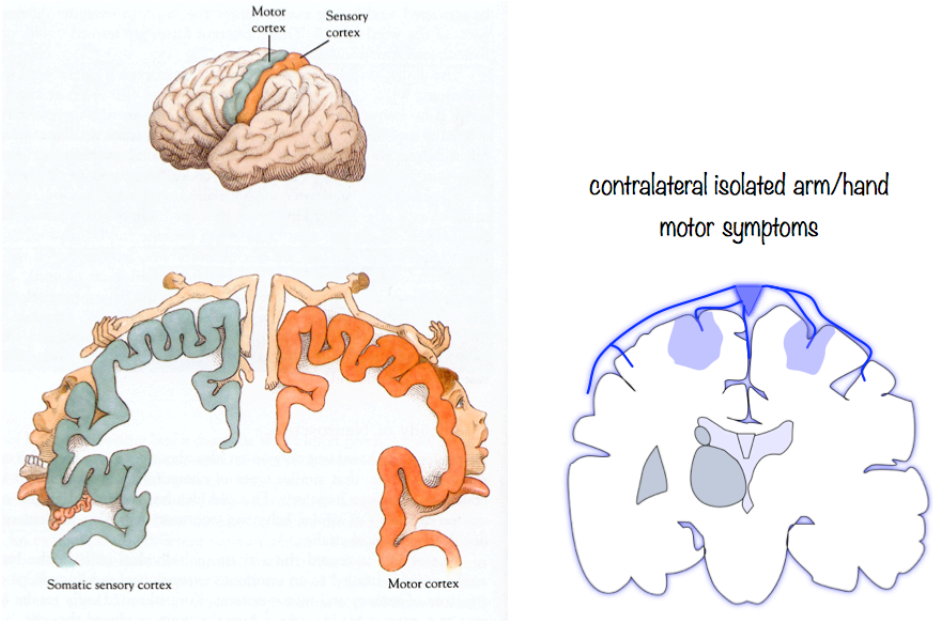

Figure 5 Parasagittal injury in the posterior frontal or parietal area due to superior sagittal sinus thrombosis may cause motor seizures and induce permanent motor deficit.

Internal cerebral vein or straight sinus thrombosis

Thrombosis of the GCV and/or the ICV puts fragile veins under pressure in the vicinity of germinal matrix or choroid plexus. This may lead to deep venous infarction [59]. The phenomenon is nearly always associated with IVH, mostly limited grade. An infarct related to ICV thrombosis may stretch as far as corpus callosum and periventricular white matter, sparing subcortical areas. When a single branch of the ICV is thrombosed, the most striking phenomenon may be unilateral haemorrhagic infarction in thalamus or caudate nucleus: thalamoventricular haemorrhage (Figure 6). Collaterals mitigate injury when occlusion of the deep venous system is not abrupt. At the moment of diagnosis the affected vein may not always be without flow. Besides propagation from thrombosis in the superior sagittal sinus along the straight sinus to the deep venous system, risk factors of primary deep venous thrombosis are congestion, meningitis and/or ventriculitis, hyperviscosity, asphyxia and genetic prothrombotic conditions.

Basal vein thrombosis

Basal vein thrombosis can induce haemorrhage with feathered margins in the centre of the temporal lobe and extending upward into infero-lateral hemi-striatum (Figure 6) [60]. The haematoma does not reach the temporal lobe convexity. The typical endstage BVR runs around the brainstem and drains posteriorly into the Galenic system, in three segments: striate, peduncular and mesencephalic.

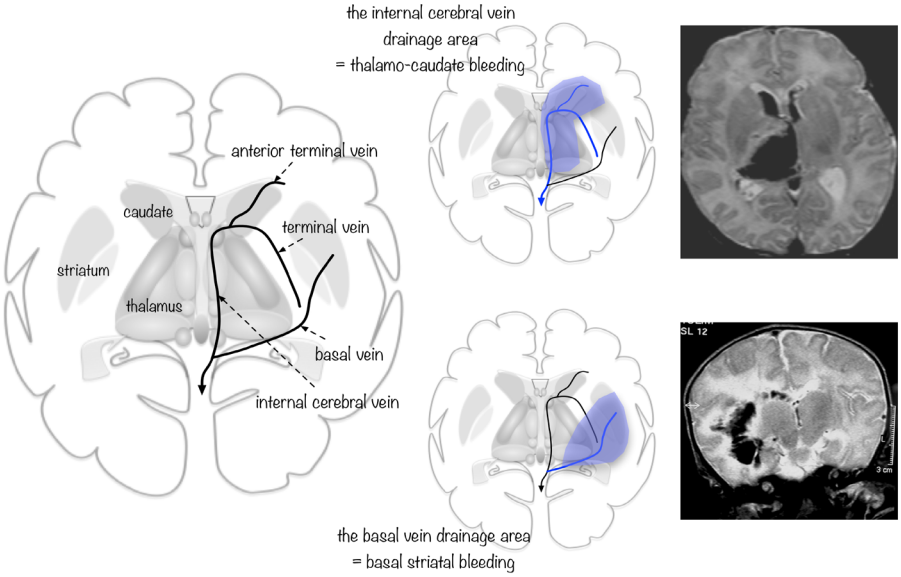

Figure 6 Templates of internal and basal cerebral vein thrombosis, with T2-weighted MRI examples.

The BVR is derived around the 11th fetal week from the formation of longitudinal anastomoses between embryonic precursors. Its formation can be complicated by anatomic variation [61]. Prospective tributaries may drain almost independently of each other into various sinuses. In about 10 % the BVR does not even connect to the GCV. The sonographic study of the BVR is possible with high-quality Doppler technique, but its horizontal course and variability present sources of difficulty.

Transverse sinus thrombosis

Haemorrhage into the temporal lobe (basal and temporal parts) or around the tentorium and in cerebellum may be associated with TS thrombosis [62, 63]. In adults several patterns of TS bridging veins have been described: between torcular and the curve to the SiS, bridging veins may form multiple entries, gather into a candelabra or into tentorial lakes. Tentorial lakes of type I mainly drain to straight sinus, torcular and mesial/middle TS, of type II to lateral TS and transverse-petrosal junction [64, 65]. A large draining vein of the cerebral convexity into the TS, the vein of Labbé, is connecting the SMCVs to the vein of Trolard and indirectly to the SSS, but this vein can also be absent. Young infants are more vulnerable to subdural haematoma because of relatively large venous lakes in the dura around the posterior fossa [66]. The orifices of bridging veins in the TS share some characteristics: they are oval with semicircular superior dural reinforcement and follow an orientation opposite to venous flow. Smooth muscle layers at the dural reinforcement suggest that these venous orifices are sphincters [67]. Development, variation in end stage anatomy and maturation of these sphincters will codetermine what type

of temporal lobe haematoma follows thrombosis of affected veins (Figure 7). A recent study reports a high incidence of TS thrombosis in VLBW infants below 29 weeks of gestation (4.4% of the cohort [52]). Ultrasound can confirm or refute flow gaps observed with MR venography [68]. That ultrasound, including color Doppler, can depict sinovenous thrombosis at an early stage, presents therapeutic options prior to parenchymal injury. The transverse to sigmoid transmission may be a developmental, neonatal venous achilles heel, for the following reasons.

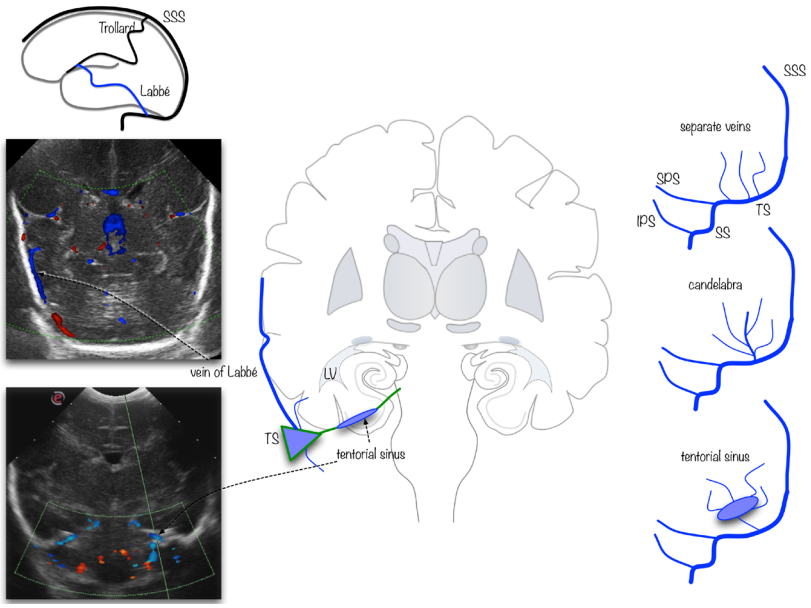

Figure 7 Bridging veins related to the transverse sinus may enter in separate trunks, gather in candelabra formation or drain with an intermediary tentorial lake; a large collector is the parieto-temporal vein of Labbé.

Relative jugular obstruction in the fetal period. From a relatively high and straight early fetal position, the StS is flattened and displaced downward by enlarging cerebral hemispheres. Several intrafalcine veins connect the primitive axis of ICV, GCV and StS below, with the SSS above. If such vein persists after birth it is called a persistent falcine sinus. Finally, in the 9th or 10th fetal month, the StS typically drains into the left limb of the SSS. The TS on each side is small and plexiform in its medial part at the fetal age of 3 months and begins to balloon from its lateral end later in the fourth fetal month, gradually extending medially to reach the confluence and becoming evenly enlarged by the 5th month [9]. This may be due to a narrow calibre of the sigmoid sinuses and jugular bulbs at the moment. Sigmoid sinuses are slender at the 80 mm stage; only after birth pressure waves entrain progressive dilatation of the superior jugular vein into a bulb, which then acts as a reservoir and suction pump, gently draining blood from the

brain into the internal jugular vein. During dilatation of the TS in fetal life, the occipital and marginal sinuses also dilate, emissary veins develop in condylar and mastoid areas, septae and fenestrae may be formed in unevenly dilated sinuses and lacunae (pouches) from near the TS (later forming tentorial lakes).

TS develops asymmetrically (Figure 8). Venous drainage dominance has been studied extensively in adults, for instance with bilateral carotid angiograms [69]. All studies confirmed drainage mainly to the right side in 41 %, equal drainage in 38 %, drainage mainly to the left in 19 %; 2 %

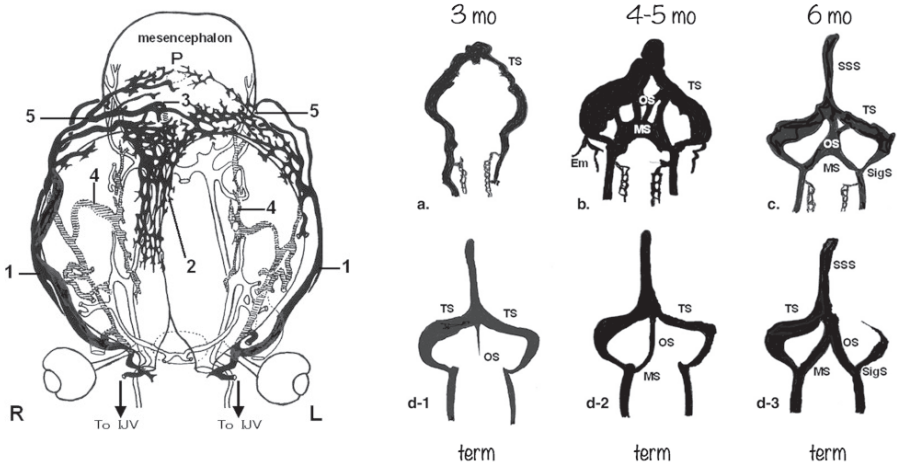

Figure 8 Developing cranial venous system in a fetus at 23-mm CR, stage 6 (40–44 days), viewed from above. The anterior dural plexus, from which the sagittal and straight sinus (RS) are derived, drains to the right side predominantly in all. 1 = primitive transverse sinus; 2 = sagittal plexus, which will join the anterior portion of the SSS in adults; 3 = primitive straight sinus; 4 = tentorial sinus; 5 = primitive marginal sinus, which will join the posterior portion of the SSS in adults. Medial situated plexus-formed venous channels will join the bifurcated limbs and then fuse into the posterior portion of the SSS. IJV, internal jugular vein; L, left; P, pineal body; R, right. Reproduced from Padget 1957.
Schematic drawing of the development of the transverse sinus (TS) and occipital sinus (OS). (a) Three-month-old fetus: the TS is small in caliber. The OS has not developed. (b) Four-month-old to 5-month-old fetus: the TS balloons from its lateral end in the 4th month and gradually extends medially to reach the confluence, becoming relatively even in caliber in the 5th month. Underdeveloped sigmoid sinus (SigS) and superior jugular bulb, whereas OS channels appear well developed and connect to the medial part of the TS with either the marginal sinus (MS) or the distal end of the SigS (ie, the superior jugular bulb). (c) Six-month-old to 7- month-old fetus: despite attenuation of the ballooning, the enlarged configuration of the OS will be sustained until birth. The OS have regressed into a single venous channel along the cerebellar falx. (d) After birth. (d-1) to (d-3) represent various development of the OS: short and rudimentary (d-1), medium sized (d-2), and large sized (d-3). The large-sized TS may be associated with contralateral aplastic or hypoplastic TS and/or SigS. Em, emissary veins. Reproduced from Okudera et al. 1994.

showed drainage only to the right and 0.53% only to the left. On CT venograms of adults the SSS drains into the TS in patterns similar to those observed post mortem or with angiography [70, 71]. Persistent occipital sinuses are recognized in about 60 %, persistent falcial sinuses in 2.5%. A rare normal type is the common pool (9%), a coalescence of channels, which usually implies equality. In the abnormal strict unilateral type one TS, typically the right, is minute; in such instances the possibility of an anomalous configuration of the great veins above the heart should be considered. The relative straight course of the venous system down to the superior caval vein on the right, is probably the reason why the growing hemisphere preferentially drains via the SSS to the right TS: venous drainage on the left is more circuitous via the innominate vein. There is no doubt about the significance of the relation between heart or respiratory function and pressure waves in the intracranial veins [72]. This relationship accounts for the postnatal development of the jugular bulbs as well. Accordingly an asymmetry of the internal jugular veins was noted with ultrasound in 62.5% of adult patients: the dominant vein was the right in 68% [73]. In a study of intracranial sinuses with two-dimensional time-of-flight magnetic resonance venography, the mean calibre of the right TS was greater than the contralateral sinus (6.5 mm±1.84 vs 5.1 mm±1.72)[74]. Partial linear flow gaps in this study never involved the distal TS (oval ones did) and linear flow gaps were not observed in the dominant TS. Variation of venous anatomy may not only be relevant for sinovenous thrombosis: only adult patients with hypoplasia or occlusion of the ipsilateral cranial venous drainage seem to develop early fatal edema after large middle cerebral artery infarction [75]. This hints to a role for cranial venous outflow abnormalities in the development of brain edema following adult arterial ischaemic stroke.

By compression of the jugular veins in the lower neck, Cowan and Thoresen, attempting to measure cerebral blood flow, registered a drop in flow velocities in the superior sagittal sinus in many neonates; asymmetrical findings were compatible with the above reported asymmetrical adult TS anatomy [76]. Escape along non-jugular veins seemed common and variable. This functional venous asymmetry has been confirmed in term neonates using MR venography [77]. In a recent neonatal cadaver study [78] termination patterns were reclassified into six types, taking into account the presence of occipital sinuses (OS): the SSS showed continuity with right TS (TS) (with OS) (30.3%) (Type I); or multiple OSs (21.2%) (Type II). The SSS continued with left TS (with OS) (12.1% (Type III); or with multiple OSs (6.1%) (Type IV); the SSS showed continuity with both TS (9.1%) (Type V); SSS symmetrically bifurcated, the confluens sinuum had a large OS (21.2%) (Type VI). Prior knowledge of venous asymmetry might have an influence on the decision to use deep jugular venous lines for neonatal venous access.

The tentorial sinus dwindles. Newborn infants still have a tentorial sinus draining into the TS. In adults the SMCV has usually connected to the cavernous sinus by the intermediary sphenoparietal sinus (SPS) and there is no tentorial sinus. However, variations of para-cavernous sinus veins are common [79]. The tentorial sinus is a collector formed by disappearance of the anterior dural plexus around vascular stage 6 (24 mm CRL). Subsequent growth of the hemisphere

causes the tentorial sinus to elongate posteriorly, and the anterior portion is shifted medially, merging into the cavernous sinus. The fetal SMCV drains through the tentorial sinus into the transverse rather than into the cavernous sinus. The pro-otic sinus develops from the stem of the middle dural plexus by the 17- to 20 mm stage; it contributes to the cavernous sinus, the SPS, the meningeal sinus, the anterior parietal temporal diploic veins in the 3 month-old embryo and part of the transverse sinus. Contrary to many reports, San Millan Ruiz [80], in a human postmortem study, contradicted the existence of a SMCV draining into the SPS. Suzuki and Matsumoto in 2000 [81] investigated variations of the SMCV by using 3D CT angiography and classified into 7 types, including the sphenoparietal, cavernous, emissary, superior petrosal, basal, squamosal and undeveloped types (Figure 9). Tanoue et al. [79] simplified the variations

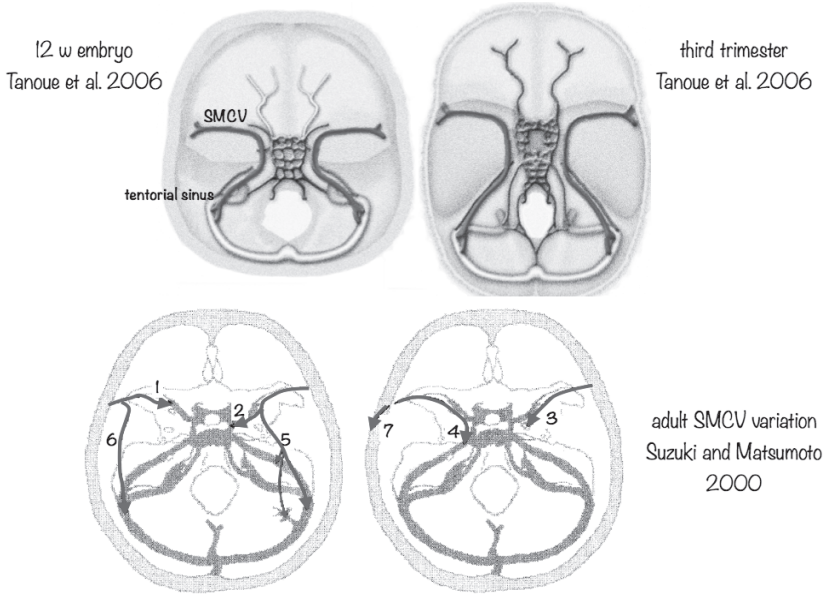

Figure 9 after Suzuki and Matsumoto 2000, Chung and Weon 2005 and Tanoue et al. 2006): (1) Sphenoparietal type (54 %): the SMCV enters the sphenoparietal sinus and runs along the lesser wing of the sphenoid bone into the cavernous sinus. (2) Cavernous type (7 %): the SMCV directly enters the anterior end of the cavernous sinus. (3) Emissary type (12 %): the SMCV turns posteriorly to join the sphenoidal emissary veins, and passes to the pterygoid plexus. (4) Superior petrosal type (2 %): the SMCV runs along the lesser wing, turns downward along the anterior inner wall of the middle cranial fossa, then runs along its floor medially to the foramen ovale to join the superior petrosal sinus. (5) Basal type (2 %): the SMCV turns downward along the anterior wall of the middle cranial fossa, then runs lateral to the foramen ovale, to join the transverse sinus through the lateral tentorial or superior petrosal sinus. (6) Squamosal type (2 %): the SMCV fails to turn medially to join the sinus along the lesser wing, and instead turns posteriorly backward along the inner aspect of the temporal squama to join the transverse or lateral tentorial sinus. (7) Undeveloped type (9 %): the SMCV is absent, and superficial sylvian drainage is through a large channel into the superior sagittal or transverse sinus. (8) Undetermined (8 %).

into 4 subtypes. Secondary intradural cavernous sinus anastomosis of the SMCV is seen on CT angiography in 44%, but the most prevalent pattern is without anastomosis with the cavernous sinus [61]. Tributaries of the BVR may connect with the cavernous sinus via the SMCV or superior petrosal sinus. In term infants it is possible to visualize a large tentorial venous vessel that enters the transverse sinus through a keyhole with high and turbulent velocities (Figure 10). The natural involution of this vessel still has to be studied in foetuses and preterm infants.

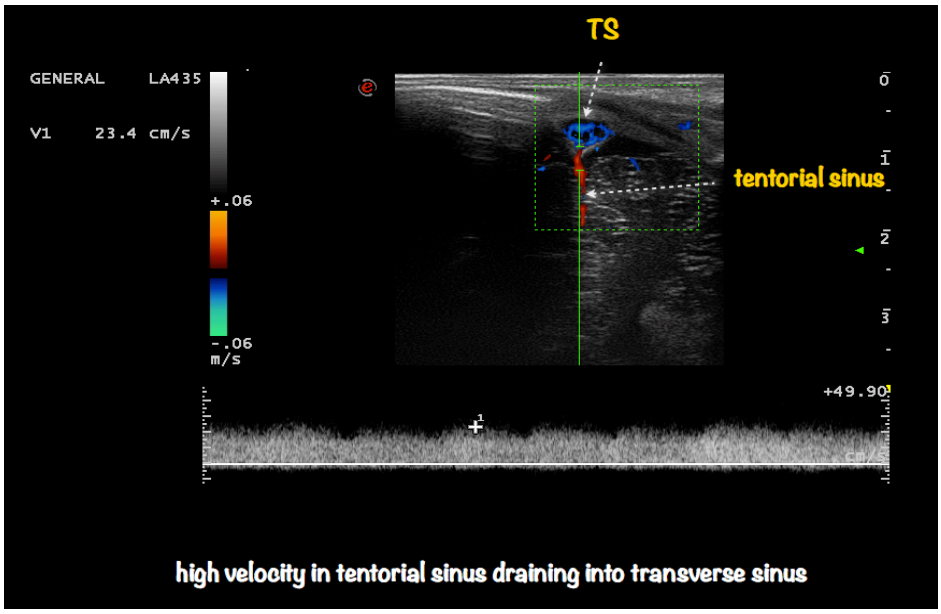

Figure 10 Tentorial vein entering a transverse sinus visualized at 18 MHz through the left asterion of a term infant.

Lobar haematoma and contusion

Lobar haematoma outside deep grey matter is observed in each region of the neonatal cerebrum, often associated with a subdural or subarachnoid extra-axial component [63, 82-88] (Figure 11). The presenting sign is apnoea or (multi)focal convulsive activity but some lobar haematomas are a chance finding [89]. On occasion they are of prenatal origin. Some are a haemorrhagic conversion of total or partial pial arterial infarction. Haemostatic failure, especially thrombocytopenia, is in itself a sufficient cause of haemorrhage within the temporal lobe (arising in the molecular layer, just under the subarachnoid membrane). Some reports suggest that TS thrombosis may cause temporal lobar haemorrhage. Lobar lesions warrant a diligent search for evidence of trauma, haemostatic failure, prothrombotic tendency and also vascular malformation (saccular arterial aneurysm, arterio-venous malformation, cavernous angioma). Astrocytoma is a rare cause of neonatal lobar haematoma.

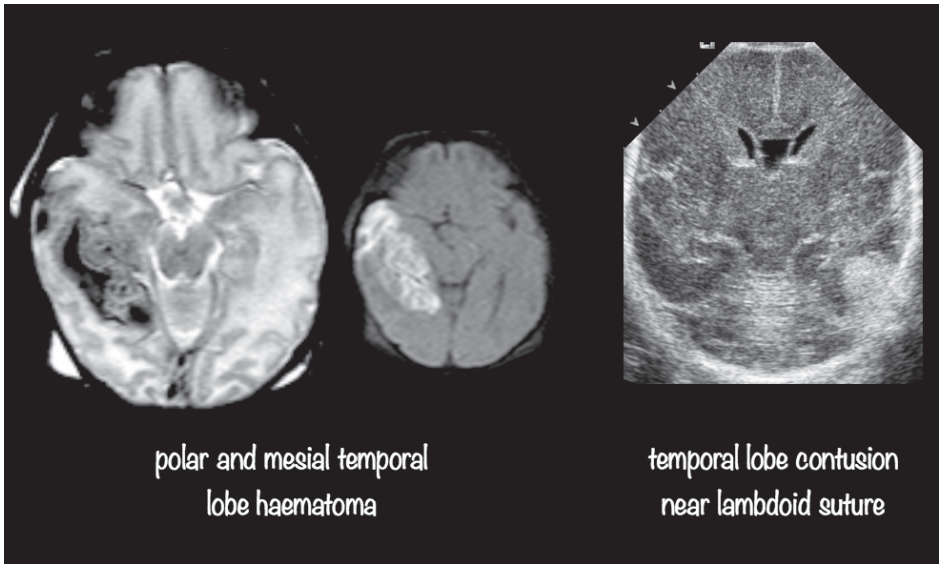

Figure 11 *Left image:* Term infant with unexplained polar and mesial temporal lobe haematoma with infarction, presenting with apnoea; arterial templates do not fit this lesion; vasculary anomaly was excluded by clinical and imaging follow-up. *Right image:* Preterm vaginal breech delivery: subcortical haematoma near a suture is compatible with contusion.

Primary haemorrhage was the most common lesion found in an *ECMO* cohort with an incidence of 8.8% and an unsuspected predilection of lobar bleeding for the left hemisphere [90]. Both asymmetrical brain venous drainage and a shift of blood volume to the left hemisphere upon right jugular vein cannulation, play a role in site predominance of sinovenous thrombosis and lobar haematoma associated with ECMO. In term neonates, not treated with ECMO, there is no side difference in the prevalence of lobar haemorrhage. Neonates treated with ECMO have a logical higher risk of ipsilateral arterial infarction and venous occlusion due to the catheters inserted; ligation of the right jugular vein increases the risk of thrombosis in the proximal right TS, due to sluggish blood flow or stasis at some stage.

Contusion refers to unexpected limited surface haematomas near a bony edge or fracture following delivery with excessive moulding, and it may reflect vascular (probably venous) injury (Figure 11). Other examples are haematoma into the medulla following excessive force on the neck during delivery, and contusional injury of the inferior cerebellar surfaces during difficult breech or instrumental delivery (occipital osteodiastasis). A peculiar neonatal variant of contusion by vigorous chest therapy has been reported: subarachnoid haemorrhage resulted in a fatal pattern of cavitating necrosis in both parietal lobes of extremely preterm infants [91]. This entity is thereafter discussed as shaken newborn syndrome [92, 93].

Open vessel venous ischaemia: polycythaemia and dehydration

Several types of brain damage have been reported in association with neonatal polycythaemia. Linguistic, aritmetic and fine motor problems have been observed following neonatal polycythaemia. Imaging correlates are rare however. Unilateral lobar haemorrhage was reported in term infants by Slovis et al. 1984[94] (temporal) and by Bergman et al. 1985[83] (parietal). Sinovenous thrombosis was associated with a high haematocrit in a few older studies [95, 96]. More reports cover the association between dehydration and venous thrombosis [97-104]. Rheological properties of blood dramatically worsen under dehydration by an increase of plasma and blood viscosity, an enhancement of erythrocyte aggregation and a reduction of oxygen transport into tissues. That venous flow requires consideration of the additional factor viscosity supports a venous mechanism of brain injury, whereas arterial blood flow is mainly determined by pressure gradient and arterial diameter. Red blood cell aggregation in veins might be a key factor in "blood flow structure" [105, 106]. Given the small number of reports that link arterial ischaemic brain stroke to neonatal polycythaemia [107-109] one can infer that this association is questionable. For reasons described above, haemorrhagic lesions near the temporal pole might be

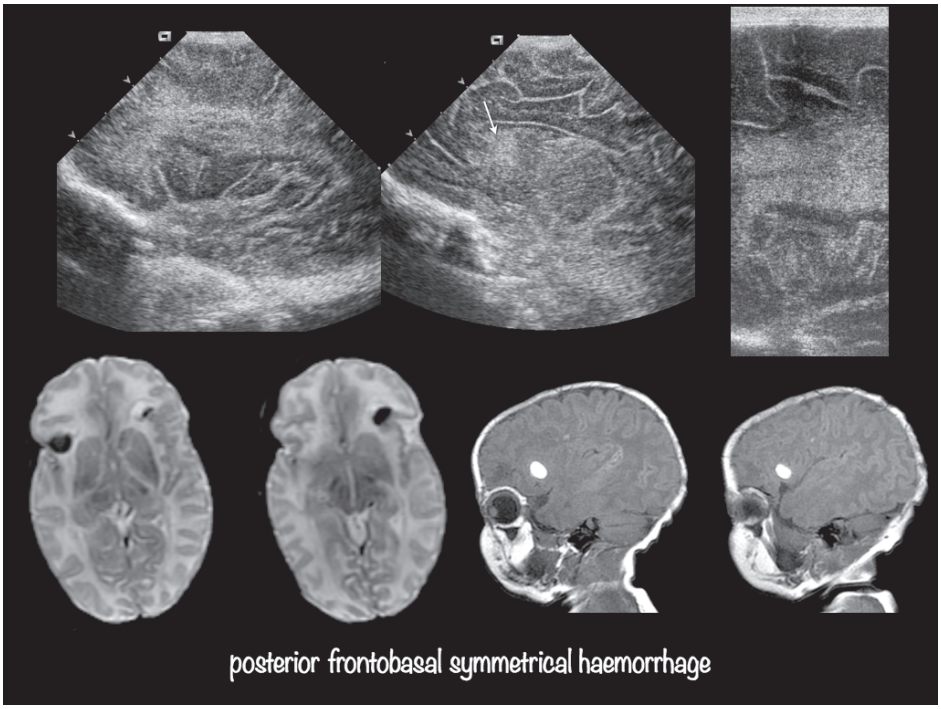

Figure 12 Near term infant following partial exchange transfusion for polycythaemia: symmetrical posterior basofrontal haemorrhage is surrounded by extensive hyperechoic areas with high white matter signal on T2 MRI; arrow points to hyperechoic caudate area. On US the lesions appeared less circumscript, suggesting a role for perilesional congestion in adjacent white matter. The absence of cavitation in the third week after birth suggested the tissue was not entirely infarcted.

linked to developmental changes involving the tentorial sinus and SMCV. Bilateral and almost symmetrical lesions in one personal observation of polycythaemia (Figure 12) were haemorrhagic given the high signal on T1 and low signal on T2 MRI. Location in the orbitofrontal area just anterior to the insula were unlike any other brain lesion observed in the newborn. Normal diffusion-weighted images in the face of low ADC values have been explained by hyperviscosity, interpreted as a T2-wash out phenomenon [110]. Conversely, others have suggested that congestion without necrosis causes increased ADC values [63]. Using CT with contrast, congestion presents as an area of low perfusion hyperaemia [111], but the need for irradiation excludes CT in the neonatal period. We need reports of brain lesions associated with neonatal hyperviscosity, and have to focus on veins around them.

Reversible dilatation of the vein of Galen and sinuses following difficult delivery may be one way of documenting the link between trauma and IVH [112, 113]. Dilatation may mimick vein of Galen malformation on superficial inspection.

Other venous lesions

Vascular anomalies involving veins

(Vein of Galen and arteriovenous malformation excluded)

Developmental venous anomaly

A cerebral developmental venous anomaly (DVA) is considered a "variant" of venous drainage, with an incidence in adult autopsies of 2.6% [80, 114]. Characteristic is an umbrella-like convergence of multiple venules that merge into a dilated collector vein, which drains either superficially into a cortical vein or sinus or into the subependymal deep venous system, or in a minority of cases into both. Until recent little was known about neonatal DVA appearances on MRI and even less about the findings on cUS/Doppler ultrasound [115](Figure 13). While the ultrasound appearance - dilated slow flow collector vein surrounded by increased echogenicity - is striking in some cases, it is subtle in others and only detected retrospectively, once the diagnosis is made with MRI. DVA can be mistaken for (haemorrhagic) parenchymal infarction when positioned adjacent to the lateral ventricle. The absence of breakdown into a porencephalic cyst excludes infarction. Doppler ultrasound can help to recognize a DVA by depicting blood flow in the collector vein, typically localized in the centre of the hyperechogenicity [116]. "Arterialized" DVAs have somewhat larger than normal arteries within them [80, 117] and flow in them may be pulsatile. It is uncertain how increased arterial flow into some DVAs relates to possible haemorrhagic transformation and how DVA relates to cavernous haemangioma [118]. An association with disorders of neuroblast migration has been observed [119]. Serial imaging during early infancy has learnt that imaging findings of DVA vary over time. This challenges the idea that DVAs are a stable variation of venous angioarchitecture.

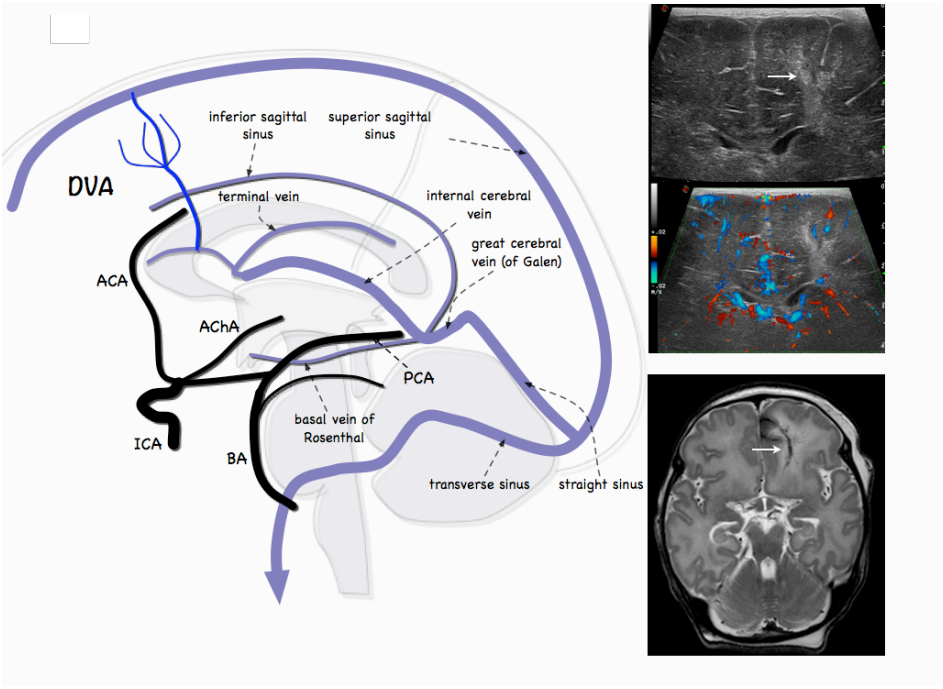

Figure 13 Typical DVA in two different neonates: top: Doppler negative but grey scale positive flow in a linear anomaly spanning the left frontal lobe at 35 weeks; bottom: term infant with left frontal DVA on T2 weighted MRI (courtesy Linda de Vries).

Sinus pericranii

This is a soft-tissue mass in the frontal region along or close to the midline (Figure 14); eccentric locations are rare. By definition it is a network of thin-walled veins that form a varix on the external table of the skull and connect through multiple diploic holes with the underlying dilated sinus; this varix is continuous with the pericranial veins of the scalp and is not directly fed by a large artery. Three different types of SP have been recognized [120]: (1) closed system (with accessory drainage); (2) transcranial collateral which involves a communication between the intra- and extracranial venous systems (dominant brain drainage); (3) an epicranial vascular anomaly draining entirely intracranially. Reported associations suggest a role for vascular wall anomalies as a mechanism [121]: meningocele, cerebrofacial arteriovenous metameric syndrome (CAMS-III), facial haemangioma, intracranial venous anomaly [solitary DVA, vein of Galen hypoplasia, vein of Galen aneurysmal malformation (VGAM), dural sinus malformation (DSM) and intraosseous AVM], craniosynostosis, von Hippel-Lindau disease, blue rubber naevus syndrome. Some sinus pericranii have followed previous sinus thrombosis or trauma.

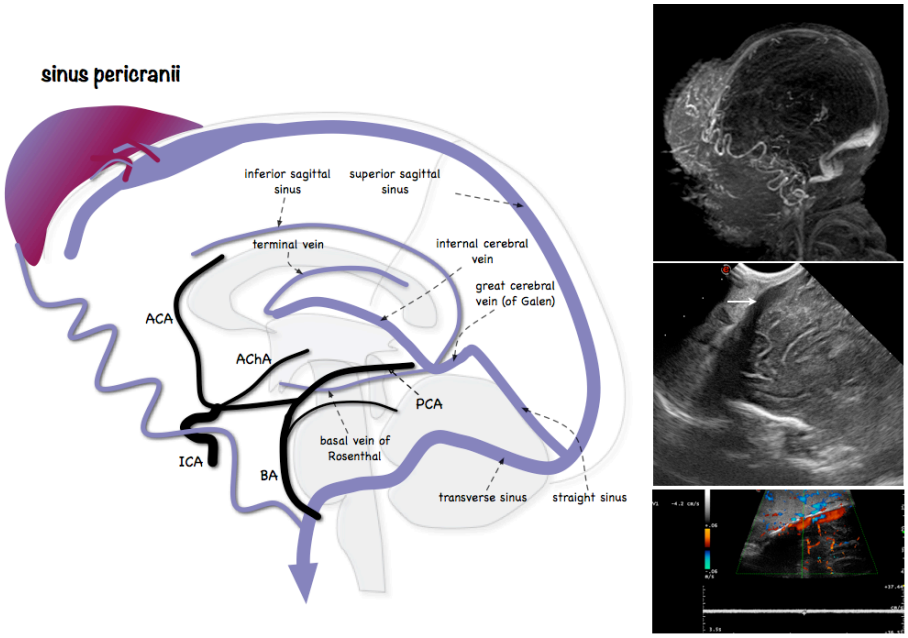

Figure 14 Typical sinus pericranii draining a frontal angioma. The arrow points to the dilated SSS. Venous flow in larger vessels in the angioma.

Cerebral angiodysplasia

Brain vascular abnormalities associated with renal agenesis have been named cerebral angiodysplasia. At postmortem Valdivieso and Scholtz [122] described a large number of anomalous small vessels in the pia and underlying cortex with infarction and gliosis of the cortex and subjacent white matter; dilatation and thrombosis was seen within vessels of capillary or venous nature, associated with calcification and infarction. Ultrasound and MR data of a similar entity were presented by Mul et al.[123]. Similar angiodysplasia has been reported in association with vein of Galen aneurysm.

Cerebellar vascular dysplasia

Focal isolated hyperechoic cerebellar lesions, without mass effect, are rare in the fetus. A cavernous angioma of the cerebellum complicated by haemorrhage has been reported in a fetus of 23 weeks, revealed by such focal lesion[124]. The diagnosis of "capillary telangiectasia" can be confirmed by a typical post-gadolinium MR pattern, even before birth. Only a few cases of cerebellar haemorrhage due to capillary telangiectasia were published: an autopsy case involving a fetus of five months [125], a four-month-old infant where surgical evacuation of the haematoma was deemed necessary [126] and three third trimester foetuses with a focal hyperechoic lesion [127].

The cerebellar haemangioblastoma typical of Von Hippel-Lindau disease, has been reported in the newborn [128]. An alarm sign may be multiple cutaneous angiomata. It is a solid, macrocystic or mixed solid and cystic benign tumor of polygonal stromal cells with lipid droplets, embedded in a reticulin network with mastocytes and a rich microvascular maze containing large vessels as well (simulating an AVM). The mass is round or polycyclic, displaces normal cerebellar tissue and keeps contact with pia mater. It presents with posterior fossa hypertension (tonic seizures, lowered consciousness), rarely with subarachnoid haemorrhage. Other preferential locations are in retina and spinal cord (mimicking syringomyelia), or in the medulla near the area postrema. Cerebral haemangioblastoma is exceptional.

Sturge-Weber syndrome

Is a neurocutaneous entity presenting with a facial port-wine nevus, glaucoma, seizures and hemiparesis. Characteristic is absence of cortical veins compensated for by centripetal venous drainage via enlarged medullary collaterals or anomalous deep veins (a.o. choroidal) into the GCV. Nonthrombotic veno-occlusive processes commence in utero and progress postnatally. The underlying parenchyma may undergo necrosis, with calcification. Lobar haemorrhage is one of the complications observed [129]. (progressive) Deep venous outflow occlusion with frontal venous collaterals can complicate imaging findings [130-132] and it is suggested to be a factor in accelerated myelination [133]. Hydrocephalus and megalencephaly may be related to venous changes [134]. MRI features include leptomeningeal angiomatosis, cortical and pial calcification, and vascular changes in choroid plexus. SWI is superior to T1-Gd in identifying enlarged veins, cortical gyriform abnormalities and grey matter/white matter junction abnormalities [135]. High-resolution BOLD MR venography also allows early diagnosis of venous anomalies in SWS [136].

Hereditary haemorrhagic telangiectasia (Weber-Rendu-Osler disease)

Typical presentation of this autosomal dominant small venule disease is with recurrent epistaxis in the second or third decade of life. Punctate well-marginated flat red telangiectatic lesions or raised pinhead angiomata are covering lips, palms, tongue, nasal mucosa and palate; such features are almost by definition absent in the newborn. The disease has been reported to involve almost any body organ. Cerebrovascular malformations, affecting at least 10 per cent of adults with this disorder, include arteriovenous malformation, arterial aneurysm, capillary telangiectasia, venous angioma and carotido-cavernous fistula. Presentation with lobar or subarachnoid haematoma in the neonatal period has been reported on few occasions [137]. An affected newborn with ruptured berry aneurysm has been described [138].

Infantile subdural haematoma

Intrinsic brain and dural veins separate early in development. Most primary venous anastomoses between pia and dura resorb. Remaining anastomoses develop into bridging veins, between 10 and 18 large veins that eventually penetrate the dura–arachnoid interface and

travel for a variable distance within the dura before entering the superior sagittal sinus. These veins are not fragile and only rupture under considerable force, making them improbable sources of subdural haematoma in the absence of major trauma. Key and Retzius in 1875 noted the presence of a fine capillary network located along the inner portion of the dura, with particularly high vascularity in infancy [139]. Penetrating branches of the meningeal arteries leave the superficial dural surface and extend to within 5 to 15 µm of the dural border cell layer, to end in a rich capillary network. The dural venules of this network are permeable and innervated by branches of the trigeminal nerve. These "leaky" vessels near the dura–arachnoid interface are candidates for the source of subdural bleeding [140, 141].

Le Gros Clark in 1920 emphasized that lateral lacunae are part of a dense parasagittal "meshwork of veins "[142]. While they may play a dominant role in the adult, arachnoid granulations are not fully formed in the infant; at the age of six months they are still invisible, but by 18 months they are obvious on close inspection; they appear first in areas where the parieto-occipital and central veins open into the sagittal sinus, from where they spread forwards and backwards.

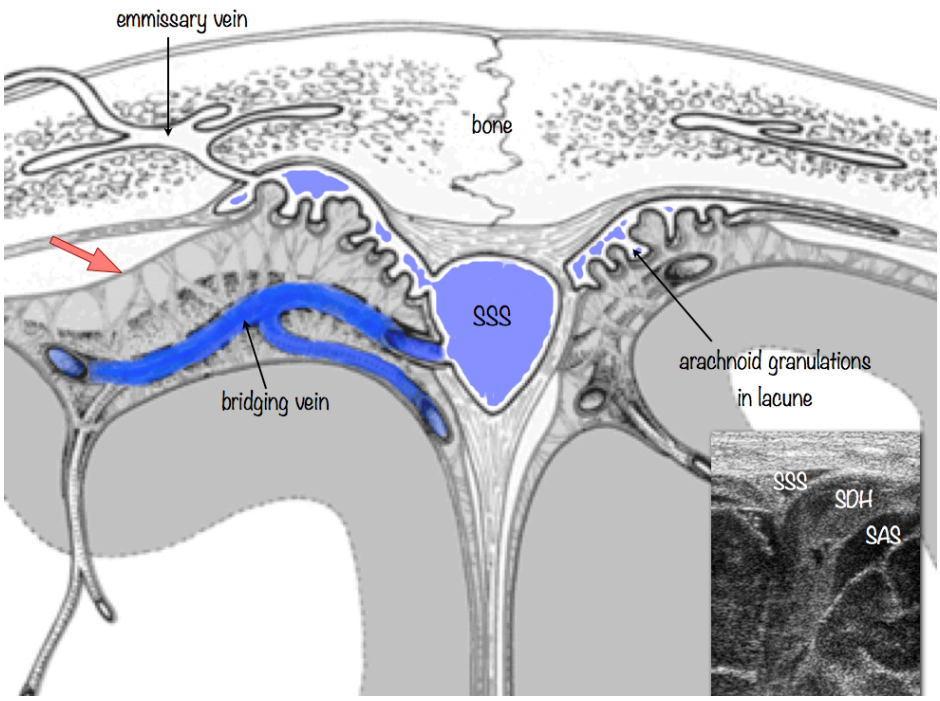

Figure 15 The adult subdural and subarachnoid spaces around the superior sagittal sinus (SSS). Emissary veins and arachnoid granulations are related to lacunae, cerebral bridging veins have separate entries into the sinus. The origin (arrow) of infantile subdural haematoma is in the vascular inner dural layer. Inset: vitamin K deficiency with late neonatal subdural haematoma (SDH)(SAS=subarachnoid space)(coronal 10 MHz US scan).

Arachnoid granulations occur abundantly in the parasagittal venous plexus [143], where they are interdigitated between the trabeculae of the dura. The bridging veins independently usually enter the sinus beneath the parasagittal venous plexus. The intimate relationship between the parasagittal venous plexus and arachnoid villi might bear relevance to the known association of SDH to states of both increased (benign extracerebral collections of infancy) and decreased CSF volume (spontaneous intracranial hypotension)(Figure 15) [140].

References

1. Padget DH. The cranial venous system in man in reference to development, adult configuration, and relation to the arteries. Am J Anat. 1956; **98**(3): 307-55.
2. Laurichesse-Delmas H, Grimaud O, Moscoso G, Ville Y. Color Doppler study of the venous circulation in the fetal brain and hemodynamic study of the cerebral transverse sinus. Ultrasound Obstet Gynecol. 1999; **13**(1): 34-42.
3. Kostovic I, Judas M, Rados M, Hrabac P. Laminar organization of the human fetal cerebrum revealed by histochemical markers and magnetic resonance imaging. Cereb Cortex. 2002; **12**(5): 536-44.
4. Raybaud C, Ahmad T, Rastegar N, Shroff M, Al Nassar M. The premature brain: developmental and lesional anatomy. Neuroradiology. 2013.
5. Raets MM, Dudink J, Govaert P. Neonatal disorders of germinal matrix. J Matern Fetal Neonatal Med. 2013.
6. Padget D. The development of the cranial venous system in man from the view point of comparative anatomy; 1957.
7. Raybaud C. Normal and abnormal embryology and development of the intracranial vascular system. Neurosurg Clin N Am. 2010; **21**(3): 399-426.
8. Nakamura Y, Okudera T, Hashimoto T. Vascular architecture in white matter of neonates: its relationship to periventricular leukomalacia. J Neuropathol Exp Neurol. 1994; **53**(6): 582-9.
9. Okudera T, Huang YP, Ohta T, Yokota A, Nakamura Y, Maehara F, et al. Development of posterior fossa dural sinuses, emissary veins, and jugular bulb: morphological and radiologic study. AJNR Am J Neuroradiol. 1994; **15**(10): 1871-83.
10. Okudera T, Huang YP, Fukusumi A, Nakamura Y, Hatazawa J, Uemura K. Micro-angiographical studies of the medullary venous system of the cerebral hemisphere. Neuropathology. 1999; **19**(1): 93-111.
11. Kuban KC, Gilles FH. Human telencephalic angiogenesis. Ann Neurol. 1985; **17**(6): 539-48.
12. Kehrer M, Blumenstock G, Ehehalt S, Goelz R, Poets C, Schoning M. Development of cerebral blood flow volume in preterm neonates during the first two weeks of life. Pediatr Res. 2005; **58**(5): 927-30.
13. Meek JH, Tyszczuk L, Elwell CE, Wyatt JS. Cerebral blood flow increases over the first three days of life in extremely preterm neonates. Arch Dis Child Fetal Neonatal Ed. 1998; **78**(1): F33-7.
14. Rademaker KJ, Groenendaal F, Jansen GH, Eken P, de Vries LS. Unilateral haemorrhagic parenchymal lesions in the preterm infant: shape, site and prognosis. Acta Paediatr. 1994; **83**(6): 602-8.
15. Bassan H, Benson CB, Limperopoulos C, Feldman HA, Ringer SA, Veracruz E, et al. Ultrasonographic features and severity scoring of periventricular hemorrhagic infarction in relation to risk factors and outcome. Pediatrics. 2006; **117**(6): 2111-8.
16. Dudink J, Lequin M, Weisglas-Kuperus N, Conneman N, van Goudoever JB, Govaert P. Venous subtypes of preterm periventricular haemorrhagic infarction. Arch Dis Child Fetal Neonatal Ed. 2008; **93**(3): F201-6.
17. Perlman JM, Volpe JJ. Are venous circulatory abnormalities important in the pathogenesis of hemorrhagic and/or ischemic cerebral injury? Pediatrics. 1987; **80**(5): 705-11.
18. Gould SJ, Howard S, Hope PL, Reynolds EO. Periventricular intraparenchymal cerebral haemorrhage in preterm infants: the role of venous infarction. J Pathol. 1987; **151**(3): 197-202.
19. Takashima S, Mito T, Ando Y. Pathogenesis of periventricular white matter hemorrhages in preterm infants. Brain Dev. 1986; **8**(1): 25-30.
20. Nakamura Y, Okudera T, Fukuda S, Hashimoto T. Germinal matrix hemorrhage of venous origin in preterm neonates. Hum Pathol. 1990; **21**(10): 1059-62.
21. Nakamura Y, Okudera T, Hashimoto T. Microvasculature in germinal matrix layer: its relationship to germinal matrix hemorrhage. Mod Pathol. 1991; **4**(4): 475-80.
22. Ghazi-Birry HS, Brown WR, Moody DM, Challa VR, Block SM, Reboussin DM. Human germinal matrix: venous origin of hemorrhage and vascular characteristics. AJNR Am J Neuroradiol. 1997; **18**(2): 219-29.

23. Govaert P, Smets K, Matthys E, Oostra A. Neonatal focal temporal lobe or atrial wall haemorrhagic infarction. Arch Dis Child Fetal Neonatal Ed. 1999; **81**(3): F211-6.
24. Taylor GA. Effect of germinal matrix hemorrhage on terminal vein position and patency. Pediatr Radiol. 1995; **25 Suppl 1**: S37-40.
25. Deeg KH, Lode HM. [Trans-fontanellar Doppler sonography of the intracranial veins in infants. Part II—pathology]. Ultraschall Med. 2006; **27**(2): 164-75.
26. Ramenghi LA, Fumagalli M, Groppo M, Consonni D, Gatti L, Bertazzi PA, et al. Germinal matrix hemorrhage: intraventricular hemorrhage in very-low-birth-weight infants: the independent role of inherited thrombophilia. Stroke. 2011; **42**(7): 1889-93.
27. Harteman JC, Groenendaal F, van Haastert IC, Liem KD, Stroink H, Bierings MB, et al. Atypical timing and presentation of periventricular haemorrhagic infarction in preterm infants: the role of thrombophilia. Dev Med Child Neurol. 2012; **54**(2): 140-7.
28. Staudt M. Reorganization after pre- and perinatal brain lesions. J Anat. 2010; **217**(4): 469-74.
29. Marin-Padilla M. Developmental neuropathology and impact of perinatal brain damage. I: Hemorrhagic lesions of neocortex. J Neuropathol Exp Neurol. 1996; **55**(7): 758-73.
30. Govaert P, Lequin M, Korsten A, Swarte R, Kroon A, Barkovich AJ. Postnatal onset cortical dysplasia associated with infarction of white matter. Brain Res. 2006; **1121**(1): 250-5.
31. Ramenghi LA, Gill BJ, Tanner SF, Martinez D, Arthur R, Levene MI. Cerebral venous thrombosis, intraventricular haemorrhage and white matter lesions in a preterm newborn with factor V (Leiden) mutation. Neuropediatrics. 2002; **33**(2): 97-9.
32. Arrigoni F, Parazzini C, Righini A, Doneda C, Ramenghi LA, Lista G, et al. Deep medullary vein involvement in neonates with brain damage: an MR imaging study. AJNR Am J Neuroradiol. 2011; **32**(11): 2030-6.
33. Breedveld G, de Coo IF, Lequin MH, Arts WF, Heutink P, Gould DB, et al. Novel mutations in three families confirm a major role of COL4A1 in hereditary porencephaly. J Med Genet. 2006; **43**(6): 490-5.
34. Verbeek E, Meuwissen ME, Verheijen FW, Govaert PP, Licht DJ, Kuo DS, et al. COL4A2 mutation associated with familial porencephaly and small-vessel disease. Eur J Hum Genet. 2012; **20**(8): 844-51.
35. Mochida GH, Ganesh VS, Felie JM, Gleason D, Hill RS, Clapham KR, et al. A homozygous mutation in the tight-junction protein JAM3 causes hemorrhagic destruction of the brain, subependymal calcification, and congenital cataracts. Am J Hum Genet. 2010; **87**(6): 882-9.
36. Rutherford MA, Supramaniam V, Ederies A, Chew A, Bassi L, Groppo M, et al. Magnetic resonance imaging of white matter diseases of prematurity. Neuroradiology. 2010; **52**(6): 505-21.
37. Verney C, Monier A, Fallet-Bianco C, Gressens P. Early microglial colonization of the human forebrain and possible involvement in periventricular white-matter injury of preterm infants. J Anat. 2010; **217**(4): 436-48.
38. Verney C, Pogledic I, Biran V, Adle-Biassette H, Fallet-Bianco C, Gressens P. Microglial reaction in axonal crossroads is a hallmark of noncystic periventricular white matter injury in very preterm infants. J Neuropathol Exp Neurol. 2012; **71**(3): 251-64.
39. Counsell SJ, Rutherford MA, Cowan FM, Edwards AD. Magnetic resonance imaging of preterm brain injury. Arch Dis Child Fetal Neonatal Ed. 2003; **88**(4): F269-74.
40. Ramenghi LA, Fumagalli M, Righini A, Bassi L, Groppo M, Parazzini C, et al. Magnetic resonance imaging assessment of brain maturation in preterm neonates with punctate white matter lesions. Neuroradiology. 2007; **49**(2): 161-7.
41. Wigglesworth JS, Pape KE. Pathophysiology of intracranial haemorrhage in the newborn. J Perinat Med. 1980; **8**(3): 119-33.
42. Limperopoulos C, Benson CB, Bassan H, Disalvo DN, Kinnamon DD, Moore M, et al. Cerebellar hemorrhage in the preterm infant: ultrasonographic findings and risk factors. Pediatrics. 2005; **116**(3): 717-24.
43. Muller H, Beedgen B, Schenk JP, Troger J, Linderkamp O. Intracerebellar hemorrhage in premature infants: sonographic detection and outcome. J Perinat Med. 2007; **35**(1): 67-70.

44. Johnsen SD, Tarby TJ, Lewis KS, Bird R, Prenger E. Cerebellar infarction: an unrecognized complication of very low birthweight. J Child Neurol. 2002; **17**(5): 320-4.
45. Pape KE WJ. Haemorrhage, Ischaemia and the Perinatal Brain. Clinics in Developmental Medicine. London: Spastics International Medical Publications; 1979.
46. Ecury-Goossen GM, Dudink J, Lequin M, Feijen-Roon M, Horsch S, Govaert P. The clinical presentation of preterm cerebellar haemorrhage. Eur J Pediatr. 2010; **169**(10): 1249-53.
47. Pape KE, Armstrong DL, Fitzhardinge PM. Central nervous system patholgoy associated with mask ventilation in the very low birthweight infant: a new etiology for intracerebellar hemorrhages. Pediatrics. 1976; **58**(4): 473-83.
48. Gveric-Ahmetasevic S, Colic A, Gveric T, Gasparovic VE, Pavlisa G, Ozretic D. Coexistance of cerebral sinovenous thrombosis and Dandy Walker malformation in newborn. Coll Antropol. 2011; **35 Suppl 1**: 303-7.
49. Ushiwata I, Saiki I, Murakami T, Kanaya H, Konno J, Wada S. [Transverse sinus thrombosis accompanied by intracerebellar hemorrhage: a case report]. No Shinkei Geka. 1989; **17**(1): 51-5.
50. Fumagalli M, Ramenghi LA, Mosca F. Palpebral ecchymosis and cerebral venous thrombosis in a near term infant. Arch Dis Child Fetal Neonatal Ed. 2004; **89**(6): F530.
51. Berfelo FJ, Kersbergen KJ, van Ommen CH, Govaert P, van Straaten HL, Poll-The BT, et al. Neonatal cerebral sinovenous thrombosis from symptom to outcome. Stroke. 2010; **41**(7): 1382-8.
52. Raets MM, Sol JJ, Govaert P, Lequin MH, Reiss IK, Kroon AA, et al. Serial Cranial US for Detection of Cerebral Sinovenous Thrombosis in Preterm Infants. Radiology. 2013.
53. Bailey OT. Results of long survival after thrombosis of the superior sagittal sinus. Neurology. 1959; **9**: 741-6.
54. Bailey OT, Hass, G.M. Dural sinus thrombosis in early life. Journal of Pediatrics. 1958; **11**: 755-72.
55. Byers RK, Hass, G.M. Thrombosis of the dural venous sinuses in infancy and childhood. American Journal of Diseases of Children. 1933; **45**: 1161-83.
56. Ehlers H CC. Thrombosis of internal cerebral veins in infancy and childhood. Journal of Pediatrics. 1936; **8**: 600-23.
57. Moharir MD, Shroff M, Pontigon AM, Askalan R, Yau I, Macgregor D, et al. A prospective outcome study of neonatal cerebral sinovenous thrombosis. J Child Neurol. 2011; **26**(9): 1137-44.
58. Moharir MD SM, MacGregor D Clinical and radiographic features of thrombosis propagation in neonatal and childhood cerebral sinovenous thrombosis. . Ann Neurology. 2006; **60 (suppl)**: S141.
59. Govaert P, Achten E, Vanhaesebrouck P, De Praeter C, Van Damme J. Deep cerebral venous thrombosis in thalamo-ventricular hemorrhage of the term newborn. Pediatr Radiol. 1992; **22**(2): 123-7.
60. Govaert P, Swarte R, Oostra A, Zecic A, Vanzieleghem B, Van Langenhove P. Neonatal infarction within basal cerebral vein territory. Dev Med Child Neurol. 2001; **43**(8): 559-62.
61. Chung JI, Weon YC. Anatomic variations of the deep cerebral veins,tributaries of Basal vein of rosenthal: embryologic aspects of the regressed embryonic tentorial sinus. Interv Neuroradiol. 2005; **11**(2): 123-30.
62. Baram TZ, Butler IJ, Nelson MD, Jr., McArdle CB. Transverse sinus thrombosis in newborns: clinical and magnetic resonance imaging findings. Ann Neurol. 1988; **24**(6): 792-4.
63. Eichler F, Krishnamoorthy K, Grant PE. Magnetic resonance imaging evaluation of possible neonatal sinovenous thrombosis. Pediatr Neurol. 2007; **37**(5): 317-23.
64. Guppy KH, Origitano TC, Reichman OH, Segal S. Venous drainage of the inferolateral temporal lobe in relationship to transtemporal/transtentorial approaches to the cranial base. Neurosurgery. 1997; **41**(3): 615-9; discussion 9-20.
65. Muthukumar N, Palaniappan P. Tentorial venous sinuses: an anatomic study. Neurosurgery. 1998; **42**(2): 363-71.
66. Browder J, Kaplan HA, Krieger AJ. Venous lakes in the suboccipital dura mater and falx cerebelli of infants: surgical significance. Surg Neurol. 1975; **4**(1): 53-5.

67. Dagain A, Vignes R, Dulou R, Delmas JM, Riem T, Guerin J, et al. [Study of the junction between the cortical bridging veins and basal cranial venous sinus] Etude anatomique du drainage des veines corticales inferieures dans le sinus transverse. Neurochirurgie. 2009; **55**(1): 19-24.
68. Miller E, Daneman A, Doria AS, Blaser S, Traubici J, Jarrin J, et al. Color Doppler US of normal cerebral venous sinuses in neonates: a comparison with MR venography. Pediatr Radiol. 2012; **42**(9): 1070-9.
69. Durgun B, Ilgıt ET, Cizmeli MO, Atasever A. Evaluation by angiography of the lateral dominance of the drainage of the dural venous sinuses. Surg Radiol Anat. 1993; **15**(2): 125-30.
70. Ayanzen RH, Bird CR, Keller PJ, McCully FJ, Theobald MR, Heiserman JE. Cerebral MR venography: normal anatomy and potential diagnostic pitfalls. AJNR Am J Neuroradiol. 2000; **21**(1): 74-8.
71. Fukusumi A, Okudera T, Takahashi S, Taoka T, Sakamoto M, Nakagawa H, et al. Anatomical evaluation of the dural sinuses in the region of the torcular herophili using three dimensional CT venography. Acad Radiol. 2010; **17**(9): 1103-11.
72. Taylor GA, Walker LK. Intracranial venous system in newborns treated with extracorporeal membrane oxygenation: Doppler US evaluation after ligation of the right jugular vein. Radiology. 1992; **183**(2): 453-6.
73. Lichtenstein D, Saifi R, Augarde R, Prin S, Schmitt JM, Page B, et al. The Internal jugular veins are asymmetric. Usefulness of ultrasound before catheterization. Intensive Care Med. 2001; **27**(1): 301-5.
74. Manara R, Mardari R, Ermani M, Severino MS, Santelli L, Carollo C. Transverse dural sinuses: incidence of anatomical variants and flow artefacts with 2D time-of-flight MR venography at 1 Tesla. Radiol Med. 2010; **115**(2): 326-38.
75. Yu W, Rives J, Welch B, White J, Stehel E, Samson D. Hypoplasia or occlusion of the ipsilateral cranial venous drainage is associated with early fatal edema of middle cerebral artery infarction. Stroke. 2009; **40**(12): 3736-9.
76. Cowan F, Thoresen M. Ultrasound study of the cranial venous system in the human new-born infant and the adult. Acta Physiol Scand. 1983; **117**(1): 131-7.
77. Widjaja E, Shroff M, Blaser S, Laughlin S, Raybaud C. 2D time-of-flight MR venography in neonates: anatomy and pitfalls. AJNR Am J Neuroradiol. 2006; **27**(9): 1913-8.
78. Kopuz C, Aydin ME, Kale A, Demir MT, Corumlu U, Kaya AH. The termination of superior sagittal sinus and drainage patterns of the lateral, occipital at confluens sinuum in newborns: clinical and embryological implications. Surg Radiol Anat. 2010; **32**(9): 827-33.
79. Tanoue S, Kiyosue H, Okahara M, Sagara Y, Hori Y, Kashiwagi J, et al. Para-cavernous sinus venous structures: anatomic variations and pathologic conditions evaluated on fat-suppressed 3D fast gradient-echo MR images. AJNR Am J Neuroradiol. 2006; **27**(5): 1083-9.
80. San Millan Ruiz D, Gailloud P. Cerebral developmental venous anomalies. Childs Nerv Syst. 2010; **26**(10): 1395-406.
81. Suzuki Y, Matsumoto K. Variations of the superficial middle cerebral vein: classification using three-dimensional CT angiography. AJNR Am J Neuroradiol. 2000; **21**(5): 932-8.
82. Pierre-Kahn A, Renier D, Sainte-Rose C, Flandin C, Hirsch JF. [Acute intracranial hematoma in neonates at term. Apropos of 17 cases]. Ann Pediatr (Paris). 1985; **32**(5): 419-25.
83. Bergman I, Bauer RE, Barmada MA, Latchaw RE, Taylor HG, David R, et al. Intracerebral hemorrhage in the full-term neonatal infant. Pediatrics. 1985; **75**(3): 488-96.
84. Hayashi T, Harada K, Honda E, Utsunomiya H, Hashimoto T. Rare neonatal intracerebral hemorrhage. Two cases in full-term infants. Childs Nerv Syst. 1987; **3**(3): 161-4.
85. Hanigan WC, Powell FC, Palagallo G, Miller TC. Lobar hemorrhages in full-term neonates. Childs Nerv Syst. 1995; **11**(5): 276-80.
86. Sandberg DI, Lamberti-Pasculli M, Drake JM, Humphreys RP, Rutka JT. Spontaneous intraparenchymal hemorrhage in full-term neonates. Neurosurgery. 2001; **48**(5): 1042-8; discussion 8-9.
87. Huang AH, Robertson RL. Spontaneous superficial parenchymal and leptomeningeal hemorrhage in term neonates. AJNR Am J Neuroradiol. 2004; **25**(3): 469-75.

88. Tramonte JJ, Goodkin HP. Temporal lobe hemorrhage in the full-term neonate presenting as apneic seizures. J Perinatol. 2004; **24**(11): 726-9.
89. Hoogstraate SR, Lequin MH, Huysman MA, Ahmed S, Govaert PP. Apnoea in relation to neonatal temporal lobe haemorrhage. Eur J Paediatr Neurol. 2009; **13**(4): 356-61.
90. Raets MM, Dudink J, Ijsselstijn H, van Heijst AF, Lequin MH, Houmes RJ, et al. Brain Injury Associated With Neonatal Extracorporeal Membrane Oxygenation in the Netherlands: A Nationwide Evaluation Spanning Two Decades. Pediatr Crit Care Med. 2013.
91. Cross JH, Harrison CJ, Preston PR, Rushton DI, Newell SJ, Morgan ME, et al. Postnatal encephaloclastic porencephaly—a new lesion? Arch Dis Child. 1992; **67**(3): 307-11.
92. Williams AN, Sunderland R. Neonatal shaken baby syndrome: an aetiological view from Down Under. Arch Dis Child Fetal Neonatal Ed. 2002; **87**(1): F29-30; discussion F.
93. Rushton DI. Neonatal shaken baby syndrome—historical inexactitudes. Arch Dis Child Fetal Neonatal Ed. 2003; **88**(2): F161; author reply F-2.
94. Slovis TL, Shankaran S, Bedard MP, Poland RL. Intracranial hemorrhage in the hypoxic-ischemic infant: ultrasound demonstration of unusual complications. Radiology. 1984; **151**(1): 163-9.
95. Schubiger G, Schubiger O, Tonz O. [Superior sagittal sinus thrombosis is the newborn—diagnosis by computerized tomography]. Helv Paediatr Acta. 1982; **37**(2): 193-9.
96. Konishi Y, Kuriyama M, Sudo M, Konishi K, Hayakawa K, Ishii Y. Superior sagittal sinus thrombosis in neonates. Pediatr Neurol. 1987; **3**(4): 222-5.
97. Anderson WR, Quie PG. Cyanosis, seizures, and hypernatremia in a two-week-old infant. Minn Med. 1968; **51**(1): 97-103.
98. Aicardi J, Goutieres F. [Intracranial venous thromboses. Complication of acute dehydration in infants]. Arch Fr Pediatr. 1973; **30**(8): 809-29.
99. Hilliard TN, Marsh MJ, Malcolm P, Murdoch IA, Wood BP. Radiological case of the month. Sagittal sinus thrombosis in hypernatremic dehydration. Arch Pediatr Adolesc Med. 1998; **152**(11): 1147; discussion 8.
100. Gebara BM, Everett KO. Dural sinus thrombosis complicating hypernatremic dehydration in a breast-fed neonate. Clin Pediatr (Phila). 2001; **40**(1): 45-8.
101. van Amerongen RH, Moretta AC, Gaeta TJ. Severe hypernatremic dehydration and death in a breast-fed infant. Pediatr Emerg Care. 2001; **17**(3): 175-80.
102. Fitzgerald KC, Williams LS, Garg BP, Carvalho KS, Golomb MR. Cerebral sinovenous thrombosis in the neonate. Arch Neurol. 2006; **63**(3): 405-9.
103. Soman TB, Moharir M, DeVeber G, Weiss S. Infantile spasms as an adverse outcome of neonatal cortical sinovenous thrombosis. J Child Neurol. 2006; **21**(2): 126-31.
104. Nwosu ME, Williams LS, Edwards-Brown M, Eckert GJ, Golomb MR. Neonatal sinovenous thrombosis: presentation and association with imaging. Pediatr Neurol. 2008; **39**(3): 155-61.
105. McHedlishvili G. Red blood cell aggregability in blood. Criteria for scoring the techniques. Clin Hemorheol Microcirc. 1998; **19**(2): 161-2.
106. Tikhomirova IA. The effect of dehydration on macro- and microrheological blood properties. Clin Hemorheol Microcirc. 2002; **26**(2): 85-90.
107. Amit M, Camfield PR. Neonatal polycythemia causing multiple cerebral infarcts. Arch Neurol. 1980; **37**(2): 109-10.
108. Clancy R, Malin S, Laraque D, Baumgart S, Younkin D. Focal motor seizures heralding stroke in full-term neonates. Am J Dis Child. 1985; **139**(6): 601-6.
109. Dawkins RR, Marshall TL, Rogers MS. Prenatal gangrene in association with twin-twin transfusion syndrome. Am J Obstet Gynecol. 1995; **172**(3): 1055-7.
110. Casey S. "T2 washout": an explanation for normal diffusion-weighted images despite abnormal apparent diffusion coefficient maps. AJNR Am J Neuroradiol. 2001; **22**(8): 1450-1.
111. Kato Y, Takeda H, Furuya D, Nagoya H, Deguchi I, Fukuoka T, et al. Subarachnoid hemorrhage as the initial presentation of cerebral venous thrombosis. Intern Med. 2010; **49**(5): 467-70.

112. Komiyama M, Kitano S, Sakamoto H, Ehara E, Miyagi N, Kusuda S. Rapid normalization of marked dilatation of the cerebral duro-venous system in a newborn infant mimicking a great vein of Galen varix. Pediatr Neurosurg. 2001; **35**(3): 149-52.
113. Hunt RW, Loughnan P, Fink AM, Volpe JJ, Inder TE. Magnetic resonance demonstration in the newborn of generalized cerebral venous dilation with spontaneous resolution. Eur J Paediatr Neurol. 2002; **6**(5): 289-92.
114. Truwit CL. Venous angioma of the brain: history, significance, and imaging findings. AJR Am J Roentgenol. 1992; **159**(6): 1299-307.
115. Horsch dV, Cowan, Groenendaal, Benders, Lequin, Paris, Govaert. Developmental Venous Anomaly in the Newborn Brain. Unpublished manuscript. 2013.
116. Chang CL, Chiu NC. Developmental venous anomaly found by cranial US in a neonate. Pediatr Radiol. 2010; **40**(3): 374.
117. Oran I, Kiroglu Y, Yurt A, Ozer FD, Acar F, Dalbasti T, et al. Developmental venous anomaly (DVA) with arterial component: a rare cause of intracranial haemorrhage. Neuroradiology. 2009; **51**(1): 25-32.
118. Cakirer S. De novo formation of a cavernous malformation of the brain in the presence of a developmental venous anomaly. Clin Radiol. 2003; **58**(3): 251-6.
119. Riel-Romero RM, Mattingly M. Developmental venous anomaly in association with neuromigrational anomalies. Pediatr Neurol. 2005; **32**(1): 53-5.
120. Févre M, Modec, L Sinus pericranii et tumeurs vasculaires extracraniennes communiquant avec la circulation intracranienne. J Chir. 1936; **47**(561-588).
121. Gandolfo C, Krings T, Alvarez H, Ozanne A, Schaaf M, Baccin CE, et al. Sinus pericranii: diagnostic and therapeutic considerations in 15 patients. Neuroradiology. 2007; **49**(6): 505-14.
122. Valdivieso EM, Scholtz CL. Diffuse meningocerebral angiodysplasia and renal agenesis: a case report. Pediatr Pathol. 1986; **6**(1): 119-26.
123. Mul D, Lequin M, Govaert P. Bilateral renal agenesis, cerebral angiodysplasia and esophageal atresia. Eur J Paediatr Neurol. 2006; **10**(1): 23-6.
124. Sharony R, Kidron D, Aviram R, Beyth Y, Tepper R. Prenatal diagnosis of fetal cerebellar lesions: a case report and review of the literature. Prenat Diagn. 1999; **19**(11): 1077-80.
125. Trash. Vascular malformation of the cerebellum. Archives Pathology. 1963; **75**: 65-9.
126. Bland LI, Lapham LW, Ketonen L, Okawara SH. Acute cerebellar hemorrhage secondary to capillary telangiectasia in an infant. A case report. Arch Neurol. 1994; **51**(11): 1151-4.
127. Guibaud L, Garel C, Annie B, Pascal G, Francois V, Vavasseur C, et al. Prenatal diagnosis of capillary telangiectasia of the cerebellum—ultrasound and MRI features. Prenat Diagn. 2003; **23**(10): 791-6.
128. Diguet A, Laquerriere A, Eurin D, Chanavaz-Lacheray I, Magdeleine Ruchoux M, Rossi A, et al. Fetal capillary haemangioblastoma: an exceptional tumour. A review of the literature. Prenat Diagn. 2002; **22**(11): 979-83.
129. Aguglia U, Latella MA, Cafarelli F, Le Piane E, Gangemi A, Labate A, et al. Spontaneous obliteration of MRI-silent cerebral angiomatosis revealed by CT angiography in a patient with Sturge-Weber syndrome. J Neurol Sci. 2008; **264**(1-2): 168-72.
130. Cure JK, Holden KR, Van Tassel P. Progressive venous occlusion in a neonate with Sturge-Weber syndrome: demonstration with MR venography. AJNR Am J Neuroradiol. 1995; **16**(7): 1539-42.
131. Yallapragada AV, Cure JK, Holden KR. Sturge-Weber syndrome variant with atypical intracranial findings: case report. J Child Neurol. 2006; **21**(2): 155-7.
132. Slasky SE, Shinnar S, Bello JA. Sturge-Weber syndrome: deep venous occlusion and the radiologic spectrum. Pediatr Neurol. 2006; **35**(5): 343-7.
133. Porto L, Kieslich M, Yan B, Zanella FE, Lanfermann H. Accelerated myelination associated with venous congestion. Eur Radiol. 2006; **16**(4): 922-6.
134. Fishman MA, Baram TZ. Megalencephaly due to impaired cerebral venous return in a Sturge-Weber variant syndrome. J Child Neurol. 1986; **1**(2): 115-8.

135. Hu J, Yu Y, Juhasz C, Kou Z, Xuan Y, Latif Z, et al. MR susceptibility weighted imaging (SWI) complements conventional contrast enhanced T1 weighted MRI in characterizing brain abnormalities of Sturge-Weber Syndrome. J Magn Reson Imaging. 2008; **28**(2): 300-7.
136. Mentzel HJ, Dieckmann A, Fitzek C, Brandl U, Reichenbach JR, Kaiser WA. Early diagnosis of cerebral involvement in Sturge-Weber syndrome using high-resolution BOLD MR venography. Pediatr Radiol. 2005; **35**(1): 85-90.
137. Delaney HM, Rooks VJ, Wolfe SQ, Sawyer TL. Term neonate with intracranial hemorrhage and hereditary hemorrhagic telangiectasia: a case report and review of the literature. J Perinatol. 2012; **32**(8): 642-4.
138. Roy C, Noseda G, Arzimanoglou A, Harpey JP, Binet MH, Vaur C, et al. [Rendu Osler disease revealed by ruptured cerebral arterial aneurysm in an infant]. Arch Fr Pediatr. 1990; **47**(10): 741-2.
139. Key A RG. Studien in der Anatomie des Nervensystems und des Bindegewebes. Stockholm, Sweden: Samson and Waller; 1875-1876.
140. Mack J, Squier W, Eastman JT. Anatomy and development of the meninges: implications for subdural collections and CSF circulation. Pediatr Radiol. 2009; **39**(3): 200-10.
141. Hannah. The aetiology of subdural hematoma: an anatomical and pathological study. J Nerve Ment Dis 1936; **84**: 169–86.
142. Clark LG. On the Pacchionian bodies. Journal of Anatomy. 1920; **55** (Pt1): 40-8.
143. Grzybowski DM, Herderick EE, Kapoor KG, Holman DW, Katz SE. Human arachnoid granulations Part I: a technique for quantifying area and distribution on the superior surface of the cerebral cortex. Cerebrospinal Fluid Res. 2007; **4**: 6.

CHAPTER 3

SERIAL CRANIAL ULTRASOUND DETECTS CEREBRAL SINOVENOUS THROMBOSIS IN PRETERM INFANTS

M.M.A. Raets, J.J. Sol, P. Govaert, M.H. Lequin, I.K.M. Reiss,
A.A. Kroon, I.M. Appel, J.Dudink

Radiology, 2013 Aug 28. [Epub ahead of print].

Abstract

Purpose: To report the incidence of CSVT in a prospective cohort of preterm infants less than 29 weeks of gestation.

Materials and Methods: The local medical ethics review board approved this study and written parental consent was obtained. Preterm infants below 29 weeks of gestation admitted to our neonatal intensive care unit were prospectively studied with cranial ultrasound (cranial US). The scan protocol included visualization with color Doppler imaging of the superior sagittal and transverse sinus through the anterior (8.5 MHz probe) and mastoid fontanel (13 MHz probe). When feasible, magnetic resonance imaging was performed to confirm cranial US-diagnosed CSVT. The differences between preterm infants with and without CSVT were analyzed by Mann-Whitney tests for continuous variables and by Fishers' exact tests for categorical data.

Results: Cranial US documented CSVT in 11 of 249 preterm infants less than 29 weeks. Transverse sinuses were most frequently affected (in all 11 CSVT patients). All infants with CSVT were asymptomatic. Postnatal age at diagnosis ranged from 5 to 34 days. The mean gestational age was significantly lower in infants with CSVT (25.9 weeks versus 26.8 weeks, P= 0.038). Of the risk factors studied only duration of mechanical ventilation was associated with CSVT; it was significantly longer in the CSVT group.

Conclusion: Systematic serial cranial US of infants below 29 weeks of gestational age showed a remarkably high incidence of CSVT of 4.4%. Cranial US including color Doppler imaging with scans through the mastoid fontanel can detect CSVT at an early stage. Management of this possibly important condition needs attention.

Introduction

Neonatal cerebral sinovenous thrombosis (CSVT) is reported to be a rare finding with high morbidity. Improved neuroimaging techniques and clinical vigilance have led to detection of more cases recently. A recent Dutch retrospective cohort study suggested an incidence of 1 to 12 per 100,000 neonates [2, 3]. This is higher than suggested by the Canadian Registry (0.67 per 100.000) [3], but probably still an underestimation, as only late preterm and term neonates with clinical symptoms suggestive of CSVT were screened.

Venous "outflow" obstruction due to CSVT may lead to venous hypertension -leading to hemorrhage- and ischemia, and thus cause parenchymal damage [4, 5]. Early treatment of CSVT may be important to reduce the risk of brain damage and of recurrent thrombosis.

Different diagnostic imaging techniques are used, e.g. computed tomography (CT), magnetic resonance imaging (MRI) and cranial ultrasound (cranial US). CT carries the disadvantage of ionizing radiation and requires intravenous administration of contrast agents. MRI including venography is comparable with CT without the disadvantages of ionizing radiation [5]. However MRI requires transport and in most cases sedation [6].

Transfontanellar cranial US is a safe and non-invasive method which can be performed bedside, even when a patient is clinically unstable [7]. Cranial US is nearly universally available at neonatal intensive care units (NICUs), which allows serial imaging. Therefore cranial US is the preferred method for brain imaging in daily practice in the NICU. The role of cranial US for detecting CSVT is controversial. Yang et al. [8] state that cranial US should not be used primary to detect CSVT, however several authors have reported that cranial US including color Doppler is feasible to screen the intracranial venous system in neonates [9-12]. Through the anterior fontanel, color Doppler allows visualization of the deep venous system including: internal cerebral veins, inferior sagittal sinus, great cerebral vein and straight sinus. The superior sagittal sinus and both transverse sinuses at the insertion of the cerebellar tentorium can be visualized through the anterior fontanel. Through both mastoid fontanels parts of the transverse and sigmoid sinuses can be studied.

We hypothesized that CSVT in premature infants is underestimated because clinical signs can be subtle. The purpose of this study was to report the incidence of CSVT in a prospective cohort of preterm infants less than 29 weeks of gestation.

Materials and Methods

The local medical ethics review board approved this study and written parental consent was obtained. This study was performed in the NICU of the Sophia Children's Hospital / Erasmus Medical Center Rotterdam. This tertiary multidisciplinary NICU with 30 beds serves the South-Western Netherlands.

Between November 1st, 2010, and June 30th, 2012, all newly admitted preterm infants below 29 weeks of gestation were eligible. Those with congenital malformations were excluded, as were those with unknown gestational age.

The following data were prospectively collected for the duration of the NICU stay; (from medical charts and computerized patient data management system); gestational age, birth weight, head circumference, Score for Neonatal Acute Physiology – Perinatal Extension- II (SNAPPE-II) score [13], gender, respiratory support, age at CSVT diagnosis, and potential risk factors for CSVT (maternal, perinatal and neonatal). Simultaneous with the present study, our center participated in a multicenter randomized controlled trial, entitled "Systemic Hydrocortisone To Prevent Bronchopulmonary Dysplasia" in preterm infants (the SToP-BPD study)[14]. In total, five infants were included in both studies, two infants with CSVT and three infants without CSVT. These infants were excluded for the analysis of postnatal use of steroids due to uncertain medication (placebo versus hydrocortisone).

All included preterm infants were prospectively studied with cranial US including color Doppler according to a local standard protocol (on day 0, 1, 2, and 7 after birth and then once a week until discharge). Deviation of protocol occurred on clinical grounds (by example

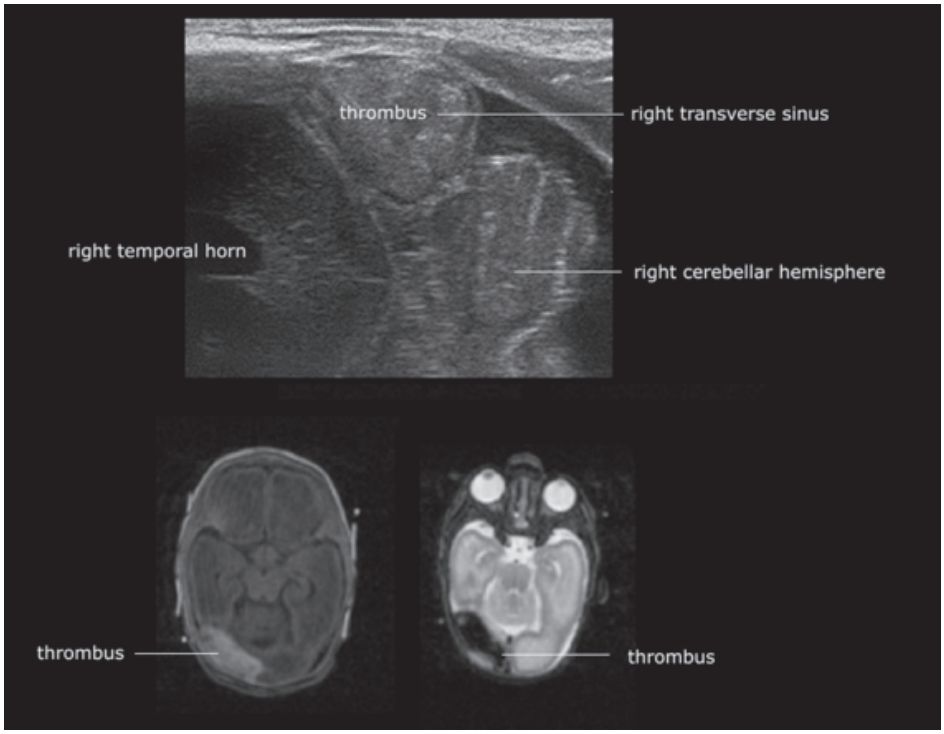

Figure 1 Top image: an overview through the mastoid fontanel showing a thrombus in the right transverse sinus. Below right: T1 weighted MR image, showing hypersignal intensity of the thrombus, and below

hemodynamic instability). Cranial US screening was performed and real time reviewed by two authors (MR, physician with 4 years and PG neonatologist with 25 years experience in cranial US), with expertise in neonatal cranial ultrasound and consensus was reached in every case.

We used serial color Doppler imaging of the intracranial venous system including both internal cerebral veins, superior sagittal sinus (anterior and mid sinus) and both transverse sinuses at the insertion of the cerebellar tentorium, through the anterior fontanel with a 8.5 MHz convex probe. If the transverse sinuses were not visualized through the anterior fontanel, additional images of the transverse and sigmoid sinuses were acquired through the mastoid fontanel with a high frequency linear probe (13 MHz). These additional images with color Doppler added maximum five minutes to the duration of the routine examination. An Esaote MyLab 70 (Genoa, Italy) was used for imaging.

CSVT was diagnosed if there was partial or total absence of flow and/or partial or complete thrombus was seen in the above-mentioned sinuses. Partial flow was indicated by color findings and pulse wave. If the infants' condition allowed for it, the cranial US diagnosis was verified with MRI scans (figure 1). In our center MRI is performed according to standard protocol at 30 weeks of postmenstrual age, if the patients are hemodynamically stable and can manage transport to another department. Preterm infants are evaluated in the outpatient clinic at 6 weeks corrected age, 6 months, 1 year and 2 year of age. We performed chart review for outcome analysis, these outcome data were collected as standard care.

Statistical analysis

Statistical analysis was performed using SPSS version 17 for windows (IBM, NY, NY). The differences between preterm infants with and without CSVT were analyzed by Mann-Whitney tests for continuous variables and by Fisher's exact tests for categorical data. A two-sided significance level of $P < .05$ was used.

Results

During the study period 265 infants below 29 weeks of gestational age were admitted. 16 were excluded (figure 2), leaving 249 to be included in this study. CSVT was diagnosed in 11 preterm infants, 4.4 % of the study cohort. These were all asymptomatic. The postnatal age at diagnosis ranged from five to 34 days (mean 18.5 days, ±10.6 SD). There was no gender predominance (five males, six females).

Thrombosis was found in the transverse sinuses in all; in one case the superior sagittal was also involved. No side-to-side differences were found: six were on the left, five on the right.

MRI was performed in nine infants with sonographically diagnosed CSVT but could not be assessed in two MRI scans due to motion artifacts. MRI confirmed CSVT in these seven infants; MRI documented no additional findings in these infants. MR was performed in 138 of 238

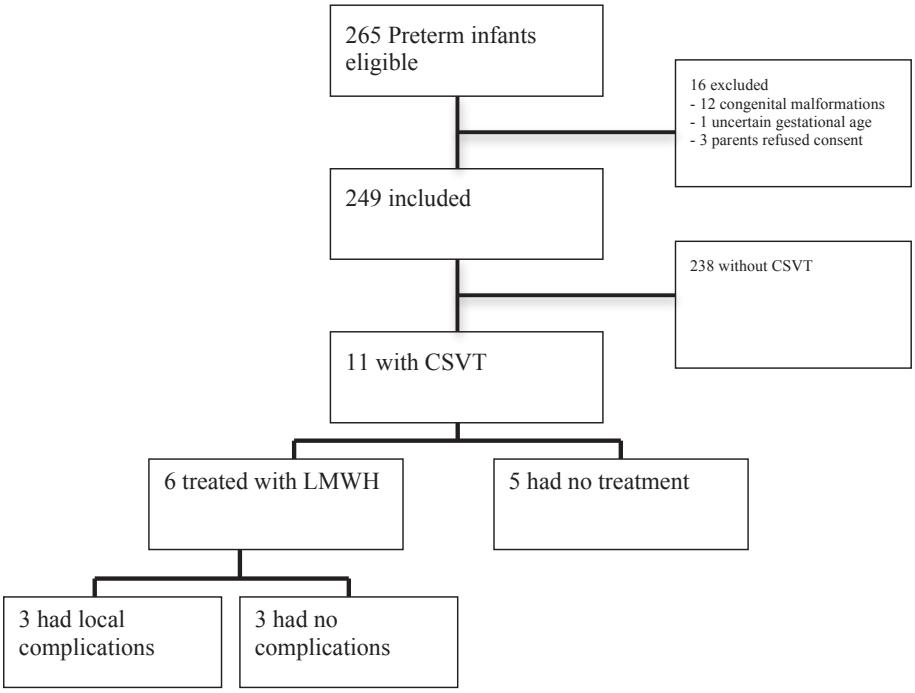

Figure 2- Patient flow chart

neonates without sonographic findings of CSVT. In two infants CSVT was picked up by MRI where it had not been diagnosed on cranial US. In one of these patients cranial US, without additional color Doppler imaging, was performed for clinical indications prior to MRI. During that study the neonatologists with experience in color Doppler were not present and therefore regular cranial US was performed without targeted color Doppler. After this study we adjusted the clinical imaging protocol on our unit.

In the second infant MRI was performed in week 5 after birth, however the most recent cranial US was performed 8 days before MRI.

Partial thrombosis in the transverse sinus was documented in eight, in three the transverse sinus was completely obstructed with thrombus (figure 3).

The mean gestational age of the infants with CSVT was significantly lower (25.9 weeks versus 26.8 weeks) (table 1; P = .038). Birth weight (843.7 grams versus 927.6 grams), head circumference and SNAPPE-II scores [13] were not significantly different (P= .291; P=.052 and P=.906 respectively).

One infant with CSVT died due to the complications of extreme prematurity (intestinal perforation, hemodynamic instability with circulatory failure); thrombosis was not the cause of death.

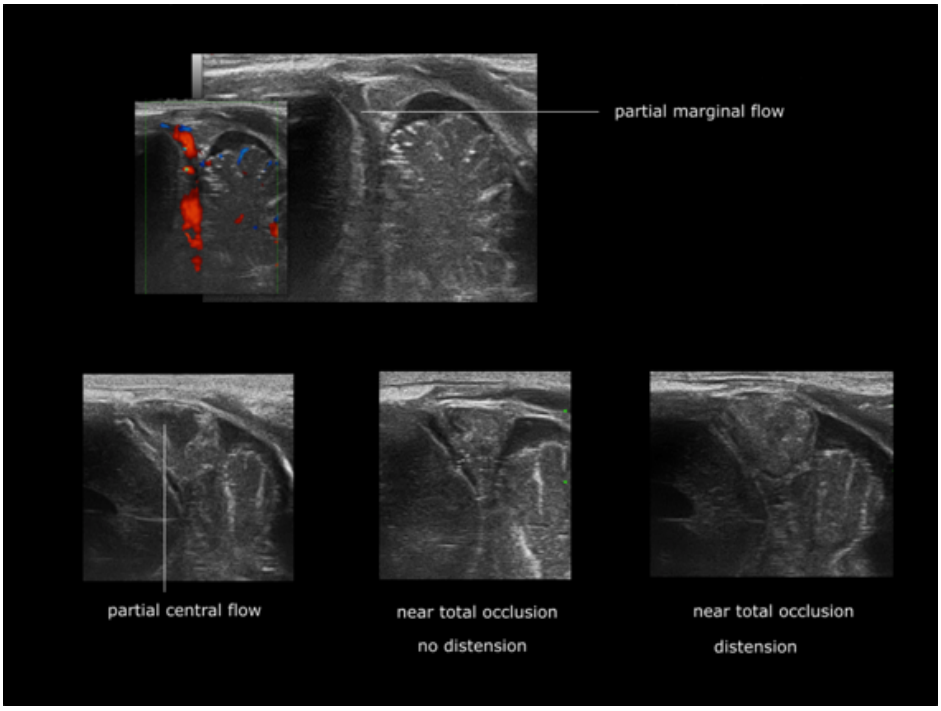

Figure 3 Top image: image through the mastoid fontanel, showing thrombus with partial flow. Bottom images: on the right CUS showing a thrombus with partial central flow, in the middle a near total occlusion without distension of the transverse sinus and on the left near total occlusion with distention of the transverse sinus.

Table 1 Patient Characteristics

	CSVT (n=11)	No CSVT (n=238)	P-value
Gestational age at birth, mean ± SD, (range), weeks	25.9 ± 1.4 (24-28.4)	26.8 ±1.5 (23.9-28.9)	**0.038**
Birth weight, mean ± SD, (range), grams	843.7 ± 213.8 (615-1185)	927.6 ± 270.9 (360-1610)	0.291
Head circumference, mean ± SD, (range), cm	23 ± 1.4 (21-25.2)	24.2 ± 2.1(19.5-29.3)	0.052
SNAPPE-II-score, mean ± SD, (range)	24.2 ± 13.2 (0-45)	27.8 ± 22.8(0-118)	0.906
Male gender, n (%)	5 (45.5%)	132 (55.5%)	0.514

SNAPPE-II score= Score for Neonatal Acute Physiology – Perinatal Extension- II

The incidence of maternal risk factors such as chorioamnionitis and premature rupture of membranes (PROM) was slightly higher in the CSVT group (table 2), but these differences were not significant. Seven of the 11 infants with CSVT had blood culture proven sepsis during the neonatal period (p= .218). Postnatal use of corticosteroids was not significantly associated with thrombosis (p= .264). Duration of conventional mechanical ventilation was significantly longer

Table 2 Risk factors

	CSVT (n=11)	No CSVT (n=238)	P-value
Maternal			
Preeclampsia/HELLP, n (%)	1 (9.1%)	35 (14.7%)	1.00
PPROM, n (%)	4 (36.4%)	51 (21.4%)	0.266
Chorioamnionitis, n (%)	5 (45.5%)	56 (23.5%)	0.179
Perinatal			
Cesarean section, n (%)	7 (63.6%)	121 (50.8%)	0.582
Apgar score 5 minutes post partum, mean ± SD, (range)	7.1 ± 1 (5-9)	7.3 ± 1.8 (1-10)	0.375
Neonatal			
Postnatal steroids, n (%)	0/9	34/238 (14.3%)	0.617
PDA, n (%)	9 (81.8%)	104 (43.7%)	0.153
HFV, n (%)	7 (63.6%)	197 (82.1%)	0.209
HFV duration, mean ± SD, (range), hours	136.3 ± 79.3 (46.48-283.68)	85.2 ± 93.4 (4.1-435.08)	0.057
Mean Airway Pressure HFV, mean ± SD, (range), mmHg	16.4 ± 1.5 (14.5-18.3)	16.6 ± 2.9 (10-25)	0.795
Delta P HFV, mean ± SD, (range)	45 ±6.7 (40-58)	46.7 ± 11.7 (13-71)	0.523
CMV duration § , mean ± SD, (range), hours	363.7 ± 190.9 (78.88-706.38)	226.1 ± 235.2 (2.5-1607)	**0.012**
Mean Airway Pressure CMV, mean ± SD, (range), mmHg	12.1 ± 2.8 (6.7-16.2)	10.8 ± 3.6 (5.5-24)	0.241
Sepsis, n (%)	7 (63.6%)	106 (44.5%)	0.235

PPROM = premature rupture of membranes, PDA= patent ductus arteriosus, HFV= high frequency ventilation, CMV= conventional mechanical ventilation

in infants with CSVT (367.3 versus 226.1 hours, p=.038). Ventilator settings did not significantly differ between the groups (table 2).

Six infants with almost complete vessel occlusion were treated with subcutaneous low molecular-weighted heparin (LMWH). Three of these infants suffered from bleeding at the area of cannula insertion, following LMWH treatment which was ended when the bleeding epidsode was diagnosed. The other three completed therapy for two to six weeks without any side effects (e.g. intracranial hemorrhage, local bleeding at insertion side). These infants showed recanalisation.

Five infants were not treated with LMWH; these infants had partial thrombosis with sufficient flow along the thrombus. Spontaneous resolution was seen in four of these patients, within 6 to 34 days after thrombus was documented. One infant showed propagation of the thrombus, intraventricular hemorrhage was a contra-indication in this infant; he died due to complications of extreme prematurity. One infant had recently undergone abdominal surgery because of necrotizing enterocolitis; Cranial US monitoring showed a stable thrombus and sufficient flow; therefore it was decided not to start LMWH.

Table 3 Overview of CSVT patients

Patient	GA at birth	Gender	Days to positive cranial US for CSVT (GA at CSVT)	Days at negative cranial US prior to positive MRI	Cranial US findings	Side	Days postpartum MRI	MRI findings	LMWH	Complications due to LMWH	CSVT course (days after diagnosis)	Follow-up
1	24 6/7	Female	34 (29 5/7)	30 days	Complete SSS and TS thrombosis	Left	34	SSS and left TS thrombosis	Yes	No	Recanalization (17 days)	At 2 years: Normal
2	26 4/7	Male	24 (30 5/7)	N.A.	Partial TS thrombosis	Right	29	No intracranial lesions, no signs of CSVT	Yes	Yes, local haemorrhage after 17 days of treatment	Reduced (52 days)	At 2 years: MDI 100 PDI 107*
3	26	Female	7 (27)	N.A.	Partial TS thrombosis	Left	N.A.	N.A.	No	N.A.	Resolved without therapy (22 days)	At 2 years: MDI 90 PDI 100*
4	25 3/7	Male	32 (30)	24 days	Complete TS thrombosis	Right	32	Right TS thrombosis	Yes	No	Recanalization (23 days)	At 1 year normal
5	27 3/7	Female	8 (28 4/7)	N.A.	Partial TS thrombosis	Left	22	PWML in centrum semiovale. No signs of CSVT	Yes	No	Reduced (22 days)	At 1 year normal
6	28 3/7	Female	13 (30 2/7)	N.A.	Partial TS thrombosis	Left	22	Absent flow-void in SSS compatible with CSVT	No	N.A.	Reduced (32 days)	At 6 mths normal
7	26 1/7	Female	24 (29 4/7)	N.A.	Partial TS thrombosis	Right	24	Right TS thrombosis	No	N.A.	Reduced (60 days)	At 6 mnths abnormal
8	24 1/7	Male	19 (26 6/7)	N.A.	Complete TS thrombosis	Left	47	CSVT could not be assessed due to severe motion artefacts	Yes	Yes, local haemorrhage after 17 days of treatment	Recanalization (22 days)	At 6 mnths mild-moderate abnormal
9	24 4/7	Female	23 (27 6/7)	N.A.	Complete TS thrombosis	Left	71	bilateral remmants of IVH, evident asymmetry in TS, suspect for CSVT	Yes	Yes, local haemorrhage after 19 days of treatment	Recanalization (43 days)	At 6 mnths normal
10	26 6/7	Male	9 (28 1/7)	N.A.	Partial TS thrombosis	Left	41	CSVT could not be assessed due to severe motion artefacts	No	N.A.	Resolved without therapy (6 days)	At 6 mnths abnormal
11	24	Male	5 (24 5/7)	N.A.	Partial TS thrombosis, with propagation of the thrombus	Right	N.A.	N.A.	No, because of IVH	N.A.	Propagation of the thrombus (11 days)	Deceased

TS= transverse sinus, SSS= superior sagittal sinus, PWML= punctate white matter lesions, IVH= intraventricular haemorrhage, LMWH= low molecular-weighted heparin*= BSID-III[1], N.A.= Not applicable

Discussion

Our study found a 4.4% incidence of CSVT, higher than others have previously reported [2, 3]. This study also shows that cranial US including color Doppler imaging and scans through the mastoid fontanel can detect transverse sinus thrombosis at an early stage, allowing consideration of therapeutic options prior to the development of stroke or hemorrhage. The technique further allows serial assessment of the process and effect of treatment.

Miller et al [12] compared MRV with color Doppler US in the evaluation of normal cerebral venous sinuses. They found that color Doppler US was highly specific in detecting true-negative cases of cerebral thrombosis in suspected neonates [12]. The inter-observer and inter-modality reading agreement rates were high.

Fitzgerald et al reported on a cohort of 42 neonates studied with CT and MR between 1986 and 2005 [15]. Clinical presentation was variable and included seizures, apnea, poor feeding, lethargy and thrombocytopenia. Two-thirds had multiple symptoms. The superior sagittal and transverse sinuses were most commonly involved. Long-term sequelae were found in 79% of the infants (cognitive and motor impairment,epilepsy).

deVeber et al [3] reported an incidence of CSVT was 0.67 cases per 100,000 children per year [3]. Thirty-eight per cent had neurological deficits including motor impairment (80%), cognitive impairment (10%), development delay (9%), speech, and visual impairment (both 6%). 12 infants died, 6 due to the sinovenous thrombosis [3]. These outcome data are comparable with the study of Berfelo et al [2].

Reported risk factors in the neonatal period were dehydration, sepsis, perinatal complications (hypoxia, PROM, maternal infection, placental abruption or gestational diabetes) and prothrombotic disorders [3, 16]. We found a tendency towards higher prevalence of sepsis and maternal risk factors including PROM and chorioamnionitis in patients with CSVT; however these differences were not significant.

Patent ductus arteriosus (PDA) showed a trend to higher incidence in infants with CSVT than in infants without CSVT. In our NICU the first step of PDA treatment is fluid restriction to 140-150 ml/kg/dg. Perhaps this relative dehydration plays a role in the mechanisms leading to CSVT. Sluggish blood flow or stasis at some stage can induce thrombosis, a phenomenon observed in neonates treated with Extra Corporal Membrane Oxygenation (ECMO) using right jugular vein cannulation [17]. Birth trauma with displacement of the occipital bone can also decrease flow in the superior sagittal sinus and induce thrombosis [18]. We hypothesized that high mean airway pressure could lead to reduced venous return, stasis and thrombosis in the transverse sinus. Different ventilator settings were studied. High frequency ventilation did not significantly increase the risk for developing CSVT. The only significant difference was found in duration of mechanical ventilation in affected infants. Mean airway pressure did not differ between the groups. It may well be that infants who need ventilatory support are sicker and develop other

risk factors for CSVT (e.g. sepsis or dehydration); alternatively, prolonged mechanical ventilation may increase the risk of venous thrombosis per se.

There are normal variants in the distribution of blood flow in the transverse sinuses; different studies show that the right transverse sinus is dominant in the majority of human adults [19-23] and neonates[22]. However in our cohort we found no side-to-side difference.

Management of CSVT is controversial[24]. There are no randomized trials, although there are some data regarding safety of anticoagulation in neonates with CSVT [3, 25, 26]. Duration of treatment or optimal dosing is not known. Recanalization of thrombotic veins is faster in neonates than older children; therefore treatment for 6 weeks is thought to be sufficient [27]. The 'Chest guidelines 9th edition'[27] recommends that neonates with CSVT without substantial intracranial hemorrhage should be treated with LMWH, at least for 6 weeks and no longer than three months. Intracranial hemorrhage should be monitored radiologically for 5-7 days and treatment should not start until there are signs of thrombosis propagation [27]. In our cohort, we treated six infants with LMWH; local hemorrhagic complications occurred in three. Intracranial hemorrhage was not a sequel in any infant in this study. The other infants were not treated due to the partial nature of the occlusion with sufficient flow in the transverse sinus and distal sigmoid sinus.

Our study has limitations. For optimal ultrasound visualization of the venous system: anterior, posterior and mastoid fontanel on both sides should be evaluated. However because this is time-consuming and because of NIDCAP principles [28] changing head and body positions are considered exhausting for the patients, we tried to minimalize scanning time. Therefore we presumed that if flow was visualized through the anterior fontanel this would confidently exclude clinically relevant CSVT. However this could implicate that the incidence we found still underestimates the overall incidence of CSVT. The straight sinus and vein of Galen were not included in this study. Further research is needed to study these vessels as well.

Due to the small sample size and univariate analysis, the associations we report needs confirmation from further research.

Our cohort is too young to determine long-term outcome. Neurodevelopmental outcome can provide insight in effects of asymptomatic thrombosis, effect of treatment, and the need for treatment of these infants. We also have no extensive data on genetic prothrombotic tendencies in these infants. Another limitation is that intra- and interobserver is lacking due to the study design.

Before the start of this study a standard treatment protocol was not in place. Treatment was decided on an individual basis and depended on images acquired with cranial US, risk factors and clinical status of the patient. Further research will be necessary with protocols tailored to diagnostic and therapeutic options.

These results raise many questions especially regarding safety of treatment. Is it necessary to treat all asymptomatic partial thrombosis given the side effects of treatment? How is the long-term neurodevelopmental outcome with or without treatment?

In summary, this study illustrates – using serial cranial US with color Doppler – that the incidence of CSVT in preterm infants is higher than previously reported. Preterm CSVT is probably a multifactorial condition and further research is needed to identify risks, treatment options and outcome.

References

1. Bayley. Bayley Scales of Infant and Toddler Development (BSID-III). 2006; **3rd edn.**: Harcourt Assessment/Psychological Corporation, San Antonio.
2. Berfelo FJ, Kersbergen KJ, van Ommen CH, Govaert P, van Straaten HL, Poll-The BT, et al. Neonatal cerebral sinovenous thrombosis from symptom to outcome. Stroke. 2010; **41**(7): 1382-8.
3. deVeber G, Andrew M, Adams C, Bjornson B, Booth F, Buckley DJ, et al. Cerebral sinovenous thrombosis in children. N Engl J Med. 2001; **345**(6): 417-23.
4. Kenet G, Lutkhoff LK, Albisetti M, Bernard T, Bonduel M, Brandao L, et al. Impact of thrombophilia on risk of arterial ischemic stroke or cerebral sinovenous thrombosis in neonates and children: a systematic review and meta-analysis of observational studies. Circulation. 2010; **121**(16): 1838-47.
5. Kersbergen KJ, Groenendaal F, Benders MJ, de Vries LS. Neonatal cerebral sinovenous thrombosis: neuroimaging and long-term follow-up. J Child Neurol. 2011; **26**(9): 1111-20.
6. Plaisier A, Raets MM, van der Starre C, Feijen-Roon M, Govaert P, Lequin MH, et al. Safety of routine early MRI in preterm infants. Pediatr Radiol. 2012.
7. van Wezel-Meijler G, Steggerda SJ, Leijser LM. Cranial ultrasonography in neonates: role and limitations. Semin Perinatol. 2010; **34**(1): 28-38.
8. Yang JY, Chan AK, Callen DJ, Paes BA. Neonatal cerebral sinovenous thrombosis: sifting the evidence for a diagnostic plan and treatment strategy. Pediatrics. 2010; **126**(3): e693-700.
9. Deeg KH, Lode HM. [Trans-fontanellar Doppler sonography of the intracranial veins in infants—part I—Normal values] Transfontanellare Doppler-Sonographie der Hirnvenen im Sauglingsalter—Teil I—Normalbefunde. Ultraschall Med. 2005; **26**(6): 507-17.
10. Taylor GA. Intracranial venous system in the newborn: evaluation of normal anatomy and flow characteristics with color Doppler US. Radiology. 1992; **183**(2): 449-52.
11. Bezinque SL, Slovis TL, Touchette AS, Schave DM, Jarski RW, Bedard MP, et al. Characterization of superior sagittal sinus blood flow velocity using color flow Doppler in neonates and infants. Pediatr Radiol. 1995; **25**(3): 175-9.
12. Miller E, Daneman A, Doria AS, Blaser S, Traubici J, Jarrin J, et al. Color Doppler US of normal cerebral venous sinuses in neonates: a comparison with MR venography. Pediatr Radiol. 2012.
13. Richardson DK, Corcoran JD, Escobar GJ, Lee SK. SNAP-II and SNAPPE-II: Simplified newborn illness severity and mortality risk scores. J Pediatr. 2001; **138**(1): 92-100.
14. Onland W, Offringa M, Cools F, De Jaegere AP, Rademaker K, Blom H, et al. Systemic Hydrocortisone To Prevent Bronchopulmonary Dysplasia in preterm infants (the SToP-BPD study); a multicenter randomized placebo controlled trial. BMC Pediatr. 2011; **11**: 102.
15. Fitzgerald KC, Williams LS, Garg BP, Carvalho KS, Golomb MR. Cerebral sinovenous thrombosis in the neonate. Arch Neurol. 2006; **63**(3): 405-9.
16. Govaert P, Ramenghi L, Taal R, Dudink J, Lequin M. Diagnosis of perinatal stroke II: mechanisms and clinical phenotypes. Acta Paediatr. 2009; **98**(11): 1720-6.
17. Wu YW, Miller SP, Chin K, Collins AE, Lomeli SC, Chuang NA, et al. Multiple risk factors in neonatal sinovenous thrombosis. Neurology. 2002; **59**(3): 438-40.
18. Govaert P, Voet D, Achten E, Vanhaesebrouck P, van Rostenberghe H, van Gysel D, et al. Noninvasive diagnosis of superior sagittal sinus thrombosis in a neonate. Am J Perinatol. 1992; **9**(3): 201-4.
19. Browning H. The confluence of dural venous sinuses. Am J Anat. 1953; **93**(3): 307-29.
20. Dora F, Zileli T. Common variations of the lateral and occipital sinuses at the confluens sinuum. Neuroradiology. 1980; **20**(1): 23-7.
21. Ayanzen RH, Bird CR, Keller PJ, McCully FJ, Theobald MR, Heiserman JE. Cerebral MR venography: normal anatomy and potential diagnostic pitfalls. AJNR Am J Neuroradiol. 2000; **21**(1): 74-8.
22. Widjaja E, Shroff M, Blaser S, Laughlin S, Raybaud C. 2D time-of-flight MR venography in neonates: anatomy and pitfalls. AJNR Am J Neuroradiol. 2006; **27**(9): 1913-8.

23. Alper F, Kantarci M, Dane S, Gumustekin K, Onbas O, Durur I. Importance of anatomical asymmetries of transverse sinuses: an MR venographic study. Cerebrovasc Dis. 2004; **18**(3): 236-9.
24. Moharir MD, Shroff M, Pontigon AM, Askalan R, Yau I, Macgregor D, et al. A prospective outcome study of neonatal cerebral sinovenous thrombosis. J Child Neurol. 2011; **26**(9): 1137-44.
25. Heller C, Heinecke A, Junker R, Knofler R, Kosch A, Kurnik K, et al. Cerebral venous thrombosis in children: a multifactorial origin. Circulation. 2003; **108**(11): 1362-7.
26. Barron TF, Gusnard DA, Zimmerman RA, Clancy RR. Cerebral venous thrombosis in neonates and children. Pediatr Neurol. 1992; **8**(2): 112-6.
27. Monagle P, Chan AK, Goldenberg NA, Ichord RN, Journeycake JM, Nowak-Gottl U, et al. Antithrombotic therapy in neonates and children: Antithrombotic Therapy and Prevention of Thrombosis, 9th ed: American College of Chest Physicians Evidence-Based Clinical Practice Guidelines. Chest. 2012; **141**(2 Suppl): e737S-801S.
28. Als H, Lawhon G, Brown E, Gibes R, Duffy FH, McAnulty G, et al. Individualized behavioral and environmental care for the very low birth weight preterm infant at high risk for bronchopulmonary dysplasia: neonatal intensive care unit and developmental outcome. Pediatrics. 1986; **78**(6): 1123-32.

PART II

CHAPTER 4

INCIDENTAL SONOGRAPHIC DIAGNOSIS OF NEONATAL CAROTID OCCLUSION

M.M.A. Raets, M.H. Lequin, A. Plaisier, J. Dudink, P. Govaert

Acta Paediatrica, 2013 Apr; 102(4):e187-190.

Abstract

Cranial ultrasonography including colour Doppler can detect neonatal carotid flow problems at an early stage, even before symptoms occur. Different pathogeneses can be identified. The condition is more frequent than previously reported. If the circle of Willis is fully developed this can prevent brain injury even in case of total carotid flow obstruction. In conclusion screening of the carotid artery in critical ill neonates may detect complications of treatment at an early stage.

Introduction

Imaging of the brain in preterm and term infants is important. It can be used for detection of abnormalities which may correlate with the clinical presentation or it can be performed to rule out or screen for abnormalities. In an optimal setting, magnetic resonance imaging (MRI) is the best neuroimaging technique due to its good spatial resolution, excellent soft-tissue contrast and quantitation of brain injury [1-3]. However the use of MRI is hampered because it requires transport, sometimes sedation, such that critically ill neonates may not be stable enough to be scanned. Therefore, serial imaging is difficult.

Transfontanellar cranial ultrasound (CUS) is a safe and non-invasive method which can be performed bedside, even when a patient is unstable[4] . CUS is nearly universally available on NICUs which allows serial imaging. Therefore CUS is the method of choice for brain imaging in daily practice in the neonatal intensive care unit. Extensive Doppler visualisation of the circle of Willis is not done routinely. In many cases only Doppler measurements are performed in the superior sagittal sinus to check its patency and in the pericallosal artery, to screen for luxury perfusion or increased resistance index. There is no additional training necessary to visualize the carotid arteries if the echographist is used to work with colorDoppler. One is able to screen for the carotid arteries in a coronal plane through the foramen of Monro.

With six case histories, we illustrate that CUS with extensive colour Doppler of many intracranial vessels, including the circle of Willis is feasible and that it can detect flow problems at an early, even pre-symptomatic stage.

In our center all infants are scanned according to standard protocol, including coronal and sagittal/parasagittal planes through the anterior fontanel and colour Doppler visualisation of different intracranial vessels (carotid arteries, basilar artery, ACA, MCA, striatal arteries, both jugular veins and transverse sinus). We identified uncommon carotid pathology in six patients during one year (6 of 190 patients). In the context of this paper we will only focus on these six patients. Images were obtained with the 8 MHz probe of an Esaote My Lab 70 (Genova, Italy). Ethical approval was obtained from the local ethics committee.

Case 1: a preterm infant, born at 26 weeks gestation, was admitted in September 2010. He exhibited complications associated with Infant Respiratory Distress Syndrome, which was treated with mechanical ventilation. Initial routine CUS was normal. Because enteral feeding proved difficult, a Broviac catheter was inserted into the right internal jugular vein 11 days after birth, and CUS was performed 4 days after insertion. An unexpected phenomenon was observed with colour Doppler sonography (Figure 1): the left internal carotid artery exhibited anterograde blood flow toward the circle of Willis, whereas the right internal carotid artery presented retrograde cranio-cervical flow.

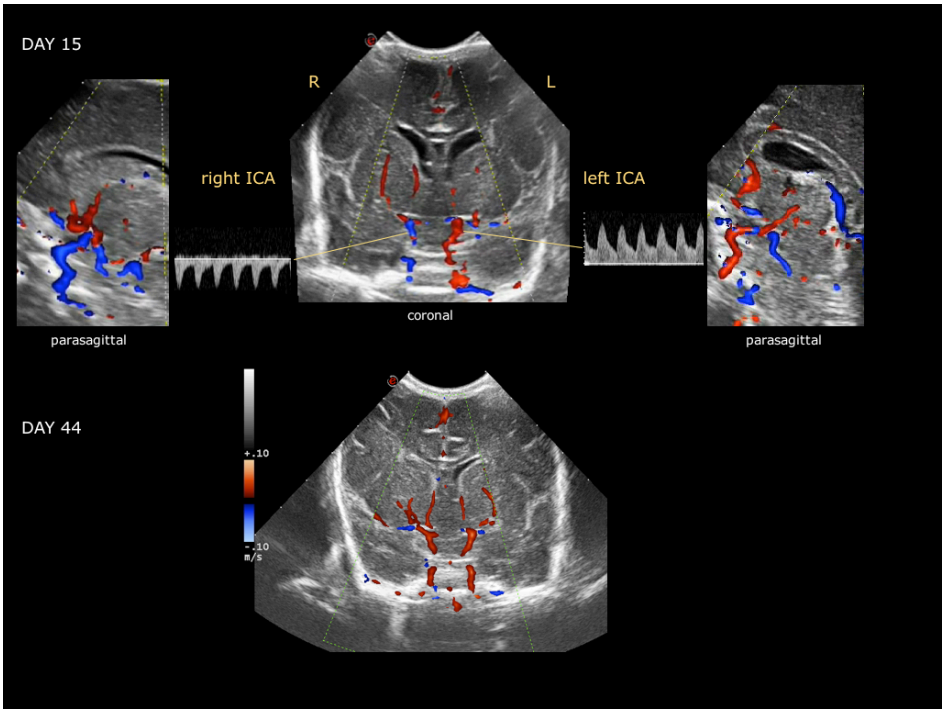

Figure 1 Composition of colour Doppler images (through the anterior fontanelle) on day 15 and day 44 after birth: the top row depicts coronal (in the middle) and sagittal scans of the flow direction in both carotid arteries, including velocity profiles. Normalization is illustrated in the bottom coronal image.

Axial images illustrated reversed flow in the A1 segment of the right anterior cerebral artery and forward flow through the right posterior communicating artery from the P1 segment of the posterior cerebral artery (Figure 2). Ultrasound of the neck documented thrombus in the common carotid artery proximal to the bifurcation. Because the circle of Willis was fully developed and competent, flow was maintained and a stroke did not occur. The surgeon noted that the right common carotid artery had been accidentally punctured. MRI was performed and included "time of flight" images on day 25. These data showed asymmetrical signal intensity in the carotid arteries. After team debate we decided not to treat this thrombosis due to the risk for embolism. On day 20 however a thrombosis in the left transverse sinus was documented and treatment with low molecular-weighted heparin (LMWH) was started. By week 7, the right internal carotid artery had regained forward flow (Figure 1). Serial CUS showed no focal lesions until discharge at 35 weeks postmenstrual age.

Case 2: a preterm infant born at 27 weeks of gestation was admitted in April 2011. She needed ventilator support by IRDS, intubation proved difficult. Three days of respiratory support was given non-invasively. On day 5 an urgent tracheotomy was necessary because of respiratory insufficiency, difficult intubation by laryngeal edema and velopharyngeal hypotonia. The

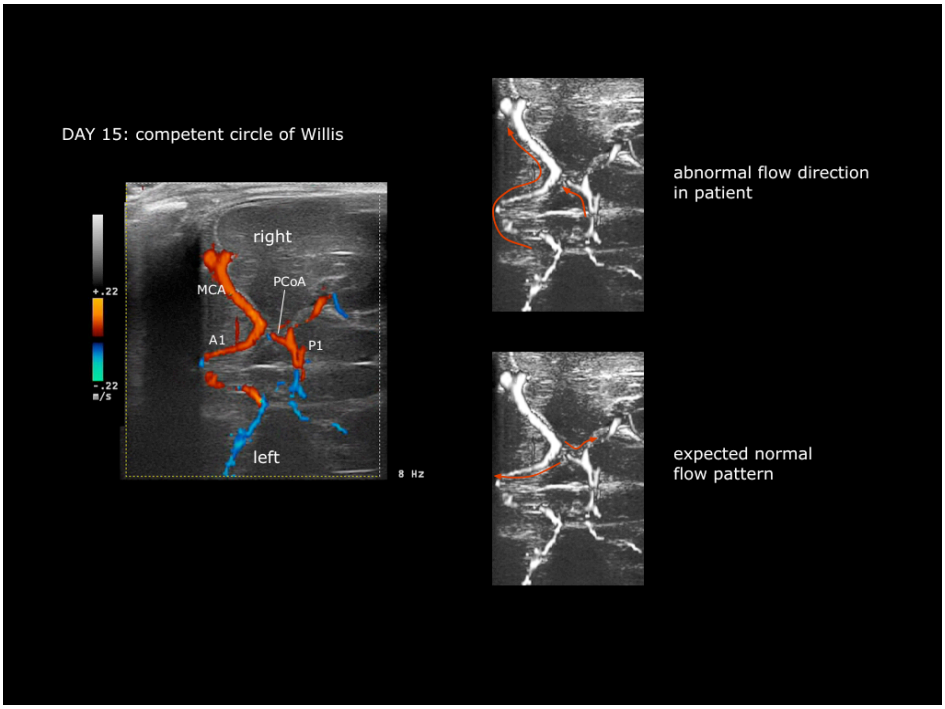

Figure 2 Axial colour Doppler image through the right sphenoid fontanelle on day 15. Adjacent schemes illustrate expected and abnormal flow direction.

procedure was difficult and the surgeon ligated a vessel in the operating area. On day 11 after birth standard CUS revealed retrograde flow in the right internal carotid artery. Axial images were comparable to Figure 1. In retrospect the vessel ligated during the procedure must have been the right internal carotid artery. Genetic counseling and DNA diagnostics confirmed 22q11deletion.

Case 3: a preterm infant born at 31 weeks of gestation was admitted in May 2011. Pregnancy and delivery were uncomplicated. CUS on admission documented extensive intraventricular haemorrhage complicated by venous infarction of the right anterior terminal vein. Serial CUS illustrated a transient absence of flow in the left carotid artery. Adjuvant images were obtained through the sphenoid fontanel, compensatory flow through the circle of Willis was not seen. A Rickham drain was inserted for post-haemorrhagic ventricular dilatation. A few days after insertion the head circumference remained stable and further tapping of cerebrospinal fluid was not necessary.

Case 4: a near term infant was admitted in June 2011 because of seizures within 24 hours after birth. Pregnancy and delivery were uncomplicated. CUS showed extensive intraventricular haemorrhage right without venous infarction and a transient absence of flow in the left carotid

artery. He was treated with anti-epileptic drugs and frequently monitored for post-hemorrhagic ventricular dilatation; only one lumbar puncture was indicated.

Case 5: a preterm infant, first of twins, born at 34 weeks of gestation, was admitted in April 2011 because of respiratory insufficiency due to pneumothorax. The second postnatal day he was transferred to the paediatric intensive care unit for extra-corporal membrane oxygenation (ECMO) to treat persistent pulmonary hypertension. CUS after ECMO failed to document brain injury, whereas retrograde filling of the internal carotid artery was present. His course was complicated by severe bronchopulmonary dysplasia.

Case 6: a near term infant, second of twins, was admitted because of seizures within 24 hours after birth. Pregnancy and delivery were uncomplicated. CUS on admittance did not reveal haemorrhage or other lesions. The MR-DTI sequence documented stroke in the posterior trunk of the left MCA and a perforator stroke in the left thalamus. Additional colour Doppler imaging after MRI showed absent flow in the left carotid artery, with compensatory flow to the left MCA along the anterior communicating artery (figure 3.). Because of a suspected thrombus in the carotid artery the patient was treated with heparin. After five days the left carotid artery regained forward flow.

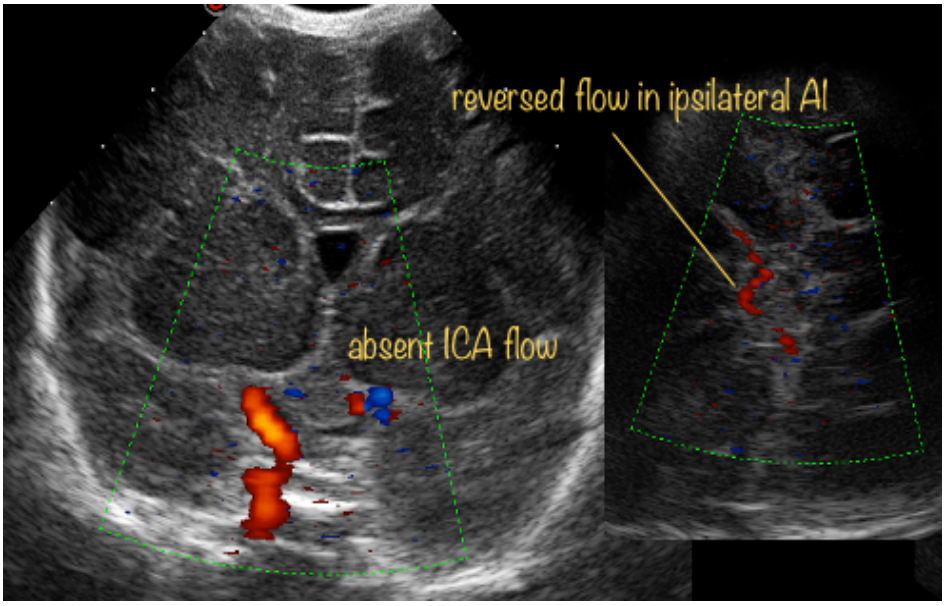

Figure 3 Absent flow in the left carotid artery, with compensatory flow to the left MCA along the anterior communicating artery

Discussion

The history of the first two patients illustrates how acute complete obstruction of the common carotid artery can be missed in an extremely low birth weight (ELBW) preterm infant due to a lack of symptoms because of sufficient collateral flow through the circle of Willis. These observations also demonstrate the potential of CUS to document changes in the condition of an ELBW infant. With transfontanellar colour and power Doppler imaging, we investigated flow in vessels high up in the neck and documented the competence of the anterior and posterior parts of the circle of Willis to detect pre-symptomatic flow problems. The images of patient 1, 2 and 5 suggest obstruction of the right common carotid artery and retrograde filling of the internal carotid artery from the circle of Willis. The explanation for these observations was that obstruction was located below the bifurcation, which conserved anterograde flow in the right external carotid artery. If an internal carotid artery is obstructed, the contralateral carotid artery may augment flow and perfuse the area supplied by the affected anterior cerebral artery; this mechanism, together with forward flow through the posterior communicating artery ipsilateral to the obstruction, sustains perfusion of the middle cerebral artery on the affected side [5, 6][Figure 1,2]. The images in patient 6 were compatible with ICA thrombosis between the bifurcation and the circle of Willis.

Some discussion of the variability of the circle of Willis is warranted. Our findings suggest that colour Doppler and power angiography data allow to study the circle of Willis in appropriate clinical settings (e.g. before and after ECMO, jugular or carotid cannulation, and aortic surgery). Thomas Willis described his "circle" in 1664: it is generally a 9-sided polygon that is completely formed in the 52-day-old embryo [2]. Variations result from different mechanisms [7, 8], which may be developmental (genetic or acquired), but may also result from structural changes acquired during adulthood [3]. The definition of a normal circle is debatably based on a study by Alpers et al. who found a 52 % incidence of normal circles in a postmortem population without brain injury [5]. The circle can be incomplete because of a lack of polygonal components or can have more than nine vessels forming the polygon [9]; vessels may also be present as expected but exhibit asymmetric caliber and flow. ICA agenesis or hypoplasia is most often unilateral and rare (< 1/10,000 individuals). Perfusion of the MCA on the affected side may occur through a transcavernous collateral from the contralateral ICA, from intact parts of the circle of Willis or from anastomoses with the external carotid artery [10, 11]. The main vascular supply of the brain during bilateral agenesis of the ICA is the vertebrobasilar system [12-14]. CUS is useful in detecting unilateral carotid artery agenesis [10, 11, 15, 16].

The remarkable phenomenon of acute competence of the circle of Willis is also observed in many neonates who are treated with arterio-venous ECMO, where the right carotid artery is cannulated (patient 5). This procedure may predispose such patients to brain injury; the incidence of cerebrovascular injury ranges from 10 to 52 % [17].

Patient 3,4 and 6 had different flow patterns and did not show retrograde flow in the carotid artery. In these patients flow was absent or seriously decreased in the left carotid artery, which spontaneously restored within days. Cerebral vasospasm as complication of subarachnoid haemorrhage is well-known and can result in neurologic deficits. Only three pediatric cases are reported of intraventricular haemorrhage leading to vasospasm [18-20]. We hypothesize that patient 3 and 4, both with intraventricular haemorrhage, had no visible Doppler signal of the left internal carotid artery due to (transient) vasospasm. Patient 6 had an ICA thrombosis proximal to the bifurcation.

Puncture of the carotid artery, seen in patient 1, is a complication of jugular vein catheter insertion, and the incidence is approximately 8,5-23% [21, 22]. However (complete) obstruction of the common carotid artery has not yet been reported in a preterm infant, although Broviac catheters are frequently inserted.

Management of cerebral arterial thrombosis is still controversial. Recurrent arterial ischemic stroke or carotid dissection is treated with LMWH at least for six weeks[23]. However treatment strategies for carotid thrombosis are not specifically described in these guidelines. Therefore we decided not to treat in the acute phase because of the risk of embolism.

In conclusion targeted CUS including colour Doppler can detect flow problems at an early even presymptomatic stage. Different pathogeneses can be identified for carotid flow problems. The neonatal circle of Willis is competent in preventing brain injury if fully developed. Screening of the carotid artery in critical ill neonates can detect complications of treatment at an early stage. There is a place for routine insonation of the large neck vessels in critically ill neonates.

References

1. Huppi PS, Dubois J. Diffusion tensor imaging of brain development. Semin Fetal Neonatal Med. 2006; **11**(6): 489-97.
2. Rutherford MA. What's new in neuroimaging? Magnetic resonance imaging of the immature brain. Eur J Paediatr Neurol. 2002; **6**(1): 5-13.
3. Counsell SJ, Rutherford MA, Cowan FM, Edwards AD. Magnetic resonance imaging of preterm brain injury. Arch Dis Child Fetal Neonatal Ed. 2003; **88**(4): F269-74.
4. van Wezel-Meijler G, Steggerda SJ, Leijser LM. Cranial ultrasonography in neonates: role and limitations. Semin Perinatol. 2010; **34**(1): 28-38.
5. Hartkamp MJ, van Der Grond J, van Everdingen KJ, Hillen B, Mali WP. Circle of Willis collateral flow investigated by magnetic resonance angiography. Stroke. 1999; **30**(12): 2671-8.
6. van Laar PJ, Hendrikse J, Klijn CJ, Kappelle LJ, van Osch MJ, van der Grond J. Symptomatic carotid artery occlusion: flow territories of major brain-feeding arteries. Radiology. 2007; **242**(2): 526-34.
7. Vasovic L, Milenkovic Z, Pavlovic S. Comparative morphological variations and abnormalities of circles of Willis: a minireview including two personal cases. Neurosurg Rev. 2002; **25**(4): 247-51.
8. Arey B. Developmental Anatomy. 6th Edn Saunders, Philadelphia. 1954: 364-73.
9. Vasovic LP. The tenth vascular component in a rare form of the cerebral arterial circle of fetuses. Cells Tissues Organs. 2004; **178**(4): 231-8.
10. Lee JH, Oh CW, Lee SH, Han DH. Aplasia of the internal carotid artery. Acta Neurochir (Wien). 2003; **145**(2): 117-25; discussion 25.
11. Given CA, 2nd, Huang-Hellinger F, Baker MD, Chepuri NB, Morris PP. Congenital absence of the internal carotid artery: case reports and review of the collateral circulation. AJNR Am J Neuroradiol. 2001; **22**(10): 1953-9.
12. Tasar M, Yetiser S, Tasar A, Ugurel S, Gonul E, Saglam M. Congenital absence or hypoplasia of the carotid artery: radioclinical issues. Am J Otolaryngol. 2004; **25**(5): 339-49.
13. Sun J, Jiang D, Zhang S. Bilateral internal carotid artery agenesis with artery compression of the brain parenchyma. J Neurol Sci. 2008; **272**(1-2): 191-3.
14. Gonzalez-Cuyar LF, Lam-Himlin D, Tavora F, Burke A, Castellani RJ. Bilateral internal carotid absence: a case report of a rare congenital anomaly. Cardiovasc Pathol. 2008; **17**(2): 113-6.
15. Harps E, Helmke K. Diagnosis of congenital absence of internal carotid artery by power angio sonography. Eur Radiol. 1998; **8**(7): 1245-7.
16. Lie T. Congenital anomalies of the carotid arteries. Amsterdam: Exerpta Medica. 1968: 35-51.
17. Bulas DI, Taylor GA, O'Donnell RM, Short BL, Fitz CR, Vezina G. Intracranial abnormalities in infants treated with extracorporeal membrane oxygenation: update on sonographic and CT findings. AJNR Am J Neuroradiol. 1996; **17**(2): 287-94.
18. Spader HS, Doberstein CE, Rao AJ, Jayaraman MV. Central fever as an early predictor of vasospasm in a child with isolated intraventricular hemorrhage. Clin Neurol Neurosurg. 2011; **113**(2): 146-9.
19. Yanaka K, Hyodo A, Tsuchida Y, Yoshii Y, Nose T. Symptomatic cerebral vasospasm after intraventricular hemorrhage from ruptured arteriovenous malformation. Surg Neurol. 1992; **38**(1): 63-7.
20. Pendharkar AV, Guzman R, Dodd R, Cornfield D, Edwards MS. Successful treatment of severe cerebral vasospasm following hemorrhage of an arteriovenous malformation. Case report. J Neurosurg Pediatr. 2009; **4**(3): 266-9.
21. Verghese ST, McGill WA, Patel RI, Sell JE, Midgley FM, Ruttimann UE. Ultrasound-guided internal jugular venous cannulation in infants: a prospective comparison with the traditional palpation method. Anesthesiology. 1999; **91**(1): 71-7.
22. Karapinar B, Cura A. Complications of central venous catheterization in critically ill children. Pediatr Int. 2007; **49**(5): 593-9.
23. Monagle P, Chan AK, Goldenberg NA, Ichord RN, Journeycake JM, Nowak-Gottl U, et al. Antithrombotic therapy in neonates and children: Antithrombotic Therapy and Prevention of Thrombosis, 9th

ed: American College of Chest Physicians Evidence-Based Clinical Practice Guidelines. Chest. 2012; **141**(2 Suppl): e737S-801S.

CHAPTER 5

RISK FACTORS, CLINICAL PRESENTATION AND NEUROIMAGING FINDINGS OF NEONATAL PERFORATOR STROKE

G.M. Ecury-Goossen, M.M.A. Raets, M.H. Lequin,
M. Feijen-Roon, P. Govaert, J. Dudink

Stroke, 2013 Aug; 44(8): 2115-20.

Abstract

Background and Purpose – To date, studies on neonatal stroke have mainly focused on cortical stroke. We have focused on perforator strokes, non-cortical strokes in the arterial vascular perforator area. We sought to identify risk factors and to evaluate clinical presentation and neuroimaging findings for neonatal perforator stroke, which seems to be under-recognized.

Methods – All infants admitted to our tertiary intensive care unit in almost twelve years diagnosed with postnatal brain imaging to have a perforator stroke were enrolled in this study. Demographic, perinatal and postnatal data were evaluated.

Results – 79 perforator strokes were detected in 55 patients (28 male) with a median gestational age of 37 1/7 weeks (range 24 1/7 to 42 1/7 weeks, 25 preterm). Perforator stroke was asymptomatic in most patients (58%). Initial diagnosis was predominantly made with cranial ultrasound (80%) in the first week of life (60%). Risk factors for stroke were present in all cases: maternal, fetal or perinatal. Likely pathogenic mechanisms were prolonged birth asphyxia (16%), hypoxia or hypotension (15%), embolism (15%), infection (15%), acute blood loss (9%) and birth trauma (9%).

Conclusions – Previously described risk factors for developing neonatal main artery stroke are probably also associated with neonatal perforator stroke. Perforator stroke is often asymptomatic, but cranial ultrasound is a reliable diagnostic tool in diagnosing perforator stroke.

Introduction

Advances in neuroimaging techniques have greatly improved detection and understanding of neonatal stroke.[1] Reported incidence of neonatal stroke in term newborns ranges from 1 in 2300 to 1 in 5900.[1-3] Benders et al. reported an incidence of 7 in 1000 preterm admissions.[4] In most cases of neonatal stroke, the middle cerebral artery (MCA) is involved. For each of the cerebral arteries, main branch (cortical or pial) or perforator branch involvement can be distinguished.[5] To date, studies on neonatal stroke have mainly focused on cortical stroke. Perforator stroke is apparently still under-recognized and little is known about risk factors and clinical presentation.

To gain more insight into risk factors, clinical presentation and neuroimaging findings of neonatal perforator stroke, we report the largest cohort to date of neonates diagnosed with perforator stroke.

Patients and methods

All infants admitted to our tertiary (neonatal) intensive care unit between August 1999 and April 2011 and diagnosed with perforator stroke by postnatal cranial ultrasound (CUS) and/or magnetic resonance imaging (MRI) were enrolled. The study was approved by the medical ethical committee of the Erasmus Medical Centre Rotterdam, the Netherlands.

Perforator stroke involves the perforators of the anterior choroidal artery (AChA), anterior cerebral artery (ACA), middle cerebral artery (MCA), posterior cerebral artery (PCA) and posterior

Table 1 Perforator stroke classification

Vessel	Arterial perforator vessel	Territory
ACA	Heubner's	Rostroventral and lateral part of caudate head Lateral part of anterior limb of internal capsula (ALIC)
MCA	Lenticulostriate	Posterior part caudate head Lateral part globus pallidus Putamen
PCA		Lateral, inferior and paramedian parts of thalamus
AchA		Medial part of globus pallidus Posterior limb of internal capsula (PLIC) Amygdaloid nuclei
PCoA		Supero-anterior part of medial thalamic nuclei
Circle of Willis	Hypothalamus Thalamus	 Superolateral parts of thalamus

ACA= anterior cerebral artery, AchA= anterior choroidal artery, MCA= middle cerebral artery, PCA= posterior cerebral artery, PCoA=posterior communicating artery

communicating artery (PCoA), supplying amongst others thalamus, striatum, posterior limb of the internal capsule (PLIC) and centrum semiovale (table 1)[6].

The anatomy of basal ganglia perforators is detailed in previous papers.[5, 6] Perforator stroke was defined as a well-delineated hyperechoic lesion in thalamus and/or striatum on CUS (figure 1). Isolated lesions in centrum semiovale were not included, as these can not only be caused by focal arterial infarction in a terminal lateral striatal MCA branch. An alternative explanation could be by a stroke of a ventriculopetal cortical arterial branch of the MCA with occlusion away from the surface as it courses in white matter. Also, isolated lesions in the centrum semiovale can be confused with punctuate white matter lesions. On MRI perforator stroke was defined as a well-lineated lesion, hypointense on T1-weighed imaging, hyperintense in T2-weighed imaging, hypointense on apparent diffusion coefficient maps and hyperintense on diffusion-weighted imaging (DWI).

All preterm infants had been screened by standard local CUS protocol, as a matter of clinical routine. This entailed at least two ultrasound studies in the first week of life, followed by weekly ultrasound studies until discharge. Term infants at risk for brain damage are screened with cranial ultrasound at the discretion of the attending physician. Sonograms were obtained using a Sequoia (Siemens, Mountain View, California) or an Esaote system (Mylab 70, Genova Italy). MRI

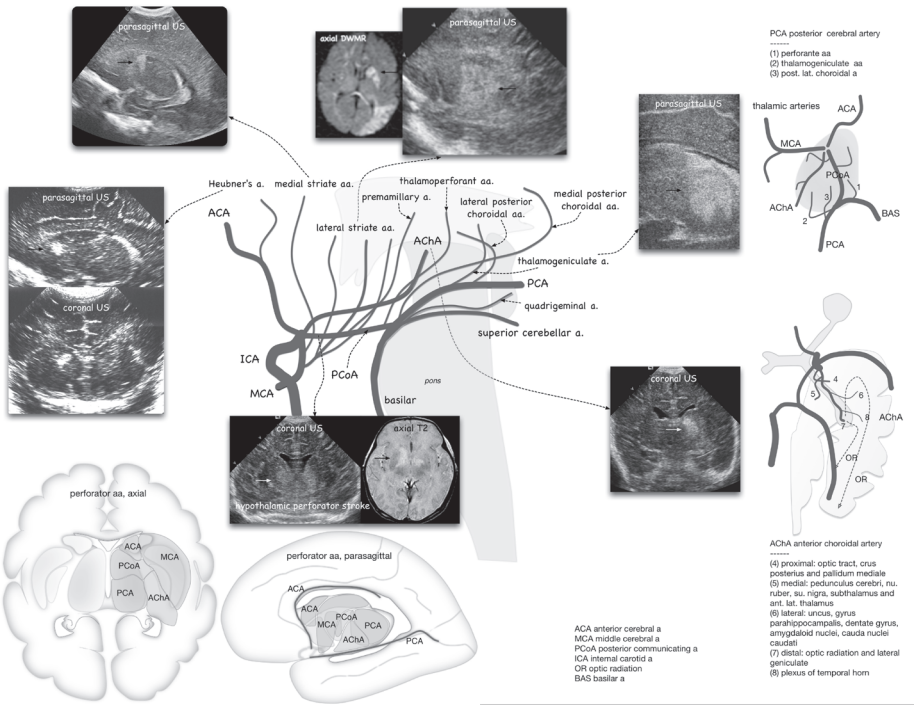

Figure 1 Axial and parasagittal perforator templates with illustrative cranial ultrasound and/or MRI images.

scanning was performed on a 1.5-T GE EchoSpeed scanner (GE Medical Systems, Milwaukee, Wisconsin), using an MR-compatible incubator provided with a specialized high-sensitivity neonatal head coil. Perforator strokes first diagnosed with MRI (ML), were reviewed by two neonatologists (JD, PG) who also reviewed all CUS and remaining MRI studies independently and sought consensus for questionable imaging findings.

Demographic, perinatal, postnatal and short-term follow-up data were retrieved from the medical records. Perinatal data included delivery, gestational age, gender, birth weight, Apgar score, and umbilical cord pH. Postnatal data included respiratory support, CRIB (Clinical Risk Index for Babies) score[7], the presence of central venous catheters, necrotizing enterocolitis (NEC), hypoglycemia, sepsis, and congenital heart disease. Clinical symptoms and neuroimaging findings preceding the radiological diagnosis of perforator stroke were reviewed.

Clinical phenotypes for perinatal stroke were classified by etiological mechanisms of neonatal stroke: infection, birth trauma, embolism, arteriopathy, blood loss, ECMO, asphyxia, prothrombotic condition, or unclassifiable.[8]

Results

Patient characteristics and risk factors

55 patients were included in this study, 0.7% of all 7713 patients admitted to our NICU during the study period, 0.5% of admitted preterm infants and 0.6% of admitted very low birth weight infants (birth weight < 1500 grams). Patient characteristics are shown in table 2. Twenty-five patients were born preterm (< 37 weeks postmenstrual age), 17 of whom before 32 weeks postmenstrual age. Eight mothers had received antenatal betamethasone. Vacuum extractor

Table 2 Patient characteristics

	No. (%) or median (range)
Gestational age, weeks	37 1/7 (24 1/7- 42 1/7)
Birth weight, grams	2640 (550-4440)
Male	28 (51%)
Singleton	48 (87%)
SGA	12 (22%)
Apgar score 1 minute (n=53)	5 (0-10)
Apgar score 5 minutes (n=54)	8 (2-10) n=14 Apgar ≤ 5
Umbilical cord pH (n=31)	7.18 (6.73-7.39) n=10 pH ≤ 7.05
CRIB score (n=54)	2 (0-13)
Age at diagnosis of perforator stroke, days	6 (1-82)

SGA= small for gestational age, CRIB= clinical risk index for babies

was used in five cases, and was unsuccessful in one, in which emergency caesarean section was then needed. Sixteen other patients were delivered by emergency caesarean section because of suspected fetal distress. Eighteen patients were diagnosed with birth asphyxia according to Levene's criteria.[9]

Risk factors for developing stroke are summarized in table 3. Data on placental histology were recorded in only 15 cases. These data could not be retrieved for the 39 outborn children. In 8 of 15 cases the placenta was classified as abnormal (table 3). There were no cases reported of perinatal stroke in a sibling. In two cases family history was positive for stroke. In both multiple family members suffered a stroke before the age of 50 years.

Thirteen children had culture proven sepsis, five had culture-proven meningitis (1 *Listeria monocytogenes*, 1 *E. Coli*, 3 *Group B Streptococcus*). Forty-five children had one or more central venous catheters before perforator stroke was diagnosed. Diagnosis of perforator stroke was followed by ultrasound evaluation of the catheter and major veins and/or heart in 24 cases. This revealed thrombosis in five (n=2 thrombosis around the tip of the catheter, n=3 venous thrombosis) and multiple air configurations in the liver in one patient (with an umbilical vein

Table 3 Risk factors for stroke

	No (%)
Maternal	
Pre-eclampsia/ HELLP syndrome	6 (11%)
Pregnancy induced- /pre-existing diabetes	3 (5%)
Placental abnormalities	8/15 (53%) n=3 chorioamnionitis, n=4 infarction, n=1 abruption
Perinatal	
Complicated delivery*	21 (38%)
Perinatal asphyxia	18 (33%)
Fetomaternal transfusion	6 (11%)
Neonatal	
Sepsis/Meningitis	18 (33%)
Patent ductus arteriosus	12 (22%)
Congenital heart defect	3 (5%)
ECMO	0 (0%)
Central venous catheter	45 (82%)
Hypoglycemia (≤ 2 mmol/l)	8 (15%)
Polycythemia (hematocrit > 65%)	8 (15%)
Prothrombotic risk factors	2/27 (7%)
NEC	6 (11%)

***forceps, vacuum extraction or ceasarian section**

HELLP= hemolytic anemia , elevated liver enzymes, low platelet count, ECMO= extra-corporeal membrane oxygenation, NEC= necrotizing enterocolitis.

catheter). Prothrombotic screening was done in 27 patients, revealing heterozygosity for factor V Leiden in two cases. Etiological mechanisms leading to the perforator stroke are summarized in table 4.

Table 4 Etiological mechanisms leading to perforator stroke

	Term (n=30)	Preterm (n=25)	Total
Infection			
Sepsis	1	2	3
Meningitis	4	1	5
Birth trauma	2	3	5
Embolism			
Proven thrombosis of catheter	1	1	2
Proven venous thrombosis	2	1	3
Suspected thrombosis	2	0	2
Suspected Air embolism	0	1	1
Arteriopathy	1	1	2
Acute blood loss	3	2	5
Birth asphyxia	6	3	9
Prothrombotic condition	0	0	0
Other			
Prolonged hypoxia/hypotension	3	5	8
Unclassifiable	5	5	10

Neuroimaging

Neuroimaging revealed 79 perforator strokes in 55 patients (table 5); right-sided in 21, left-sided in 20, and bilateral in 14. These 14 patients had two to four perforator strokes each. Of these fourteen, none had symmetrical deep gray matter injury and only one was diagnosed with birth asphyxia according to Levene's criteria[10].

Table 5 Perforator stroke

	Right	Left	Total
ACA Heubner's	6	4	10
MCA	13	19	32
PCA	7	11	18
AChA	6	2	8
PCoA	5	3	8
Circle of Willis	1	2	3
	38	41	79

In 44 patients (80%), the stroke was first identified with CUS. In 27 of them additional MRI was obtained, confirming the diagnosis of perforator stroke in all 27. In 10 patients (18%) the stroke was first diagnosed by MRI. In one patient the stroke was first diagnosed on a CT scan made elsewhere because of convulsions and later confirmed with MRI in our hospital.

In 33 patients (60%), the perforator stroke was diagnosed in the first week of life. Three patients with previous normal CUS findings were diagnosed with routine CUS after the age of 28 days. These were born preterm (between 28 and 31 weeks gestational age) and were diagnosed at term equivalent age.

13 patients had concomitant cortical stroke. In none of these patients perforator stroke could be explained solely by the concomitant cortical stroke. Table 6 gives an overview of all associated intracerebral lesions in this cohort.

Table 6 Associated intracerebral lesions

	No.
Cortical MCA stroke	11
Cortical PCA stroke	2
Watershed lesions	4
Grade II IVH and watershed lesions	1
Germinal matrix haemorrhage	2
Hydrocephalus	2
Cerebellar haemorrhage	1
Lissencephaly	1

Presenting symptoms and clinical course

Perforator stroke was asymptomatic in 32 patients (58%), all diagnosed with routine neuroimaging. Twenty other patients (36%) had clinical seizures prior to the diagnosis of perforator stroke. Eighteen of these twenty patients were diagnosed with conditions which are known to cause seizures, such as cortical stroke, birth asphyxia and meningitis. Eight patients presented with apnea, which was probably related to prematurity, not to perforator stroke. One patient with meningitis presented with hypertonia. One patient presented with unexplained diminished arousal response and was later diagnosed with multiple perforator strokes (right MCA lateral striate stroke, left circle of Willis, left PCA thalamic stroke).

None of the patients in this cohort received thrombolytic therapy. Six patients died before the age of one month. None of these deaths was related to perforator stroke, but rather to cardiopulmonary insufficiency due to other neonatal complications.

Discussion

To our knowledge, this is the largest cohort of newborns with perforator stroke studied. Both preterm and term infants were included. We found that perforator stroke was asymptomatic in most patients (58%). Most strokes were first diagnosed using CUS (80%), predominantly in the first week of life (60%). Still, 40% were diagnosed *after* the first week of life and 5% were diagnosed with routine CUS after the age of 28 days. These numbers illustrate the importance of routine serial CUS screening in infants admitted to a neonatal intensive care unit. Right-sided lesions occurred as frequently as left-sided lesions. Various likely pathogenic mechanisms for the development of perforator stroke could be distinguished, most often birth asphyxia, prolonged hypoxia or hypotension, embolism, and infection. It seems likely that previously described risk factors for developing neonatal main artery stroke can also apply to neonatal perforator stroke. Maternal, fetal or perinatal risk factors were present in all cases.

Pregnancy is considered to be a natural prothrombotic state. Thrombosis on the fetal side of the placenta can potentially lead to embolism in the fetal brain as a result of right-to-left direction of blood flow in the fetal ductus arteriosus and patency of the foramen ovale. Placental disorders may be under-recognized in neonatal stroke, as placentas are often not adequately examined or have been discarded before stroke becomes apparent.[11] We had data on placental abnormalities for only 15 mothers. More than half of them had placental abnormalities that could be regarded as a risk factor for developing stroke, specifically placental infarction, chorioamnionitis and placental abruption.[12-14]

In five patients, birth trauma was considered responsible for the occurrence of perforator stroke. Breech or forceps delivery can lead to indirect arterial injury by traction-elongation-torsion. Subdural bleeding after a complicated delivery can lead to compression and/or spasm of the MCA or its branches, thus leading to stroke. In one case birth trauma led to tentorium tear and uncal herniation, presumably leading to compression of the PCA and thus to PCA artery stroke.[15]

Perinatal arterial ischemic stroke has been reported to coincide with hypoxic-ischemic encephalopathy and hypoxic-ischemic encephalopathy has been suggested to be a risk factor for perinatal stroke.[16] Birth asphyxia can lead to congestion, endothelial injury and intravascular coagulation, thus leading to stroke.[17] Hypoxic-ischemic encephalopathy is more often present in full-term infants than in preterm infants with stroke.[18] This was also the case in the present study.

In this cohort, five perforator strokes were most likely related to meningitis. The perforator arteries course through the infected meninges to reach the brain parenchyma, and subarachnoid inflammation may encompass the major vessels of the circle of Willis. It has been suggested that local vasculopathy induced by infection and inflammation leads to thrombosis, resulting in occlusion of the arteries.[19]

Embolism was the most likely mechanism of stroke in 15% of patients in this cohort.

In two cases embolism was suspected, but not proven by ultrasound imaging; in one case from a femoral vein catheter used for exchange transfusion for jaundice, in another case from a suspected thrombus in a patient with an indwelling femoral vein catheter and abnormal anatomy of the inferior vena cava. In five cases proven thrombosis of a venous catheter or proven venous thrombosis most likely led to perforator stroke. In one patient abdominal ultrasound imaging revealed multiple air configurations in the liver, which probably led to air embolism, causing the stroke. These events could have been prevented by avoiding the use of central venous catheters. However, this is not always feasible, especially in a NICU setting. We recommend to critically evaluate the necessity of maintaining a central venous catheter.

In a study on risk factors for perinatal arterial stroke in preterm infants, hypoglycemia was the only independent risk factor identified in the neonatal period.[18] In the present study, hypoglycemia was present in 8 patients, 7 of whom were preterm. In the subgroup of preterm infants 7 of 25 (28 %) had hypoglycemia preceding the diagnosis of perforator stroke, compared to 1 of 33 term infants. It is not certain whether hypoglycemia did indeed precede perforator stroke, in view of the delay in detecting ultrasound abnormalities in infants with stroke.[18]

Prothrombotic screening at our institution has evolved over the years. Currently it entails antithrombin, protein S and protein C levels, factor V Leiden mutation and factor II G20210A mutation. In some cases screening is broadened to include lupus anticoagulans, MTHR C677T mutation and homocysteine levels. Twenty-eight patients (51%) in our study were not adequately screened for prothrombotic factors. Moreover, protein S, C and antithrombin levels were often not repeated after the neonatal period, so congenital deficiencies could not be ruled out. Two patients, both with isolated perforator stroke, were diagnosed with factor V Leiden heterozygosity. It is unlikely that only the presence of factor V Leiden led to isolated perforator stroke.[20] These patients had multiple other risk factors, particularly acute blood loss. Earlier studies have found that prothrombotic coagulation factors are present in more than half of neonatal main artery strokes, but it has been suggested that they likely play only a minor role in the pathogenesis of stroke.[11, 20]

In two patients stroke was most likely related to arteriopathy. One of these patients had Miller-Dieker lissencephaly, the other idiopathic infantile arterial calcification. Infantile arterial calcification has been related with cerebral infarction.[21]

Perinatal stroke is probably under-recognized because symptoms are subtle or absent and neonates may not undergo appropriate neuroimaging to identify stroke. It may be diagnosed serendipitously, as in the case of a term infant who was a control subject in a study of perinatal stroke and was diagnosed with a stroke on MRI.[22] In the present study, perforator stroke was usually first identified with CUS – probably because CUS is the first choice imaging modality at our NICU. There is no evidence that CUS is superior to MRI in detecting a stroke. In 27 of 44 patients in which perforator stroke was first identified with CUS, subsequent MRI was obtained. MRI confirmed the diagnosis of perforator stroke in all of these 27 cases, illustrating that CUS is reliable in diagnosing perforator stroke. Cranial ultrasound is an essential part of the routine

care in high-risk infants admitted to our NICU. Its major advantages are its safety, relatively low cost, the fact that it can be performed at bedside and can be repeated as often as necessary, making it the most suitable tool for serial imaging of the neonatal brain[23]. The value of CUS in detecting neonatal stroke has been described previously.[5, 24]

In preterm neonates, sequential routine neuroimaging led to the diagnosis of perforator stroke. In term infants, indications for neuroimaging such as birth asphyxia and convulsions ultimately led to the diagnosis. Cortical stroke in full-term infants most often presents with seizures, apnea and non-focal neurologic signs. [1, 25] Preterm infants are often free of symptoms, and cortical stroke is often diagnosed using routine cranial imaging. In the present study, perforator stroke was indeed asymptomatic in more than half of patients. Convulsions were a possible presenting symptom in one third of patients, mostly term neonates. In all but two patients these could be related to a more likely cause, such as concurrent cortical stroke, birth asphyxia and meningitis. The remaining two patients had multiple perforator strokes, possibly explaining the clinical presentation of seizures.

In (term) infants with perinatal stroke the left MCA is preferentially affected.[4] In our cohort, however, there was no side preference. We have no obvious explanation for this. It is not explained by preferential direction of emboli; there was also no left-sided preference in the subgroup of patients in whom embolism was the most likely pathogenic mechanism.

According to the definition provided by the Workshop on Ischemic Perinatal Stroke, neonatal ischemic stroke is diagnosed after birth and on or before the 28th postnatal day.[26] We chose to also include three neonates diagnosed after 28 days of life. These had normal CUS results prior to detection of perforator stroke. They were born preterm and were diagnosed at term corrected age with routine cranial ultrasound while still admitted. Two of them had proven thrombosis of a central venous catheter; one was diagnosed after developing NEC. This illustrates that perforator strokes in preterm infants can be diagnosed after the 28th day of life, especially when multiple risk factors are present.

Our report has limitations inherent to its retrospective design. As risk factors were studied retrospectively, risk analysis was incomplete and possibly biased. In relating the cases of perforator stroke to a clinical phenotype, ascertainment bias is inevitable.

Conclusion

In this cohort of neonatal perforator stroke various likely pathogenic mechanisms could be distinguished, notably prolonged hypoxia or hypotension, birth asphyxia, embolism, infection, acute blood loss, and birth trauma. Previously described risk factors for developing neonatal main artery stroke can probably also be applied to neonatal perforator stroke. In experienced hands, CUS is reliable in diagnosing perforator stroke. Isolated perforator strokes are most likely under-recognized, as clinical symptoms are almost always lacking. Routine serial CUS is

therefore recommended, especially in preterm neonates. In combination with cortical stroke, hypoxic-ischemic encephalopathy or meningitis, convulsions can be a presenting symptom, especially in term neonates. Insight gained from ongoing follow-up of this neonatal perforator stroke cohort will help more accurately predict neurodevelopmental outcome.

References

1. Nelson KB, Lynch JK. Stroke in newborn infants. Lancet Neurol. 2004; **3**(3): 150-8.
2. Lee J, Croen LA, Backstrand KH, Yoshida CK, Henning LH, Lindan C, et al. Maternal and infant characteristics associated with perinatal arterial stroke in the infant. JAMA. 2005; **293**(6): 723-9.
3. Chabrier S, Husson B, Dinomais M, Landrieu P, Nguyen The Tich S. New insights (and new interrogations) in perinatal arterial ischemic stroke. Thromb Res. 2011; **127**(1): 13-22.
4. Benders MJ, Groenendaal F, De Vries LS. Preterm arterial ischemic stroke. Semin Fetal Neonatal Med. 2009; **14**(5): 272-7.
5. Abels L, Lequin M, Govaert P. Sonographic templates of newborn perforator stroke. Pediatr Radiol. 2006; **36**(7): 663-9.
6. Govaert P. Sonographic stroke templates. Semin Fetal Neonatal Med. 2009; **14**(5): 284-98.
7. The CRIB (clinical risk index for babies) score: a tool for assessing initial neonatal risk and comparing performance of neonatal intensive care units. The International Neonatal Network. Lancet. 1993; **342**(8865): 193-8.
8. Govaert P, Ramenghi L, Taal R, Dudink J, Lequin M. Diagnosis of perinatal stroke II: mechanisms and clinical phenotypes. Acta Paediatr. 2009; **98**(11): 1720-6.
9. Levene MI LR. Chapter: The asphyxiated newborn infant, pages 405-426. Edinburgh: Churchil Livingstone 1995.
10. Swarte R, Lequin M, Cherian P, Zecic A, van Goudoever J, Govaert P. Imaging patterns of brain injury in term-birth asphyxia. Acta Paediatr. 2009; **98**(3): 586-92.
11. Rutherford MA, Ramenghi LA, Cowan FM. Neonatal stroke. Arch Dis Child Fetal Neonatal Ed. 2012; **97**(5): F377-84.
12. Cheong JL, Cowan FM. Neonatal arterial ischaemic stroke: obstetric issues. Semin Fetal Neonatal Med. 2009; **14**(5): 267-71.
13. Elbers J, Viero S, MacGregor D, DeVeber G, Moore AM. Placental pathology in neonatal stroke. Pediatrics. 2011; **127**(3): e722-9.
14. Lynch JK. Epidemiology and classification of perinatal stroke. Semin Fetal Neonatal Med. 2009; **14**(5): 245-9.
15. Govaert P, Vanhaesebrouck P, de Praeter C. Traumatic neonatal intracranial bleeding and stroke. Arch Dis Child. 1992; **67**(7 Spec No): 840-5.
16. Ramaswamy V, Miller SP, Barkovich AJ, Partridge JC, Ferriero DM. Perinatal stroke in term infants with neonatal encephalopathy. Neurology. 2004; **62**(11): 2088-91.
17. Voorhies TM, Lipper EG, Lee BC, Vannucci RC, Auld PA. Occlusive vascular disease in asphyxiated newborn infants. J Pediatr. 1984; **105**(1): 92-6.
18. Benders MJ, Groenendaal F, Uiterwaal CS, Nikkels PG, Bruinse HW, Nievelstein RA, et al. Maternal and infant characteristics associated with perinatal arterial stroke in the preterm infant. Stroke. 2007; **38**(6): 1759-65.
19. Hernandez MI, Sandoval CC, Tapia JL, Mesa T, Escobar R, Huete I, et al. Stroke patterns in neonatal group B streptococcal meningitis. Pediatr Neurol. 2011; **44**(4): 282-8.
20. Cnossen MH, van Ommen CH, Appel IM. Etiology and treatment of perinatal stroke; a role for prothrombotic coagulation factors? Semin Fetal Neonatal Med. 2009; **14**(5): 311-7.
21. van der Sluis IM, Boot AM, Vernooij M, Meradji M, Kroon AA. Idiopathic infantile arterial calcification: clinical presentation, therapy and long-term follow-up. Eur J Pediatr. 2006; **165**(9): 590-3.
22. Mercuri E, Cowan F, Gupte G, Manning R, Laffan M, Rutherford M, et al. Prothrombotic disorders and abnormal neurodevelopmental outcome in infants with neonatal cerebral infarction. Pediatrics. 2001; **107**(6): 1400-4.
23. van Wezel-Meijler G, Steggerda SJ, Leijser LM. Cranial ultrasonography in neonates: role and limitations. Semin Perinatol. 2010; **34**(1): 28-38.

24. Cowan F, Mercuri E, Groenendaal F, Bassi L, Ricci D, Rutherford M, et al. Does cranial ultrasound imaging identify arterial cerebral infarction in term neonates? Arch Dis Child Fetal Neonatal Ed. 2005; **90**(3): F252-6.
25. Kirton A, Armstrong-Wells J, Chang T, Deveber G, Rivkin MJ, Hernandez M, et al. Symptomatic neonatal arterial ischemic stroke: the International Pediatric Stroke Study. Pediatrics. 2011; **128**(6): e1402-10.
26. Raju TN, Nelson KB, Ferriero D, Lynch JK, Participants N-NPSW. Ischemic perinatal stroke: summary of a workshop sponsored by the National Institute of Child Health and Human Development and the National Institute of Neurological Disorders and Stroke. Pediatrics. 2007; **120**(3): 609-16.

CHAPTER 6

BRAIN INJURY ASSOCIATED WITH NEONATAL ECMO IN THE NETHERLANDS. A NATIONWIDE EVALUATION SPANNING TWO DECADES

M.M.A. Raets, J. Dudink, H. IJsselstijn, A.F.J. van Heijst, M.H.Lequin, R.J. Houmes, E.D. Wildschut, I.K.M Reiss, P. Govaert, D. Tibboel.

Pediatric Critical Care Medicine, 2013 Oct 10. [Epub ahead of print].

Abstract:

Objective: Our objective is to determine the incidence of and to classify ultrasound proven brain injury during neonatal ECMO in the Netherlands.

Design: Retrospective, nationwide study (Rotterdam and Nijmegen), spanning two decades. Cranial ultrasound images were reviewed independently by two investigators without knowledge of primary diagnosis, outcome, type of ECMO, or statistics. The scans were reviewed for lesion type and timing, with the use of a refined classification method for focal brain injury

Patients: 676 neonates were studied.

Main results: ECMO type was veno-arterial in 88%. Brain abnormalities were detected in 17.3%: primary hemorrhage was most frequent (8.8%). Stroke was identified in 5% of the total group, with a notable significant preference for the left hemisphere (in 70%). Lobar hematoma (prevalence 2.2 %) was also significantly left predominant.

Conclusion: The incidence of brain injury found with CUS in the Netherlands of the patients treated with ECMO during the neonatal period was 17.3%. Primary hemorrhage was the largest group of lesions, not clearly side-specific except for lobar bleeding, most probably related to changes in venous flow. Arterial ischemic stroke occurred predominant in the left hemisphere.

Introduction:

In 1976 Bartlett and colleagues were the first to successfully perform extracorporeal membrane oxygenation (ECMO) in a newborn with respiratory failure due to meconium aspiration syndrome [1, 2]. In the Netherlands neonatal ECMO was first applied in two infants at Radboud University Nijmegen Medical Center [3]. Since 1989 ECMO has evolved from an experimental treatment for moribund newborns to a life-saving technology for selected patients [4]. Technical changes have been introduced over the years. For example, the intermittent opening of the veno-arterial bypass bridge is no longer applied since 2001 because this affected cerebral blood flow velocities and presented a risk of brain injury [5].

In the veno-arterial (VA) type of ECMO, unilateral cannulation of the right carotid artery and internal jugular vein (often with ligation) as classically used when applying veno-arterial (VA) ECMO, in combination with systemic heparinisation, increases the risk of intracranial hemorrhage [6]. For this reason – and in line with guidelines and previous reports – in the Netherlands ECMO is not offered to patients born at a gestational age of less than 34 weeks or with a birth weight of less than two kilograms [7]. Reported prevalence of brain injury in neonates treated with ECMO range from 10 to 52% [6, 8-10]. One study used a neuroimaging score to predict neurodevelopmental outcome [6]. During ECMO treatment neuroimaging can detect major bleedings, leading to adjustment of (anti-coagulant) treatment. Type and location of lesions can predict neurodevelopmental outcome. Early recognition and physiotherapy can positively influence outcome. Monitoring of brain injury is therefore important for treatment and outcome. Transfontanellar cranial ultrasound (CUS) is the best method to screen for brain injury. It is a safe and non-invasive technique, and can be performed bedside, even in unstable patients [11].

We report a study reviewing the types of brain injury seen in all neonates receiving neonatal ECMO in the Netherlands over the past two decades. We applied a refined classification system of focal lesions, aiming at better understanding of the different types of lesions, their distribution, and their underlying mechanisms. Furthermore this study sought to identify possible influences of prematurity, type of ECMO, intermittent closure of the bridge and primary diagnosis on the development of intracranial lesions during neonatal ECMO.

Materials and Methods

Between September 1989 and October 2010, a total of 677 neonates received ECMO-treatment in either of the two ECMO centers in the Netherlands (Erasmus MC - Sophia Children's Hospital, Rotterdam and University Medical Center St Radboud, Nijmegen). Eligibility criteria have been described earlier [12]. VA-ECMO was the only type applied in patients born before 2004, consisting of veno-arterial bypass via the right common carotid artery and right internal jugular vein. Veno-venous (VV) ECMO was introduced in 2004 and applied in 71 cases (nine patients

started with VV-ECMO and were later converted to VA-ECMO). Prospectively recorded data on gestational age, birth weight, sex, primary diagnosis and type of ECMO were extracted from the electronic patient data management systems and medical reports. During this study period no major changes in the detection of the anti-coagulation status occurred. As part of the nation-wide protocol, anti coagulant therapy is guided by repeated measurement of the Activated Clotting Time (ACT) at two hour intervals. Before the start of ECMO a complete coagulation status is determined including (PT, PTT, fibrinogen, INR). In Nijmegen heparin is also included in the coagulation status. The basic therapy guidance is the determination of the ACT as indicated before, as well as having fibrinogen levels above 1 mg/ml, platelet count of more then 100.000 and keeping factor V within normal ranges. These data are corrected for eventual drops of hematocrit, eventually correction in case the hematocrit is less then 0.3 l/l. ATIII and TEG were only determined after finalization of the data collection for this study. So hemoglobin, hematocrit and thrombocytes are routinely determined three times a day. APTT, PT, fibrinogen once daily. The respective medical ethics review boards approved this study.

Neuroimaging

All patients had cranial ultrasound (CUS) screening prior to and serially during ECMO (started daily, with lower frequency after stabilization).

In Nijmegen all survivors had a post-ECMO MRI before discharge, except for 15 infants with normal CUS. In Rotterdam CT and MRI are not performed according to a standard protocol, however in the recent years MRI was more frequently used post-ECMO.

In Rotterdam (379 infants) the following neuroimaging techniques were used: 34 MRI scans (9%), 8 CT scans (2.1%), in two infants both CT and MRI (0.5%) and solely CUS in 335 infants (88.4%). In Nijmegen (297 infants) 201 CT- or MRI scans (68%) and solely CUS in 95 infants (32%). Only CUS was performed in 63.5% of the total cohort.

If (late) CT/ MRI scans were available the CUS diagnosis was verified with those images. This study focused on CUS alone.

All CUS scans were reviewed by two authors (M.R. and P.G.) with solid expertise in neonatal cranial ultrasound. They had no knowledge of indication for ECMO, neurodevelopmental outcome, primary diagnosis by the radiologist, or type of ECMO. Consensus reading was reached between the authors in all cases. The scans were reviewed for lesion type and timing, with the use of a refined classification method for focal brain injury (figure 1). This method classifies focal lesions in a detailed way allowing to study their pathogenesis [13]. Agreement between authors and radiologist was high (115/117, 98.3%).

Statistical analysis

Statistical analysis was performed using SPSS version 17 Windows.

Descriptive statistics are reported for all variables. Mean value and standard deviation are reported for continuous variables, and median values and range for non-normally distributed

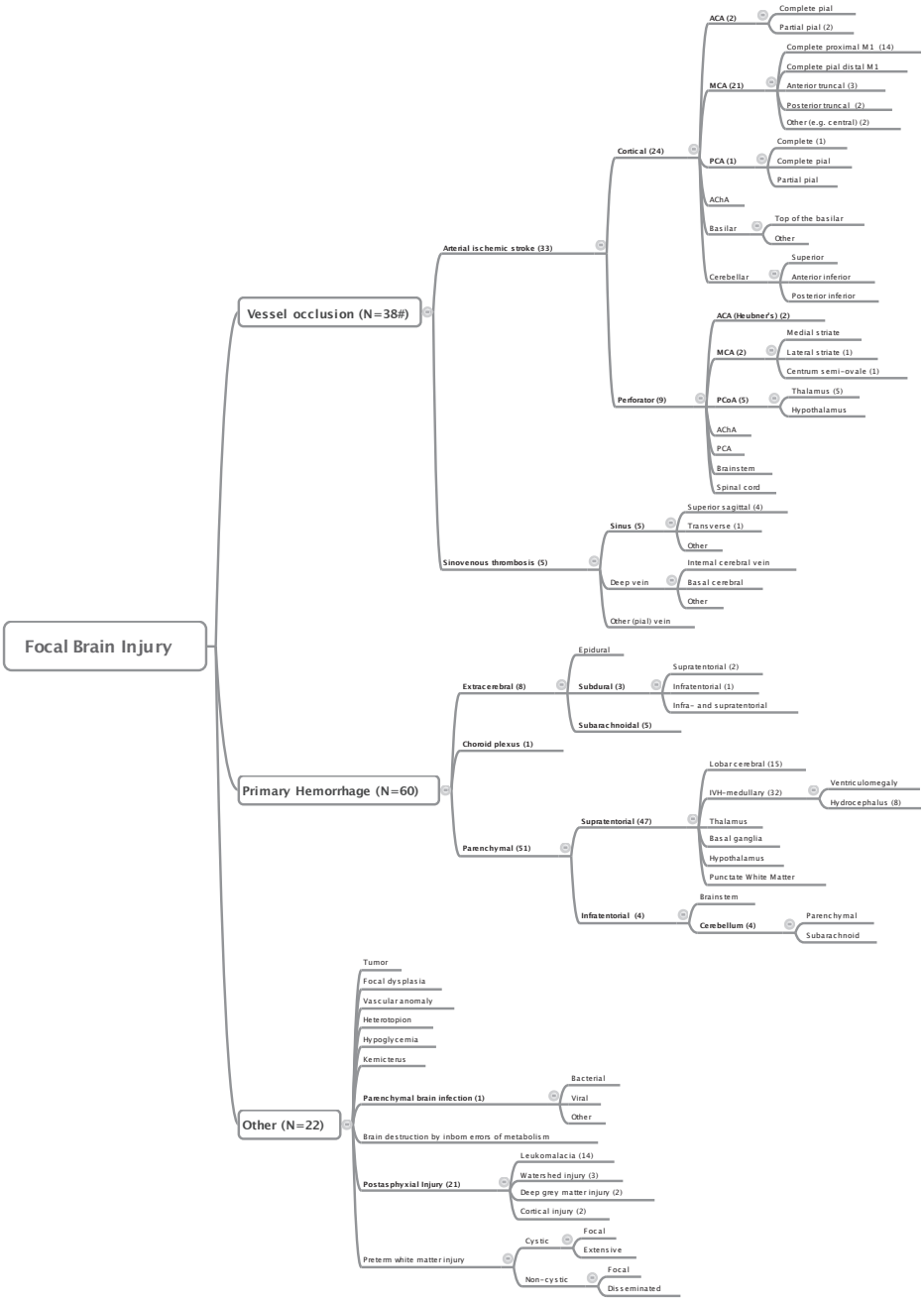

Figure 1 Focal brain injury including incidence of lesions
four patients have more than one lesion, ACA = anterior cerebral artery , MCA = medial cerebral artery, PCA= posterior cerebral artery, AChA = anterior choroidal artery, PCoA= posterior communicating artery, IVH= intraventricular hemorrhage

variables. Pearson's correlation coefficients served to establish proportional differences between two categorical scaled variables; the Mann-Whitney U test was applied for continuous variables. A p-value of less than 0.05 was considered statistically significant.

Results

The number of neonates receiving ECMO in the period under consideration was 677 (398 boys), of whom 487 infants survived (72 %). One boy was excluded from analysis because neuroimaging was lacking. Demographic data and primary diagnosis are summarized in Table 1 in relation to CUS findings and reported according to the different diagnostic categories of the Extracorporeal Life Support Organization (ELSO) registry. Birth weight and sex were significantly different between the groups. Intracranial lesions were observed in 17.3% of all patients. Survival in patients without abnormalities on CUS was 75.5% versus 54.7% in patients with abnormalities.

Table 1 Demographical data and primary diagnosis

Demographic data	**CUS findings**		**P-value**
	Normal (n=560)	Abnormal (n=116)	
GA at birth, mean ± SD	39.6 ± 2.0	38.4 ± 2.3	<0.01
GA > 37 weeks, n *	533	83	
GA 34-37 weeks, n *	60	26	
GA < 34 weeks, n *	1	2	
BW, mean ± SD	3345 ± 611	3105 ± 555	< 0.01
Male gender, n (%)	316 (56.6)	81 (68)	< 0.05
Survival, n (%)	423 (75.5)	63 (54.3)	< 0.05
Type of ECMO			
Veno-arterial (VA), n	489	107	
Veno-venous (VV), n	63	8	
VA converted to VV	8	1	
Diagnosis, n (%)			
MAS	232 (41.5)	29 (24.8)	0.012
CDH	161 (28.6)	39 (34.2)	
PPHN	66 (11.8)	13 (11.2)	
RDS	8 (1.4)	0	
Sepsis	52 (9.3)	22 (19)	
Pneumonia	7 (1.3)	0	
Other	34 (6.1)	13 (11.2)	

MAS= meconium aspiration syndrome, CDH= congenital diaphragmatic hernia, PPHN= persistent pulmonary hypertension of the neonate, RDS= respiratory distress syndrome. * GA data were missing in 16 infants

Stroke (hemorrhagic and/or ischemic) had been documented in 94 infants (13.9%). Primary hemorrhage was the commonest type of lesion; it was seen in 60 infants (8.8% of all). No lateralization was observed for primary hemorrhage as a group. Intraventricular hemorrhage (IVH) was the most frequent subtype of hemorrhage.

To analyze the influence of age on risk of lesions we compared findings in infants born < 37 weeks of gestation and infants born ≥ 37 weeks of gestation. Gestational age data were missing in 16 infants; four of them had lesions (IVH, arterial ischemic stroke (AIS), sinus thrombosis (ST) and post-asphyxial injury). The incidence of lesions was significantly higher in preterm compared to term infants, 28 of 89 (31.5%) versus 83 of 571 (14.5%) respectively (P-value < 0.01). Primary hemorrhage was the most common lesion in the preterm infants, i.e. in 21 of 28 infants. Three infants below 34 weeks of gestation were treated with ECMO, IVH was documented in two.

Lobar hemorrhage was seen in 15 patients, in 12 located on the left. There was no side predominance for cerebellar and extracerebral hemorrhage (Table 2).

Vessel occlusion (ischemic stroke) was seen in 34 of all 676 infants (5%): four had thrombosis in the superior sagittal sinus, 30 were diagnosed with arterial ischemic stroke (located on the left in 70 %).

The incidence of intracranial lesions in infants on VV-ECMO treatment was lower than in infants on VA-ECMO treatment (12.7% versus 17.4%; p-value 0.102).

Three quarters of the lesions occurred within 72 hours after starting ECMO. The interval after which lesions occurred ranged widely, until 139 days. One patient developed stroke following

Table 2 Overview of lesions related to diagnosis, type of ECMO and survival

Neuroimaging	**No. patients**	**Lesions**			**Type of ECMO**			**Survival**	
		Right	**Left**	**Bilateral**	**VA**	**VV**	**VA-VV**	**Yes**	**No**
Normal	**560**	**.**	**.**	**.**	**489**	**63**	**8**	**423**	**137**
Vessel occlusion	**34**	**9**	**19**	**2**	**30**	**3**	**1**	**20**	**14**
Arterial ischemic	30	9	19	2	27	2	1	18	12
Sinovenus	4	.	.	.	3	1	.	2	2
Primary haemorrhage	**60**	**15**	**29**	**16**	**55**	**5**	**0**	**32**	**28**
Extracerebral	8	3	4	1	6	2	0	5	3
Choroid plexus	1	0	0	1	1	0	0	1	0
Parenchymal-cerebellar	4	2	2	0	4	0	0	2	2
Parenchymal-lobar	15	2	12	1	12	3	0	7	8
Parenchymal-IVH	32	8	11	13	32	0	0	17	15
Other	**22**	**0**	**0**	**22**	**22**	**0**	**0**	**11**	**11**
Total	**676**	**24**	**48**	**40**	**596**	**71**	**9**	**486**	**190**

removal of the veno-arterial catheters. Removal had probably resulted in an embolic event given the fact that seizures were seen a few hours after removal and CUS later documented AIS.

Injury other than stroke included symmetrical post-asphyxial damage in 2.2%. Only 5 of the 676 patients had documented intracranial lesions prior to the ECMO-procedure: leukomalacia, punctate white matter lesions, IVH grade II, AIS in the left thalamus, and thrombosis of the superior sagittal sinus.

In two of the 116 patients with lesions the nature of the lesion conflicted with the previous diagnosis of the radiologist. In one case the lesion was classified as AIS of the medial cerebral artery whereas the radiologist had diagnosed a hemorrhagic infarction reported as lobar hemorrhage; in the second case a peritentorial subdural hematoma had not been reported previously.

To evaluate the impact of technical changes on the incidence of lesions over time we considered four periods (1989-1995, 1996-2000, 2001-2005, 2006-2010). There were no significant differences between the different time periods (p-value 0.102; figure 2).

Neonates with meconium aspiration syndrome had significantly fewer brain lesions compared to other diagnosis groups (p-value 0.012; table 2).

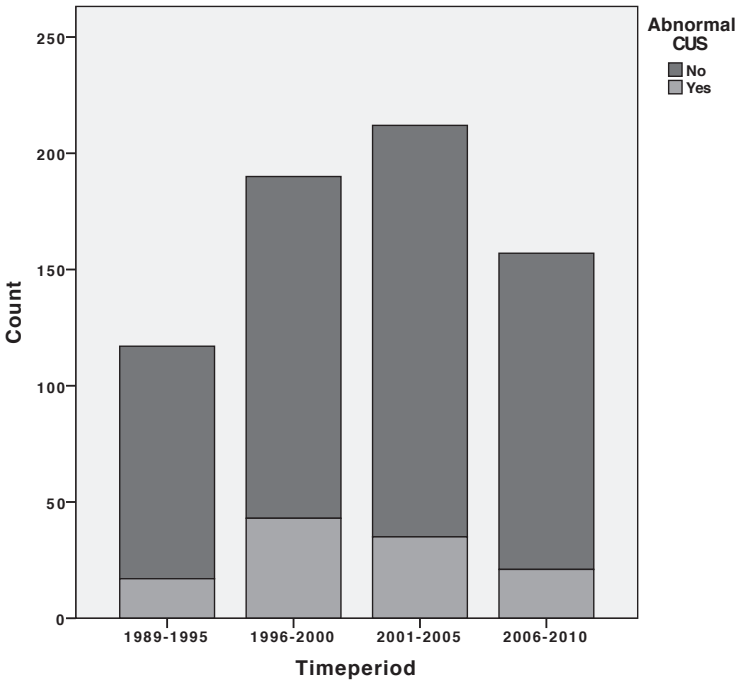

Figure 2 Number of (ab)normal CUS in different time periods, according to ECMO type. T1= 1989-1995, T2= 1996-2000, T3= 2001-2005, T4= 2006-2010

Table 3 Overview of different studies including neuroimaging and neonatal ECMO

		Imaging method			Lesions					ECMO type		
Author,year	**No. of patients**	**CUS**	**CT**	**MRI**	**No. of lesions**	**Hemorrhagic**	**Vessel occlusion**	**other**	**Localization**	**VA**	**VV**	**Survival**
Ahmad, 1999 [9]	51	+	+	-	18/51 (35%)	6/51 (11.8%)	1/51 (2%)	11/51 (21.2%)		+	+	61%
Babcock, 1988 [36]	50	+	+	-	22/50 (44%)	8/50 (16%)	9/50 (18%)	5/50 (10%)	No side difference	+	-	82%
Bartlett, 1986 [37]	100	+	-	-	only haemorrhagic lesions documented, 29/100 (29%)	29/100 (29%)	-	-	-	+	+	72%
Bowerman, 1985 [38]	28	+	-	-	8/28 (28.6%)	8/28 (28.6%)	-	-	-	+	-	-
Bulas, 1986 [8]	388 *	+	+	-	203/386 (52%)	116/386 (30%)	17/386 (4.4%)	70/386 (17.6%)	No side difference	+	-	83%
Campbell, 1988	35	+	+	-	6/35 (17.1%)	6/35 (17.1%)	-	-	No side difference (4/35 r, 3/35 l)			-
Cilley, 1986 [39]	35				only hemorrhagic lesions documented, 10/35 (28.6%)	10/35 (28.6%)	-	-	No side difference	+	-	-
Glass, 1989 [40]	42 ^	+	+	-	18/42 (42.8%)	13/42 (30%)		5/42 (11.9%)		+	-	84%
Griffin, 1992	24	+	-	+	3/24 (12.5%)	Not documented	Not documented	3/24 (12.5%)		+	-	91%
Lazar,1994 [41]	74	+	+	+	19/74 (25.7%)	3/74 (4%)	16/74 (21.6%)	-	No side difference	+	-	76%
Mendoza, 1991	180	+	+	-	106/180 (59%)	10/180 (5.6%)	6/180 (3.3%)	90/180 (50%)	Stroke 5/6 right sided	+	-	
Taylor, 1987	46 ^	+	+	-	18/46 (39.1%)	6/46 (13%)	5/46 (10%)	7/46 (16.1%)		+	-	84%
Taylor, 1989	146	+	+	-	66/148 (45%)	42/148 (28.8%)	4/148 (3%)	20/148 (13.2%)		+	-	
ELSO registry 1990-2012	25746	+	+	-	3736/25746 (29.3%)	1902/25746 (7.3%)	1834/25746(7%)			+	+	85%
Raets, 2012	676	+	+	+	116/676 (17.3%)	60/676 (8.8%)	34/676 (5%)	22/676 (3.3%)	Stroke left predominant	+	+	72%

*=2 infants without neuroimaging, 386 included, ^= subset of original study population

Discussion

The incidence of CUS-proven brain injury in neonates treated with ECMO in the Netherlands over the past two decades was established at 17.3%. Primary hemorrhage was the most common presentation; lobar bleeding was predominantly found in the left hemisphere. The incidence of AIS was 5%, likewise predominantly in the left hemisphere.

The 17.3% incidence was comparable to incidences reported in the literature (Table 3). An exception is a study by Bulas et al. reporting a 52% prevalence of intracranial abnormalities. This study, however, included findings such as a widened interhemispheric fissure and ventriculomegaly; their data are from the first 12 years of ECMO treatment [8]. Some interpreted widening of the interhemispheric fissure on ultrasound as generalized capillary leakage, others suggested that an increase of sagittal sinus pressure lowers the cerebrospinal fluid passage in the arachnoid villi [10-13]. We classified scans showing only a widened interhemispheric fissure as normal. The striking left side predominance of lobar bleeding found in the present study has not been reported by others. On the other hand, side predominance of lobar bleeding was not found in term neonates not treated with ECMO [14-16]. Parenchymal hemorrhage is uncommon in healthy term neonates and the pathogenesis is still unclear. It may be caused by trauma, asphyxia, and vascular malformation, but also be the result of hemorrhagic conversion of an embolic arterial infarction or venous compression/occlusion [15, 17]. Neonates treated with ECMO are at higher risk of arterial infarction and venous occlusion due to catheters inserted. Hypothetically, ligation of the right internal jugular vein may increase the risk of thrombosis in the proximal right transverse sinus, due to sluggish blood flow. We withheld the diagnosis of thrombosis of the superior sagittal sinus in four infants, one also with thrombosis in one transverse sinus, all four in the Rotterdam cohort. Neither center performed CUS according to standard protocol; consequently images of the superior sagittal sinus and transverse sinus were most often missing. Therefore it is highly likely that sinovenous thrombosis was underreported. Prospective studies documenting patency of superior sagittal and both transverse sinus are necessary to determine the incidence of clinically relevant sinus thrombosis during neonatal ECMO. Berfelo et al [18] concluded that sinovenous thrombosis during the neonatal period unassociated with ECMO is equally underestimated because of the nonspecific clinical presentation and insufficient use of appropriate imaging tools. With CUS the patency of sinuses can only be examined directly under the different fontanels. The side predominance of sinovenous thrombosis may be due to both asymmetrical brain venous drainage and a shift of blood volume to the left hemisphere upon right internal jugular vein cannulation.

Although ECMO is generally not offered to infants born below 34 weeks of gestation in view of the risk of intracranial hemorrhage, the cohort counted three infants treated under 34 weeks' gestational age. Two of them indeed developed intracranial hemorrhage. A comparison of preterm (born < 37 weeks of gestation) and term infants in the present study confirmed a significantly higher incidence of intracranial lesions in the preterm infants, especially primary

hemorrhage. These findings support the current practice of setting the age limit of 34 weeks' gestational age. We realize that ECMO in late preterm infants results in significant higher morbidity, as recently documented [19]. Our results reveal that AIS predominantly occurs in the left hemisphere. This is unexpected in view of ligation of the right common carotid artery. Conflicting data are reported on this issue. Stroke in a non-ECMO population has a discrete preference for the left hemisphere [20-25], but the mechanism behind this vulnerability is not clear. Some authors [26, 27] found a higher prevalence of lesions in the right hemisphere in ECMO-treated infants. Mendoza et al. reported ischemic lesions in six of 180 neonates treated with ECMO; right-sided in five and left-sided in one [26]. Schumacher et al. reported eight infants with right-sided AIS. Others did not find lateralization [6, 20, 28-31]. An important modulator in this context is the circle of Willis. If the circle is competent, blood flow to the right hemisphere is guaranteed. Van Heijst et al. [28] examined ten infants during cannulation for VA-ECMO with Doppler CUS and Near Infrared Spectroscopy (NIRS). They found changes in cerebral oxygenation and hemodynamics but no difference between right and left hemisphere due to competence of the circle of Willis: implementation of VA-ECMO induces changes in hemodynamics and cerebral oxygenation, but the effect is reversible and symmetric. Raju et al. [32] studied three infants with Doppler CUS through the mastoid fontanel: reperfusion of the right hemisphere was documented in all three following common carotid artery ligation. In two, velocities in the right middle and anterior cerebral arteries were lower than the velocities pre-ECMO and the velocities in the control patients; the other showed no side-to-side difference upon ligation of the common carotid artery. Follow-up of these infants showed that the velocities on the right side normalized and that compensatory increase occurred in the contralateral left hemisphere. We argue that if AIS associated with right carotid ligation does not occur predominantly in the right hemisphere, the circle of Willis must be competent enough to guarantee cerebral blood flow via the left carotid artery and the basilar artery to the right part of the brain. After ligation of the carotid artery, stroke occurred in 5% of the patients, therefore competence of the circle of Willis exceeds 95% in this cohort. A different pathogenesis must explain predominance of left-sided AIS. The continuous heparinisation during ECMO increases the risk of hemorrhage in general; however when heparinisation is insufficient thrombosis may occur at fragile sites in the artificial system. This mechanism presents an increased risk of embolization. Our hypothesis is that thrombosis may occur on catheters lying in the aortic arch; with compensatory high flow through left carotid and basilar artery, embolic complications will tend to occur in territories of left brain arteries.

Although the technical aspects of ECMO treatment has changed over the years, such as the intermittent opening of the bypass bridge, no significant changes in incidence of brain injury in successive periods were found (figure 2). Information from this current study is important to interpret data on neurodevelopment in ECMO-treated neonates that are being collected longitudinally until 18 years of age [33-35].

One of the limitations of this study is the retrospective design. However the scans were adequate and sufficient for review in retrospect. Ultrasound is a dynamic process and images were not obtained using a standard protocol; therefore some diagnoses were underestimated, sinovenous thrombosis for example.

Conclusion

We report here for the first time the predominance of the left sided lesions and the early occurrence of the lesions in the ECMO course. Furthermore, the incidence of brain injury remains unchanged despite overall improvement in the ECMO management. These findings suggest that additional pathological mechanisms may underlie the development of brain injury in ECMO. Prospective studies may need to focus on asymptomatic sinovenous thrombosis, on anti-coagulation monitoring and on the prevention of thrombus formation in the ECMO-system of patients with subsequent potential embolisation.

References

1. Bartlett RH, Gazzaniga AB, Jefferies MR, Huxtable RF, Haiduc NJ, Fong SW. Extracorporeal membrane oxygenation (ECMO) cardiopulmonary support in infancy. Trans Am Soc Artif Intern Organs. 1976; **22**: 80-93.
2. Bartlett RH, Andrews AF, Toomasian JM, Haiduc NJ, Gazzaniga AB. Extracorporeal membrane oxygenation for newborn respiratory failure: forty-five cases. Surgery. 1982; **92**(2): 425-33.
3. Geven WB, van de Wal HJ, Festen C. [2 successful treatments with extracorporeal membrane oxygenation in neonates with severe respiratory problems]. Ned Tijdschr Geneeskd. 1990; **134**(45): 2200-2.
4. Finer N. Neonatal selection criteria for ECMO. In: ECMO, Extracorporeal cardiopulmonary support in critical care Zwischenberger JB, Steinhorn RH, Bartlett RH eds Extracorporeal Life Support Organization Ann Arbor. 2000: 357-62.
5. De Mol AC, Van Heijst AF, Van der Staak FH, Liem KD. Disturbed cerebral circulation during opening of the venoarterial bypass bridge in extracorporeal membrane oxygenation. Int J Artif Organs. 2008; **31**(3): 266-71.
6. Taylor GA, Glass P, Fitz CR, Miller MK. Neurologic status in infants treated with extracorporeal membrane oxygenation: correlation of imaging findings with developmental outcome. Radiology. 1987; **165**(3): 679-82.
7. Stolar CJ, Snedecor SM, Bartlett RH. Extracorporeal membrane oxygenation and neonatal respiratory failure: experience from the extracorporeal life support organization. J Pediatr Surg. 1991; **26**(5): 563-71.
8. Bulas DI, Taylor GA, O'Donnell RM, Short BL, Fitz CR, Vezina G. Intracranial abnormalities in infants treated with extracorporeal membrane oxygenation: update on sonographic and CT findings. AJNR Am J Neuroradiol. 1996; **17**(2): 287-94.
9. Ahmad A, Gangitano E, Odell RM, Doran R, Durand M. Survival, intracranial lesions, and neurodevelopmental outcome in infants with congenital diaphragmatic hernia treated with extracorporeal membrane oxygenation. J Perinatol. 1999; **19**(6 Pt 1): 436-40.
10. Griffin MP, Minifee PK, Landry SH, Allison PL, Swischuk LE, Zwischenberger JB. Neurodevelopmental outcome in neonates after extracorporeal membrane oxygenation: cranial magnetic resonance imaging and ultrasonography correlation. J Pediatr Surg. 1992; **27**(1): 33-5.
11. van Wezel-Meijler G, Steggerda SJ, Leijser LM. Cranial ultrasonography in neonates: role and limitations. Semin Perinatol. 2010; **34**(1): 28-38.
12. Beck R, Anderson KD, Pearson GD, Cronin J, Miller MK, Short BL. Criteria for extracorporeal membrane oxygenation in a population of infants with persistent pulmonary hypertension of the newborn. J Pediatr Surg. 1986; **21**(4): 297-302.
13. Govaert P, Ramenghi L, Taal R, de Vries L, Deveber G. Diagnosis of perinatal stroke I: definitions, differential diagnosis and registration. Acta Paediatr. 2009; **98**(10): 1556-67.
14. Dale ST, Coleman LT. Neonatal alloimmune thrombocytopenia: antenatal and postnatal imaging findings in the pediatric brain. AJNR Am J Neuroradiol. 2002; **23**(9): 1457-65.
15. Huang AH, Robertson RL. Spontaneous superficial parenchymal and leptomeningeal hemorrhage in term neonates. AJNR Am J Neuroradiol. 2004; **25**(3): 469-75.
16. Sandberg DI, Lamberti-Pasculli M, Drake JM, Humphreys RP, Rutka JT. Spontaneous intraparenchymal hemorrhage in full-term neonates. Neurosurgery. 2001; **48**(5): 1042-8; discussion 8-9.
17. Bergman I, Bauer RE, Barmada MA, Latchaw RE, Taylor HG, David R, et al. Intracerebral hemorrhage in the full-term neonatal infant. Pediatrics. 1985; **75**(3): 488-96.
18. Berfelo FJ, Kersbergen KJ, van Ommen CH, Govaert P, van Straaten HL, Poll-The BT, et al. Neonatal cerebral sinovenous thrombosis from symptom to outcome. Stroke. 2010; **41**(7): 1382-8.
19. Ramachandrappa A, Rosenberg ES, Wagoner S, Jain L. Morbidity and mortality in late preterm infants with severe hypoxic respiratory failure on extra-corporeal membrane oxygenation. J Pediatr. 2011; **159**(2): 192-8 e3.

20. Campbell LR, Bunyapen C, Holmes GL, Howell CG, Jr., Kanto WP, Jr. Right common carotid artery ligation in extracorporeal membrane oxygenation. J Pediatr. 1988; **113**(1 Pt 1): 110-3.
21. Mannino FL, Trauner DA. Stroke in neonates. J Pediatr. 1983; **102**(4): 605-10.
22. Mantovani JF, Gerber GJ. 'Idiopathic' neonatal cerebral infarction. Am J Dis Child. 1984; **138**(4): 359-62.
23. Ment LR, Duncan CC, Ehrenkranz RA. Perinatal cerebral infarction. Ann Neurol. 1984; **16**(5): 559-68.
24. Levy MS, Share JC, Fauza DO, Wilson JM. Fate of the reconstructed carotid artery after extracorporeal membrane oxygenation. J Pediatr Surg. 1995; **30**(7): 1046-9.
25. Clancy R, Malin S, Laraque D, Baumgart S, Younkin D. Focal motor seizures heralding stroke in full-term neonates. Am J Dis Child. 1985; **139**(6): 601-6.
26. Mendoza JC, Shearer LL, Cook LN. Lateralization of brain lesions following extracorporeal membrane oxygenation. Pediatrics. 1991; **88**(5): 1004-9.
27. Schumacher RE, Barks JD, Johnston MV, Donn SM, Scher MS, Roloff DW, et al. Right-sided brain lesions in infants following extracorporeal membrane oxygenation. Pediatrics. 1988; **82**(2): 155-61.
28. Van Heijst A, Liem D, Hopman J, Van Der Staak F, Sengers R. Oxygenation and hemodynamics in left and right cerebral hemispheres during induction of veno-arterial extracorporeal membrane oxygenation. J Pediatr. 2004; **144**(2): 223-8.
29. Lago P, Rebsamen S, Clancy RR, Pinto-Martin J, Kessler A, Zimmerman R, et al. MRI, MRA, and neurodevelopmental outcome following neonatal ECMO. Pediatr Neurol. 1995; **12**(4): 294-304.
30. Bulas DI, Glass P, O'Donnell RM, Taylor GA, Short BL, Vezina GL. Neonates treated with ECMO: predictive value of early CT and US neuroimaging findings on short-term neurodevelopmental outcome. Radiology. 1995; **195**(2): 407-12.
31. Taylor GA, Fitz CR, Glass P, Short BL. CT of cerebrovascular injury after neonatal extracorporeal membrane oxygenation: implications for neurodevelopmental outcome. AJR Am J Roentgenol. 1989; **153**(1): 121-6.
32. Raju TN, Kim SY, Meller JL, Srinivasan G, Ghai V, Reyes H. Circle of Willis blood velocity and flow direction after common carotid artery ligation for neonatal extracorporeal membrane oxygenation. Pediatrics. 1989; **83**(3): 343-7.
33. Hanekamp MN, Mazer P, van der Cammen-van Zijp MH, van Kessel-Feddema BJ, Nijhuis-van der Sanden MW, Knuijt S, et al. Follow-up of newborns treated with extracorporeal membrane oxygenation: a nationwide evaluation at 5 years of age. Crit Care. 2006; **10**(5): R127.
34. Nijhuis-van der Sanden MW, van der Cammen-van Zijp MH, Janssen AJ, Reuser JJ, Mazer P, van Heijst AF, et al. Motor performance in five-year-old extracorporeal membrane oxygenation survivors: a population-based study. Crit Care. 2009; **13**(2): R47.
35. Spoel M, Laas R, Gischler SJ, Hop WJ, Tibboel D, de Jongste JC, et al. Diagnosis-related deterioration of lung function after extracorporeal membrane oxygenation. Eur Respir J. 2012.
36. Babcock DS, Han BK, Weiss RG, Ryckman FC. Brain abnormalities in infants on extracorporeal membrane oxygenation: sonographic and CT findings. AJR Am J Roentgenol. 1989; **153**(3): 571-6.
37. Bartlett RH, Gazzaniga AB, Toomasian J, Coran AG, Roloff D, Rucker R. Extracorporeal membrane oxygenation (ECMO) in neonatal respiratory failure. 100 cases. Ann Surg. 1986; **204**(3): 236-45.
38. Bowerman RA, Zwischenberger JB, Andrews AF, Bartlett RH. Cranial sonography of the infant treated with extracorporeal membrane oxygenation. AJR Am J Roentgenol. 1985; **145**(1): 161-6.
39. Cilley RE, Zwischenberger JB, Andrews AF, Bowerman RA, Roloff DW, Bartlett RH. Intracranial hemorrhage during extracorporeal membrane oxygenation in neonates. Pediatrics. 1986; **78**(4): 699-704.
40. Glass P, Miller M, Short B. Morbidity for survivors of extracorporeal membrane oxygenation: neurodevelopmental outcome at 1 year of age. Pediatrics. 1989; **83**(1): 72-8.
41. Lazar EL, Abramson SJ, Weinstein S, Stolar CJ. Neuroimaging of brain injury in neonates treated with extracorporeal membrane oxygenation: lessons learned from serial examinations. J Pediatr Surg. 1994; **29**(2): 186-90; discussion 90-1.

CHAPTER 7

PRETERM CEREBRAL MICROCIRCULATION ASSESSED WITH COLOUR DOPPLER: A PILOT STUDY.

M.M.A. Raets, P.Govaert, T.G.Goos, I.K.M. Reiss,
R.C.J. de Jonge, J. Dudink.

Submitted

Abstract

Aim: Pilot study to explore feasibility of a colour Doppler technique for monitoring cerebral perfusion at the level of microvessels.

Methods: Between March 1st, 2011, and January 30th, 2013, all admitted infants born before 29 weeks of gestation were eligible for Doppler imaging. Perfusion images were acquired in a standard coronal plane. Image quality was assessed by two authors (MR,PG). The region of interest (ROI) was manually selected. A segmentation tool was developed to separate colour data from the greyscale 2D images, leading to a percentage and number of colour pixels in the image (Doppler colour index; DCI). Intra- and interobserver agreement was analysed.

Results: Intra- and interobserver agreement for placement of ROIs were good (bias -0.24 resp. -0.74 percentage points). Colour Doppler was able to depict microvessels in cortex, white matter and deep grey matter. The median DCI in a region of cortex-white matter was 7.8% with a wide range (1.4%-25.6%). There was no significant difference between the left and right hemisphere (Mann-Whitney U, P-value 0.61). Clinically relevant observations were tabulated, e.g. distant effect of GMH on regional perfusion.

Conclusion: Sonographic small vessel visualisation may help understand pathogenic mechanisms related to perfusion and is valuable to monitor effects of treatment.

Introduction

Many prematurely born children develop long-term neurodevelopmental problems. One accepted risk factor for such problems is cerebrovascular instability and the treatment thereof, which may lead to lesions such as germinal matrix or intraventricular haemorrhage with or without venous infarction, bilateral white matter injury associated with low brain perfusion, and perforator stroke [1, 2]. Fragility of matrix microvessels [3] and presence of arterial end zones in periventricular white matter are involved in the pathogenesis of these lesions [1, 2]. As therapeutic options for preterm brain injury are lacking, clinicians focus on prevention – for which we need monitoring. Several methods are available.

The essence of haemodynamic monitoring lies in detecting perfusion values that are inadequate for timely tissue metabolism. This coupling is related to cerebrovascular autoregulation [1]. Other methods to measure cerebral blood flow include: ^{133}Xenon clearance, positron emission tomography (PET), and contrast enhanced or arterial spin labelling MRI. Radioactivity exposure, need for intravenous injection of contrast, and the need for transport limit their clinical application for serial bedside monitoring [2]. Much used conventional surrogates such as blood pressure, diuresis, heart rate and limb oxygen saturation are poor surrogates for brain perfusion in preterm infants. Besides blood pressure and pulse monitoring, near-infrared spectroscopy (NIRS) has gained acceptance in the neonatal intensive care setting. However NIRS does not allow visualization of vessel perfusion [2].

Evans et al. [4] investigated superior vena cava flow with ultrasound: this flow reflects global upper body flow without interference by shunts that confound early measurements of cardiac output (patent ductus arteriosus, open foramen ovale). The authors concluded, however, that the standard of this examination is probably too high for daily practice [4].

Doppler ultrasound is a non-invasive method that can be performed at bedside, but measurement of intracranial vessel diameter and flow characteristics is still problematic [5, 6]. Kehrer et al. reported a Doppler method to measure diameters and flow in internal carotid and basilar artery [5, 6].

Current ultrasound technique permits visualization of vessels with flow around 2 cm/sec, enabling to visualize corticofugal arteries as well as corticopetal and ventriculopetal veins. Medial and lateral subependymal veins can be followed along their path of drainage into the terminal and internal cerebral veins (figure 1).

Our objective was to explore in a pilot study the feasibility of a colour Doppler imaging technique to monitor regional cerebral perfusion at the level of microvessels. We describe the technique and present the first results of this pilot study, together with illustrative clinical findings.

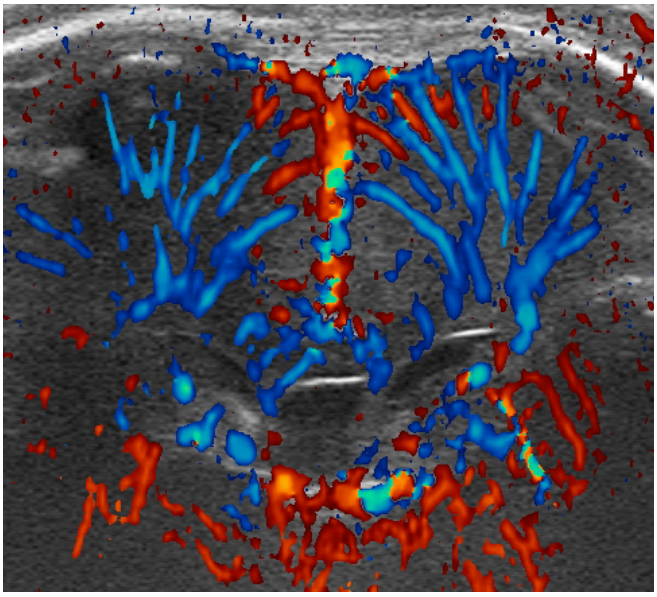

Figure 1 Cranial ultrasound image including colour Doppler. Coronal view at level of Monro, with 13 Mhz probe showing both hemispheres with microvessels in the periventricular white matter.

Methods

This study was performed in the NICU of the Erasmus MC - Sophia Children's Hospital, Rotterdam, the Netherlands. Between March 1st, 2011 and January 30th, 2013, all newly admitted preterm infants below 29 weeks of gestation were eligible, except if congenital malformations were present or when precise gestational age was not clear (figure 2).

The local medical ethics board approved this study and parental consent was obtained.

Data on gestational age, birth weight, head circumference, Score for Neonatal Acute Physiology – Perinatal Extension- II (SNAPPE-II) score [7], and gender were prospectively collected from medical charts and the computerized patient data management system.

All infants were prospectively studied with cranial US including colour Doppler according to a standard protocol (on days 0, 1, 2, and 7 after birth and then once a week until discharge).

Specific imaging of the microvessels in the cortex and white matter was obtained at the level of the foramen of Monro in a standard coronal plane, with a high frequency linear probe (13 MHz) (figure 1)(Esaote MyLab 70, Genoa, Italy). A standard preset was used, so images could be compared between patients and all images were acquired by one observer (MR). Settings included pulse repetition frequency of 250 MHz, Doppler frequency of 7.7 Hz, gain of 50% and a depth of 30 mm. The mechanical and thermal indices were always kept below 1. Due to sensitivity of the Doppler settings motion artefacts were common. Images with motion artefacts,

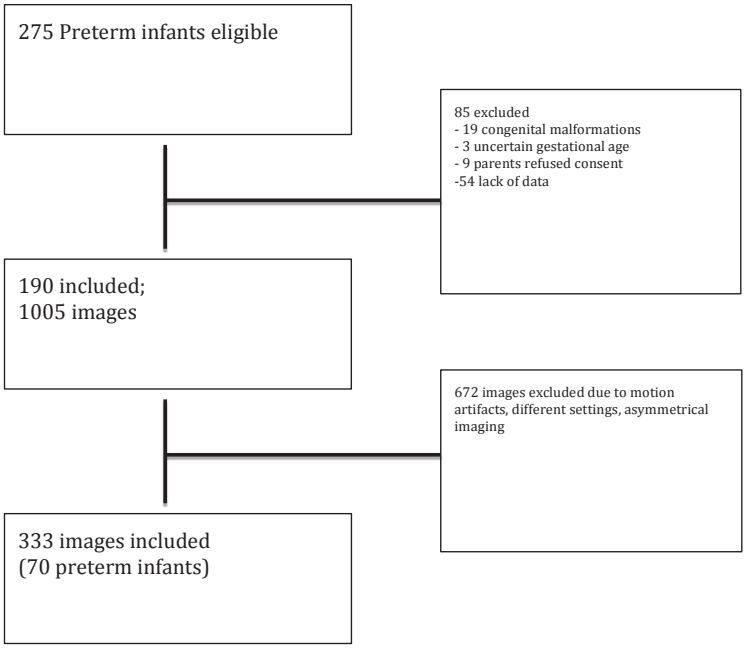

Figure 2 Patient flow chart

different setting (despite protocol) and asymmetrical pictures (probe misfit) were excluded from analysis (figure 2). Image quality was assessed by two authors (MR, PG).

The region of interest (ROI) was manually selected. These ROIs were placed in white matter and cortex. A horizontal line was drawn from the corpus callosum to the upper edge of the lateral ventricle, the hemisphere was contoured and vessels in the falx cerebri and meninges were excluded. Both hemispheres were analysed separately (figure 3).

Manual placement of ROI could be the only factor influencing our results, because one observer acquired all images, by standard settings and segmentation was automated with dedicated software. Therefore authors' intra- and interobserver agreement for placement of region of interest (ROI) was assessed in a subset of images included in this study and measured by our outcome measure DCI.

Offline digital analysis was performed using dedicated software written in Labview 2011 (National Instruments, Austin, USA). A segmentation tool was developed to separate colour data from the greyscale 2D images, leading to a percentage and number of colour pixels in the image (Doppler colour index; DCI). Flow towards probe is presented in red; flow away from probe in blue. Due to sensitive settings and unknown filtering parameters, only total colour (red and blue) was used, not the allocated velocities. The findings were not in any way calibrated against objective flow measures.

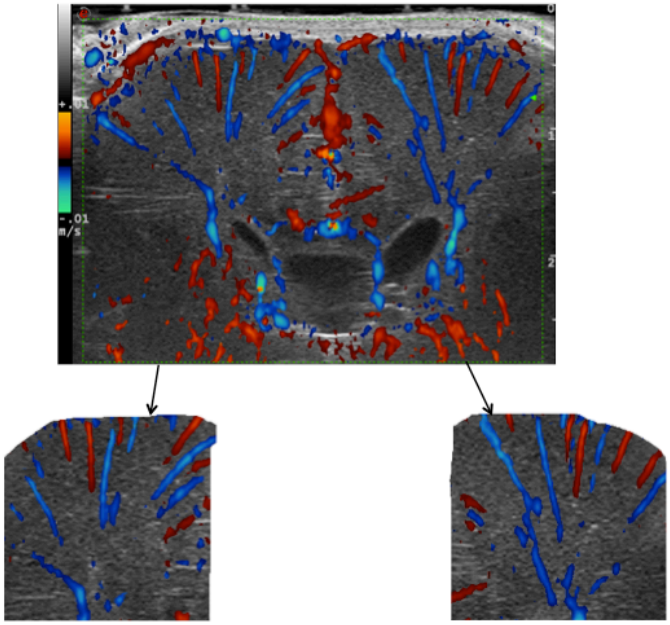

Figure 3 Top image: Cranial ultrasound image including colour Doppler. Coronal view at level of Monro, with 13 Mhz probe showing both hemispheres with microvessels in the periventricular white matter. Below left: region of interest: periventricular white matter right hemisphere Below

Statistical analysis

Descriptive statistics are reported for all variables. Median value and range are presented for continuous variables. The difference DCI between left and right hemisphere was analysed using Mann Whitney U test. A P-value two-sided of less than 0.05 was considered statistically significant. Intra- and interobserver agreement for DCI after manual placement of ROI was evaluated by the method of Bland and Altman and with the intraclass correlation coefficient (ICC). ICC was analysed with a two-way mixed model. The following cut-off values were used: bad agreement ($k < 0$), little agreement (k= 0-0.20), moderate agreement (k= 0.21-0.40), reasonable agreement (k= 0.41-0.60), good agreement (k= 0.61-0.80) and excellent agreement (k= 0.8-1).

Results

During the study period 275 infants below 29 weeks of gestation were admitted, of whom 85 were excluded from this study (figure 2). In the remaining 190 infants a total of 1005 images of the microvessels were obtained, of which 672 were excluded for quality reasons (see methods). This left 333 images of 70 preterm infants to be analysed. Demographical data and basic patient characteristics of these infants are presented in table 1.

Table 1 Patient characteristics

	Study population
Gestational age at birth, median (range), weeks	26.5 (23.9-28.9)
Birth weight, median (range), grams	884.4 (520-1367)
Head circumference, median (range), cm	24 (20.2-27.6)
SNAPPE-II-score, median (range)	23.2 (0-71)
Male gender, n (%)	32 (45.7%)

Median DCI was 7.84% (range 1.4%-32.6%) in the left hemisphere and 7.67% (range 1.4%-25.6%) in the right hemisphere. There is no significant difference in DCI between the left and right hemisphere (Mann-Whitney U test, P-value 0.61).

Intraobserver agreement was subject to a bias of -0.24 percentage point (95% limits of agreement -1.51, +1.03). Interobserver agreement was subject to a bias of -0.74 percentage point (95% limits of agreement -2.95, +1.47). The Bland-Altman plots are presented in figure 4.

The ICC for intraobserver agreement was 0.98; and the ICC for interobserver agreement was 0.95.

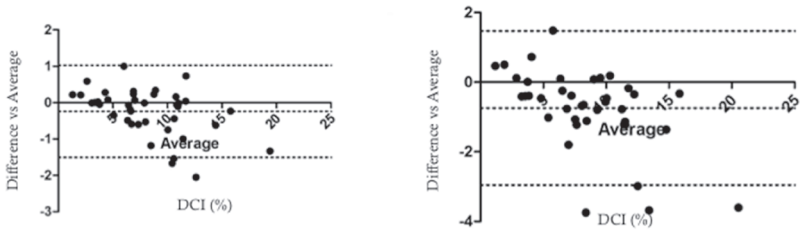

Figure 4 Left image: Bland Altman plot for intraobserver agreement, lines indicating mean with 95% limits of agreement.
Right image: Bland Altman plot for interobserver agreement, lines indicating mean bias with 95% limits of agreement.

Illustrative cases

Two study infants developed a germinal matrix haemorrhage leading to asymmetrical perfusion in periventricular white matter (figure 5).

In another extremely low birth weight infant of 24 weeks, NIRS documented more than 90% regional cerebral saturation and ultrasound showed high cerebral Doppler perfusion (figure 1, DCI right 23.8%, left 32.6%). Long-term data of this infant are not available, because of late neonatal death.

Hardly any vessels were visualised in a very low birth weight infant of 28 weeks with pulmonary hypertension. During the ultrasound study the infant was hemodynamic unstable, on high frequency ventilation with NO and inotropics (figure 6). The infant was not responding to NO and cerebral perfusion did not change during therapy.

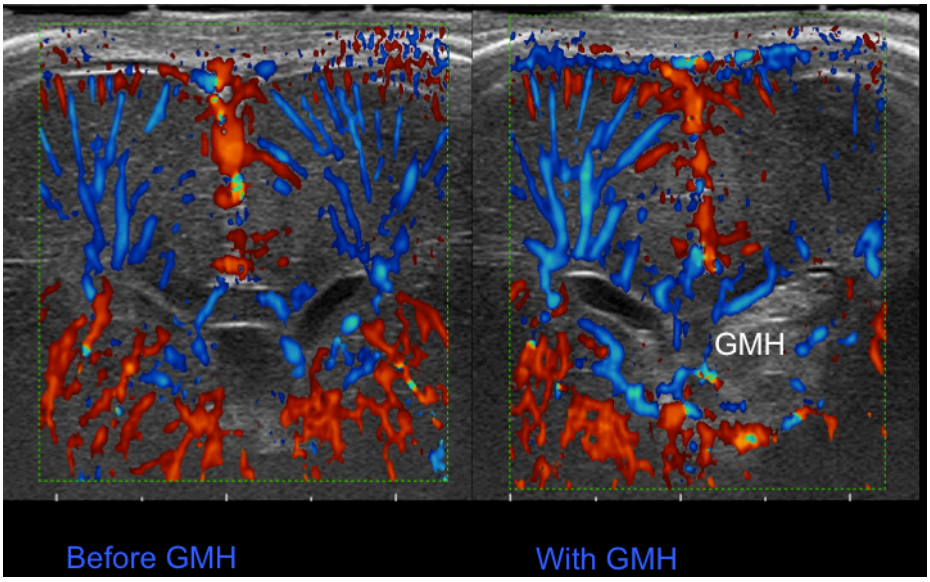

Figure 5 Left image: Cranial ultrasound image including colour Doppler. Coronal view at level of Monro, with 13 Mhz probe showing both hemispheres with microvessels in the periventricular white matter. Image before germinal matrix haemorrhage, symmetrical perfusion

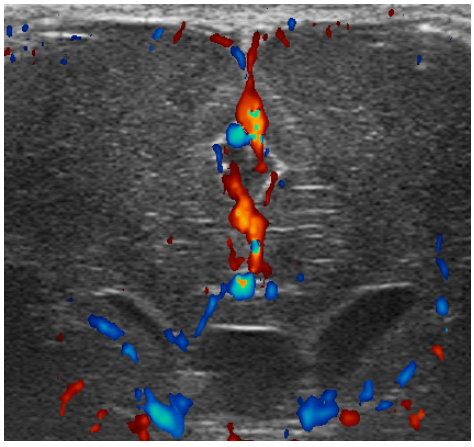

Figure 6 Cranial ultrasound image including colour Doppler. Coronal view at level of Monro, with 13 Mhz probe showing both hemispheres almost no microvessels are visible in the periventricular white matter.

Discussion

With this pilot we demonstrated that cerebral hemisphere microvessels can be visualised with colour Doppler. Given the wide variation in DCI between and within patients at different moments, this method might reflect changing patterns of cerebral blood flow. The combined results from both statistical analysis methods (Bland-Altman and ICC) were interpreted as being consistent with good to excellent agreement between observers for placement of ROIs. During the study period, two preterm infants with subependymal haemorrhage developed asymmetrical perfusion in periventricular white matter, prior to venous infarction in both. These images illustrate that arterial perfusion is reduced before obstruction of venous drainage in the terminal vein. If the findings from this pilot study would be confirmed, application of this technique might well provide "in vivo" insight into the effect of haemorrhage on locoregional perfusion and e.g. development of periventricular venous infarction.

NIRS has recently found its way into standard care. It measures cerebral oxygen saturation; a mixture of arterial and venous blood, and oxygen use can be calculated by using the arterial oxygen saturation [8]. The measurement will reflect differences in tissue oxygen uptake between different locations [9]. Due to higher metabolic activity oxygen uptake in the brain is higher than in other organs, with cerebral regional oxygen saturations between 60-80%. Lower values could reflect increased oxygen extraction or decreased oxygen delivery [9]. In one patient in the present study, higher cerebral oxygen saturations corresponded with a rich vessel visualisation, indicating increased cerebral blood flow. If we can refine this DCI tool and calibrate it against true flow values, the ultrasound technique combined with NIRS may permit to detect states of discrepant high or low perfusion.

Quantitative measurement of cerebral blood flow with CUS remains difficult. Measuring fractional moving blood volume (FMBV) seems a reproducible technique that correlates with actual tissue perfusion [10-12]. This technique is already used in utero to quantify foetal regional blood flow [13, 14] and in preterm neonates to quantify neonatal region cerebral perfusion [15]. It is based on acoustic amplitude changes in moving targets and not on changes in the Doppler shift. Heck et al. studied neonatal regional cerebral blood flow in the basal ganglia and subependymal area [15]. They concluded from their pilot study that experienced operators can measure FMBV using power Doppler and that practical and clinical usefulness of measuring FMBV in the neonate should be further evaluated. Previous FMBV studies confirmed the correlation of actual tissue perfusion by phantom experiments [10-12].

This study generated several problems. First, due to the sensitivity of the Doppler settings motion artefacts were common and we had to exclude almost two third of the images. These motion artefacts restrict clinical usefulness especially in patients ventilated on high frequency oscillation. Second, reference values are lacking because we did not study other clinical parameters and other surrogates of perfusion in this pilot study; therefore we cannot draw inferences about normal preterm brain perfusion. Third, hindbrain-forebrain comparison is not possible

because deep grey matter and cerebellum were not studied. Fourth, we realise that with the use of other manufacturers' probes and settings, microvessels may be presented in a different manner, which precludes extrapolation of our findings.

Further research should focus on normal cerebral microcirculation correlated with NIRS in different clinical settings (e.g. patent ductus arteriosus, use of inotropic agents or hypocapnia). In addition, the hypothesis that visualisation of microvessels corresponds with cerebral blood flow should be confirmed by calibration with a flow phantom. In vitro calibration methods as described by Rubin et al. offer no solution, however, as the vessels in the field of interest have small diameters [16]. It is not yet known if this can be accomplished with commercially available hardware. As we do not exactly know what filtering techniques and algorithms are used, analysis should start on a higher level before it is processed for display. In the end, routine clinical use requires that the analysis should be implemented in the ultrasound machine at the bedside.

In conclusion, DCI ultrasound measurement can contribute to the study of preterm brain injury. Further research is needed to evaluate clinical implementation, correlate with actual tissue perfusion and determine reference values for preterm infants.

References

1. Greisen G, Borch K. White matter injury in the preterm neonate: the role of perfusion. Dev Neurosci. 2001; **23**(3): 209-12.
2. Liem KD, Greisen G. Monitoring of cerebral haemodynamics in newborn infants. Early Hum Dev. 2010; **86**(3): 155-8.
3. Raets MM, Dudink J, Govaert P. Neonatal disorders of germinal matrix. J Matern Fetal Neonatal Med. 2013.
4. Evans N, Kluckow M, Simmons M, Osborn D. Which to measure, systemic or organ blood flow? Middle cerebral artery and superior vena cava flow in very preterm infants. Arch Dis Child Fetal Neonatal Ed. 2002; **87**(3): F181-4.
5. Kehrer M, Blumenstock G, Ehehalt S, Goelz R, Poets C, Schoning M. Development of cerebral blood flow volume in preterm neonates during the first two weeks of life. Pediatr Res. 2005; **58**(5): 927-30.
6. Kehrer M, Krageloh-Mann I, Goelz R, Schoning M. The development of cerebral perfusion in healthy preterm and term neonates. Neuropediatrics. 2003; **34**(6): 281-6.
7. Richardson DK, Corcoran JD, Escobar GJ, Lee SK. SNAP-II and SNAPPE-II: Simplified newborn illness severity and mortality risk scores. J Pediatr. 2001; **138**(1): 92-100.
8. Naulaers G, Meyns B, Miserez M, Leunens V, Van Huffel S, Casaer P, et al. Use of tissue oxygenation index and fractional tissue oxygen extraction as non-invasive parameters for cerebral oxygenation. A validation study in piglets. Neonatology. 2007; **92**(2): 120-6.
9. Marin T, Moore J. Understanding near-infrared spectroscopy. Adv Neonatal Care. 2011; **11**(6): 382-8.
10. Hernandez-Andrade E, Jansson T, Ley D, Bellander M, Persson M, Lingman G, et al. Validation of fractional moving blood volume measurement with power Doppler ultrasound in an experimental sheep model. Ultrasound Obstet Gynecol. 2004; **23**(4): 363-8.
11. Welsh A. Quantification of power Doppler and the index 'fractional moving blood volume' (FMBV). Ultrasound Obstet Gynecol. 2004; **23**(4): 323-6.
12. Welsh AW, Rubin JM, Fowlkes JB, Fisk NM. Standardization of power Doppler quantification of blood flow in the human fetus using the aorta and inferior vena cava. Ultrasound Obstet Gynecol. 2005; **26**(1): 33-43.
13. Cruz-Martinez R, Figueras F, Hernandez-Andrade E, Benavides-Serralde A, Gratacos E. Normal reference ranges of fetal regional cerebral blood perfusion as measured by fractional moving blood volume. Ultrasound Obstet Gynecol. 2011; **37**(2): 196-201.
14. Hernandez-Andrade E, Jansson T, Figueroa-Diesel H, Rangel-Nava H, Acosta-Rojas R, Gratacos E. Evaluation of fetal regional cerebral blood perfusion using power Doppler ultrasound and the estimation of fractional moving blood volume. Ultrasound Obstet Gynecol. 2007; **29**(5): 556-61.
15. Heck S, Schindler T, Smyth J, Lui K, Meriki N, Welsh A. Evaluation of neonatal regional cerebral perfusion using power Doppler and the index fractional moving blood volume. Neonatology. 2012; **101**(4): 254-9.
16. Rubin JM, Bude RO, Fowlkes JB, Spratt RS, Carson PL, Adler RS. Normalizing fractional moving blood volume estimates with power Doppler US: defining a stable intravascular point with the cumulative power distribution function. Radiology. 1997; **205**(3): 757-65.

PART III

CHAPTER 8

MATURATION OF ECHOGENICITY IN PRETERM STRIATUM

M.M.A. Raets, R. de Goederen, R.C.J. de Jonge,
L.A. Ramenghi, I.K.M. Reiss, I.V. Koning, P. Govaert, J. Dudink.

Submitted

Abstract

Background: Preterm infants are at risk of brain injury. Cranial ultrasound is an imaging technique frequently used in neonatal care to detect and monitor brain injury. Anatomical structures and abnormalities can be distinguished by differences in echogenicity.

Our primary objective was to reliably measure sonographic grey values in the basal ganglia of preterm infants. Secondary objectives included the influence of gestational age at birth on echogenicity and aspects of deep grey matter change at 30 weeks corrected GA.

Methods: We prospectively collected CUS-data of 229 preterm infants below 29 weeks of gestation. Parasagittal images through the gangliothalamic ovoid were assessed on mean grey value in putamen and globus pallidus. The measured regions of interest (ROI) were chosen within the same 'time gain compensation' segment. Intra- and interobserver for placement of ROI were analyzed.

Results: The method used proved to be reliable for measuring grey values in putamen and globus pallidus, as it produced a reliable globus pallidus to putamen ratio (GPP ratio). Mean GPP ratio was 0.786 (± 0.085). Extreme preterm infants have significantly lower GPP at birth than did preterm infants above 28 weeks (0.755 ± 0.081 vs 0.808 ± 0.091; P-value <0.01). At 30 weeks corrected GA this was still the case (0.723 ± 0.051 vs. 0.818 ± 0.063; P-value <0.01).

Conclusion: The putamen of extremely preterm infants is more hyperechoic then putamen of preterm infants of 29 weeks of gestation. Objective measurement of grey values can help to study brain injury.

Introduction

Advances in prenatal and neonatal care have led to increased survival of infants born preterm, but neonatal morbidity and neurological sequelae are still of concern [1-3]. Transfontanellar cranial ultrasound (CUS) is traditionally used to detect major brain abnormalities, such as intraventricular hemorrhage (IVH), periventricular hemorrhagic infarction (PVHI), post-hemorrhagic ventricular dilatation (PHVD) and (cystic) periventricular leukomalacia ((c)PVL).

In addition to severe pathologies subtler alterations of brain structure may influence outcome [4]. White matter injury in preterm infants correlates with impaired development of basal ganglia and thalamus [4-6].

In very preterm infants putamen seems more hyperechoic than it is in term or near term infants [7]. CUS transmits radio-frequency signals of which the echoes are detected (raw data) and processed in several steps, leading to grey values of speckles that construct an image. Speckles result from interference patterns of sound waves with tissue. The speckle patterns contain true time information (relative values only), but also noise [8]. Anatomical structures and their injuries can be distinguished by different degrees of echogenicity. Routine measurements are hardly possible because most CUS devices do not provide bedside access to raw data and measurement of grey values in images. Even more importantly, grey values change with different probe physics, beam settings and post processing of the image frame. Another issue is time gain compensation (TGC). Reflected signals returning from deeper in the tissue travel a longer distance and are therefore more attenuated. In the absence of raw data, it is thus important to measure grey values in the same TGC segment [8].

The primary objective of this study was to find a way to reliably measure relative grey values in basal ganglia of preterm infants. Secondary objectives included the influence of gestational age at birth on echogenicity of deep grey matter and aspects of deep grey matter change at 30 weeks corrected GA. It was hypothesized that postnatal maturation would differ from prenatal maturation.

Methods

This study is part of a large prospective cohort study conducted in the NICU of the Sophia Children's Hospital Rotterdam between May 2010 and January 2013. All infants born below 29 weeks GA were eligible. Exclusion criteria were uncertain GA, no parental consent or congenital brain abnormalities. Seventy of the 333 eligible preterm infants were excluded, leaving 263 infants in this study. The local medical ethics review board approved this study.

Image acquisition

All included infants were prospectively studied with CUS according to a standard protocol (on days 0, 1, 2, and 7 after birth and then once a week until discharge) using an Esaote MyLab 70 (Genoa, Italy) with a convex probe (8.5 MHz). Standard settings included a depth of 76 mm, persistence of 11, gain of 70% and frequency of 8.5 MHz. All images were acquired by one observer (MR) and digitally stored in an Esaote MyLab environment that allows easy reviewing. Lesions were reviewed by two authors (MR, PG). For this sub-study we only used one parasagittal image through basal ganglia per patient. Images were evaluated on two criteria. (1) Good visibility of the entire ganglio-thalamic ovoid with anterior horn of the lateral ventricle up to and including choroid plexus. (2) Good visibility of putamen (below anterior limb of internal capsule), globus pallidus and thalamus in the ganglio-thalamic ovoid. Parasagittal images of 229 preterm infants met these criteria. The globus pallidus/putamen (GPP ratio) after birth was established from images acquired within the first week; the GPP at 30 weeks corrected age from images at 30 weeks (cross-sectional). The GPP ratio is obtained by dividing the grey value of globus pallidus by the grey value of putamen.

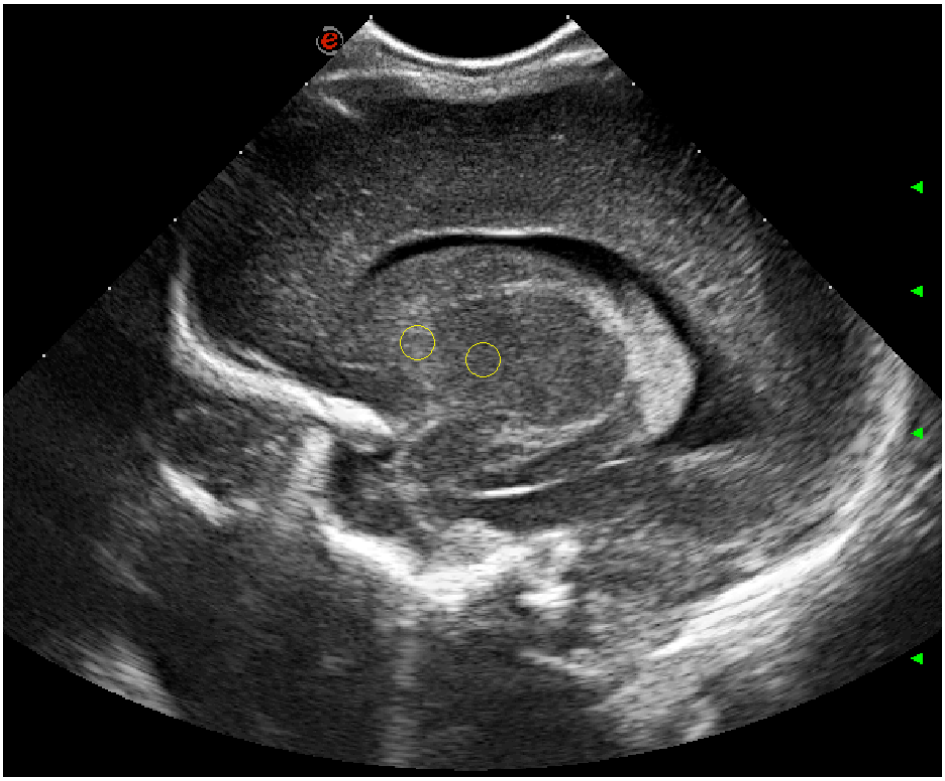

Figure 1 Parasagittal ultrasound image through the anterior fontanel, containing two ROIs in the same time gain compensation segment. From left to right: putamen and globus pallidus

Grey value measurements were made on a personal computer, using the Java image processing program ImageJ (NIH, MD, USA). Grey values of putamen and globus pallidus were independently measured in all images by two authors (MR, RdG). Round regions of interest (ROIs) of identical size were used. Grey values may range from 0 (black) to 255 (white). Only GPP ratios were established because due to attenuation differences (e.g. hair) that had occurred despite standard ultrasound settings, real values were difficult to compare. Absolute values were only used to determine whether changes in GPP ratio were the result of changes in putamen (denominator) or in globus pallidus (numerator). In order to avoid biased echogenicity findings, we positioned the ROIs in the same TGC segment (figure 1).

Statistical analysis

Statistical analysis of all data was performed using SPSS Statistics 20 (IBM, NY, US) and GraphPad Prism 5 (GraphPad Software, San Diego, CA, USA).

Intra- and interobserver agreement for grey values after manual placement of ROI was evaluated by the method of Bland and Altman [9] and with the intraclass correlation coefficient (ICC). ICC was analysed with a two-way mixed model. Cut-off values were the following: bad agreement (k < 0), little agreement (k= 0-0.20), moderate agreement (k= 0.21-0.40), reasonable agreement (k= 0.41-0.60), good agreement (k= 0.61-0.80) and excellent agreement (k= 0.8-1) [10].

Descriptive statistics are reported for all variables. Median value and range are presented for non-normal distributed continuous variables, mean and standard deviations are presented

Table 1 Demographic data

	N=229
GA at birth, weeks (median, range)	26 5/7 (23 6/7-28 6/7)
< 25 weeks, n (%)	33 (14.4%)
25-26 weeks, n (%)	31 (13.5%)
26-27 weeks, n (%)	48 (21%)
27-28 weeks, n (%)	64 (28%)
>28 weeks, n (%)	52 (23.1%)
Birth weight, grams (median, range)	900 (365-1610)
Male gender, n (%)	124 (54.2%)
Head circumference, cm (median, range)	24.0 (19.7-29.8)
Abnormal CUS, n (%)	96 (41.9%)
Intraventricular haemorrhage	75 (32.7%)
Perforator stroke	3 (1.3%)
Sinovenous thrombosis	11 (4.8%)
Preterm white matter injury	5 (2.2%)
Extracerebral haemorrhage	2 (0.9%)

for normally distributed data. Differences between extreme preterm infants below 26 weeks and preterm infants of older than 28 weeks GA were analysed with Mann-Whitney U test for continuous variables and Fisher's Exact test for categorical data. Linear regression was used for putamen and globus pallidus changes with gestational age in days.

A two-sided P-value of less than 0.05 was considered statistically significant.

Results

The 229 included infants had a median GA of 26 5/7 (23 6/7-28 6/7) weeks and median birth weight of 900 (365-1610) grams. Ultrasound scans of 96 children showed brain lesions i.e. IVH (n=75), perforator stroke (n=3), sinus thrombosis (n=11), preterm white matter injury (n=5) and extracerebral hemorrhage (n=2). Demographic data are presented in table 1.

Intraobserver rating for grey value of putamen showed a bias of -0.42 (95% limits of agreement: -7.55-6.70; for grey value of globus pallidus a bias of 0.07 (95% limits of agreement: -5.87-6.02). Interobserver rating for grey value of putamen showed a bias of 5.45 (95% limits of

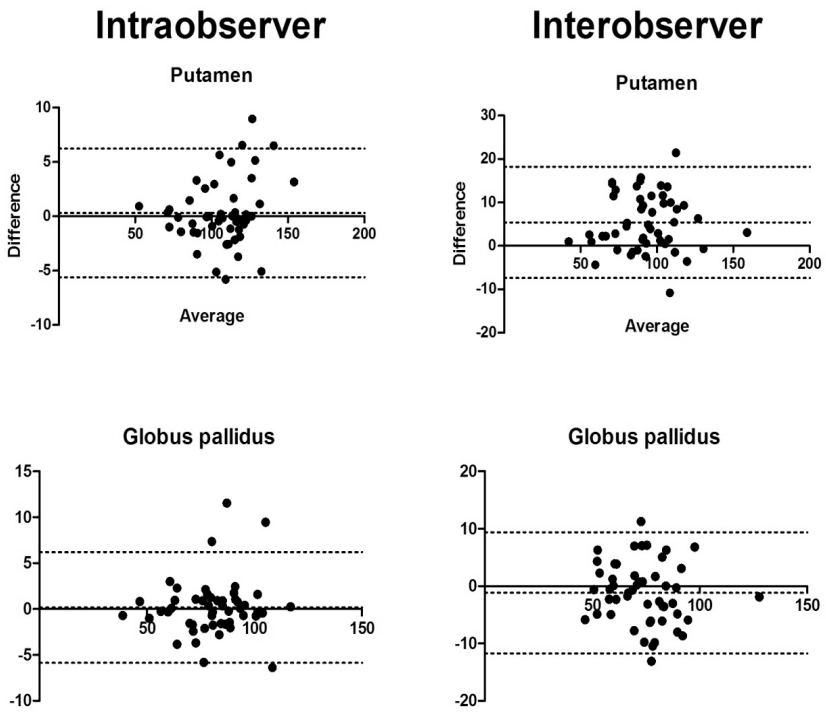

Figure 2 Bland Altman plots for intra and interobserver agreement

agreement: -7.26-18.16); for grey value of globus pallidus a bias of -1.16 (95% limits of agreement: -11.82-9.49). The Bland Altman plots are presented in figure 2.

Regarding putamen, the ICC for intraobserver reliability was 0.988 that for interobserver reliability 0.927. Regarding globus pallidus, the ICC for intraobserver reliability was 0.982 that for interobserver reliability 0.936. This represents excellent agreement.

The mean overall GPP ratio was 0.786 (± 0.085 SD). GPP ratio after birth was significantly lower in extremely preterm infants (n=64; GPP 0.755 ± 0.081) compared with preterm infants above 28 weeks (n=53; GPP 0.808 ± 0.091) (P < 0.01) (Table 2).

Table 2 GPP ratios

	< 26 weeks GA	> 28 weeks GA
After birth	0.755 ± 0.081 (n=64)	0.808 ± 0.091 (n=53)
At 30 weeks corrected age	0.723 ± 0.051(n=28)	0.818 ± 0.063 (n=38)

P-values < 0.01

At 30 weeks corrected GA infants born below 25 weeks GA (n=28) had a significantly lower GPP ratio than infants born after 28 weeks GA (n=38): i.e. 0.723 ± 0.051 versus 0.818 ± 0.063, respectively (P< 0.01) (Table 2).

Z-score of birth weight and head circumference and incidence of abnormal CUS was significantly different between two groups (preterm < 26 weeks of GA and preterm of > 28 weeks GA). There was no sex difference between the groups (table 3).

Linear regression: crude coefficient for grey values of putamen to GA (in weeks): - 2.065 (95%CI: -3.884;-0.240) P-value 0.027; corrected coefficient to birth weight (z-score) and head circumference (z-score): -1.523 (95%CI: -3.482;0.436) P-value 0.127.

Linear regression: crude coefficient for grey values of globus pallidus to GA (in weeks): -0.045 (95%CI: -1.504;1.414) P-value 0.952; corrected coefficient to birth weight (z-score) and head circumference (z-score): 0.263 (95%CI: -1.307;1.834) P-value 0.741.

Table 3 Demographic data compared between two groups

	< 26 wk	>28 wk	P-Value
GA, median (range)	24 6/7 (23 6/7-25 6/7)	28 2/7 (28-28 6/7)	<0.01 #
BW (grams) median (range)	706 (365-1030)	1120 (460-1610)	<0.01 #
BW-SD median (range)	-1.26 (-3.80-1.00)	-0.28 (-4.50-2,72)	< 0.01#
HC (cm) median (range)	22.3 (20-25.6)	25.8 (20.3-29.8)	<0.01#
HC-SD median (range)	-0.78 (-3.00-1.72)	-0.14 (-4.20-2.60)	< 0.01#
Male gender, n	32/64	29/54	0.711*
Abnormal CUS	56.3%	20.8%	< 0.01 *

*= fisher exact, # Mann Whitney U test

Although abnormal CUS findings were more frequent in extreme preterm infants, GPP was not significantly different between infants with abnormal CUS findings and infants with normal CUS findings (Mann-Whitney U test, P-value 0.218).

Discussion

Our results suggest reliable placement of and measurement of grey values in ROIs in deep grey matter nuclei on parasagittal CUS images between different observers. At 30 weeks corrected GA, GPP ratios in preterm infants born below 26 weeks of gestation were lower than those in preterm infants born at 28 weeks of gestation. This difference was irrespective of z-score birth weight/head circumference or abnormal CUS findings. The lower GPP ratio in extreme preterm infants is explained by relatively more hyperechoic putamen.

In a previous study putamen in preterm infants subjectively seemed hyperechoic, probably due to a physiological process [11]. Our results confirm by objective measurement that putamen is more hyperechoic compared with globus pallidus. Between 24 and 27 weeks of GA putamen is estimated to contain ~ 3 fold more neurons (or cells) than globus pallidus [12]. Since cell density influences echogenicity, this histological difference is at least part of the explanation. In addition, myelination around globus pallidus starts earlier than myelination around putamen [13].

An additional finding is that at 30 weeks corrected age the GPP ratio is still significantly lower in extreme preterm infants, which implies sustained relative hyperechogenicity of putamen. One possible explanation is that delayed "normal" maturation in these infants, results in fewer cells to be eliminated from putamen. Alternatively the persistent hyperechoic character of putamen could be due to a subtle, general impairment of brain development [4, 14]. Johnston et al. studied selective damage to basal ganglia in the newborn [15]. They hypothesized that these nuclei were either damaged or protected according to their place and function in the neuronal circuit. Neuronal excitation results in damage to putamen, thalamus and cerebral cortex. The globus pallidus, on the other hand, is inhibited by the putamen, thus protecting it from sequential damage [15]. Selip et al. studied the effects of hypoxic-ischemic injury to grey matter in rat pups [16]. They concluded that even without severe white matter injury, activated microglia and reactive astrocytes infiltrate damaged grey matter regions [16]. A recent study by Supramaniam et al. showed that periventricular white matter injury was associated with a higher number of microglia in periventricular white matter, and thus higher cell density [17]. These studies suggest that even if there is no apparent damage on CUS, the basal ganglia could still be damaged due to poorly defined insults. Injurious activation of microglia thus leads to higher cell density, which explains higher grey values on CUS.

Some CUS studies used integrated backscatter (IBS) analysis for quantitative measurement in the brain [18-20]. This somehow draws on raw data, but the technique cannot be reproduced with other machines. Fujimoto et al. reported higher IBS values in preterm infants compared

with term infants in each ROI placed, consistent with the presence of more echoic signal. In preterm infants these IBS values decreased within 28 days after birth [18]. Ichihashi et al. studied 25 preterm infants (mean GA 32 weeks) and confirmed that IBS values decreased with increasing GA [19]. Mullaart et al. studied white and grey matter in preterm infants with grey values (compared to our method): their ROIs were not in the same TGC, however calibration was with the use of a grey scale phantom [21]. They also reported decreasing white matter grey values with increasing GA [21].

Our method has several limitations. First, due to attenuation differences between patients actual grey values are impossible to compare. Therefore we had to use ratios. Secondly, objective measurement of white matter would also be of interest to study genuine white matter injury, but as we restricted ourselves to the same TGC segment we could not compare with a ROI in white matter. Thirdly, ROIs were manually placed in an offline analysis setting. This makes implementation in daily clinical still difficult. Fourthly, our cohort is too young to determine long-term neurodevelopmental outcome. Such outcome data could provide more insight in physiology versus pathology of preterm deep grey matter.

In conclusion we found an objective method to compare echogenicity of the basal ganglia. With this method we demonstrated that extreme preterm infants have a lower GPP ratio at birth and at 30 weeks corrected age. Hyperechogenicity of the putamen during neonatal development might be of physiological relevance, but could also be due to pathophysiological processes. Future attempts to tackle the remaining questions could incorporate raw (RF) data, calibrated by a phantom [20].

References

1. Doyle LW, Roberts G, Anderson PJ. Outcomes at age 2 years of infants < 28 weeks' gestational age born in Victoria in 2005. J Pediatr. 2010; **156**(1): 49-53 e1.
2. Draper ES, Zeitlin J, Fenton AC, Weber T, Gerrits J, Martens G, et al. Investigating the variations in survival rates for very preterm infants in 10 European regions: the MOSAIC birth cohort. Arch Dis Child Fetal Neonatal Ed. 2009; **94**(3): F158-63.
3. Schlapbach LJ, Adams M, Proietti E, Aebischer M, Grunt S, Borradori-Tolsa C, et al. Outcome at two years of age in a Swiss national cohort of extremely preterm infants born between 2000 and 2008. BMC Pediatr. 2012; **12**: 198.
4. Volpe JJ. Brain injury in premature infants: a complex amalgam of destructive and developmental disturbances. Lancet Neurol. 2009; **8**(1): 110-24.
5. Inder TE, Warfield SK, Wang H, Huppi PS, Volpe JJ. Abnormal cerebral structure is present at term in premature infants. Pediatrics. 2005; **115**(2): 286-94.
6. Lin Y, Okumura A, Hayakawa F, Kato K, Kuno T, Watanabe K. Quantitative evaluation of thalami and basal ganglia in infants with periventricular leukomalacia. Dev Med Child Neurol. 2001; **43**(7): 481-5.
7. van Wezel-Meijler G, Leijser LM, Wiggers-de Bruine FT, Steggerda SJ, van der Grond J, Walther FJ. Diffuse hyperechogenicity of basal ganglia and thalami in preterm neonates: a physiologic finding? Radiology. 2011; **258**(3): 944-50.
8. Vansteenkiste E, Govaert P, Conneman N, Lequin M, Philips W. Segmentation of white matter flaring areas in ultrasound images of very-low-birth-weight preterm infants. Ultrasound Med Biol. 2009; **35**(6): 991-1004.
9. Bland JM, Altman DG. Statistical methods for assessing agreement between two methods of clinical measurement. Lancet. 1986; **1**(8476): 307-10.
10. Altman. Practical Statistics for Medical Research. London: Chapman & Hall; 1991.
11. Leijser LM, Klein RH, Veen S, Liauw L, Van Wezel-Meijler G. Hyperechogenicity of the thalamus and basal ganglia in very preterm infants: radiological findings and short-term neurological outcome. Neuropediatrics. 2004; **35**(5): 283-9.
12. Itoh K, Suzuki K, Bise K, Itoh H, Mehraein P, Weis S. Apoptosis in the basal ganglia of the developing human nervous system. Acta Neuropathol. 2001; **101**(2): 92-100.
13. Hasegawa M, Houdou S, Mito T, Takashima S, Asanuma K, Ohno T. Development of myelination in the human fetal and infant cerebrum: a myelin basic protein immunohistochemical study. Brain Dev. 1992; **14**(1): 1-6.
14. de Kieviet JF, Zoetebier L, van Elburg RM, Vermeulen RJ, Oosterlaan J. Brain development of very preterm and very low-birthweight children in childhood and adolescence: a meta-analysis. Dev Med Child Neurol. 2012; **54**(4): 313-23.
15. Johnston MV, Hoon AH, Jr. Possible mechanisms in infants for selective basal ganglia damage from asphyxia, kernicterus, or mitochondrial encephalopathies. J Child Neurol. 2000; **15**(9): 588-91.
16. Selip DB, Jantzie LL, Chang M, Jackson MC, Fitzgerald EC, Boll G, et al. Regional differences in susceptibility to hypoxic-ischemic injury in the preterm brain: exploring the spectrum from white matter loss to selective grey matter injury in a rat model. Neurol Res Int. 2012; **2012**: 725184.
17. Supramaniam V, Vontell R, Srinivasan L, Wyatt-Ashmead J, Hagberg H, Rutherford M. Microglia activation in the extremely preterm human brain. Pediatr Res. 2013; **73**(3): 301-9.
18. Fujimoto C, Yamashita Y, Kanda H, Harada E, Maeno Y, Matsuishi T. In vivo quantitative ultrasonic evaluation of neonatal brain with a real time integrated backscatter imaging system. Brain Dev. 2003; **25**(6): 411-5.
19. Ichihashi K, Yada Y, Takahashi N, Homma Y, Momoi M. Integrated backscatter of the brain of preterm infants. J Perinat Med. 2008; **36**(3): 253-5.
20. Strowitzki M, Brand S, Jenderka KV. Ultrasonic radio-frequency spectrum analysis of normal brain tissue. Ultrasound Med Biol. 2007; **33**(4): 522-9.

21. Mullaart RA, Thijssen JM, Rotteveel JJ, Valckx FM, van Geemen AJ. Quantitative ultrasonography of the periventricular white and grey matter of the developing brain. Ultrasound Med Biol. 1999; **25**(4): 527-30.

CHAPTER 9

SERIAL CRANIAL ULTRASONOGRAPHY AND EARLY MRI ARE COMPLEMENTARY IN DETECTING PRETERM BRAIN INJURY

A. Plaisier, M.M.A. Raets, P. Govaert, M. Feijen – Roon,
I.K.M. Reiss, L.S. Smit, M. H. Lequin, J. Dudink.

Submitted

Abstract

Background: Magnetic resonance imaging (MRI) is considered superior in detecting preterm brain injury, but its clinical use is challenged. Advanced serial cranial ultrasonography (CUS) has acquired great clinical value. We hypothesized that dedicated serial CUS is equally effective in diagnosing preterm brain damage as a routine MRI scan at 30 weeks postmenstrual age and excels in clinical feasibility.

Methods: We prospectively collected data of 307 infants born <29 weeks gestational age. Serial CUS and MRI were performed according to standard clinical protocol. In case of instability, MRI was postponed or cancelled. Brain images were assessed by independent experts and compared between modalities.

Results: Serial CUS was performed in all infants, MRI was often postponed (n = 58) or canceled (n = 127). Injury was found in 146 infants (47.6%). Clinical characteristics differed significantly between groups that were subdivided according to timing of MRI. 61 discrepant imaging findings were found. MRI was superior in identifying cerebellar hemorrhages; CUS in detection of acute intraventricular hemorrhage and cerebral sinovenous thrombosis.

Conclusions: Advanced serial CUS seems highly effective in diagnosing preterm brain injury, but may miss cerebellar abnormalities. Although MRI does identify these lesions, clinical additional value is limited. Improved safety, better availability and tailored procedures are essential for MRI to increase its value in clinical care.

Introduction

With the World Health Organization reporting increasing numbers of infants born preterm (over 15 million/year) and increased survival rates, there is a growing recognition that many of these infants may develop long term neurodevelopmental problems [1, 2]. Not surprisingly, preterm birth is rapidly becoming the leading cause of neurodevelopmental impairment in childhood [3]. Early objective diagnosis of brain injury in preterm infants is important for prognostication and decision making in neonatal intensive care. Current neuroimaging tools are suited for quantitative assessment of preterm brain injury and thus can provide insight into pathogenesis of brain injury in preterm infants [4]. Magnetic resonance imaging (MRI) is a powerful, non-ionizing neuroimaging tool with several advanced techniques to evaluate preterm brains: diffusion tensor imaging (DTI), functional MRI, volumetric MRI, and proton magnetic resonance spectroscopy allow quantification of disturbances in brain maturation and elucidate brain connectivity and functionality of infants born preterm. Therefore, quantitative MRI promises to provide early proxy biomarkers of long term outcome [4, 5]. MRI is considered the best method to detect and quantify diffuse non-cystic white matter (WM) injury [6] and is increasingly performed at preterm age to provide early diagnosis of lesions [2]. However, MRI is expensive, time consuming and challenging for critically ill infants. Furthermore, technical background of advanced MRI modalities is a complex matter and imaging accuracy depends on many aspects, including acquisition and processing methodology [7-10]. MRI seems therefore limited as a practical clinical tool to detect most common reported preterm brain lesions on which outcome data are available.

Cranial ultrasonography (CUS) is relatively cheap, directly available and allows serial bedside scanning with limited disturbance for the infant. Color Doppler imaging enables sequential monitoring of intracranial hemodynamic adaptation after birth. Traditionally, CUS is used to detect lesions, such as germinal matrix and intraventricular hemorrhage (GMH-IVH), post-hemorrhagic ventricular dilatation and periventricular leukomalacia (PVL). Its value to detect brain lesions is increasing, owing to technical developments such as high-resolution ultrasound (<200 micron), quantitative measurements (linear, volumetric, raw data and texture analysis), and use of supplemental acoustic windows (mastoid and posterior fontanel) [11-17]. Limitations of CUS include observer-dependency [18], problems to detect posterior fossa abnormalities and cerbral cortical changes, and the challenge of reproducible objective measurement [15].

Based on comparative studies between MRI and CUS regarding abilities to predict outcome, MRI is proposed as imaging method of choice for high risk preterm infants [19-21]. However, these studies did not use additional acoustic windows, high-resolution ultrasound, and Doppler imaging – as recommended by others [11, 22-24]. And, most importantly, the limitations of MRI in clinical context are often not fully considered.

In order to raise awareness regarding feasibility of routine, clinical MRI scanning in a vulnerable population, we performed this prospective study. Our aims were to investigate detection

accuracy and clinical feasibility of serial CUS from birth until discharge compared with a routine MRI scan obtained from 30 weeks' postmenstrual age (PMA) onwards, in infants born <29 weeks' gestational age (GA). We hypothesized that dedicated advanced serial CUS is equally effective as a single routine MRI scan at 30 weeks PMA to diagnose most common brain lesions in infants born very preterm and has greater clinical value due to higher availability for critically ill preterm infants.

Patients and Methods

Patients

Between May 2010 and January 2013, preterm infants born below 29 weeks GA were recruited prospectively. Standard clinical neuroimaging included serial CUS from birth until discharge and MRI at 30 weeks PMA (29 4/7 – 30 4/7 weeks). Of the 336 eligible infants, 29 were excluded because of congenital malformation (n = 18), uncertainty regarding gestational age (n = 5) or refusal of parental informed consent (n = 6). The institutional review board approved this study and parental consent was obtained for all participants.

Cranial ultrasonography

Serial CUS was performed by an experienced observer using an Esaote MyLab 70 (Genova, Italy). According to standard clinical protocol, images were obtained in standard sections; six coronal and five sagittal / parasagittal planes through the anterior fontanel, at days 0, 1, 2 and 7, and subsequently, once a week until discharge. Additional images of the cerebellum and transverse sinus were acquired through the mastoid fontanel. Serial color Doppler imaging was performed to assess the intracranial (sino-) venous and arterial system (Fig. 1). Images were acquired with a convex, 8.5 MHz probe. To obtain higher resolution of superficially located areas, a high frequency linear probe (13 MHz) was used at the anterior and mastoid fontanel.

Magnetic resonance imaging

MRI procedures were carried out according to protocol [8]: MRI scanning was postponed if patients were hemodynamically and respiratory unstable, which was evaluated by the attending neonatologist and nursing staff. All infants were accompanied by trained staff and were placed in an MRI-compatible incubator, which allowed controlled temperature and humidity and MR-compatible pulse oximetry and ventilation. Moldable earplugs and neonatal earmuffs protected the infants from auditory noise; sedative drugs were not administered.

Imaging data were acquired with a 1.5T GE EchoSpeed scanner (General Electrics Healthcare Technologies, Waukesha, WI) (Fig. 2). Axial T2-weighted fast-spin echo MRI data were obtained with the following parameter settings: repetition time (TR): 13100 ms; echo time (TE): 139 ms; flip angle: 90°; slice thickness: 1.2 mm; field of view: 190 x 190 mm^2. Axial 3D T1-SPGR MRI data

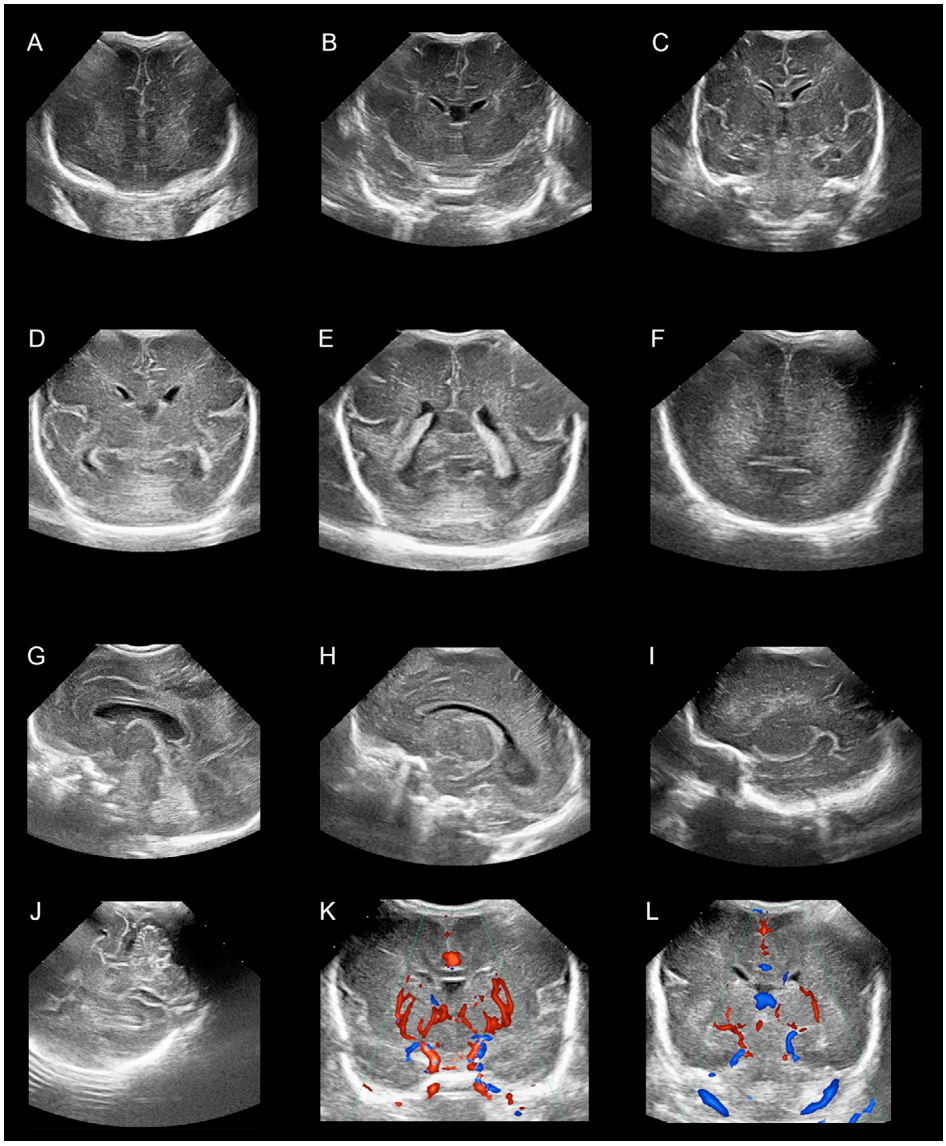

Figure 1 Ultrasound images were obtained in six coronal (A-F) and five sagittal/parasagittal planes (G-I) through the anterior fontanel. Additional images were acquired through the mastoid fontanel (J) to visualize the cerebellum and color Doppler images (K-L) were acquired to assess arterial and (sino-) venous systems.

were acquired using: TR: 9 ms; TE: 3 ms; flip angle: 15˚; slice thickness: 1.6 mm; field of view: 150 x 150 mm^2. DTI was performed using a single-shot-echo-planar-imaging sequence with diffusion gradients in 25 non-collinear directions, TR: 11725 ms; TE: 85.6 ms; slice thickness: 3 mm; field of view: 220 x 220 mm^2; *b* value: 750 s/mm^2; number of non-diffusion-weighted images: 3.

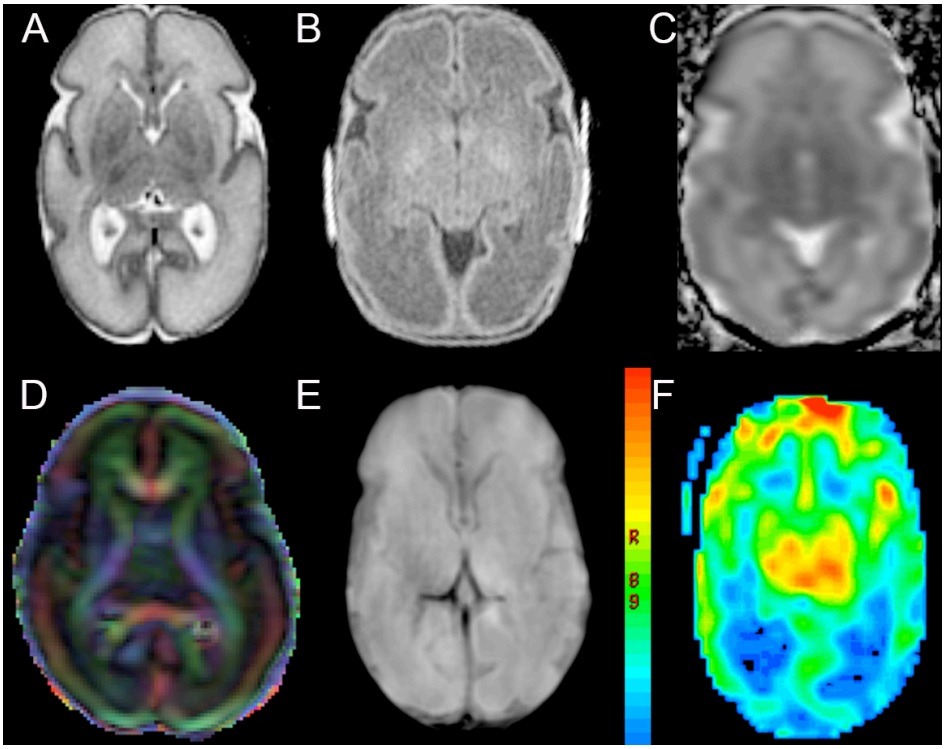

Figure 2 Applied MRI sequences: A: axial T2-weighted fast-spin echo; B: axial 3D T1-SPGR; diffusion tensor imaging, C: apparent diffusion coefficient-map and D: color-coded directionality map (red represents fibers in the left–right direction, blue represents fibers in the superior–inferior direction, and green represents fibers in the anterior–posterior direction); E: susceptibility weighted imaging, and F: arterial spin labeling.

For the sake of optimization during the study, advanced sequences were added to scanning protocol: susceptibility weighted imaging (SWI) was performed using: TR: 75 ms; TE: 48 ms; flip angle: 20˚; slice thickness: 2.2 mm; field of view: 210 x 210 mm^2. Arterial spin labeling was executed using: TR: 4200 ms; TE: 10 ms; flip angle: 155˚; post label delay: 1025 ms; slice thickness: 4 mm; field of view: 220 x 220 mm^2.

Assessment of brain injury

CUS and MRI data were assessed for signs of preterm brain injury by experienced authors independently (MR, PG for CUS and AP, ML for MRI) using a detailed classification system [25]. In all cases, consensus was reached between authors. IVH was graded according to Papile et al. [26]. WM abnormalities were classified into cystic PVL and diffuse non-cystic WM injury; the latter were defined as periventricular inhomogeneous echodensities on CUS or diffuse WM lesions on MRI [6, 23]. Cerebellar hemorrhage was categorized into folial or lobar cerebellar hemorrhage [27].

Statistical analysis

Statistical analysis was performed using SPSS version 20.0.0.1. Descriptive statistics were applied to patient characteristics and neonatal morbidities. GA was calculated from the first date of the last menstrual period; severity of illness was assessed with the score for neonatal acute physiology perinatal extension [28]; intrauterine growth restriction was defined as birth weight below two standard deviations; persistent ductus arteriosus was recorded if it required treatment, and necrotizing enterocolitis was diagnosed by pneumatosis intestinalis, hepatobiliary gas, or free intraperitoneal air on radiography. Proportional differences between imaging groups were investigated with Pearson's Chi-squared test. One-way ANOVA served to test differences between imaging group means. Combined sum of findings by CUS and MRI served as golden standard for calculation of sensitivity to detect injury patterns. A *p*-value of <0.05 (two-sided) was considered statistically significant.

Results

Descriptive statistics

307 Infants (170 boys) were included in this study, with mean GA of 26 weeks, 5 days and birth weight of 922 grams. 28 infants (9.1%) did not receive prenatal steroid therapy. Additional clinical characteristics are listed in Table 1. All 307 infants were serially scanned using CUS. In contrast, MRI was not performed at all in 127 infants, as 57 died before 30 weeks PMA; 55 were transferred to other hospitals before the MRI scan could be performed; and scanning was not performed in 15 due to logistic difficulties.

At 30 weeks PMA, 73 infants were considered not stable enough for MRI scanning; 58 of them were eventually scanned at a later time. Thus, three different groups with regard to MRI scanning are distinguished: group I: MRI scanning at 30 weeks PMA (n = 122); group II: MRI scanning after 30 weeks PMA (n = 58), and group III: no MRI scanning (n =127) (Fig. 3).

Patterns of preterm injury (Fig. 4)

Combined imaging findings

Injury patterns found either with CUS or MRI are listed in Table 1. GMH-IVH was detected in 100 infants, WM injury in 10, cerebellar hemorrhage in 21; cerebral sinovenous thrombosis (CSVT) in 11, and in 4 infants perforator stroke was identified.

Ultrasonographic findings

180 infants (58.6%) had normal CUS. GMH-IVH was seen in 80 infants (26.7%); in 23 this was limited to germinal matrix (7.5%), in 39 it was assigned IVH grade II (12.7%), in six IVH grade III (2.0%) and in 12 (3.9%) hemorrhage was complicated by parenchymal infarction. WM injury

Table 1 Descriptive statistics

	Total (*n* = 307)
Gestational age, mean ± SD[a] (weeks)	26.7 ± 1.5
Birth weight, mean ± SD (grams)	922 ± 256
Head circumference, mean ± SD (cm)	24.1 ± 2.1
Male gender, *n* (%)	170 (55.4%)
Apgar score at 5 minutes, mean ± SD	7 ± 2
Antenatal steroids	
None	28 (9.1%)
1 dose, *n* (%)	88 (28.7%)
2 doses, *n* (%)	187 (60.9%)
Intrauterine growth restriction, *n* (%)	42 (13.7%)
SNAPPE-score[b], mean ± SD	26 ± 21
Postnatal steroids, *n* (%)	43 (14.0%)
Necrotizing enterocolitis, *n* (%)	45 (14.7%)
Persistent ductus arteriosus, *n* (%)	142 (46.3%)
Death, *n* (%)	61 (19.9%)
Postmenstrual age at MRI scan, mean ± SD (weeks)	31.03 ± 2.3
No signs of brain injury, *n* (%)	161 (52.4%)
Germinal matrix and intraventricular hemorrhage (GMH-IVH), *n* (%)	100 (32.6%)
GMH, *n* (%)	39 (12.7%)
Limited IVH grade II, *n* (%)	43 (14.0%)
Extensive IVH grade III, *n* (%)	6 (2.0%)
Periventricular hemorrhagic infarction, *n* (%)	12 (3.9%)
White matter injury, *n* (%)	10 (3.3%)
Diffuse non-cystic white matter injury, *n* (%)	7 (2.3%)
Cystic periventricular leukomalacia, *n* (%)	3 (1.0%)
Cerebellar hemorrhage, *n* (%)	21 (6.8%)
Folial hemorrhage, *n* (%)	9 (2.9%)
Lobar hemorrhage, *n* (%)	12 (3.9%)
Cerebral sinovenous thrombosis, *n* (%)	11 (3.6%)
Perforator stroke, *n* (%)	4 (1.3%)
Inconsistent imaging findings on CUS and MRI, *n* (%)	61 (19.9%)

[a] standard deviation; [b] score for neonatal acute physiology perinatal extension

was sonographically detected in seven infants (2.2%); in four of them (1.3%) it was diffuse non-cystic WM injury, and in three (1.0%) cystic PVL was detected. Lobar cerebellar hemorrhage was identified in 10 infants (3.3%). Folial cerebellar hemorrhages were not recognized with CUS. CSVT was present in 11 infants; in all infants, the transverse sagittal sinus was involved, in one

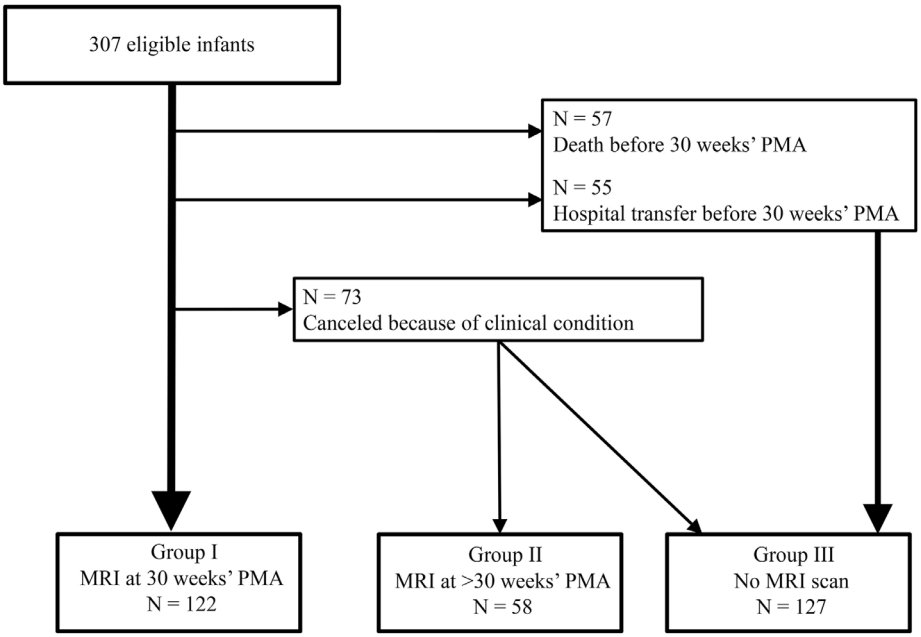

Figure 3 Flowchart of formation of neuroimaging groups.

infant there was also almost complete thrombosis of the superior sagittal sinus. Four infants presented with a perforator stroke on CUS.

MRI findings

MRI was performed in 180 infants and did not show any injury in 112 infants (62.2%). GMH-IVH was present in 43 infants (23.8%): GMH in 20 (11.1%); IVH-II in 14 (7.7%), and periventricular hemorrhagic infarction in nine infants (5.0%). WM injury was detected in eight infants (4.4%); in seven (3.9%) this was diffuse non-cystic WM injury and one infant had cystic PVL. Cerebellar hemorrhage was detected with MRI in 15 infants (8.3%); lobar in six and folial in nine. CSVT was identified on MRI in two infants; perforator stroke was not detected at all by MRI.

Differences between imaging groups

Clinical characteristics between the three MRI imaging groups differed significantly (Table 2). In general, infants in imaging group I were born with higher GA and birth weight and seemed to have fewer complications: intrauterine growth restriction, persistent ductus arteriosus, supplementation of postnatal steroids and death were significantly less common, and score for severity of illness was significantly lower: 19 compared with 27 and 34 of groups II and III respectively. Occurrence of necrotizing enterocolitis and pattern of preterm brain injury did not significantly differ between imaging groups (Table 2).

Table 2 Differences between imaging groups

	Group I (*n* = 122)	Group II (*n* = 58)	Group III (*n* = 127)	*p*-value
Gestational age, mean ± SD[a] (weeks)	27.1 ± 1.3	26.5 ± 1.3	26.4 ± 1.6	**
Birth weight, mean ± SD (grams)	994 ± 224	864 ± 181	880 ± 297	**
Head circumference, mean ± SD (cm)	24.7 ± 1.8	23.8 ± 1.7	23.7 ± 2.3	**
Male gender, *n* (%)	58 (47.5%)	35 (60.3%)	77 (60.6%)	
Apgar score at 5 minutes, mean ± SD	8 ± 1	8 ± 2	7 ± 2	*
Antenatal steroids				†
None	12 (9.8%)	5 (8.6%)	11 (8.7%)	
1 dose, *n* (%)	35 (28.7%)	14 (24.1%)	39 (30.7%)	
2 doses, *n* (%)	72 (59.0%)	39 (67.2%)	76 (59.8%)	
Intrauterine growth restriction, *n* (%)	9 (7.4%)	8 (13.8%)	25 (19.7%	*
SNAPPE[b]-score, mean ± SD	19 ± 16	27 ± 16	34 ± 25)	**
Postnatal steroids, *n* (%)	5 (4.1%)	12 (20.7%)	26 (20.5%)	**
Necrotizing enterocolitis, *n* (%)	11 (9.0%)	9 (15.5%)	25 (19.7%)	†
Persistent ductus arteriosus, *n* (%)	44 (36.1%)	41 (70.7%)	57 (44.9%)	**
Death, *n* (%)	2 (1.6%)	2 (3.4%)	57 (44.9%)	**
Postmenstrual age at MRI scan, mean ± SD (weeks)	30.1 ± 0.3	33.0 ± 3.3	-	-
No signs of brain injury, *n* (%)	58 (47.5%)	27 (46.6%)	76 (59.8%)	†
Germinal matrix and intraventricular hemorrhage (GMH-IVH), *n* (%)	42 (34.4%)	19 (32.8%)	39 (30.7%)	†
GMH, *n* (%)	18 (14.7%)	7 (12.1%)	14 (11.0%)	
Limited IVH grade II, *n* (%)	19 (15.6%)	8 (13.8%)	16 (12.6%)	
Extensive IVH grade III, *n* (%)	-	-	6 (4.7%)	
Periventricular hemorrhagic infarction, *n* (%)	5 (4.1%)	4 (6.9%)	3 (2.4%)	
White matter injury, *n* (%)	8 (6.6%)	-	2 (1.6%)	†
Diffuse non-cystic white matter injury, *n* (%)	7 (5.7%)	-	-	
Cystic periventricular leukomalacia, *n* (%)	1 (0.8%)	-	2 (1.6%)	
Cerebellar hemorrhage, *n* (%)	9 (7.4%)	6 (10.3%)	6 (4.7%)	†
Folial hemorrhage, *n* (%)	5 (4.1%)	4 (6.9%)	-	
Lobar hemorrhage, *n* (%)	4 (3.3%)	2 (3.4%)	6 (4.7%)	
Cerebral sinovenous thrombosis, *n* (%)	5 (4.1%)	4 (6.9%)	2 (1.6%)	†
Perforator stroke, *n* (%)	-	2 (3.4%)	2 (1.6%)	†
Inconsistent imaging findings on CUS and MRI, *n* (%)	41 (33.6%)	20 (34.5%)	-	†

[a] standard deviation; [b] score for neonatal acute physiology perinatal extension
* p<0.05; ** p<0.01; † not significant

Discrepant imaging findings on CUS and MRI

Table 3 compares imaging findings of CUS with MRI findings in the 180 infants who were scanned by both techniques. Inconsistencies were predominantly found for GMH-IVH in 38 infants, cerebellar hemorrhage in 11 and CSVT in seven infants. MRI had higher sensitivity to detect GMH and identified all posterior fossa abnormalities, but in 27 infants, CUS excelled in the acute detection of IVH grade II-III, perforator strokes and CSVT, as these lesions were no longer clearly visible on MRI at the time of scanning. Findings for WM injury were discrepant in three infants.

Table 3 Discrepant imaging findings on CUS and MRI

	Imaging findings			Accuracy	
	CUS	MRI		SensitivityCUS	Sensitivity MRI
		+	-		
Germinal matrix hemorrhage, *n* = 25	+	4	5	36.0%	80.0%
	-	16	-		
Intraventricular hemorrhage, grade II-III, *n* = 27	+	10	13	85.2%	51.9%
	-	4	-		
Diffuse non-cystic white matter injury, *n* = 7	+	4	0	57.1%	100%
	-	3	-		
Folial cerebellar hemorrhage, *n* = 9	+	0	0	0%	100%
	-	9	-		
Lobar cerebellar hemorrhage, *n* = 6	+	4	0	66.7%	100%
	-	2	-		
Cerebral sinovenous thrombosis, *n* = 9	+	2	7	100%	22.2%
	-	0	-		
Perforator stroke, *n* = 2	+	0	2	100%	0%
	-	0	-		

Discussion

This study demonstrates that many infants born very preterm suffer from brain injury and CUS effectively detects most common lesions. CUS has higher clinical feasibility than MRI, which cannot always be performed in severely ill infants. However, despite mastoid fontanel scanning, CUS remains inferior to identify small posterior fossa abnormalities. As MRI provides additional diagnostic information, we would recommend to optimize safety and feasibility of MRI procedures.

Comprehensive application of CUS, usage of supplemental acoustic windows, color Doppler imaging, higher transducer frequencies and careful interpretation of images by an experienced observer results in high accuracy to identify certain lesions. CUS provided better assessment

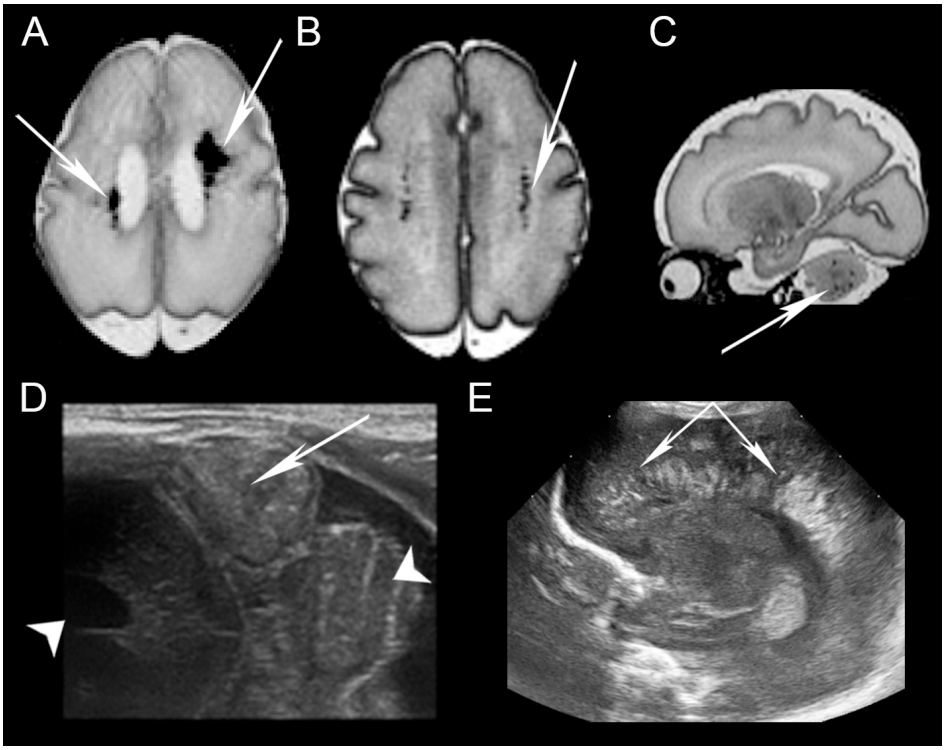

Figure 4 Examples of brain injury patterns on MRI (A-C) and CUS (D-E): A: bilateral periventricular hemorrhagic infarction on axial T2-weighted scan, note the ventricular dilatation caused by intraventricular hemorrhage; B: punctate white matter lesions on axial T2-weighted scan; C: multiple folial cerebellar hemorrhages on sagittal T2-weighted scan; D: cerebral sinovenous thrombosis in transverse sinus on cranial ultrasound, assessed through mastoid fontanel, note the large mass (arrow) between the lateral ventricle (left arrowhead) and cerebellum (right arrowhead), and E: periventricular leukomalacia on parasagittal cranial ultrasound, assessed through the anterior fontanel.

of injury than MRI in 27 infants, mostly because of higher sensitivity to detect IVH grade II-III, perforator stroke and CSVT. These lesions seem to correlate with adverse long term outcome and would have been missed if serial CUS had not been performed, leading to less prognostic accuracy [29, 30].

The higher sensitivity of CUS to detect IVH grade II-III seems mainly attributable to the consecutive application of CUS. Conventional MRI was unable to detect intraventricular blood and/or ventricular dilatation, possibly due to the resolving nature of IVH. Parodi et al. [31] recently reported a lower sensitivity (60%) of CUS to detect grade I-II GMH-IVH compared with SWI. The authors point out the unique possibilities of SWI to detect subependymal and/or intraventricular hemosiderin depositions and accentuate that dedicated timing and application of advanced MRI sequences is quite valuable in assessing the preterm brain.

In the present study, CUS was insufficient to detect diffuse non-cystic WM injury in three infants only. All other diffuse WM lesions on MRI were already detected on CUS by

inhomogeneous echodensities on CUS. This confirms the assumption that inhomogeneous hyperechogenicities are the CUS correlates of punctate WM lesions and stresses the value of sequential and advanced CUS to monitor and detect diffuse non-cystic WM injury [13, 15, 22-24]. However, MRI is needed to assess the extent and localization of WM injury for its full impact on long term outcome [32].

In correspondence with current literature [33, 34], MRI in the present study excelled in the detection of posterior fossa abnormalities: it confirmed all cerebellar hemorrhages detected with CUS and identified all folial and two lobar cerebellar hemorrhages that had been missed with CUS. Although cerebellar hemorrhages seen only on MRI seem to correlate with more optimistic outcomes than those visible on CUS [16], neurologic abnormalities are common; Tam et al. [34] reported abnormal neurologic examinations at age 3-6 years in 50% of infants with cerebellar hemorrhage seen only on MRI, compared with 16% of children without cerebellar hemorrhage. Furthermore, disrupted cerebellar development in preterm infants is suggested to contribute significantly to poor outcome [35].

In addition to the detection of limited cerebellar haemorrhage, neonatal care may clearly benefit from quantitative MRI sequences that could provide early objective biomarkers of outcome [4]. However, MRI is a complex technique with limitations in the very young. Our study design dictated MRI scanning at 30 weeks' PMA, but depending on clinical condition, scanning was postponed or cancelled in 185 infants (60%). Inherently, infants scanned at 30 weeks' PMA may likely have been the most healthy ones. Postponement or cancellation seems rather worrying because especially preterm infants with severe illness are at risk of brain injury and may benefit most from early MRI scanning [36, 37]. Moreover, more premature babies are surviving than ever before and related brain injury is on the rise [1]. It would be essential, therefore, to considerably improve the applicability of MRI. This includes: 1) safety improvement: transfers and monitoring of critically ill infants to the MR suite should be optimized and MRI sequences can be shortened to reduce procedure times [10, 38]; 2) tailored MRI scanning: indications, usage of sequences and timing to scan should be established more individually. For instance, MRI may be unnecessary for infants with uncomplicated history and absence of brain injury on ultrasound scans, provided that CUS was performed serially, comprehensively and carefully by an experienced observer [22]. But MRI would be required, even in case of critical illness, when CUS is inconclusive on the need to continue intensive care. And 3) improved availability: a dedicated neonatal MRI scanner in the vicinity of the NICU would improve its accessibility and overcome logistic problems.

Important limitations of this study should be addressed: 1) imaging group III was heterogeneous because it included both deceased patients and infants transferred to other hospitals before the MRI could take place. Inclusion of deceased patients may have influenced clinical characteristics; 2) due to absence of correlation between injury patterns and long term neurodevelopmental outcome in our study population, we were not able to demonstrate clinical relevance of all findings; 3) because strategies were being optimized over the course of this

study, SWI was not performed in all MRI procedures, which may have led to lower sensitivity to detect low-grade GMH-IVH compared with other studies [31]; 4) in this study, we observed imaging findings of routine, clinical MRI scans, as such, we were not able to perform post processing of advanced MRI sequences to obtain quantitative measurements of injury. We are aware that sophisticated use of MRI sequences, such as DTI, volumetric MRI and proton MR spectroscopy, which are usually performed in the context of research, would undoubtedly result in greater value of MRI. And, 5) due to logistic problems, our prospective study did not include term equivalent MRI scanning. As a result, we might not have been able to detect 'typical' characteristics of WM abnormality at term, such as thinning of corpus callosum, ventricular enlargements [32] and diffuse excessive high signal intensities [39]. Our results could therefore not be compared with other studies. However, MRI was performed at mean PMA of 31 weeks, but was still unable to detect some lesions that were previously detected with serial advanced CUS. We argue therefore that performance of CUS to detect acute brain lesions accurately would have been higher if MRI had been performed at term-equivalent age. Moreover, experienced use of CUS at term corrected age is well able to detect callosal thinning, ventricular enlargement and presence of small WM cysts [22].

Conclusion

Serial advanced CUS is adequate to detect and monitor preterm brain injury and therefore deserves more appreciation in neonatal neurology. MRI is invaluable as it allows objective quantitative assessment of microstructural brain properties and is superior to detect posterior fossa abnormalities. However, clinical use in preterms is currently limited because of safety and logistic issues. These issues need to be addressed in view of the increasing demand for quantitative biomarkers of outcome. Furthermore, dual use of sequential CUS and MRI provides high sensitivity to detect common patterns of preterm brain injury. Future research should therefore focus on the improvement of their complementary applications.

References

1. Gulland A. Fifteen million and rising—the number of premature births every year. BMJ. 2012; **344**: e3084.
2. Plaisier A, Govaert P, Lequin MH, Dudink J. Optimal Timing of Cerebral MRI in Preterm Infants to Predict Long-Term Neurodevelopmental Outcome: A Systematic Review. AJNR Am J Neuroradiol. 2013.
3. Wood NS, Marlow N, Costeloe K, Gibson AT, Wilkinson AR. Neurologic and developmental disability after extremely preterm birth. EPICure Study Group. N Engl J Med. 2000; **343**(6): 378-84.
4. Ment LR, Hirtz D, Huppi PS. Imaging biomarkers of outcome in the developing preterm brain. Lancet Neurol. 2009; **8**(11): 1042-55.
5. Smyser CD, Snyder AZ, Shimony JS, Blazey TM, Inder TE, Neil JJ. Effects of white matter injury on resting state FMRI measures in prematurely born infants. PLoS One. 2013; **8**(7): e68098.
6. Rutherford MA, Supramaniam V, Ederies A, Chew A, Bassi L, Groppo M, et al. Magnetic resonance imaging of white matter diseases of prematurity. Neuroradiology. 2010; **52**(6): 505-21.
7. Heemskerk AM, Leemans A, Plaisier A, Pieterman K, Lequin MH, Dudink J. Acquisition Guidelines and Quality Assessment Tools for Analyzing Neonatal Diffusion Tensor MRI Data. AJNR Am J Neuroradiol. 2013; **34**.
8. Plaisier A, Raets MM, van der Starre C, Feijen-Roon M, Govaert P, Lequin MH, et al. Safety of routine early MRI in preterm infants. Pediatr Radiol. 2012; **42**(10): 1205-11.
9. Mathur AM, Neil JJ, McKinstry RC, Inder TE. Transport, monitoring, and successful brain MR imaging in unsedated neonates. Pediatr Radiol. 2008; **38**(3): 260-4.
10. Rutherford M, Biarge MM, Allsop J, Counsell S, Cowan F. MRI of perinatal brain injury. Pediatr Radiol. 2010; **40**(6): 819-33.
11. Leijser LM, de Vries LS, Cowan FM. Using cerebral ultrasound effectively in the newborn infant. Early Hum Dev. 2006; **82**(12): 827-35.
12. Govaert P, De Vries LS. An atlas of neonatal brain sonography. 2nd ed. London: Mac Keith Press; 2010.
13. Ciambra G, Arachi S, Protano C, Cellitti R, Caoci S, Di Biasi C, et al. Accuracy of transcranial ultrasound in the detection of mild white matter lesions in newborns. Neuroradiol J. 2013; **26**(3): 284-9.
14. Graca AM, Cardoso KR, da Costa JM, Cowan FM. Cerebral volume at term age: Comparison between preterm and term-born infants using cranial ultrasound. Early Hum Dev. 2013.
15. van Wezel-Meijler G, Steggerda SJ, Leijser LM. Cranial ultrasonography in neonates: role and limitations. Semin Perinatol. 2010; **34**(1): 28-38.
16. Steggerda SJ, Leijser LM, Wiggers-de Bruine FT, van der Grond J, Walther FJ, van Wezel-Meijler G. Cerebellar injury in preterm infants: incidence and findings on US and MR images. Radiology. 2009; **252**(1): 190-9.
17. Leijser LM, Srinivasan L, Rutherford MA, Counsell SJ, Allsop JM, Cowan FM. Structural linear measurements in the newborn brain: accuracy of cranial ultrasound compared to MRI. Pediatr Radiol. 2007; **37**(7): 640-8.
18. Reynolds PR, Dale RC, Cowan FM. Neonatal cranial ultrasound interpretation: a clinical audit. Arch Dis Child Fetal Neonatal Ed. 2001; **84**(2): F92-5.
19. Maalouf EF, Duggan PJ, Counsell SJ, Rutherford MA, Cowan F, Azzopardi D, et al. Comparison of findings on cranial ultrasound and magnetic resonance imaging in preterm infants. Pediatrics. 2001; **107**(4): 719-27.
20. Miller SP, Cozzio CC, Goldstein RB, Ferriero DM, Partridge JC, Vigneron DB, et al. Comparing the diagnosis of white matter injury in premature newborns with serial MR imaging and transfontanel ultrasonography findings. AJNR Am J Neuroradiol. 2003; **24**(8): 1661-9.
21. Mirmiran M, Barnes PD, Keller K, Constantinou JC, Fleisher BE, Hintz SR, et al. Neonatal brain magnetic resonance imaging before discharge is better than serial cranial ultrasound in predicting cerebral palsy in very low birth weight preterm infants. Pediatrics. 2004; **114**(4): 992-8.

22. Horsch S, Skiold B, Hallberg B, Nordell B, Nordell A, Mosskin M, et al. Cranial ultrasound and MRI at term age in extremely preterm infants. Arch Dis Child Fetal Neonatal Ed. 2010; **95**(5): F310-4.
23. Leijser LM, Liauw L, Veen S, de Boer IP, Walther FJ, van Wezel-Meijler G. Comparing brain white matter on sequential cranial ultrasound and MRI in very preterm infants. Neuroradiology. 2008; **50**(9): 799-811.
24. de Vries LS, Benders MJ, Groenendaal F. Imaging the premature brain: ultrasound or MRI? Neuroradiology. 2013.
25. Govaert P, Ramenghi L, Taal R, de Vries L, Deveber G. Diagnosis of perinatal stroke I: definitions, differential diagnosis and registration. Acta Paediatr. 2009; **98**(10): 1556-67.
26. Papile LA, Burstein J, Burstein R, Koffler H. Incidence and evolution of subependymal and intraventricular hemorrhage: a study of infants with birth weights less than 1,500 gm. J Pediatr. 1978; **92**(4): 529-34.
27. Ecury-Goossen GM, Dudink J, Lequin M, Feijen-Roon M, Horsch S, Govaert P. The clinical presentation of preterm cerebellar haemorrhage. Eur J Pediatr. 2010; **169**(10): 1249-53.
28. Richardson DK, Corcoran JD, Escobar GJ, Lee SK. SNAP-II and SNAPPE-II: Simplified newborn illness severity and mortality risk scores. J Pediatr. 2001; **138**(1): 92-100.
29. Patra K, Wilson-Costello D, Taylor HG, Mercuri-Minich N, Hack M. Grades I-II intraventricular hemorrhage in extremely low birth weight infants: effects on neurodevelopment. J Pediatr. 2006; **149**(2): 169-73.
30. Berfelo FJ, Kersbergen KJ, van Ommen CH, Govaert P, van Straaten HL, Poll-The BT, et al. Neonatal cerebral sinovenous thrombosis from symptom to outcome. Stroke. 2010; **41**(7): 1382-8.
31. Parodi A, Morana G, Severino MS, Malova M, Natalizia AR, Sannia A, et al. Low-grade intraventricular hemorrhage: is ultrasound good enough? J Matern Fetal Neonatal Med. 2013.
32. Woodward LJ, Anderson PJ, Austin NC, Howard K, Inder TE. Neonatal MRI to predict neurodevelopmental outcomes in preterm infants. N Engl J Med. 2006; **355**(7): 685-94.
33. Fumagalli M, Bassi L, Sirgiovanni I, Mosca F, Sannia A, Ramenghi LA. From germinal matrix to cerebellar haemorrhage. J Matern Fetal Neonatal Med. 2013.
34. Tam EWY, Rosenbluth G, Rogers EE, Ferriero DM, Glidden D, Goldstein RB, et al. Cerebellar hemorrhage on magnetic resonance imaging in preterm newborns associated with abnormal neurologic outcome. J Pediatr. 2011; **158**(2): 245-50.
35. Messerschmidt A, Brugger PC, Boltshauser E, Zoder G, Sterniste W, Birnbacher R, et al. Disruption of cerebellar development: potential complication of extreme prematurity. AJNR Am J Neuroradiol. 2005; **26**(7): 1659-67.
36. Zwicker JG, Grunau RE, Adams E, Chau V, Brant R, Poskitt KJ, et al. Score for neonatal acute physiology-II and neonatal pain predict corticospinal tract development in premature newborns. Pediatr Neurol. 2013; **48**(2): 123-9 e1.
37. Card D, Nossin-Manor R, Moore AM, Raybaud C, Sled JG, Taylor MJ. Brain metabolite concentrations are associated with illness severity scores and white matter abnormalities in very preterm infants. Pediatr Res. 2013; **74**(1): 75-81.
38. Stokowski LA. Ensuring safety for infants undergoing magnetic resonance imaging. Adv Neonatal Care. 2005; **5**(1): 14-27; quiz 52-4.
39. Skiold B, Horsch S, Hallberg B, Engstrom M, Nagy Z, Mosskin M, et al. White matter changes in extremely preterm infants, a population-based diffusion tensor imaging study. Acta Paediatr. 2010; **99**(6): 842-9.

CHAPTER 10

NEONATAL DISORDERS OF GERMINAL MATRIX

M.M.A. Raets, J. Dudink, P. Govaert.

Journal of Maternal, Fetal and Neonatal Medicine, 2013 Aug 23. [Epub ahead of print].

Abstract

The germinal matrix (GM) is a richly vascularized, transient layer near the ventricles. It produces neurons and glial cells, and is present in the foetal brain between 8 and 36 weeks of gestation. At 25 weeks it reaches a maximum volume, it subsequently withers. GM is vulnerable to haemorrhage in preterm infants. This selective vulnerability is explained by limited astrocyte end-feet coverage of microvessels, reduced expression of fibronectin and immature tight junctions. Focal lesions in the neonatal period include haemorrhage, germinolysis and stroke. Such lesions in transient layers interrupt normal brain maturation and induce neurodevelopmental sequelae.

Introduction

Between 24 and 32 weeks of gestational age (GA) brain maturation is at a critical stage with ongoing events such as growth of axons, maximum growth of the subplate and entrance of thalamic afferents into the developing cortex [1]. The germinal matrix (GM) or subventricular zone is a richly vascularized, transient layer at the surface of the ventricles, which is present in the foetal brain between 8 and 36 weeks of gestation [2]. This article reviews germinal matrix volume, function, vulnerability and lesions during the neonatal period, aiming to provide insight into their pathogenesis.

GM volume

Germinal matrix volume (GMV) reaches its maximum at 23-26 weeks gestational age [2-4]. Scott et al. studied 48 magnetic resonance imaging (MRI) scans of 39 foetuses in utero between 20-31 weeks of gestation. Using motion-corrected, automatic segmentation they measured growth trajectories, which showed that GMV peaks at 25 weeks GA [5]. Reduction of this volume happens in a site specific manner and is expected to continue until the ventricular and subventricular zones regress at 36 weeks [5]. Histopathological studies confirm this peak in volume at 25 weeks [6]. The subventricular zone partly persists as a source of progenitor cells in adults, continuing to provide interneurons for the olfactory bulb as well as oligodendrocytes through adulthood [7]. Thus the adult brain harbours multipotent progenitor cells, which have the ability to develop into neurons [7].

GM function

Germinal matrix is considered the 'factory' for production of most brain cells: glutamatergic projection neurons, GABAergic interneurons and oligodendroglial precursors in the latter part of pregnancy. After 15 weeks the subventricular zone becomes the predominant site of cell generation, forming ganglionic eminences (GE) along the lateral walls of the frontal horns of the lateral ventricles [6]. The GE is the source of neocortical GABAergic inhibitory interneurons as well as neurons for adjacent basal nuclei; it also generates precursors of oligodendrocytes and astrocytes well into the third trimester (Figure 1) [8]. Neuroblasts derived from the GE migrate tangentially to reach the cortical anlage. Radial glial fibers from the GE are seen in the second half of gestation. These radial glial fibers are a scaffold for migrating neurons [8]. GE precursor cells first migrate laterally (radially) and then change direction, entering tangential migration (Figure 2). Tangential migration is also seen in the thalamic pulvinar neurons as they arise from the telencephalic GE and migrate to the diencephalon during 5-8 months of gestation [8]. As the

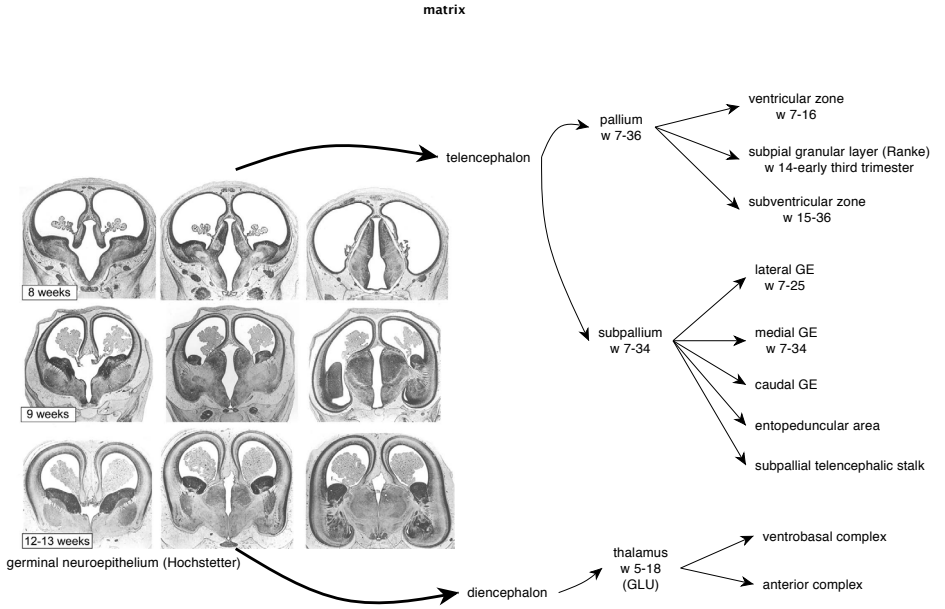

Figure 1 Role of neuroepithelium in telencephalic and diencephalic development

GE is a major source for oligodendrocytes, their number can be reduced and differentiation impaired due to haemorrhage; this may contribute to white matter injury [8].

GM vulnerability

The fragility of vessels in GM is well known but still not entirely understood. Mainly haemodynamic factors seem to cause wall rupture in small venules [9]. Preterm brain haemorrhage occurs primarily in GM (GMH or germinal matrix haemorrhage) but neither in cortex nor in white matter (WM) [10]. Matrix vascular density is increased compared with WM and cerebral cortex and the subependymal venules have a circular shape [11].

The vascular network in GM is complex: regular anatomic schemes such as arterioles, capillaries and veins are not readily applicable in this context [12]. The GM vasculature includes subependymal veins, where medullary veins from the deep white matter coalesce [12]. At 23 weeks of GA *thin-walled subependymal veins* are identified in GM; they mature with increasing GA [12, 13].

Pericytes provide structural stability to blood vessels. Braun et al. [14] illustrated, with a histopathological human and animal study, how pericytes were diminished in GM vasculature in human foetuses and preterm infants: both coverage and density were reduced in GM vasculature compared with WM and cortex (Figure 2).

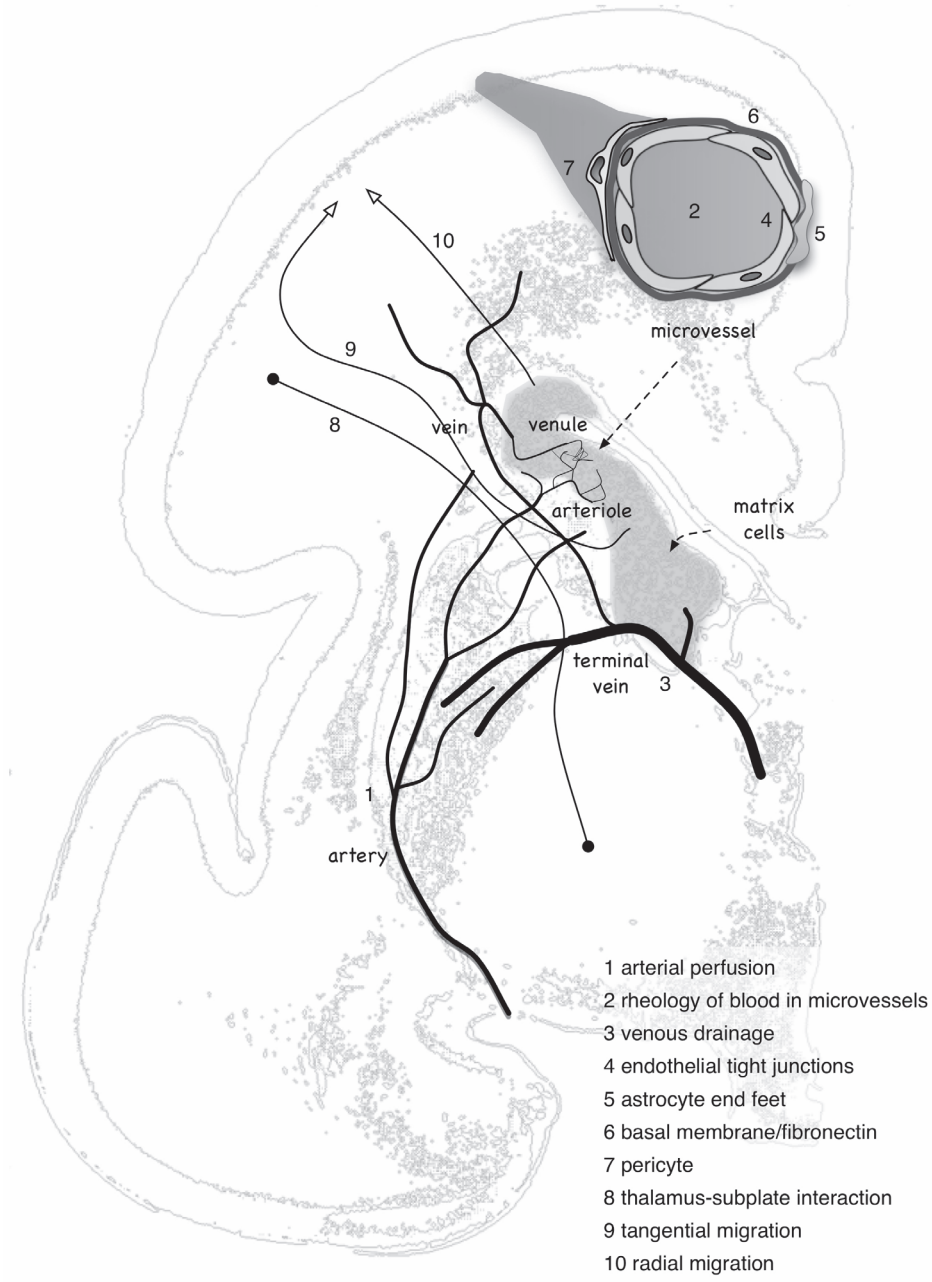

Figure 2 Overview of different factors influencing germinal matrix vulnerability

Blood-brain barrier (BBB) components include endothelial tight junctions, astrocyte end-feet coverage, basal lamina and capillary pericytes: all play a role in stabilisation of microvessels (Figure 2). Weakness of any of those components can lead to GMH [15]. Changes in BBB permeability correlate with the distribution of *tight junction proteins* [16]. Ballabh et al.[17] performed a histopathological study of endothelial tight junction molecules in different cerebral regions: primary tight junctions molecules in GM were not decreased in comparison with WM and cerebral cortex, leading to the conclusion that the tight junctions unlikely play a role in GM vulnerability [17]. Anstrom et al., on the contrary, documented that GM vessels at 24 weeks GA were characterized by thin, discontinuous lengths of tight junction immuno-reactivity, compared with a nearly continuous line in cortical vessels; tight junction protein staining in GM enhanced with increasing age in the third trimester of pregnancy [16].

El-Khoury et al. [10] studied perivascular coverage by *astrocyte end-feet* in GM compared with WM and cerebral cortex from 16 to 40 weeks GA. They documented decreased expression of the glial fibrillary acidic protein (GFAP) in end-feet along the vasculature of the GM compared with WM and cerebral cortex between 24-32 weeks GA. End-feet coverage possibly plays a role in the fragility of GM vasculature [10].

Laminin, type IV collagen and heparin sulphate proteoglycan perlecan form the basal lamina of cerebral vasculature. Together with the basal lamina, *fibronectin*, present in extracellular matrix, also plays a role in providing structural stability of vessels [15, 18]. Fibronectin regulates incorporation of fibrinogen and is, together with vascular endothelial growth factor (VEGF), critical for angiogenesis. Xu et al. [15] found that fibronectin protein levels in the GM were significantly lower than WM or cerebral cortex. Fibronectin levels in WM and cortex increased significantly with advancing GA, but not in GM. The expression of type IV collagen chains and perlecan are not different between cortex, WM or GM [15, 19]. Laminin α1 had a higher expression in GM compared with WM and cortex, the other chains did not differ. However, mutations in *type IV collagen* are known to cause foetal brain haemorrhage, hydrocephalus, porencephaly, cerebellar destruction and arterial aneurysms [20].

Prenatal lung ripening with glucocorticoids (GC) has contributed to increased survival and less morbidity in preterm infants. The incidence of GMH-IVH is reduced by 50% [21]. Vinukonda et al [21], found in a histopathological study of rabbits and human foetuses, that prenatal GCs stabilize GM vasculature through suppressed angiogenesis, pruned neovasculature and enhanced pericyte coverage [21].

In animal studies indomethacin inhibits prostaglandin synthesis and decreases cerebral blood flow. Ment et al. showed that in beagle pups pre-treated with indomethacin changes in systemic blood pressure were blunted, however there was no effect on cerebral blood flow [22]. Another study by Ment et al. demonstrated that indomethacin in beagle pups led to increased deposition of collagen V and laminin [23]. Increasing stability of the basal lamina probably explains the reduction in incidence of IVH [23]. A Cochrane review by Fowlie et al. [24] concluded that prophylactic use of indomethacin has short-term benefits in the sense that it reduces

the incidence of severe GMH-IVH. Evidence of the effect on mortality or neurodevelopmental outcome is still controversial[24].

In summary fragility of GM microvasculature is not likely due to lack of collagen, laminin or perlecan. Fibronectin is significantly lower in GM compared with WM and cortex and therefor might play a role. Tight junction protein levels in GM are comparable with WM and cortex levels, however these tight junction are immature at 23 weeks of gestation and mature with increasing GA. Perivascular coverage by astrocyte end-feet is immature in GM. Prenatal use of GCs stabilizes GM vasculature. Prophylactic use of indomethacin might have a protective effect on the development of GMH-IVH.

GM lesions

GMH/IVH risk factors and sequelae

Immaturity of organ functions in preterm infants may entrain significant changes in cerebral haemodynamics and potentially interfere with the integrity of the GM [13] (Figure 2) . The following

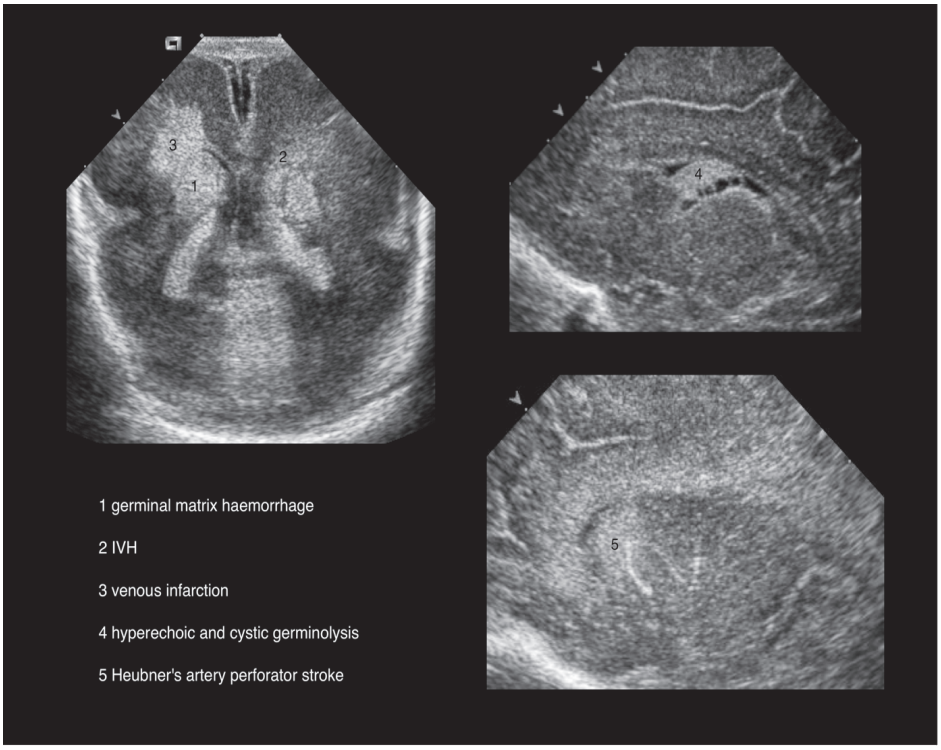

Figure 3 Germinal matrix lesions including GMH-IVH, venous infarction, germinolysis and perforator stroke.

factors have been identified as risks for GMH: low cerebral blood flow (CBF) (e.g. hypotension, asphyxia), high CBF (e.g. hypertension, volume expansion, hypercarbia, low haematocrit, pain), elevated cerebral venous pressure (e.g. respiratory distress syndrome, positive pressure ventilation, pneumothorax) and fluctuating CBF [13]. Platelet and coagulation disorders contribute to expansion rather than initiation of a spontaneous GMH [25]. Increased risk for GMH-IVH is also seen in very low birth weight infants carrier of prothrombotic mutations [26]. This suggests that besides haemodynamic changes rheological factors play a role.

The overall incidence of GMH-IVH is approximately 15% in very low birth weight infants, for extremely low birth weight infants (< 1000 grams) the incidence reaches 45% (Figure 3). GMH-IVH is typically diagnosed within the first days of life. Most infants are asymptomatic, in 15% clinical seizures are observed. Infants with periventricular haemorrhagic infarction (PVHI) have a higher incidence of seizures (40%). Post haemorrhagic ventricular dilatation occurs in half of the infants with extensive IVH [13]. PVHI is caused by occlusion of collector veins and leads to local destruction of the intermediate zone, which includes radial glial cells and thus stops cellular migration of neurons above the lesion (Figure 3).

Precursor cells already travelling cease migration and form heterotopias, these migrating cells do not reach their cortical target areas [27]. Secondarily, the cytostructure of differentiating cortical grey matter can be altered by loss of connectivity. These post-injury related changes in grey matter structure play a role in outcome [27]. The postnatal course of one 25 weeks GA preterm boy was complicated with GMH-IVH and PHVI in the first week of life [28]. An MRI scan at 34 weeks illustrated cortical dysplasia above the lesion. Disruption of final steps in cell migration, injury to the subplate and/or disruption of corticospinal axons are possible mechanisms behind this lesion paradigm [28]. Finally subarachnoid haemorrhage due to IVH may disrupt cerebellar cortex [1, 13].

Specific blood components, e.g. plasma proteins thrombin and plasmin, have toxic effects on perinatal rat subventricular zone cells. Haemoglobin and breakdown products might also play a role due to free radical mechanisms. After haemorrhage the proliferation of germinal cell populations is suppressed within 24 hours [6]. This effect can persist for up to four weeks. Although proliferation is suppressed, cell death appears to be minimal. In mouse models only a few apoptotic cells are identified in the subventricular zone after haemorrhage [6].

In survivors without ventricular dilatation and periventricular haemorrhagic infarction, neurological deficits are still present including cognitive and attention deficits. Quantitative neuroimaging at term equivalent showed a significant reduction of cortical grey matter volume of 16% in preterm infants with an uncomplicated IVH compared to those without IVH [29]. This is consistent with the literature describing possible effects of astrocytic loss on cortical development and suppressed proliferation of germinal matrix cells, which may be associated with impaired development.

Germinolysis

Haemorrhage and/or micro-infarction of GM, both in or ex utero, can cause cystic changes in the areas within one week after the event (Figure 3). The reported prevalence of pseudocysts is 1% of all healthy term infants. GM cysts are associated with several factors including non-bacterial fetopathy (CMV, rubella, toxoplasmosis), twin-to-twin transfusion, prenatal and perinatal asphyxia, inborn errors of metabolism (peroxisomal or mitochondrial disorder, organic aciduria), intra-uterine growth restriction, and anomalies of the karyotype. Several perforator stroke types may damage parts of GM. Perforator stroke is relatively common in sick preterm infants (Figure 3)[30].

Germinolysis following term birth asphyxia and in association with bronchopulmonary dysplasia further confirm the existence of microvascular infarction within striatal arteries [31]. On occasion striatal arteriopathy, a sonographic proxy of medium sized arterial injury, follows GMH. Van Baalen et al. [32] described 5 near term infants with non-cerebral infections and non-haemorrhagic echodensity of the GM on neuroimaging. Their findings favour ischaemia of the highly vascularized and highly metabolic GM as the cause for germinolysis and gliosis. An alternative explanation could be that cystic germinolysis is not due to arterial occlusion but is associated with enhanced apoptosis in this area of the brain. However, the significance of this type of matrix regression for development is still unclear. Horsch et al. [33] found 9 infants in a cohort of 86 infants below 32 weeks GA, with GMH-like lesions, which occurred after the first week of life. These infants rated lower on the Bayley score at three years of age [33].

In conclusion different lesions (haemorrhage, infarction, germinolysis) in transient zones like germinal matrix can lead to selective cell loss, alter cell migration and disrupt tract formation. The end result is white matter injury and cortical disorganisation.

References

1. Volpe JJ. The encephalopathy of prematurity—brain injury and impaired brain development inextricably intertwined. Semin Pediatr Neurol. 2009; **16**(4): 167-78.
2. Kinoshita Y, Okudera T, Tsuru E, Yokota A. Volumetric analysis of the germinal matrix and lateral ventricles performed using MR images of postmortem fetuses. AJNR Am J Neuroradiol. 2001; **22**(2): 382-8.
3. Battin MR, Maalouf EF, Counsell SJ, Herlihy AH, Rutherford MA, Azzopardi D, et al. Magnetic resonance imaging of the brain in very preterm infants: visualization of the germinal matrix, early myelination, and cortical folding. Pediatrics. 1998; **101**(6): 957-62.
4. Habas PA, Kim K, Corbett-Detig JM, Rousseau F, Glenn OA, Barkovich AJ, et al. A spatiotemporal atlas of MR intensity, tissue probability and shape of the fetal brain with application to segmentation. Neuroimage. 2010; **53**(2): 460-70.
5. Scott JA, Habas PA, Kim K, Rajagopalan V, Hamzelou KS, Corbett-Detig JM, et al. Growth trajectories of the human fetal brain tissues estimated from 3D reconstructed in utero MRI. Int J Dev Neurosci. 2011; **29**(5): 529-36.
6. Del Bigio MR. Cell proliferation in human ganglionic eminence and suppression after prematurity-associated haemorrhage. Brain. 2011; **134**(Pt 5): 1344-61.
7. Corbin JG, Gaiano N, Juliano SL, Poluch S, Stancik E, Haydar TF. Regulation of neural progenitor cell development in the nervous system. J Neurochem. 2008; **106**(6): 2272-87.
8. Ulfig N. Ganglionic eminence of the human fetal brain—new vistas. Anat Rec. 2002; **267**(3): 191-5.
9. Ghazi-Birry HS, Brown WR, Moody DM, Challa VR, Block SM, Reboussin DM. Human germinal matrix: venous origin of hemorrhage and vascular characteristics. AJNR Am J Neuroradiol. 1997; **18**(2): 219-29.
10. El-Khoury N, Braun A, Hu F, Pandey M, Nedergaard M, Lagamma EF, et al. Astrocyte end-feet in germinal matrix, cerebral cortex, and white matter in developing infants. Pediatr Res. 2006; **59**(5): 673-9.
11. Ballabh P, Braun A, Nedergaard M. Anatomic analysis of blood vessels in germinal matrix, cerebral cortex, and white matter in developing infants. Pediatr Res. 2004; **56**(1): 117-24.
12. Anstrom JA, Brown WR, Moody DM, Thore CR, Challa VR, Block SM. Subependymal veins in premature neonates: implications for hemorrhage. Pediatr Neurol. 2004; **30**(1): 46-53.
13. Bassan H. Intracranial hemorrhage in the preterm infant: understanding it, preventing it. Clin Perinatol. 2009; **36**(4): 737-62, v.
14. Braun A, Xu H, Hu F, Kocherlakota P, Siegel D, Chander P, et al. Paucity of pericytes in germinal matrix vasculature of premature infants. J Neurosci. 2007; **27**(44): 12012-24.
15. Xu H, Hu F, Sado Y, Ninomiya Y, Borza DB, Ungvari Z, et al. Maturational changes in laminin, fibronectin, collagen IV, and perlecan in germinal matrix, cortex, and white matter and effect of betamethasone. J Neurosci Res. 2008; **86**(7): 1482-500.
16. Anstrom JA, Thore CR, Moody DM, Brown WR. Immunolocalization of tight junction proteins in blood vessels in human germinal matrix and cortex. Histochem Cell Biol. 2007; **127**(2): 205-13.
17. Ballabh P, Hu F, Kumarasiri M, Braun A, Nedergaard M. Development of tight junction molecules in blood vessels of germinal matrix, cerebral cortex, and white matter. Pediatr Res. 2005; **58**(4): 791-8.
18. Hocking DC, Sottile J, Langenbach KJ. Stimulation of integrin-mediated cell contractility by fibronectin polymerization. J Biol Chem. 2000; **275**(14): 10673-82.
19. Anstrom JA, Thore CR, Moody DM, Challa VR, Block SM, Brown WR. Morphometric assessment of collagen accumulation in germinal matrix vessels of premature human neonates. Neuropathol Appl Neurobiol. 2005; **31**(2): 181-90.
20. Verbeek E, Meuwissen ME, Verheijen FW, Govaert PP, Licht DJ, Kuo DS, et al. COL4A2 mutation associated with familial porencephaly and small-vessel disease. Eur J Hum Genet. 2012; **20**(8): 844-51.
21. Vinukonda G, Dummula K, Malik S, Hu F, Thompson CI, Csiszar A, et al. Effect of prenatal glucocorticoids on cerebral vasculature of the developing brain. Stroke. 2010; **41**(8): 1766-73.

22. Ment LR, Stewart WB, Duncan CC, Scott DT, Lambrecht R. Beagle puppy model of intraventricular hemorrhage. Effect of indomethacin on local cerebral glucose utilization. J Neurosurg. 1984; **60**(4): 737-42.
23. Ment LR, Stewart WB, Ardito TA, Huang E, Madri JA. Indomethacin promotes germinal matrix microvessel maturation in the newborn beagle pup. Stroke. 1992; **23**(8): 1132-7.
24. Fowlie PW, Davis PG, McGuire W. Prophylactic intravenous indomethacin for preventing mortality and morbidity in preterm infants. Cochrane Database Syst Rev. 2010; (7): CD000174.
25. Ballabh P. Intraventricular hemorrhage in premature infants: mechanism of disease. Pediatr Res. 2010; **67**(1): 1-8.
26. Ramenghi LA, Fumagalli M, Groppo M, Consonni D, Gatti L, Bertazzi PA, et al. Germinal matrix hemorrhage: intraventricular hemorrhage in very-low-birth-weight infants: the independent role of inherited thrombophilia. Stroke. 2011; **42**(7): 1889-93.
27. Marin-Padilla M. Developmental neuropathology and impact of perinatal brain damage. I: Hemorrhagic lesions of neocortex. J Neuropathol Exp Neurol. 1996; **55**(7): 758-73.
28. Govaert P, Lequin M, Korsten A, Swarte R, Kroon A, Barkovich AJ. Postnatal onset cortical dysplasia associated with infarction of white matter. Brain Res. 2006; **1121**(1): 250-5.
29. Vasileiadis GT, Gelman N, Han VK, Williams LA, Mann R, Bureau Y, et al. Uncomplicated intraventricular hemorrhage is followed by reduced cortical volume at near-term age. Pediatrics. 2004; **114**(3): e367-72.
30. Abels L, Lequin M, Govaert P. Sonographic templates of newborn perforator stroke. Pediatr Radiol. 2006; **36**(7): 663-9.
31. Smets K, De Kezel C, Govaert P. Subependymal caudothalamic groove hyperechogenicity and neonatal chronic lung disease. Acta Paediatr. 1997; **86**(12): 1370-3.
32. van Baalen A, Rohr A. From fossil to fetus: nonhemorrhagic germinal matrix echodensity caused by mineralizing vasculitis—hypothesis of fossilizing germinolysis and gliosis. J Child Neurol. 2009; **24**(1): 36-44.
33. Horsch S, Kutz P, Roll C. Late germinal matrix hemorrhage-like lesions in very preterm infants. J Child Neurol. 2010; **25**(7): 809-14.

CHAPTER 11

GENERAL DISCUSSION

General discussion

Advances in fetal and neonatal care have increased rates of survival, however despite these advances, many infants born preterm still develop long term neurodevelopmental problems [1-5]. Epidemiological studies have shown that cerebrovascular instability during the first vulnerable weeks of life is a major risk factor for long term disability and can lead to common types of preterm brain injury such as: germinal matrix or intraventricular haemorrhage with or without venous infarction, bilateral white matter injury associated with low brain perfusion and perforator stroke [6, 7]. During the time preterm infants are admitted on the NICU (between 24 and 32 weeks of gestation) human brain development is at a critical stage with ongoing events such as growth of axons, increase of subplate to it's maximum size and entrance of thalamocortical afferents into the cortex [8]; they render the brain vulnerable to different stress factors including inflammation, hypoxia, hyperoxia and hemodynamic instability. Besides transient neuronal and axonal vulnerability, ontogenesis of the neurovascular system is known to play an important role in different types of brain injury. Monitoring brain development and early recognition of preterm brain injury is important for designing and performing neuroprotective treatment strategies. CUS allow safe, serial, bedside neuroimaging of the preterm brain. Ultrasound software improvements and more sophisticated computing algorithms together with hardware developments, have made CUS a competitive alternative for high resolution MRI brain scans. The general aim of this thesis was to provide more insight in how cerebral blood flow and brain maturation is related to preterm brain injury, studied with advanced CUS.

We prospectively performed a 3-year observational, cohort study in preterm infants born below 29 weeks of gestation. Besides normal routine serial CUS images, which included several growth indices, we decided to expand traditional scanning protocol with extensive Doppler measurements. We visualized different intracranial vessels to study normal development, anatomical variations and flow velocities. For the arterial blood flow we included carotid arteries, anterior cerebral artery, perforator arteries and pial arteries. Transverse sinuses (through the anterior fontanel at the insertion of the cerebellar tentorium), superior sagittal sinus and internal cerebral veins were studied in the venous system.

Already within the first few months of our study we identified two preterm infants in which carotid flow problems occurred. These infants were asymptomatic and normal routine CUS showed no specific lesions. Due to a competent circle of Willis major intracranial injury was prevented and these flow problems could have stayed unnoticed. With extensive CUS including colour Doppler these flow problems were timely recognized, so potential causes could be addressed and therapeutic options could be evaluated. At first we suspected an incidental finding, however after introduction of standard visualization of the circle of Willis in our clinical protocol, we identified more infants, who are described in **Chapter 4**.

Several authors have reported that CUS including colour Doppler is feasible to screen the intracranial venous system in neonates [9-12]. However routine clinical scanning of the venous

system in preterm infants is only rarely reported. Visualization of both transverse sinuses (TS) through the anterior fontanel can be challenging, but is feasible. The TS develops asymmetrically. This phenomenon is extensively studied in adults [13-16] and recently also in neonates [17]. All studies confirmed that drainage to the right TS is dominant in the majority of adults/neonates. If it was difficult to visualize TS on one side, we used the mastoid fontanel to screen TS in detail. During this study we identified eleven infants with cerebral sinovenous thrombosis (CSVT) (described in **Chapter 3**). All infants were asymptomatic and TS was affected in all infants. In the literature CSVT is reported as a rare disease with high morbidity. In the Netherlands the incidence was suggested to be 1 to 12 per 10000 neonates [18]. This seems clearly underestimated, as only late preterm and term neonates with symptoms, suggestive of CSVT, were screened [18]. We found a staggering high prevalence of 4.4% in our population. CUS including colour Doppler and scans through the mastoid fontanel can detect neonatal CSVT at an early stage, allowing therapeutic considerations prior to stroke or haemorrhage. However management of CSVT is still controversial [19]. Our study raised a few questions especially regarding treatment options. We believe that serial imaging with CUS including colour Doppler and scans through the mastoid fontanel are necessary to detect CSVT at an early stage, so prevention of stroke and haemorrhage is still possible. Due to the high incidence of local complications in our cohort, treatment is only retained for complete vessel occlusion or propagation of thrombosis after diagnosis. Further research is necessary regarding long term outcome of CSVT in preterm neonates and therapeutic options. Recently Tan et al. [20] documented that pillow decompression improves cerebral sinovenous flow, which represents a potential, non-invasive intervention in prevention and treatment of CSVT.

Beside cerebral blood flow, lesion patterns documented with CUS were studied both retrospectively and prospectively. In **Chapter 5** we describe a large cohort of infants with neonatal perforator stroke. We found that most neonates were asymptomatic and that CUS diagnosed most strokes (80%), predominantly in the first week of life. These numbers make routine serial CUS screening in admitted neonates important. Perinatal stroke is also very likely underrecognised due to subtle or absent symptoms. Therefore serial imaging with CUS is important throughout the NICU admission. Again this study gives rise to several questions about the effect on future outcome and treatment options which need to be answered in upcoming studies.

Following **Chapter 4 and 5** ECMO patients are a very interesting population to study. As stated earlier neonates are at risk for brain injury. The combination of carotid artery and jugular vein ligation with continuous heparinisation increases this risk for brain injury during ECMO. Therefore we decided to study the incidence and lesion patterns during neonatal ECMO in a nationwide cohort, spanning two decades (**Chapter 6**). All infants were screened with CUS. Additional MRI or CT scanning was not performed in all neonates, therefore we focused on CUS diagnosis and used available MRI/CT scans for confirmation. The incidence of brain injury in our cohort was 17.3%, comparable with previous studies [21-24]. Primary haemorrhage was the largest group. Stroke (AIS) occurred in 5% of the patients, with a notable preference for the left

side. This finding is unexpected in view of right carotid artery ligation. We argued that if AIS associated with right carotid ligation does not occur predominantly in the right hemisphere, the circle of Willis must be competent enough to guarantee cerebral blood flow via the left carotid artery and the basilar artery to the right part of the brain. Given the known variations of the circle of Willis [25-27], it would be interested if screening of the circle of Willis with CUS prior to ECMO could identify neonates at risk for stroke or haemorrhage during ECMO.

With ever increasing concerns about cost effectiveness, patient safety and patient friendliness, advances in CUS are making the technology increasingly attractive for routine neuroimaging. We prospectively compared serial advanced CUS to an early MRI scan for detecting most common types of preterm brain injury. **Chapter 9** showed the strengths of these neuroimaging techniques. MRI was often postponed or cancelled due to haemodynamic instability or logistic problems. Inconsistencies between the two imaging techniques were found in 48 infants (IVH, cerebellar haemorrhage, CSVT). Not surprisingly MRI was better in detecting injury in the posterior fossa (e.g. punctate cerebellar haemorrhage). However CUS was excellent in accurate detection of acute IVH and CSVT. Both techniques proved to be valuable in the neonatal period. Serial CUS proved very effective in diagnosing the common types of preterm brain injury, however cerebellar abnormalities can be missed. Although MRI identifies these lesions, clinical application is limited due to safety aspects and logistic issues. These findings are comparable with previous studies evaluating MRI and CUS [28, 29]. This study illustrates that CUS could be more accurate in detecting lesions if additional windows (e.g. mastoid fontanel) are used in standard routine CUS and with dedicated sonographers performing CUS.

Because the ontogenesis of the neurovascular system is known to play an important role in different types of brain lesions, **chapter 2** provides a comprehensive background of venous origin in perinatal brain injury and in **chapter 10** lesions of the germinal matrix are reviewed. Recent research in neuroscience has shown how these lesions in transient, vascular rich layers of development interrupt normal maturation and induce neurodevelopmental sequelae.

Alongside evaluation of "macro circulation" in large intracranial vessels we performed a pilot study to analyze whether CUS would be able to study preterm "cerebral microcirculation" (**Chapter 7)**. Our research question in this pilot study was whether colour Doppler CUS is able to monitor regional cerebral perfusion at the level of microvessels (flow velocities around 2 cm/s). A broad range in Doppler colour index (DCI) was found between patients and at different moments, therefore this method might reflect cerebral blood flow. This technique seems promising for evaluating cerebral blood flow during adaptation or to monitor therapeutic interventions on the NICU.

Chapter 8 demonstrated a technique to objectively measure grey values in preterm deep grey matter. Experienced sonographers know the putamen in extremely preterm infants is more hyperechoic compared to late preterm infants. As stated earlier ultrasound is a dynamic process and quality depends on settings and observer. Our objective was to measure grey values objectively. Globus pallidus to putamen (GPP) ratio of preterm infants at 24 weeks of

gestation was significant lower compared to preterm infants of 28 weeks GA, so the putamen is more hyperechoic in extremely preterm infants. Another interesting finding is that at 30 weeks corrected age this difference was still significant. An explanation could be that "normal" development is delayed in extreme preterm infants. But previous studies illustrated that putamen is more vulnerable to hypoxic ischemic damage compared to globus pallidus [30, 31]. Extreme preterm infants are at risk of haemodynamic instability and hypoxic-ischemic insults, therefore this persistent hyperechogenicity of the putamen might be a reflection of subtle brain injury. Further research is necessary to study this phenomenon. Attenuation effect makes direct comparison between patients difficult and analysis is now manual and offline, making clinical implementation at bedside though.

With the combined findings of the abovementioned studies, we would like to advise clinicians performing CUS in neonates to expand routine CUS. We believe that routine CUS (beside standard planes; described in **chapter 9**) should include visualization of both carotid arteries, transverse sinuses, superior sagittal sinus and that the use of additional windows (mastoid and posterior fontanel) increases detection of brain injury.

Besides better detection of brain injury, early recognition of flow problems or anatomical variations help to understand perinatal brain injury patterns and to identify infants who are at risk for developing injury at an early stage. Also providing insights for further research and hopefully preventive strategies in the near future.

Our research protocol included, beside standard routine images, imaging of the cerebral blood flow (arterial, venous and microcirculation) and focussed on brain injury patterns. Even in experienced hands it is difficult to focus on all three aspects extensively during one exam. We would like to advise other researchers to focus on one topic. Although CUS is a non-invasive imaging technique, duration of the exam should be limited to avoid discomfort in (pre)term infants.

Future perspectives

The general aim of this thesis was to provide more insight in cerebral perfusion. Our ultrasound machine has the ability to visualize micro vessels with velocities of approximately 2 cm/s. With better probes, higher frequencies and improved post-processing techniques we will be able to visualize even smaller vessels, providing more information on cerebral microcirculation. Haemodynamic monitoring is important on the NICU to timely suspect inadequate tissue perfusion. Conventional surrogates such as blood pressure, diuresis and heart rate are frequently used; however poor surrogates for brain perfusion. Ideally brain perfusion should be monitored continuously. NIRS is nowadays frequently used for trend monitoring and as a surrogate for brain metabolism/perfusion. A disadvantage is that NIRS does not allow visualization of brain vessels. Future research need to combine different (neuro)monitoring techniques to address

the microcirculation during the period on the NICU. One example could be that NIRS and amplitude-integrated electroencephalography (aEEG) are used for continuous trend monitoring, combined with additional information of colour Doppler. 'Multimodal neuromonitoring' is needed to evaluate brain metabolism and perfusion; providing insights in acute brain injury and to help neuroprotective strategies. Ideally leading to individualized therapy of the (pre) term infants on the NICU.

Collaboration with ultrasound manufacturers might lead to an integrated multimodel monitoring system: besides displaying data, automatic pattern recognition can be applied, facilitating early intervention (before clinical parameters deteriorate further).

One of ultrasounds key advantages over other imaging modalities such as CT- and MRI scans, is its increasing mobility. Innovations such as portable hand-held devices and wireless transducers (Siemens Healthcare), could give ultrasound new applications such as performing CUS during the adaptation phase in the delivery room. Combined with NIRS this will provide more information on cerebral perfusion during the very early phases of adaptation.

As stated earlier in this thesis, all images are already processed before they are presented on the ultrasound machine. The different processing algorithms are not available. To better study microcirculation or tissue characteristics the raw radiofrequency data (RF data) would be valuable. Some manufacturers provide this information and are able to extract raw RF data. In cooperation with engineers this could be a new research field. Actual microcirculation, tissue characteristics and brain development versus subtle brain injury (**chapter 8**) could be studied using this RF data. For routine clinical use implementation of these analyses, in the ultrasound machine at the bedside is mandatory.

Beside raw RF data, functional ultrasonography (fUS) is a promising application. Experimental animal studies illustrate that fUS is possible in a rat model [32]. The ability to visualize cerebral blood volume at high spatiotemporal resolution make fUS a promising technique, which can be performed bedside, in contrast with fMRI. Mace et al. induced epileptic activity in rats and with fUS they demonstrated that this technique has the possibility to identify epileptic foci and to study mechanisms of seizure spreading in vivo [32]. If proven safe, it could have a clinical application to study epileptic foci in neonates admitted at the NICU.

Another new tool in the ultrasound machine is the registration of MRI and CUS. The MRI scan of the patient is uploaded in the ultrasound machine. With this registration both imaging modalities can be compared and knowledge of both imaging modalities can be increased. This also allows study of different types of brain injury and combines the strengths of both imaging techniques (figure 1).

Other recent technological trends in ultrasound include advances for contrast-enhanced imaging, volume imaging (real time 3D images) and elastography. ShearWave Elastography (SWE), because it captures shear wave generation with patented UltraFast Imaging technology (Aixplorer, Supersonic) to quantitatively measure the stiffness of local tissues. Being less dependent on an experienced operator, SWE can record elasticity more accurately than

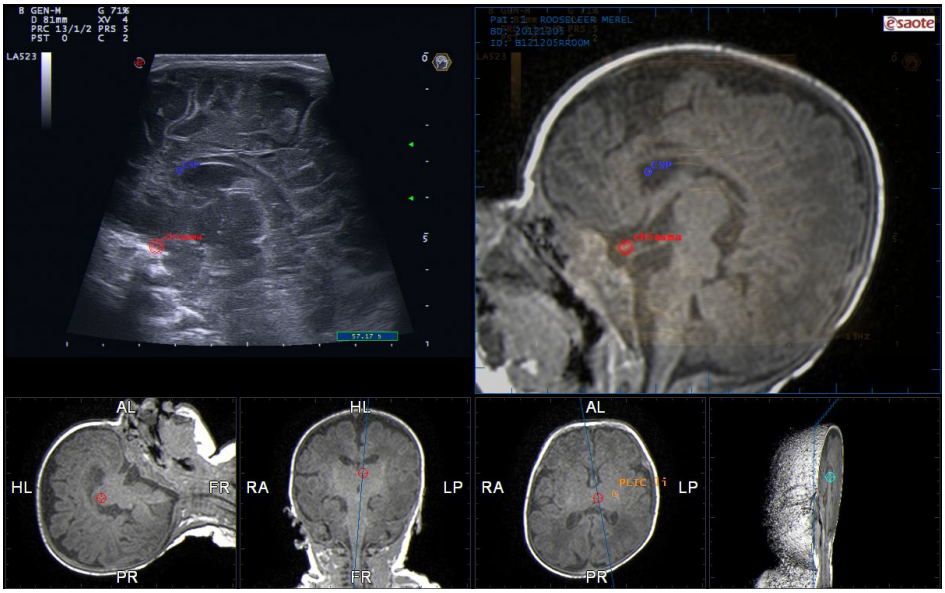

Figure 1 By courtesy of Esaote (Genoa, Italy). Bedside registration of CUS on MRI images.

conventional elastography and produce a more objective, real-time colour-coded map to show tissue stiffness. Combined with advances in colour Doppler, which include very high MHz probes (up to 80 MHz), these techniques could help us to functionally study (brain) vessels. New ultrasound tools such as these, could guide further research to study effects of preterm birth and conditions like pre-eclampsia on vascular development in preterm infants during the neonatal period. To fully understand neurovascular ontogenesis in health and disease research collaboration with the department of Obstetrics and Gynecology is important. A joined study on prenatal and postnatal brain development (DREAM study) has set these goals and is the first step in this direction.

Our ultimate aim is to finally reduce the high numbers of preterm infants with long term neurodevelopmental disabilities. New technological trends in ultrasound hardware and software, new applications and new research collaborations, all make the future of neonatal CUS research very promising.

References

1. Doyle LW, Roberts G, Anderson PJ. Outcomes at age 2 years of infants < 28 weeks' gestational age born in Victoria in 2005. J Pediatr. 2010; **156**(1): 49-53 e1.
2. Draper ES, Zeitlin J, Fenton AC, Weber T, Gerrits J, Martens G, et al. Investigating the variations in survival rates for very preterm infants in 10 European regions: the MOSAIC birth cohort. Arch Dis Child Fetal Neonatal Ed. 2009; **94**(3): F158-63.
3. Moore T, Hennessy EM, Myles J, Johnson SJ, Draper ES, Costeloe KL, et al. Neurological and developmental outcome in extremely preterm children born in England in 1995 and 2006: the EPICure studies. BMJ. 2012; **345**: e7961.
4. Schlapbach LJ, Adams M, Proietti E, Aebischer M, Grunt S, Borradori-Tolsa C, et al. Outcome at two years of age in a Swiss national cohort of extremely preterm infants born between 2000 and 2008. BMC Pediatr. 2012; **12**: 198.
5. Stoll BJ, Hansen NI, Bell EF, Shankaran S, Laptook AR, Walsh MC, et al. Neonatal outcomes of extremely preterm infants from the NICHD Neonatal Research Network. Pediatrics. 2010; **126**(3): 443-56.
6. Greisen G, Borch K. White matter injury in the preterm neonate: the role of perfusion. Dev Neurosci. 2001; **23**(3): 209-12.
7. Liem KD, Greisen G. Monitoring of cerebral haemodynamics in newborn infants. Early Hum Dev. 2010; **86**(3): 155-8.
8. Volpe JJ. The encephalopathy of prematurity—brain injury and impaired brain development inextricably intertwined. Semin Pediatr Neurol. 2009; **16**(4): 167-78.
9. Bezinque SL, Slovis TL, Touchette AS, Schave DM, Jarski RW, Bedard MP, et al. Characterization of superior sagittal sinus blood flow velocity using color flow Doppler in neonates and infants. Pediatr Radiol. 1995; **25**(3): 175-9.
10. Deeg KH, Lode HM. [Trans-fontanellar Doppler sonography of the intracranial veins in infants—part I—Normal values] Transfontanellare Doppler-Sonographie der Hirnvenen im Sauglingsalter—Teil I—Normalbefunde. Ultraschall Med. 2005; **26**(6): 507-17.
11. Miller E, Daneman A, Doria AS, Blaser S, Traubici J, Jarrin J, et al. Color Doppler US of normal cerebral venous sinuses in neonates: a comparison with MR venography. Pediatr Radiol. 2012.
12. Taylor GA. Intracranial venous system in the newborn: evaluation of normal anatomy and flow characteristics with color Doppler US. Radiology. 1992; **183**(2): 449-52.
13. Alper F, Kantarci M, Dane S, Gumustekin K, Onbas O, Durur I. Importance of anatomical asymmetries of transverse sinuses: an MR venographic study. Cerebrovasc Dis. 2004; **18**(3): 236-9.
14. Ayanzen RH, Bird CR, Keller PJ, McCully FJ, Theobald MR, Heiserman JE. Cerebral MR venography: normal anatomy and potential diagnostic pitfalls. AJNR Am J Neuroradiol. 2000; **21**(1): 74-8.
15. Browning H. The confluence of dural venous sinuses. Am J Anat. 1953; **93**(3): 307-29.
16. Dora F, Zileli T. Common variations of the lateral and occipital sinuses at the confluens sinuum. Neuroradiology. 1980; **20**(1): 23-7.
17. Widjaja E, Shroff M, Blaser S, Laughlin S, Raybaud C. 2D time-of-flight MR venography in neonates: anatomy and pitfalls. AJNR Am J Neuroradiol. 2006; **27**(9): 1913-8.
18. Berfelo FJ, Kersbergen KJ, van Ommen CH, Govaert P, van Straaten HL, Poll-The BT, et al. Neonatal cerebral sinovenous thrombosis from symptom to outcome. Stroke. 2010; **41**(7): 1382-8.
19. Moharir MD, Shroff M, Pontigon AM, Askalan R, Yau I, Macgregor D, et al. A prospective outcome study of neonatal cerebral sinovenous thrombosis. J Child Neurol. 2011; **26**(9): 1137-44.
20. Tan MA, Miller E, Shroff MM, Deveber GA, Kirton A. Alleviation of neonatal sinovenous compression to enhance cerebral venous blood flow. J Child Neurol. 2013; **28**(5): 583-8.
21. Ahmad A, Gangitano E, Odell RM, Doran R, Durand M. Survival, intracranial lesions, and neurodevelopmental outcome in infants with congenital diaphragmatic hernia treated with extracorporeal membrane oxygenation. J Perinatol. 1999; **19**(6 Pt 1): 436-40.

22. Bulas DI, Taylor GA, O'Donnell RM, Short BL, Fitz CR, Vezina G. Intracranial abnormalities in infants treated with extracorporeal membrane oxygenation: update on sonographic and CT findings. AJNR Am J Neuroradiol. 1996; **17**(2): 287-94.
23. Griffin MP, Minifee PK, Landry SH, Allison PL, Swischuk LE, Zwischenberger JB. Neurodevelopmental outcome in neonates after extracorporeal membrane oxygenation: cranial magnetic resonance imaging and ultrasonography correlation. J Pediatr Surg. 1992; **27**(1): 33-5.
24. Taylor GA, Glass P, Fitz CR, Miller MK. Neurologic status in infants treated with extracorporeal membrane oxygenation: correlation of imaging findings with developmental outcome. Radiology. 1987; **165**(3): 679-82.
25. Arey B. Developmental Anatomy. 6th Edn Saunders, Philadelphia. 1954: 364-73.
26. Vasovic L, Milenkovic Z, Pavlovic S. Comparative morphological variations and abnormalities of circles of Willis: a minireview including two personal cases. Neurosurg Rev. 2002; **25**(4): 247-51.
27. Vasovic LP. The tenth vascular component in a rare form of the cerebral arterial circle of fetuses. Cells Tissues Organs. 2004; **178**(4): 231-8.
28. Horsch S, Skiold B, Hallberg B, Nordell B, Nordell A, Mosskin M, et al. Cranial ultrasound and MRI at term age in extremely preterm infants. Arch Dis Child Fetal Neonatal Ed. 2010; **95**(5): F310-4.
29. Leijser LM, de Bruine FT, Steggerda SJ, van der Grond J, Walther FJ, van Wezel-Meijler G. Brain imaging findings in very preterm infants throughout the neonatal period: part I. Incidences and evolution of lesions, comparison between ultrasound and MRI. Early Hum Dev. 2009; **85**(2): 101-9.
30. Johnston MV, Hoon AH, Jr. Possible mechanisms in infants for selective basal ganglia damage from asphyxia, kernicterus, or mitochondrial encephalopathies. J Child Neurol. 2000; **15**(9): 588-91.
31. Selip DB, Jantzie LL, Chang M, Jackson MC, Fitzgerald EC, Boll G, et al. Regional differences in susceptibility to hypoxic-ischemic injury in the preterm brain: exploring the spectrum from white matter loss to selective grey matter injury in a rat model. Neurol Res Int. 2012; **2012**: 725184.
32. Mace E, Montaldo G, Cohen I, Baulac M, Fink M, Tanter M. Functional ultrasound imaging of the brain. Nat Methods. 2011; **8**(8): 662-4.

CHAPTER 12

SUMMARY

Summary

In **Chapter 1**- the general introduction- the increasing incidence of preterm birth and long term neurodevelopmental problems are discussed. Monitoring of brain development and early definition of brain injury is important, as is further research to reduce neurological morbidity. In the neonatal care different neuroimaging techniques are used. Cranial ultrasound (CUS) is a non-invasive, safe and bedside technique. MRI allows quantitative measurement of brain injury and offers unique anatomical detail of neonatal brain tissue. However is expensive, needs transport and therefore has limited clinical use. This thesis focus on CUS as neuroimaging technique and provides insight in cerebral blood flow.

Chapter 2 reviews disorders of neonatal brain veins, providing a comprehensive background of the venous origin in different lesion patterns. The aim of this chapter is to encourage further research in prevention of parenchymal injury related to brain veins.

In **Chapter 3** we studied the incidence of cerebral sinovenous thrombosis (CSVT) in neonates with color Doppler CUS. CSVT is a rare disease, with high morbidity. CSVT can be asymptomatic; therefore the incidence in the literature (1-12 per 100000 neonates) is probably underestimated. We documented CSVT in 11 of 249 preterm infants, leading to a 4.4% incidence. Serial CUS including color Doppler imaging through the mastoid fontanel can detect CSVT at an early stage, so prevention of haemorrhage or stroke is still possible. In our cohort we treated six of the eleven infants with low molecular-weighted heparin. In three infants local complications (haemorrhage at insertion side) occurred. One of the limitations is that long term outcome data is lacking due to the young age of the patients included in this study. Further research addressing therapeutic options and long term neurodevelopmental outcome is necessary.

Chapter 4 reports six cases, where CUS including color Doppler documented carotid artery occlusion. Different pathogenesis could be identified in these infants. A known cause is ECMO where the common carotid artery is ligated to insert the cannulas. In two infants transient spasm of the carotid artery was described. Thrombosis was the underlying pathogenesis in two other infants (one following Broviac insertion). In the last patient the carotid artery was ligated during a complicated emergency tracheostomy. We concluded that CUS including color Doppler can detect flow problems at an early stage and that the neonatal circle of Willis is competent in preventing brain injury, if fully developed.

In **Chapter 5** we retrospectively studied, to our knowledge, the largest cohort of neonatal perforator stroke. We found that most infants were asymptomatic and that CUS diagnosed most strokes (80%). Different risk factors can be identified including birth asphyxia, prolonged hypotension, embolism and infection. These risk factors are comparable with other types of perinatal stroke. Isolated perforator stroke are probably under-recognized as clinical symptoms are almost always lacking. Routine CUS is therefore recommended especially in critical ill (preterm) neonates. Insight gained from follow up of this cohort will help more accurately predict neurodevelopmental outcome.

In **Chapter 6** a nationwide cohort of neonatal ECMO patients was studied for incidence of brain injury and lesions patterns. The cohort spanned two decades. We found an incidence of 17.3% and primary haemorrhage was the largest group. Stroke occurred in 5%, with a noticeable preference to the left hemisphere. This finding is unexpected in view of right-sided carotid artery ligation; we therefore concluded that the circle of Willis is competent in 95% of the infants. The incidence of brain injury remains stable over years despite overall improvement of ECMO treatment. Further research may need to focus on asymptomatic CSVT, anti-coagulation monitoring and on the prevention of thrombus formation in the ECMO system leading to potential embolism.

In **Chapter 7** we performed a pilot study to analyse whether CUS including colour Doppler is able to study cerebral "microcirculation". With the settings used in this study we are able to visualize vessels with velocities of 1 cm/s. We measured a Doppler colour index (DCI), which had a broad range. We hypothesize that DCI might reflect cerebral blood flow. Although our pilot study has some limitations, it seems a promising technique for evaluating cerebral blood flow in the future.

Chapter 8 demonstrates a technique to objectively measure grey values in preterm striatum. In extreme preterm infants the putamen is more hyperechoic compared to preterm infants of 28 weeks of gestation. A physiological process regarding cell density and myelinisation might explain this phenomenon. An interesting finding in this study is that this difference remains significant at 30 weeks corrected age. Deep grey matter is vulnerable for hypoxic-ischemic injury, so this might also be an expression of subtle brain injury. Further research is necessary to provide more insight in this phenomenon.

Chapter 9 shows the strengths of two neuroimaging techniques, CUS and MRI, in detecting preterm brain injury. Serial CUS was performed in all patients. MRI was often postponed or cancelled. Preterm brain injury was found in 47.6% and discrepancies between the two imaging techniques was seen in 62 infants. MRI was superior in detecting fossa posterior abnormalities and CUS excelled in detection of acute intraventricular haemorrhage and CSVT. We concluded that CUS seems highly effective in diagnosing preterm brain injury but misses' abnormalities in the posterior fossa. MRI can detect these lesions, but its clinical use is limited.

Chapter 10 reviews the neonatal disorders of the germinal matrix. Beside haemorrhage, stroke and germinolysis occur in the neonatal period. These lesions in transient layers of development interrupt normal maturation and induce neurodevelopmental sequelae.

CHAPTER 13

APPENDICES

Nederlandse samenvatting

In **Hoofdstuk 1-**de algemene introductie- wordt de toename van vroeggeboorte en de gevolgen voor de latere psychomotorische ontwikkeling bediscussieerd. Bewaking van hersenontwikkeling en vroege hersenschade is belangrijk, net als verder onderzoek om de lange termijn effecten van vroeggeboorte en hersenschade te verminderen. Er worden verschillende technieken gebruikt in de neonatale zorg. Schedelechografie is niet invasief, veilig en aan het bed uitvoerbaar. MRI kan kwantitatief de hersenschade beoordelen en heeft de mogelijkheid om anatomie gedetailleerd af te beelden. MRI is echter duur, er is transport naar de MRI van zieke neonaten noodzakelijk en is daarom gelimiteerd te gebruiken in de neonatale zorg. Dit proefschrift focust op schedelechografie en geeft inzicht in de doorbloeding van de hersenen.

In **Hoofdstuk 2** wordt er een overzicht gegeven van ziektebeelden van neonatale hersenvenen, dit zijn de vaten in de hersenen exclusief de slagadres. Het hoofdstuk geeft een duidelijk overzicht van het onderliggend vaat lijden van typen hersenschade. Het doel van dit hoofdstuk is het aanmoedigen van verder onderzoek naar de preventie van schade in het hersenweefsel gerelateerd aan deze vaten.

In **Hoofdstuk 3** hebben we het voorkomen van cerebrale sino-veneuze trombose (CSVT) bij neonaten onderzocht met behulp van schedelechografie inclusief kleuren Doppler. CSVT is een zeldzame aandoening van stolsels in de aders van de hersenen met hoge morbiditeit. CSVT kan zonder symptomen en/of klachten verlopen waarbij de incidentie gerapporteerd in de literatuur (1-12 per 100000 neonaten) waarschijnlijk onderschat is. Wij diagnosticeerde CSVT in 11 van de 249 te vroeg geboren neonaten, dit geeft een incidentie van 4.4%. Herhaalde schedelechografie inclusief kleuren Doppler door de (mastoid) fontanel kan CSVT vroegtijdig detecteren, hierdoor is het voorkomen van een bloeding of infarct als gevolg van de trombose nog mogelijk. In onze onderzoeksgroep (cohort) zijn zes kinderen behandeld met antistolling (Fraxiparine). Bij drie kinderen gaf dit lokale complicaties (bloeding bij de insteekopening). In onze studie missen de lange termijn uitkomsten van deze kinderen, omdat ze nu nog te jong zijn om te testen. Verder onderzoek zal moeten kijken naar de therapeutische opties en lange termijn uitkomsten van neonaten met CSVT.

Hoofdstuk 4 bevat de casuïstiek van zes neonaten waar schedelechografie obstructie van de halsslagader detecteert. Onderliggend lijden was bij deze patiënten verschillend. Een bekende oorzaak is het gevolg van ECMO waarbij de halsslagader onderbonden wordt om de canules te kunnen plaatsen. Bij twee neonaten was er sprake van een tijdelijk spasme van de halsslagader. Trombose was het onderliggend lijden bij twee andere patiënten (een na het plaatsen van de Broviac katheter). Bij de laatste patiënt is de halsslagader onderbonden tijdens een gecompliceerde spoedtracheotomie. Wij concluderen dat schedelechografie inclusief kleuren Doppler doorstromingsproblemen vroegtijdig kan erkennen en dat de neonatale cirkel van Willis competent is om hersenschade te voorkomen, mits volledig ontwikkeld.

In **Hoofdstuk 5** onderzoeken we retrospectief, naar ons weten, het grootste cohort van neonaten met perforator infarct. Onze bevindingen tonen dat de meeste kinderen zonder symptomen en/of klachten zijn en dat schedelechografie de meeste perforator infarcten diagnosticeert (80%). Verschillende risicofactoren konden worden geïdentificeerd, inclusief zuurstoftekort rondom de geboorte, langdurige hypotensie, embolie en infectie. Deze risicofactoren zijn vergelijkbaar met andere soorten infarct in de periode rondom de geboorte. Geïsoleerd perforator infarct is zeer waarschijnlijk onderschat in de literatuur omdat bijna alle kinderen asymptomatisch zijn. Daarom raden we routine schedelechografie aan bij ernstig zieke kinderen opgenomen op de NICU. Follow up van dit cohort kan meer inzicht geven in de lange termijn gevolgen van perforator infarct en daarmee kunnen we deze lange termijn gevolgen beter voorspellen.

In **Hoofdstuk 6** is een landelijk cohort van neonatale ECMO patiënten onderzocht naar het voorkomen van hersenschade en patronen van hersenschade. Het cohort is verzameld in twee decennia. We vonden een incidentie hersenschade van 17.3% waarbij de groep bloedingen het grootst is. Infarcten vonden plaats in 5%, voornamelijk in de linker hemisfeer. Dit is een onverwachte bevinding aangezien de rechter halsslagader onderbonden wordt; wij concluderen dat cirkel van Willis in 95% van de kinderen competent genoeg is om dit op te vangen. Ondanks alle verbeteringen in de ECMO behandeling, is in ons cohort de incidentie van hersenschade over de tijd niet veranderd. Verder onderzoek moet zich wellicht focussen op asymptomatische CSVT, antistolling monitoring en op de preventie van stolsel vorming in het ECMO systeem die wellicht kan leiden tot embolieën.

In **Hoofdstuk 7** hebben we een pilotstudie verricht om te analyseren of schedelechografie inclusief kleuren Doppler gebruikt kan worden om cerebrale " microcirculatie" te bestuderen. Met de instellingen gebruikt in deze studie kunnen we micro bloedvaten visualiseren met snelheden van 1 cm/s. We hebben een Doppler color index (DCI) gemeten, deze toonde een wijde variatie. Onze hypothese is dat deze DCI waarde een afspiegeling kan zijn van de hersendoorbloeding. Ondanks dat onze studie enkele limitaties heeft, lijkt het een veelbelovende techniek om hersendoorbloeding te evalueren.

In **Hoofdstuk 8** demonstreren we een techniek die de grijswaarden van de diepe grijze kernen van preterme kinderen objectief kan beoordelen. In extreem te vroeg geboren neonaten is het putamen meer echorijk in vergelijking met te vroeg geboren kinderen van 28 weken zwangerschap. Mogelijk wordt dit verklaard door een fysiologisch proces betreffende cel dichtheid en myelinisatie. Een interessante bevinding is echter dat dit verschil in echogeniciteit blijft bestaan bij 30 weken gecorrigeerde leeftijd. De diepe grijze kernen zijn erg gevoelig voor zuurstoftekort, dus wellicht is dit dan een uiting van subtiele hersenschade van te vroeg geboren neonaten. Verder onderzoek is nodig om dit fenomeen verder te begrijpen.

Hoofdstuk 9 toont de kracht van twee neuro imaging technieken, schedelechografie en MRI, in het diagnosticeren van hersenschade bij te vroeg geboren neonaten. Schedelechografie werd verricht bij alle geïncludeerde patiënten. MRI werd frequent afgeblazen dan wel

uitgesteld. Hersenschade als gevolg van vroeggeboorte werd gevonden in 47.6% van de neonaten en discrepanties tussen de twee technieken werden gezien in 62 kinderen. MRI was superieur in het detecteren van letsels in de achterste schedelgroeve; schedelechografie excelleerde in het detecteren van acute intra-ventriculaire bloedingen en CSVT. We concluderen dat schedelechografie zeer effectief is in het detecteren van hersenschade als gevolg van vroeggeboorte, echter afwijkingen in de achterste schedelgroeve kunnen worden gemist. MRI diagnosticeert deze letsels maar de klinische toepasbaarheid is (nog) gelimiteerd.

Hoofdstuk 10 geeft een overzicht van neonatale aandoeningen van de germinale matrix. Naast bloedingen, komen infarcten en celreacties (germinolyse) voor tijdens de neonatale periode. Deze aandoeningen in tijdelijke ontwikkelingslagen (transiente lagen van de hersenontwikkeling) verstoren de normale ontwikkeling en leiden tot neurologische restverschijnselen.

Tot slot, worden in **Hoofdstuk 11** alle bevindingen in perspectief geplaatst, met aanbevelingen voor verder onderzoek.

Curriculum Vitae

Marlou Raets was born in Heerlen on 12 December 1983. She went to secondary school at the St-Janscollege in Hoensbroek. After graduating in 2001, she started medicine at the Vrije Universiteit (VU) university of Amsterdam and received her medical degree in March 2008. She started working on the Paediatric Intensive Care Unit at Leiden University Medical Center as a paediatric resident-not-in-training till March 2009. Then she started working on the Neonatal Intensive Care Unit in the Erasmus MC-Sophia in Rotterdam, the interest for neonatal neuroimaging developed here and her PhD thesis was started in 2010. During her PhD she kept working on the NICU as a paediatric resident-not-in-training. In 2014 she will continue her career and start working as a resident-in-training in the ErasmusMC-Sophia.

In 2011 she married the love of her life, Bas Kouwenberg. On December 5th 2013 their son Twan was born and they live happily together in Nieuw-Vennep.

Dankwoord

Trots ben ik op dit mooie eindresultaat van een fijn promotietraject, maar ik had het niet alleen kunnen doen en wil daarom alle betrokkenen bedanken.

Mijn promotor, professor dr. I.K.M. Reiss. Beste Irwin, dank voor de fijne samenwerking en deze leerzame ervaring. Het was prettig zowel klinisch als wetenschappelijk betrokken te zijn bij uw afdeling, het was een win-win situatie!

Mijn copromotoren dr. J. Dudink en dr. P. Govaert. Beste Jeroen, dank voor je inzet en enthousiasme de afgelopen jaren. Als ANIOS heb je me gemotiveerd voor wetenschappelijk onderzoek en je enthousiasme werkt erg aanstekelijk. Ondanks je drukke agenda was je altijd beschikbaar om te brainstormen over de lopende projecten, voor advies, of een luisterend oor. We hebben veel gelachen en ik hoop dat we onze samenwerking kunnen voortzetten in de toekomst.

Beste Paul, bedankt voor uw geduld, kennis en ondersteuning tijdens dit promotietraject, maar vooral ook voor alle gezelligheid. Ik deel uw enthousiasme voor de techniek die u mij geleerd hebt. Door de kennis die u mij heeft overgebracht, merkte ik dat de monoloog langzaam veranderde in een dialoog over schedelechografie. Een van de hoogtepunten in de afgelopen jaren was de mogelijkheid om samen een schedelechografie cursus te geven in het buitenland. Wellicht krijgen we de mogelijkheid dat een vervolg te geven.

De leden van de kleine commissie, professor dr. D. Tibboel, professor dr. G.P. Krestin en professor dr. B. Urlesberger wil ik bedanken voor hun bereidheid deel te nemen in de kleine commissie en voor hun beoordeling van het manuscript. Daarnaast wil ik professor Tibboel specifiek bedanken voor de fijne samenwerking in de ECMO-gerelateerde projecten. De overige leden wil ik hartelijk danken voor hun bereidheid zitting te nemen in de grote commissie.

Dear professor B. Urlesberger, I would like to thank you for attending this day in the Netherlands.

Alle neonatologen, fellows, arts-assistenten en verpleegkundig specialisten van de afdeling. Jullie hebben een warm team waar ik altijd met veel plezier gewerkt heb, het voelt na al die jaren als een tweede familie. Ik wil jullie allemaal bedanken, maar een aantal wil ik speciaal noemen. Beste Marijn, het was voor mij fijn om een bekend gezicht te zien op dag 1 van mijn nieuwe baan. Sindsdien ben je mijn mentor en ik wil je bedanken voor alle goede adviezen en chocolademelk-momenten. Beste Daniella, Cynthia en André, bedankt voor alles wat jullie me hebben geleerd en de gezellige Doppio momenten die we samen gedeeld hebben. Ik ga ze zeker missen. Beste Rogier, bedankt voor alle leerzame momenten en met name voor het kritisch beoordelen van artikelen en de wetenschappelijke samenwerking.

Beste Monique en George, wat heb ik veel van jullie geleerd en veel met jullie gedeeld! Voor een lach en een traan kan ik bij jullie terecht.

Beste Tom, dank voor je technische ondersteuning en de wekservice in de trein.

Graag wil ik ook alle verpleegkundigen die werkzaam zijn op de afdeling bedanken voor de mogelijkheid om de schedelecho's te verrichten en voor de ondersteuning van de patiënten.

Daarnaast wil ik alle leden van de neurogroep bedanken voor het brainstormen en het kritisch beoordelen van de artikelen en presentaties.

Ook collega's die nu elders werkzaam zijn, wil ik graag bedanken. Beste Hans, bedankt dat je me de kans hebt geboden om me op wetenschappelijk gebied te ontwikkelen. Beste Sandra, bedankt voor de begeleiding aan het begin van de onderzoeksperiode en het aanleren van de schedelechografie. Beste Leo(-natoloog), bedankt voor je vertrouwen in mij en natuurlijk alle gezellige momenten.

In de afgelopen jaren heb ik samengewerkt met enkele leergierige studenten. Dank voor de samenwerking, het verzamelen en invoeren van data en de hulp bij artikelen. Heel veel succes in jullie verdere carrière.

Alle mede-auteurs die ik wellicht nog niet genoemd heb, bedankt voor de samenwerking!

Mijn paranimfen, Annemarie en Eline. Lieve Annemarie, lieve synaps, wat fijn dat je naast me staat op die bijzondere dag! Jut en Jul werden we vaak genoemd en we waren een onafscheidelijke duo. Het was heel bijzonder om de afgelopen jaren samen te werken, ik had me geen betere buddy kunnen wensen. Dank voor alles en natuurlijk ook heel veel succes met je eigen promotie.

Lieve Eline, mijn beste vriendin. Lief en leed delen we en ik weet dat ik bij jou altijd terecht kan. Als jij naast me staat kan ik alles aan! Je houdt van aanpakken en dat werkt aanstekelijk, dat was erg fijn bij de laatste loodjes. Je hebt een super gezinnetje en ik kijk uit naar de aankomende vakanties met onze mannen. Ook je man Vincent wil ik bedanken voor zijn nuchtere blik en adviezen.

Mijn vrienden die altijd voor me klaarstaan. Lieve Jerry en Monique, vanaf het eerste jaar in de studententijd kan ik op jullie bouwen. Wat is het gezellig om jullie als bijna buren te hebben. Monique, het is heel bijzonder om hetzelfde traject met dezelfde tijdsplanning te bewandelen. Succes met je eigen promotie en het starten van de opleiding. Lieve Jerry, maar ook lieve Max en Amir, bedankt voor alle keren dat jullie me kwamen ophalen op Uilenstede. Dankzij jullie kon ik meegenieten van alle gezelligheid in bijvoorbeeld Uithoorn. Lieve Ellen, je kent me van al mijn vrienden het langst en misschien wel het beste. Jammer dat we zo ver weg van elkaar wonen maar het is fijn je als vriendin te hebben en ondanks de afstand zal dat zo blijven. Lieve

Frits en Stephanie, de kans is nu groot dat we dichter bij elkaar komen wonen, Rotterdam here we come! Op naar de spare-rib/whisky avonden.

Mijn lieve (schoon)familie. Het boek wordt te dik als ik iedereen persoonlijk ga bedanken, maar een aantal mensen wil ik toch in het bijzonder noemen. Lieve Oma en Bestemoeder, jullie zijn de liefste oma's die iemand zich kan wensen. Ondanks dat het niet meer mogelijk is om erbij te zijn in Rotterdam, weet ik dat jullie samen met mij zullen genieten op deze dag. Ik hoop nog veel bijzondere momenten met jullie te delen.

Lieve opa Joosten, dank voor het warme onthaal in de familie en alle bijzondere verhalen over vroeger en met name over Rotterdam.

Lieve schoonouders, Nico en Thea, ik wil jullie bedanken voor alle steun, interesse en betrokkenheid. Vanaf dag 1 voelde ik me thuis.

Lieve Tom, ik kan me geen leukere zwager bedenken. Naast onze serieuze gesprekken, kan ik enorm met jou lachen!

Lieve Ellen, dankzij jou weet ik hoe het voelt om een zusje te hebben, dank!

Lieve Jan en Juulz, ondanks de afstand hebben jullie mij super gesteund tijdens mijn hele promotietraject. Gelukkig is er tegenwoordig Skype, zodat het contact makkelijker is. Ik weet dat jullie Down Under met mij meevieren.

Lieve Pap en Mam, jullie hulp, oneindig vertrouwen en onvoorwaardelijke liefde hebben me zover gebracht. Bedankt voor alle steun en de kansen die jullie me geboden hebben! Het is fijn te weten dat ik altijd bij jullie terecht kan, ik hou super veel van jullie! Mam, je hebt ooit gezegd dat je dit zo graag met me wilde meemaken en die dag is gekomen! Pap, het voelt super goed om je als voorzitter van mijn fanclub te hebben. Voor de toekomst hoop ik dat ik als ouder voor Twan evenveel kan betekenen.

Lieve, lieve Bas. De liefde van mijn leven, mijn allerbeste maatje! Het is voor jou niet altijd makkelijk geweest, al die uren die werden geïnvesteerd om tot dit eindresultaat te komen, maar je hebt me altijd met alles door dik en dun gesteund! Ik had dit echt niet zonder je gekund! Ik weet zeker dat we een heel fijne toekomst tegemoet gaan samen met onze prachtige zoon Twan! Ik hou van jou!

List of publications

Raets MMA, Bosman-Vermeeren JM, Gesink-Van der Veer BJ. Tube obstruction after surgery in prone position. Netherlands Journal of Critical Care. Feb 2012; 16 (1): 26-28.

Plaisier A, **Raets MMA**, van der Starre C, Feijen-Roon M, Govaert P, Lequin MH, Heemskerk AM, Dudink J. Safety of routine early MRI in preterm infants. Pediatric Radiology. Oct 2012; 42 (10): 1205-1211.

Raets MMA, Lequin MH, Plaisier A, Dudink J, Govaert P. Incidental sonographic diagnosis of neonatal carotid artery occlusion. Acta Paediatrica. Apr 2013; 102 (4):e 187-190.

Ecury-Goossen GM, **Raets MMA**, Lequin MH, Feijen-Roon M, Govaert P, Dudink J. Risk factors, clinical presentation and neuroimaging findings of neonatal perforator stroke. Stroke. Aug 2013; 44 (8): 2115-2120.

Raets MMA, Dudink J, Govaert P. Neonatal disorders of germinal matrix. Journal of Maternal, Fetal and Neonatal Medicine. Aug 2013; Epub ahead of print.

Raets MMA, Sol JJ, Govaert P, Lequin MH, Reis IKM, Kroon AA, Appel IM, Dudink J. Serial Cranial US for detection of cerebral sinovenous thrombosis in preterm infants. Radiology. Aug 2013; Epub ahead of print.

Madderom MJ, Reuser JJ, Utens EM, van Rosmalen J, **Raets MMA**, Govaert P, Steiner K, Gischler SJ, Tibboel D, van Heijst AF, IJsselstijn H. Neurodevelopmental, educational and behavioral outcome at 8 years after neonatal ECMO: a nationwide multicenter study. Intensive care medicine. Sept 2013; 39 (9): 1584-1593.

Raets MMA, Dudink J, IJsselstijn H, van Heijst A.F.J, Lequin M.H, Houmes R.J, Wildschut E.D, Reiss I.K.M, Govaert P, Tibboel D. Brain injury associated with neonatal ECMO in the Netherlands. A nationwide evaluation spanning two decades. Pediatric Critical Care Medicine, 2013 Oct 10. Epub ahead of print.

Raets MMA, Dudink J, Raybaud C, Ramenghi LA, Lequin MH, Govaert P. Disorders of newborn brain veins. Submitted.

Raets MMA, Govaert P, Goos TG, Reiss IKM, de Jonge RCJ, Dudink J. Preterm cerebral microcirculation assessed with colour Doppler: a pilot study. Submitted.

Raets MMA, de Goederen R, de Jonge RCJ, Ramenghi LA, Reiss IKM, Koning IV, Govaert P, Dudink J. Maturation of echogenicity in preterm striatum. Submitted.

Plaisier A, **Raets MMA**, Govaert P, Feijen-Roon M, Reiss IKM, Smit LS, Lequin MH, Dudink J. Serial cranial ultrasonography and early MRI are complementary in detecting preterm brain injury. Submitted.

Van der Cammen-van Zijp MHM, Janssen AJWM, **Raets MMA**, van Rosmalen J, Govaert P, Steiner K, Gischler SJ, Tibboel D, van Heijst AFJ, IJsselstijn H. Motor performance after neonatal extracorporeal membrane oxygenation; a longitudinal evaluation. Accepted.

PhD Portfolio

Name PhD student:	M.M.A. Raets	PhD period:	2010-2014
Erasmus MC Department:	IC Neonatology	Promotor(s):	prof. dr I.K.M. Reiss
Research School:	Erasmus MC	Supervisor:	dr. P.P. Govaert/ dr J.Dudink

1. PhD training

	Year	Workload (ECTS)
General courses		
- BROK ('Basiscursus Regelgeving Klinisch Onderzoek'	2010	1
- CPO- minicursus	2010	0.3
- Biostatistical Methods I: Basic Principles (CC02)	2011	5,7
Specific courses (e.g. Research school, Medical Training)		
- MR Imaging of the neonatal brain	2010	1.4
- MRI Veiligheidsniveau 2	2011	0.3
Seminars and workshops		
- Course instructor: Cranial ultrasound for neonatologists in Burgos, Spain. With Dr P Govaert	2012	3
Presentations		
- 12de Neonatale Neurologie symposium, Utrecht	2011	0.7
- Vlaams-Nederlandse Neonatalogendag, Gent	2011	0.7
- 13de Neonatale Neurologie symposium, Amsterdam	2012	0.7
- VRA traumatisch hersenletsel, Rotterdam	2012	0.7
- The 4th congress of the European Academy of Paediatric Societies. Istanbul. (including poster symposium)	2012	1
- Vlaams-Nederlandse Neonatologendag, Antwerpen	2013	0.7
(Inter)national conferences		
- 11de Neonatale Neurologie symposium, Nijmegen.	2010	0.3
- Neuroimaging, Genetics, and Endophenotypes: Development and psychopathology, Rotterdam.	2010	0.3
- European Neonatal Neuro Experts Meeting (ENNEM): The future of neonatal brain research in Rotterdam, Rotterdam	2010	0.3
- New insights in Neonatal Neurology, Belgian society of Pediatric Neurology, Brussel.	2010	0.3
- 11th International Congress of the European Sociaty of Magnetic Resonance in Neuropediatrics, Amsterdam	2011	1.2
- 52nd Annual meeting of the European Society for Paediatric Research. Newcastle.	2011	1.2
- 5th international Euraibi meeting, Sienna		
- The 4th congress of the European Academy of Paediatric Societies. Istanbul. (including poster symposium)	2012 2012	1.2 1.2

2. Teaching		
	Year	**Workload (ECTS)**
Teaching		
- NICU nurses education, Rotterdam	2010-2011	1.4
- Cranial ultrasound: students and interns Rotterdam	2010-2012	1.4
- Cranial ultrasound: neonatologists and intensivists, Rotterdam	2012-2013	2.4
Supervising students		
- Student Venous infarction (B.Bouwen)	2012-2013	2
- Student Echogenicity (R. de Goederen)	2012-2013	2